In Situ Flash Pyrolysis of Straw

Bech, Niels; Dam-Johansen, Kim; Jensen, Peter Arendt

Publication date:
2008

Document Version
Publisher's PDF, also known as Version of record

In Situ Flash Pyrolysis of Straw

Ph.D. Dissertation

Niels Bech

Department of Chemical and Biochemical Engineering

Technical University of Denmark

2008

ISBN 978-87-91435-68-4
Printed by Frydenberg a/s, Copenhagen, Denmark

Abstract

For more than a decade straw has been utilized as fuel and made it clear that a process which could concentrate the energy in the field, remove ash, and reduce the logistic costs would improve the attractiveness of this alternative fuel significantly. These objectives can be achieved by *in situ* flash pyrolysis, where straw is converted to bio-oil in the field and char is left on the ground in order to improve soil structure and provide plant nutrients. Incondensable pyrolysis gas is also produced by the pyrolyzer but is combusted internally to provide heat for the process.

The main objectives of the Innovation Ph.D. project reported in this dissertation were to support the development of a suitable reactor for *in situ* flash pyrolysis, construct a small stationary pilot plant, characterize and test straw bio-oil as a liquid fuel, and compile a business plan for the commercialization of the results. Further objectives were to increase the knowledge on flash pyrolysis of straw and to develop a tool capable of predicting the performance of the developed reactor.

A literature study on the requirements of *in situ* flash pyrolysis found that, due to the restricted size of a vehicle, the reactor should have a small footprint and utilize gas rather than char for heating. Furthermore, in order to reduce the mechanical power consumption, the reactor should be able to operate with relatively large particles and be arranged horizontally to accommodate the shape of the vehicle. Accordingly, it was concluded that a reactor of the ablative design operating without gas recirculation would be the best choice, and the Pyrolysis Centrifuge Reactor (PCR) was developed in an attempt to accommodate these findings. It was designed as a horizontally arranged heated pipe within which a rotor creates a swirling gas wherein biomass particles are suspended. The centrifugal acceleration acting on the circulating particles cause them to be forced against the wall where reaction takes place.

Initial experimental runs showed only minor response to temperature and rotor speed variations for yields of the principal products. It was concluded that the observed behavior was caused by slow pyrolysis conditions due to a non-uniform temperature profile on the reactor pipe and by heterogeneous tar cracking in the cold zones or in the combined char separator and catch pot. Based on the observed particle hold-up time in cold flow experiments, it was concluded that the particles traveled through the reactor in plug flow. However, further investigation of the particle flow, conducted visually with a glass version of the reactor, established that the material did not travel evenly through the reactor but was retained at the reactor entrance before being quickly ejected. Accordingly, the reactor pipe and rotor were modified to ensure plug flow of particles, the heating system was split in zones to ensure a uniform temperature profile, and the char separator and catch pot were separated in order to further limit heterogeneous tar cracking.

After the system had been modified, a new series of experimental runs was performed and the yields of the principal products now varied markedly with reactor conditions. A model was developed to describe the yield distribution with reactor parameters. Solid-phase primary pyrolysis and secondary tar cracking in gas phase were treated independently in separate reactors. Conversion of the biomass particles was treated as a pseudo-surface reaction and the split between products was determined by the surface temperature of the particle. Following the primary reactions, the formed pyrolysis gas and vapors were injected into a plug flow gas phase reactor where the vapors undergo cracking to gas. The modified Broido-Shafizadeh kinetic scheme was applied in the modeling. The model could be applied directly to the pine wood experimental results, but two parameters were fitted for the straw runs. For both feedstocks, the model described the performance of the PCR acceptably. However, the model also revealed a relatively flat spatial temperature profile in the investigated particles and that the criterions for ablative pyrolysis were not satisfied. The ability of the model to describe the system despite the invalidated surface reaction assumption was attributed to that cracking of tar within the particles was negligible and that the violent movement of the particle hindered the formation of an insulating char layer.

The experimental results represent the first reported systematic investigation of straw flash pyrolysis in an ablative (*i.e.* solid convective) reactor. Modeling of the yield distribution showed that the same approach as used for wood feedstock is applicable if the catalytic effect of the ash content is incorporated. It was demonstrated that this can be accomplished simply by fitting the activation energy of the two solid pyrolysis reactions in the Broido-Shafizadeh kinetic model. The effect was shown to be a ~ 80 °C lower temperature of reaction which in combination with the catalyzed char and gas forming reaction result in higher yields of these products but also in an increased rate of conversion whereby the temperature of maximum liquid organics yield is shifted downwards.

For the reactor parameters investigated in the experimental unit, modeling showed that liquid organic yields exceeding 50 % daf. are possible if centrifugal acceleration is increased to above $3 \cdot 10^4$ g or the particle size distribution is monodisperse. The yield was expected to improve further if larger particles are employed in a reactor designed to provide sufficient residence time. This indicated that the PCR is well suited for flash pyrolysis of straw without having to finely mill the feed.

For the investigated straw particles and reactor parameters, the experimental results and the model established that the yield of liquid organics does not increase significantly above a centrifugal acceleration of 10^4 g. The highest yield at this level was predicted to be 43 % daf. at a reactor temperature of 515 °C. At these conditions, the specific capacity of the reactor on straw input was estimated to be 330 kg m^{-2} h^{-1}. The specific reactor capacity was found to be strongly influenced by centrifugal acceleration and exceeding 10^4 g of nominal centrifugal accelerations was predicted to significantly increase the capacity of the reactor.

Pilot runs were conducted, and it was concluded that straw-derived bio-oil is expected to be able to obtain a proposed *light-medium* specification if char separation is improved, water content reduced by fractional condensation, and nitrogen partitioning controlled. It was attempted to combust the samples in two domestic furnaces, normally operating on rapeseed oil, but neither unassisted ignition nor stable operation was achieved. It was concluded that the observed behavior was caused by

the significantly higher specific pre-ignition energy addition needed by bio-oil and that combustion in these burners was possible if relatively simple measures were taken to increase heat transfer to fuel droplets immediately after atomization.

The most suitable option for commercializing the intellectual property rights obtained during the project was identified by using strategic marketing planning techniques combined with analysis of selected scenarios. It was found that for the coming three years superior conditions for commercialization exit in the EU, mainly due to implementation of the first phase of the Kyoto Protocol, but on a longer time scale conditions in the US are likely to improve. Based on a SWOT analysis, two scenarios for commercialization were identified, establishing an independent research company or transferring the IPR to a multinational producer of agricultural equipment. It was concluded that the objectives of the owners are better satisfied by transferring the project to an established company in the agricultural machinery industry.

It was concluded that the objectives for the project were achieved, but several issues are still poorly understood or have not been investigated. These include the effect on yield distribution of feed water content and particle size. Solid particle movement in the reactor also needs to be investigated more fundamentally, reactor heating by combustion of pyrolysis gas verified, and the area specific reactor capacity established. The project has demonstrated that *in situ* pyrolysis of straw is a promising concept both technically and commercially, but a great deal of effort still remains.

Dansk Resumé

Erfaringerne med forbrænding af halm opnået gennem et årti har vist, at en proces der kan koncentrere energien på marken, fjerne aske og reducere logistikomkostningerne ville gøre denne alternative energikilde betydelig mere attraktiv. Disse mål kan nås med *in situ* flash pyrolyse, hvor halm bliver omdannet til bio-olie i marken og koks efterlades på jorden for at forbedre jordstrukturen og tilføre mineraler. Ikke kondenserbar pyrolysegas produceres også i processen, men bruges internt i pyrolysatoren til produktion af den nødvendige varme.

Hovedformålene med dette Innovations Ph.d. projekt var at understøtte udviklingen af en reaktor til *in situ* flash pyrolyse, konstruere et mindre stationært pilotanlæg, karakterisere og teste halm bio-olie som flydende brændstof samt udvikle en forretningsplan for kommercialisering af de opnåede resultater. Yderligere var det ønsket at undersøge flash pyrolyse af halm generelt og udvikle et værktøj, der kunne modellere den udviklede reaktors opførsel.

Ved hjælp af en litteraturundersøgelse af *in situ* flash pyrolyse blev det fastslået, at reaktoren skal være kompakt på grund af den begrænsende plads i køretøjet og bruge gas i stedet for koks til opvarmning. Reaktoren skal ydermere kunne udnytte relativt store partikler for at begrænse kraftforbruget og have en horisontalopbygning for at udnytte køretøjets form. Herudfra blev det konkluderet, at en ablativ reaktor uden gasrecirkulation var bedst egnet til opgaven, og efterfølgende blev Pyrolyse Centrifuge Reaktoren udviklet i et forsøg på at opnå disse mål. Den var designet som et horisontalt opvarmet rør med en central rotor, der skaber en roterende gasstrømning hvori biomassepartikler suspenderes. Centrifugalkraften tvinger de roterende partikler ind mod rørvæggen hvor reaktionen sker.

I den første forsøgsserie blev der kun observeret en begrænset variation i udbyttet af hovedprodukterne ved ændringer af reaktortemperatur og rotorhastighed. Det blev konkluderet, at årsagen var såkaldt langsom pyrolyse reaktionsbetingelser skabt af en ujævn temperaturfordeling på reaktorrøret, samt heterogen tjærekrakning i de kolde zoner eller i den kombinerede koksseparator og opsamlingspotte. På grundlag af den observerede hold-up tid, målt med uopvarmet reaktor, blev det konkluderet, at partiklerne bevægede sig gennem reaktoren i stempelstrømning. Efterfølgende undersøgelser af partikelstrømningen, foretaget med en glasversion af reaktoren, afslørende dog, at materialet ikke bevægede sig som først antaget, men derimod hobede sig op ved fødeporten for derefter at blive skudt ud af reaktoren. Reaktoren blev derfor modificeret således, at partiklerne bevægede sig i stempelstrømning, opvarmningen blev splittet op i zoner for at få en ensartet temperatur over røret, og koksseparatoren og opsamlingspotten blev adskilt i to enheder for at begrænse heterogen tjærekrakning.

Efter reaktoren var blevet modificeret blev der kørt en ny forsøgsserie, og nu udviste udbyttet af reaktionsprodukterne en betydelig variation med reaktorparametrene, og

en model blev udviklet for at beskrive udbyttefordelingen. Fastfase primær pyrolyse og sekundær tjærekrakning i gasfase blev behandlet uafhængigt af hinanden i to separate reaktorer. Omdannelse af partiklen blev behandlet som en pseudooverflade reaktion, og selektiviteten mellem produkterne blev bestemt af partiklens overfladetemperatur. Efter de primære reaktioner blev den dannede pyrolysegas og gasformige tjære overført til en gasfase reaktor, med stempelstrømning, hvor tjæren kunne krakke til gas. Den modificerede Broido-Shafizadeh kinetiske model blev anvendt ved modelleringen. Modellen kunne anvendes direkte på de eksperimentelle resultater opnået med fyrretræ, hvorimod to frie parametre blev estimerede ved anvendelse på halmresultaterne. I begge tilfælde beskrev modellen de eksperimentelle resultater tilfredsstillende, men afslørede samtidig, at den rumlige temperaturfordeling i partiklerne havde været relativ jævn og at kriterierne for ablativ pyrolyse ikke havde været opfyldt. Modellens evne til at beskrive produktudbytterne, trods den ikke opfyldte antagelse om overfladereaktion, blev tilskrevet, at krakning af tjære i partiklernes indre var af mindre betydning, og at den hårdhændede behandling i reaktoren forhindrede, at der kunne dannes et isolerende kokslag på overfladen.

De eksperimentelle resultater udgør den første rapporterede systematiske undersøgelse af halm flash pyrolyse i en ablativ (*solid convective*) reaktor. Modellering af udbyttedistributionen viste, at den samme metodiske tilgangsvinkel anvendt for træ er anvendelig, hvis der tages højde for den katalytiske effekt af halmens askeindhold. Det blev demonstreret, at dette kunne gøres ved at tilpasse aktiveringsenergien for de to faststof pyrolyse reaktioner i Broido-Shafizadeh modellen. Det blev vist at effekten var en ~ 80 °C lavere reaktionstemperatur, hvilket i kombination med den katalyserede koks og gas dannende reaktion resulterer i et højere udbytte af disse produkter, men også i en øget konverteringshastighed hvorved temperaturen for maksimalt tjæreudbytte sænkes.

For de reaktorparametre, der blev undersøgt i laboratoriereaktoren viste modelleringen, at et udbytte af vandfri tjære på over 50 % daf. er muligt hvis centrifugal accelerationen øges til over $3 \cdot 10^4$ g eller partikkelstørrelsesfordelingen er monodispers. Udbyttet forventes at kunne øges yderligere hvis større partikler fødes til en reaktor, der er designet til at give tilstrækkelig opholdstid. Dette indikerede at den udviklede reaktor er velegnet til flash pyrolyse af halm uden, at skulle findele råmaterialet først.

For de reaktorparametre, der blev undersøgt i laboratoriereaktoren fastslog de eksperimentelle undersøgelser og modelleringen samstemmende at udbyttet af vandfri tjære ikke øges væsentligt ved at hæve centrifugal accelerationen over 10^4 g. Det højeste udbytte ved denne værdi blev forudsagt til at være 43 % daf. ved en reaktortemperatur på 515 °C. Under disse forhold blev den specifikke reaktorkapacitet estimeret til at være 330 kg m^{-2} h^{-1}. Det blev fundet at den specifikke reaktorkapacitet var stærkt afhængig af den anvendte centrifugal acceleration, og større værdier end 10^4 g blev forudsagt til at øge reaktorkapaciteten væsentligt.

I to pilotforsøg blev der fremstillet prøver af halm bio-olie, og efter analyse af disse blev det konkluderet, at de vil kunne opfylde en fremtidig let-medium specifikation hvis separation af koks blev forbedret, vandindholdet reduceret ved partiel kondensering og nitrogenfordelingen mellem produkterne kontrolleret. Det blev forsøgt at anvende den producerede bio-olie i to husholdningskedler, udviklet til afbrænding af rapsolie, men hverken uassisteret antænding eller stabil forbrænding

blev opnået. Det blev konkluderet at begge dele skyldtes, at bio-olie dråberne krævende en betydelig højere tilførsel af energi før antændelse, og at forbrænding i sådanne systemer var mulig hvis kedlen blev modificeret således, at varmetransporten til dråberne blev forøget efter forstøvning.

Den bedste måde at kommercialisere resultaterne opnået i projektforløbet blev identificeret ved brug af strategiske marketingsplanlægningsteknikker kombineret med analyse af udvalgte scenarier. Resultatet var at for de kommende tre år er der ekstraordinært gode forhold for kommercialisering i EU, hovedsagelig på grund af implementeringen af Kyoto Protokollens første fase, men samtidig forventes det, at forholdene på længere sigt i USA og resten af verden vil forbedres. Ud fra en SWOT analyse blev to scenarier for kommercialisering identificeret, etablering af et uafhængigt forskningsfirma eller overførsel af patentrettighederne til en multinational producent af landbrugsmaskiner. Det blev konkluderet, at ejernes ønsker blev bedst tilfredsstillede ved at vælge den sidste løsning.

Slutteligt blev det konkluderet, at formålene med projektet var blevet opnåede, men at forståelse eller yderligere undersøgelser stadig mangler på flere områder. Disse områder omfatter råmaterialevandindholdets og partikelstørrelsesfordelingens indflydelse på udbyttefordelingen. Partikelstrømningen i reaktoren skal også undersøges mere fundamentalt, reaktoropvarmning ved forbrænding af pyrolysegas konfirmeres og den arealspecifikke kapacitet bestemmes. Projektet har alt i alt demonstreret, at *in situ* flash pyrolyse af halm er et lovende koncept både teknisk og kommercielt, men et betydeligt arbejde venter stadig forude.

Preface

Between 2002 and 2004, I was managing a company from St. Petersburg, Russia and had the opportunity to visit our partners in the Fore-Caucasus on several occasions. The widespread grain fields around the cities Rostov-on-Don, Krasnodar, and Stavropol brought back memories of Ukraine and especially of Midwestern USA where I had lived years back. It also started reflections on how the unused energy in the form of straw left on the field as compost could be utilized. In my childhood, we had a straw furnace at the farm where I grew up, but apart from the messy and labor intensive jobs of collecting the straw and disposing the ash, it seemed obvious that utilizing straw as fuel in power plants would not make economic sense in such scarcely populated areas. After considering several options, it seemed clear to me that employing flash pyrolysis to convert the straw to bio-oil in the field might just do the trick. Accordingly, I established contact to the head of Department of Chemical and Biochemical Engineering, Professor Kim Dam-Johansen, and he supported my ideas. Due to the project's practical nature and expected commercial interest, we applied for funding in form of an Innovation Ph.D. scholarship and were successful.

This dissertation reports the progress we have achieved so far and sketches how we plan to proceed with realizing my goal. There is still considerable work to be done before I can fire up the tractor and go bio-oil harvesting, but when I look back today, I realize that we are on the right track and have achieved what we set out to do during the project.

Financial support for the project was received from the Technical University of Denmark's Innovation Ph.D. Program and from the Nordic Energy Research Program and is gratefully acknowledged. However, the results reported in this dissertation are the fruits of the people who have contributed directly and indirectly to the project. Professor and main supervisor Kim Dam-Johansen was the first technically knowledgeable person to support the concept, and he has continued to do so throughout the years. I want to thank him and Associate Professor and co-supervisor Peter A. Jensen for the rewarding discussions we have had. At Copenhagen Business School, Managing Director and owner of Nor-Group, Troels Elgaard supervised the business plan development and contributed with support and advice during our sessions far in excess of what was expected. Engineer's Assistant, Machinist S. V. Madsen at the departmental workshop has been instrumental in constructing the reactor and the experimental set-up, and I consider him a personal friend today. The same goes for my other colleagues at the department, classmates at CBS, and participants in the Nordic BiofuelGS program who all have been supportive and contributed with valuable input. Rasmus Ebbesen, whom I meet in Russia, has been by my side all the way and has even provided his work during the bio-oil combustion trials. But above all, I want to thank my beautiful and loving wife Diana Bech who

has been there for me when things did not turn out as expected. Without you it would not have been possible.

I want to stress that all these people have had no part in possible inaccuracies and errors for which I take sole responsibility.

Niels Bech
Kgs. Lyngby, February 2008

Contents

Chapter 1: Introduction

For more than a decade straw has been utilized in Denmark as fuel in dedicated straw furnace systems or by co-combustion [1]. Besides the positive environmental impact, this practice has drawn attention to the negative aspects also associated with utilizing this solid fuel.

Despite being considered a waste material from grain production, straw handling and storage costs make it an expensive fuel compared to traditional fossil fuels. This is reflected by the fact that the costs associated with logistics are approximately five times the cost of raw straw on the field, see Figure 1.

The high logistic costs are caused in part by the low energy density. Straw has a typical lower heating value of 14.9 MJ kg^{-1} [1], and to enhance storage and transport it is compressed in Hesston bales whereby the density is increased to 139 kg m^{-3} [2]. However, the volume specific energy content is still only 2.1 GJ m^{-3} or about 7 % of the value for mineral oil products.

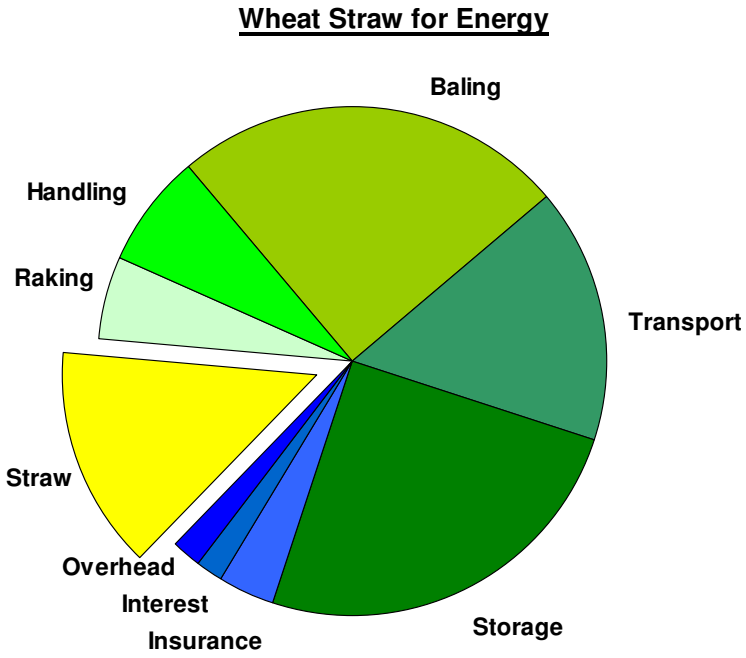

Figure 1: Distribution of costs for straw delivered in Hesston bales to power plants under Danish conditions [3, 4]. Based on data from [5].

On weight basis straw, like the biomass of other herbaceous species, contains approximately 5 % ash including a high proportion of potassium (and associated chloride) [1] due to the requirements of the fast-growing plant. When the ash is subjected to the temperatures encountered during combustion, potassium chloride is

partly melted making the ash sticky and promoting attachment to heat transfer surfaces in the boiler. The results are reduced heat transfer and energy efficiencies [6] and increased deposit formation and corrosion [7-9]. Operational costs are negatively influenced by shut-downs for cleaning and repairs and accelerated deactivation of catalytic air pollution control systems [10, 11]. In contrast to fly ash derived from coal, combustion of straw yields an ash which can not be freely utilized in cement production [12]. The potassium-rich ash may be used as fertilizer, but this option would require the ash to be stored through the winter and transported back to the field for distribution.

The aggregate effect of the above drawbacks translates into high total fuel costs which tends to reduce the attractiveness of using the CO_2 neutral straw as fuel even though it is readily available in the temperate parts of the world [13]. A process which could concentrate the energy, remove ash prior to combustion, and reduce the costs of transport and storage would clearly represent a significant step in making straw a more attractive fuel.

Flash pyrolysis is an irreversible thermo-chemical process in which organic material is rapidly heated in the absence of oxygen, whereby the material is decomposed and can be separated into distinct fractions of tar, char, and gas. Ash is largely retained in the char, whereas the tar is a homogeneous mixture of organics/water commonly referred to as bio-oil. Employing straw as raw material, the distribution between fractions is roughly 50%, 30% and 20%, respectively, on dry mass basis [13]. At 25 % wt. water content bio-oil has a lower heating value of 16 MJ kg^{-1} and a density of 1200 kg m^{-3} [14] resulting in an energy density nine times the value for raw straw. Bio-oil viscosity is comparable to that of medium or heavy fuel oil, and burners for these traditional industrial fuels can be utilized for bio-oil with few modifications [15]. Gas or char may, depending on process conditions and yields, be combusted to provide the required process heat. Obstacles with utilizing bio-oil seem to be limited to polymerization resulting in increased viscosity and layer separation following prolonged storage [16].

Interest in flash pyrolysis increased in the 1980's, and the development has presently reached a level where several large scale pilot facilities are operational [17]. These plants mainly focus on exploiting materials derived from wood, but straw and other agricultural residues such as bagasse have also been demonstrated to be suitable for the process [18]. Commercial operation has so far been visualized as pyrolysis plants employing local raw materials sourced within 25 km [19, 20], but this scheme will inevitable be burdened by many of the drawbacks experienced by conventional straw combusting power stations. These include the need to compress, transport, and store high-volume straw, and the result is that the process has the potential to eliminate the negative effects associated with the ash content, but the cost of straw-derived energy may increase further and make straw still less attractive compared to fossil fuels.

An alternative to exploiting flash pyrolysis in stationary plants is to process straw *in situ*, that is, to organize the operation on a tractor-propelled vehicle in the same fashion as a baler and convert straw to bio-oil in the field, see Figure 2. The benefits of the pyrolyzer will include that handling of straw is eliminated, char can be distributed on the field for direct recycle of nutrients, and the volumetric transport and storage space requirements are reduced substantially compared to straw. Addition of pyrolytic char to agricultural soils has been found to increase soil fertility and biomass

yield substantially [21-23] whereby long-term damage resulting from removal of organic material from the field [24] is avoided [25]. Although char left on the field decreases the potential yield of energy, the CO_2 defying potential only suffers marginally since the char represents a carbon sink created by the growing plants. In the soil, char has been found to be stable for periods on the order of 10^2 to 10^3 years [26] thus securing a viable tool for managing atmospheric CO_2 concentration.

Figure 2: Schematic presentation of the pyrolyzer in operation on the field. Straw is processed by flash pyrolysis in the pyrolyzer pulled by the tractor to obtain gas, tar (bio-oil), and char. The gas is combusted internally to provide process heat, whereas char is distributed on the field. Bio-oil is collected on board and transferred to a transport vessel on the field when full [3, 4].

The Ph.D. project reported in this dissertation has been dedicated to advancing *in situ* flash pyrolysis of straw. The main results are summarized in the following chapters, where the material is presented in chronological order, to help the reader gain an overview of the subject. However, readers who are interested in specific sub-areas are encouraged to consult the appendixes that contain detailed results and discussions of the individual investigations. References to the appendixes are included in the text in order to assist the reader locate the material which has his specific interest.

Chapter 2: Objectives and Approach

The overall objectives for this Innovation Ph.D. project were to support the development of a reactor for *in situ* flash pyrolysis of straw and to compile a business plan for the commercialization of the results. These objectives were further specified to include the goals listed below.

2.1 Scientific Goals

Due to the predominate focus on wood as feedstock in earlier studies, it was desired to increase the understanding of straw flash pyrolysis especially in relation to ablative reactors. It was planed to study the primary variables of interest which were perceived to be reactor conversion rate and yields of the principal fractions as influenced by process parameters such as reactor and gas phase temperatures, gas phase residence time, and straw particle size. The ultimate goal was to obtain a model, design equations, or procedures capable of predicting the performance of straw in the developed reactor.

2.2 Engineering Goals

The main engineering goal was to identify a reactor for *in situ* flash pyrolysis of straw by investigating the special requirements for this mode of operation. This task should ultimately result in the construction of a bench-scale unit for installation in the laboratory. The lab unit should be suitable for collecting the experimental data needed to complete the scientific goals.

It was furthermore desired to prepare the lab reactor in order to operate continuously for longer periods of time in order to approach pilot-plant scale. The ultimate goal was to obtain a small operational pilot plant in order to demonstrate the process under conditions approaching those the full scale pyrolyzer will be subjected to.

The engineering goals related to the product included characterizing and comparing bio-oil samples produced in the pilot plant runs to samples from other flash pyrolysis facilities by analyzing basic physical and chemical properties. Furthermore, it was planed that combustion trials should confirm the suitability of straw bio-oil as a liquid fuel replacement.

2.3 Commercial Goals

The commercial goals were to analyze the potential of the intellectual property rights obtained through the research and to explore possible schemes to realize this potential following the completion of the project. Since the project was organized as an Innovation Ph.D. project, the commercial findings were required to be compiled in a business plan.

Chapter 3: Results and Discussion

The main scientific, engineering, and commercial results are summarized below. For a detailed account the reader is directed to the appendixes at the back of the dissertation. In Appendix A the requirements for an *in situ* reactor are identified and recommendations for basic reactor design given. Design and specifications for the constructed bench-scale reactor system are presented in Appendix B. Appendix C contains the preliminary experimental results obtained with the reactor system [27]. The experimental results obtained with the reactor system after optimization and the model which was used to describe the results are presented in Appendix D [28]. Appendix E contains a procedure for predicting the elementary composition of fuels by use of a bomb calorimeter [29]. Appendix F reports the results of pilot runs on the experimental set-up and the combustion trials, and discusses the fuel properties of the produced bio-oil samples. Patent applications for *in situ* pyrolysis of biomass [30] and the developed reactor system [31] are presented in Appendixes G and H, respectively. Finally, Appendix I contains the business plan in form of the thesis from the Graduate Diploma in Business Administration Program at Copenhagen Business School.

3.1 Scientific and Engineering Results

3.1.1 Pyrolysis Centrifuge Reactor

Several reactor designs have been found suitable for flash pyrolysis of biomass, but the review presented in Appendix A of these reactors and the requirements of the *in situ* process (Table 1) revealed that none were well suited. The restricted size of the vehicle implies that the reactor should have a high volumetric and weight-specific capacity in order to obtain the desired capacity. In addition, it should utilize gas rather than char for heating due to the inability to store the former on board. Furthermore, in order to reduce mechanical power consumption, the reactor should be able to operate with relatively large particles and should be arranged horizontally in order to take advantage of the shape of the vehicle. It was concluded that a reactor of ablative design operating without gas recirculation was the best choice.

The Pyrolysis Centrifuge Reactor (PCR) was developed in an attempt to accommodate these findings. The concept of the PCR is described in detail in Appendix H and one manifestation is depicted in Figure 3. It consists of a horizontal, heated pipe into which particles are introduced tangentially and slide across the inner surface. The motion of the particles is caused by a swirling gas flow established by a rotor placed within the pipe. Due to the centrifugal acceleration acting on the particles firm, contact with the wall is established whereby heat transfer is maximized. Char particles are separated from the pyrolysis vapors continuously by a tangential outlet at the end of the reactor pipe. Vapors continue into the direct bio-oil condenser through ports in the rotor flange. The condenser is placed within the rotor and is supplied with

a flow of cool bio-oil through the axel at the char-discharge end. The cool bio-oil is discharged to the condenser packing through the entire condenser length by a perforated lance. Since the condenser rotates and is conical, the bio-oil flows towards the feed end. Here, a stationary scraper ensures that the liquid is removed from the condenser wall and discharged along with uncondensed gas through the hollow feed-end axel. Heating of the PCR is accomplished by a pyrolysis gas fired burner arranged around the reactor pipe.

Table 1: Requirements and constraints for an *in situ* pyrolyzer.

Specification	**Value**
Weight/volume specific capacity	As **high** as possible
Acceptable particle feed size	As **high** as possible
Bio-oil yield	As **high** as possible
Maximum weight	As **low** as possible
Heat-up time	As **low** as possible
Source of thermal energy	Pyrolysis gas
Time between service	> 250 h
Capacity	> 10 t h^{-1}
Mechanical power demand	< 112 kW
Length	< 12 m
Width	< 3.3 m
Height	< 4.0 m

Table 2: Reported flash pyrolysis yields of main fractions in weight percent of feed on moisture free basis under specified process conditions for full-scale, pilot, and bench reactors. Results have been normalized, if needed, to obtain full mass balance closure. To obtain bio-oil yield, add yields of organics and water. FB (fluid bed); AV (Ablative vortex); AP (ablative plate); Mill (ablative pyrolysis mill); VRT (vapor residence time); MSW (municipal solid waste); PS (particle size); * water of reaction estimated (not reported in source) [13].

Reactor Type	*Org. % db.*	*Gas % db.*	*Char % db.*	*Water % db.*	*Temp. °C*	*VRT ms*	*Feedstock*	*PS µm*	
FB (ash)	40	30	20	10	500	n.a.	MSW	<1200	[32]
FB	**52**	**25**	**19**	**4**	**575**	**520**	**Wheat straw**	**<595**	**[33]**
FB	69	5	14	12	500	600	Poplar	<595	[34]
Mill	34	37	17	12*	550	90,000	Pine	595-841	[35]
FB	45	15	29	11*	473	8,100	Fir	300-425	[36]
AP	59	5	26	10	600	1,710	Pine	<6250	[37]
Cone	36	40	12	12*	600	490	Pine	200	[38]
FB	**51**	**16**	**18**	**15**	**515**	**500**	**Wheat chaff**	**<1000**	**[18]**
FB	66	11	12	11	504	500	Poplar	<1000	[18]
FB	**45**	**18**	**29**	**8**	**550**	**500**	**Wheat straw**	**<250**	**[18]**
FB	**41**	**21**	**30**	**8***	**450**	**3,000**	**Wheat straw**	**<1000**	**[18]**
FB	65	10	13	12*	430	n.a.	Hardwood	<1000	[38]
AV	56	13	18	13	625	300	Pine	<3200	[39]

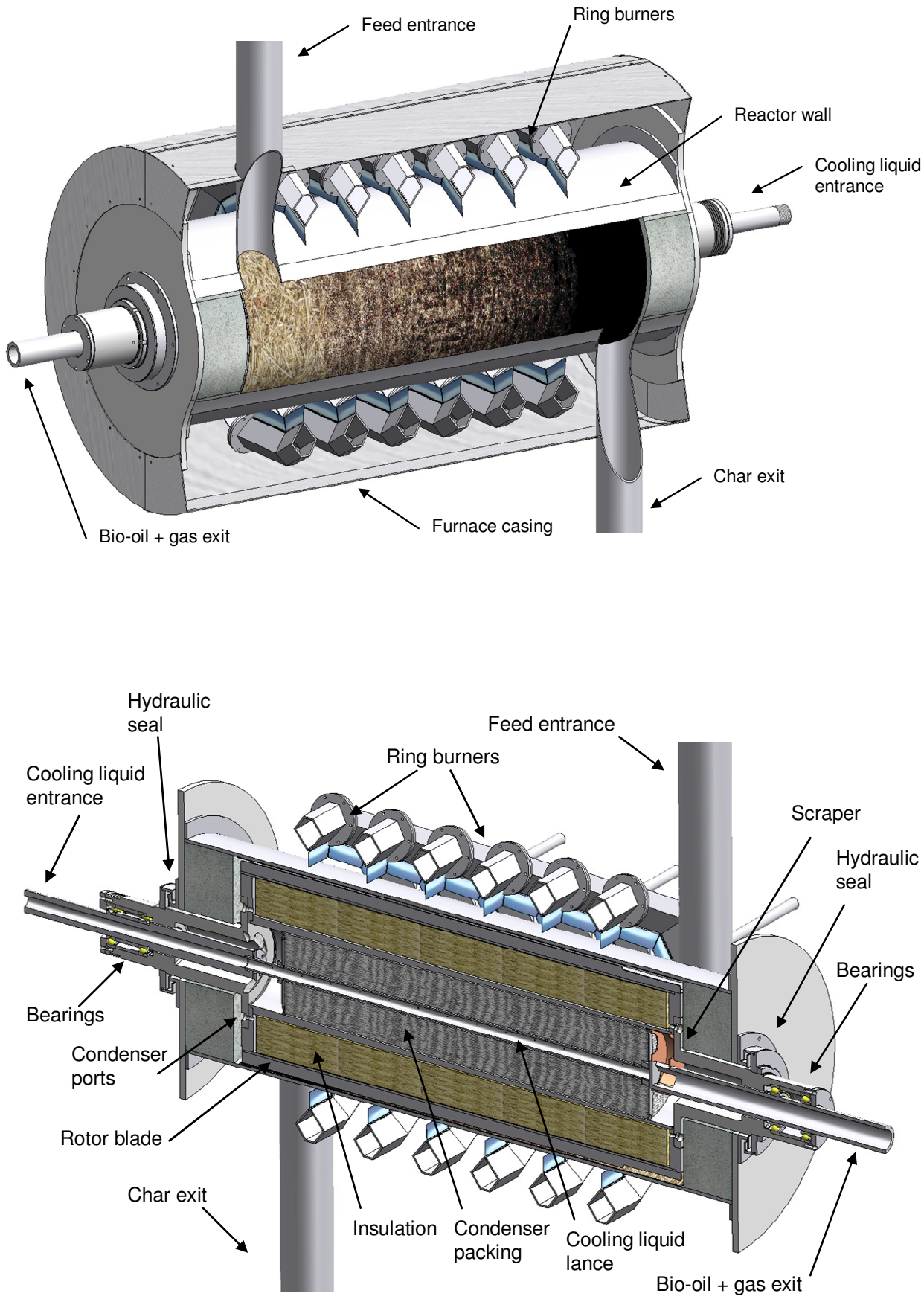

Figure 3: Pyrolysis Centrifuge reactor.

Placing the bio-oil condenser within the hot reactor and utilizing the created centrifugal acceleration for particle separation serve several purposes:

1. Utilize available space. Since the heat transfer takes place on the surface of the reactor pipe, scaling is accomplished by increasing pipe radius and/or length. For a given reactor length the available heat transfer area will be proportional to the pipe radius squared, whereas the volume within the rotor is proportional to the pipe radius cubed. Accordingly, when the reactor is scaled free space within the rotor is created that would otherwise be lost. Furthermore, since reactor, condenser, and particle separation is integrated in one unit, no bulky vapor piping is needed.

2. Reduce gas residence time. Liquid organics yield is reduced when organic vapors are cracked to gas (see Appendix A). Eliminating piping reduces the time at which vapors are kept at reactor temperature and therefore increases liquid organics yield.

3. Avoid premature condensation. Organic vapors start to condense on surfaces maintained below approximately 400 °C and cause piping to plug (see Appendix F). With no external hot piping this will not be an issue.

4. Minimize heat-up time. To avoid condensation piping needs to be heated to above 400 °C before vapors are admitted. Since external piping is eliminated, heat-up time is reduced.

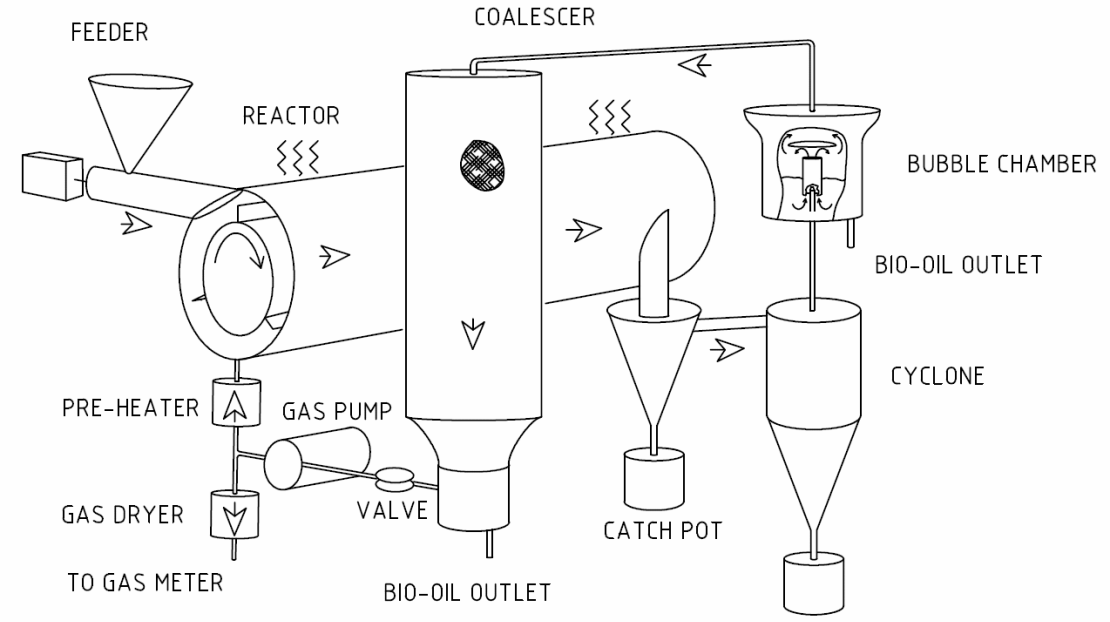

Figure 4: Simplified flow chart for the final version of the bench-scale reactor system.

A bench-scale version of the PCR was developed in order to study the performance and collect data from experiments where straw was employed as feedstock. From a review of the published flash pyrolysis results (see Table 2), it could be established that in order to maximize the yield of liquid organics, the reactor temperature would likely fall in the range 450 to 600 °C, while gas residence times as low as 500 ms were foreseen. The yield of liquid organics was expected to increase with rotor speed,

or equivalently centrifugal acceleration (*e.g.* expressed in units of gravity g), so this parameter was specified to be as high as possible but considering what could be achieved with conventional machine elements (*i.e.* bearings and axel seals).

Table 3: Specifications and main dimensions for the experimental set-up.

Reactor Specifications	**Value**	**Unit**
Overall pipe length	200	mm
Pipe length, entrance to exit (c-c)	137	mm
Pipe inner diameter, avg.	81.4	mm
Pipe particle-swept area	$3.50 \cdot 10^{-2}$	m^2
Rotor diameter	60.3	mm
Wall-to-rotor-wing clearance, min	2.2	mm
Motor, rated power max	0.37	kW
Rotor speed, max	$2.0 \cdot 10^4$	rpm
Centrifugal force at wall, max	$1.8 \cdot 10^4$	g
Reactor Heating	Horst heating cable HSQ, 4 zones	
Zone-split over full pipe length	3:1:3:4	(length)
Cable temperature, max	900	ºC
Heating power, all zones	1870	W
Tracing Temperature, max	450	ºC
Gas preheater temperature, max	540	ºC
Gas preheater power	750	W
Temperature Sensors	K-type thermocouple	
Accuracy @ 500 ºC	±2.0	ºC
Gas Pump	Rietschle Thomas VTE8 (rotary vane)	
Reactor gas volume	0.44	L
System total hot gas volume	0.50	L
Feeder	AccuRate MOD304M with centerless helix	
Feed rate (straw particles), max	2.4	$kg\ h^{-1}$
Gas Meter	IGA AC5M, positive displacement, temp. comp.	
Gas flow, max	5	$Nm^3\ h^{-1}$
Accuracy	±0.5	% vol.

Figure 4 shows a sketch of the bench-scale version of the PCR which was constructed and installed in the lab. Feed particles are dosed by the screw feeder to the tangential reactor entrance. Within the horizontally oriented reactor pipe, a three-winged rotor creates a swirling gas flow within which the particles are suspended. Due to the rotation they slide across and are forced against the reactor wall which is heated by four electrical heating elements separately controlled by thermocouples machined into the outer surface. While undergoing reaction the particles move down the reactor pipe before leaving suspended in the gas through the tangential outlet. Larger char particles are removed by a change-in-flow separator, while fines are collected by the following cyclone. Vapors are condensed in a direct condenser filled with previously produced bio-oil and cooled by a helix through which tap water flows. In order to collect the aerosols not retained by the condenser, the gas flows to a coalescer filled with fibrous

ROCKWOOL® insulation material, where droplets of bio-oil are formed and flow by gravity to a flask mounted below. The clean incondensable gas is pumped to a pre-heater before it reenters behind the rotor at the reactor inlet. Excess gas flows through a tap water cooled glass condenser before it is measured by a temperature compensated gas meter and collected. The reactor is maintained at atmospheric pressure and is controlled by setting wall temperature, rotor speed, and the gas recirculation rate by adjusting a valve in front of the gas pump. Following a run, gas residence time can be calculated based on the performance curve of the positive displacement gas pump and the yield data. Specifications and dimensions for the system are displayed in Table 3, and Appendix B contains detailed specifications and construction drawings of the lab system.

Contrary to the full-scale PCR, the experimental unit does not feature heating by combustion of the generated pyrolysis gas, internal char separation, or an integrated condenser. It was selected not to include these features due to the desire for increased temperature control, the small size of the system, and the complexity they would add. It does, however, feature the possibility for recirculation of gas in order to control gas residence time independently of feed rate and the other reactor parameters.

3.1.2 Preliminary Experimental Results

The preliminary experimental runs were conducted with the intention to collect yield data for model development and are described in detail in Appendix C. During this series of runs, the reactor system was slightly differently configured compared to the final layout described above as the change-in-flow char separator and the connected flask for particle collection were integrated in one unit. Furthermore, reactor heating had not yet been split in zones, but the entire reactor surface was heated by a single heating element controlled by a centrally mounted thermocouple. As illustrated in Figure 5, the latter feature resulted in an uneven temperature profile, and the temperature at the inlet was between 159 and 109 °C below the set-point for the temperature range 450 to 600 °C. Unfortunately, this was not discovered until later but contributed to the unexpected results as discussed below.

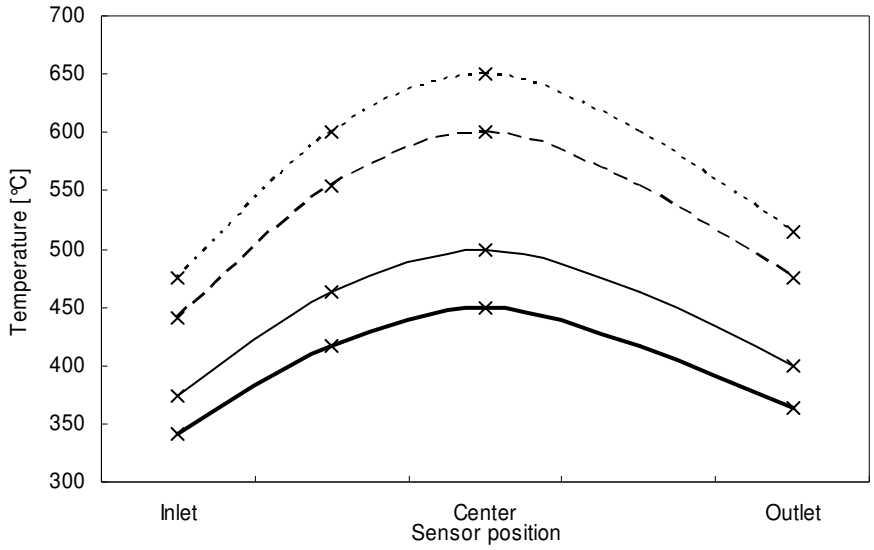

Figure 5: Temperature profiles on empty reactor pipe with position and set point (equal to center value). Results shown for set points equal to 450, 500, 600, and 650 °C.

Determining the yield of liquid organics required that the water content of the bio-oil was determined for the condenser fluid before and after a run and for the fraction of bio-oil collected from the coalescer. This is traditionally accomplished by Karl Fisher titration [14], but it was found, and reported in Appendix C, that the results obtained with this method and the measured refractive index correlated well as seen in Figure 6. Thus, water determination by refractive index measurement was used throughout the project which reduced the experimental workload considerably. Furthermore, for future full scale operation of a pyrolyzer, the found correlation will allow inline real-time determination of bio-oil water content.

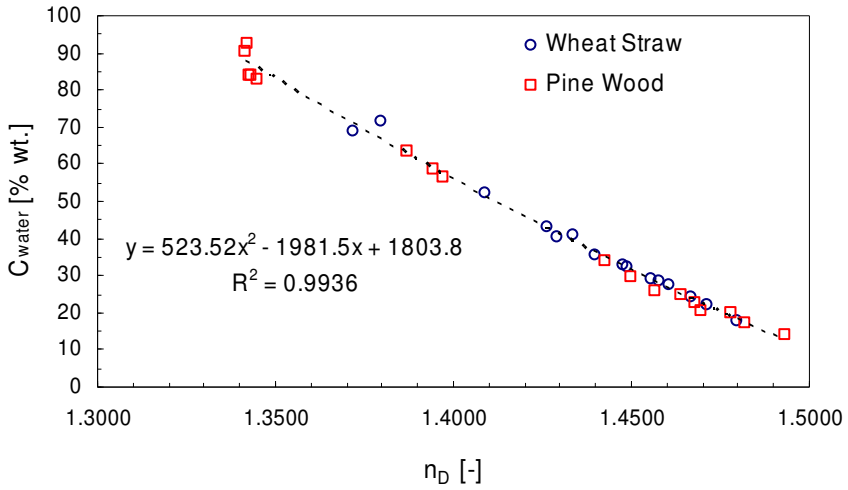

Figure 6: Water content determined by Karl Fischer titration with refractive index at 30.0 °C for wheat straw and pine wood bio-oil mixtures.

Experimental runs were performed with both wheat straw and pine wood at various combinations of nominal centrifugal acceleration ($4.9 \cdot 10^3$ – $1.7 \cdot 10^4$ g) and reactor wall temperature (480 – 620 °C), while gas residence time was fixed at 2.0±0.5 and 2.2±0.6 s for wheat and pine, respectively. The feed material was prepared by crushing pellets of wheat straw and pine wood followed by sieving to obtain particles below 1.4 mm. Mean mass diameter (MMD), as determined by sieve analysis, was 630 µm for both feeds.

For the yield of liquid, char, and gas (Figure 7), as well as the average molecular weight of the latter and the water content of the former, only slight trends were observed. This was unexpected as the yields normally change markedly within this temperature range (see *e.g.* Appendix A). Maximum yield of liquid organics was 35 % daf. for wheat straw obtained at $1.0 \cdot 10^4$ g and 524 °C. Compared to the highest reported liquid yield for ablative reactors operated with pine wood, the maximum 46 % daf. yield for pine wood at $4.9 \cdot 10^3$ g and 585 °C was 28 % (relative) below.

The particle flow behavior was investigated by measuring the hold-up time in cold runs. Due to the linear relationship found between inverse feed rate and residence time and the insensitive response to gas flow rate and rotor speed, it was concluded that the particles traveled through the reactor in plug flow. This is also reported in Appendix C.

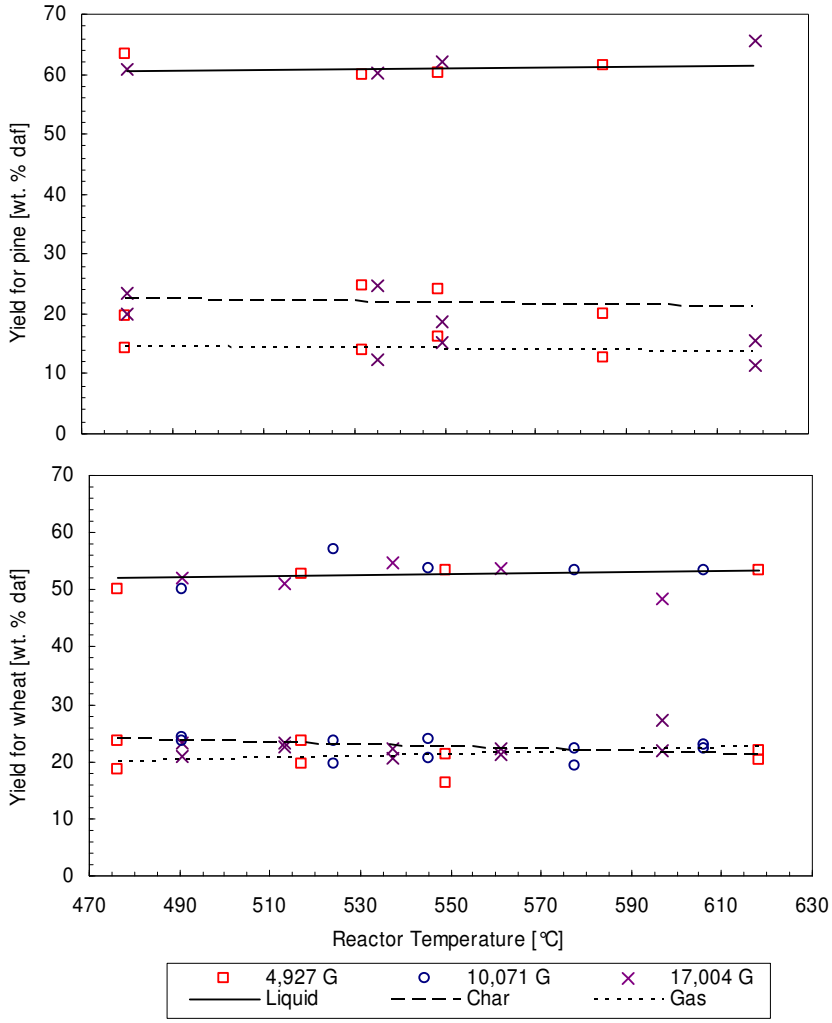

Figure 7: Yield of liquid, char, and gas for pine wood (top) and wheat straw with reactor wall temperature and centrifugal force.

Based on an analysis of earlier reported mechanisms acting to reduce liquid organics yield and a mass balance, it was in Appendix C concluded that the low liquid organics yields were caused by the non-uniform temperature profile on the reactor pipe. The identified mechanism was that particles undergoing pyrolysis did so partially through a competitive low temperature reaction (*i.e.* slow pyrolysis by R3 in Figure 13) which favors formation of char, water, and gas. In addition, heterogeneous tar cracking at the cold zones or in the combined char separator and catch pot was suspected as a possible source of especially gas. Cracking of tar within particles was ruled out as a significant mechanism due to the low specific surface area (1.2 – 1.5 m^2 g^{-1}) of the char product as measured by BET adsorption.

3.1.3 Reactor Optimization

The disappointing yield of liquid organics obtained in the preliminary runs in conjunction with the suspected causes prompted the particle flow to be investigated in more detail. Since only the extremes of the reactor pipe had been maintained at a temperature below the set-point during the initial runs, the extent of the identified slow pyrolysis conditions seemed excessive unless the solid material flow deviated from the desired mono layer plug flow. This idealized flow pattern is characterized by

that all particles rest on and travel at constant speed across the reactor surface, whereby vapors can leave the reacting particle layer without encountering cold particles on which condensation can occur or char surfaces that promote cracking of liquid organics.

A copy of the reactor pipe was fabricated in glass, whereby full view of the particle flow was possible under cold runs. These runs showed that the observed hold-up time was not caused by particles progressively filling the surface of the reactor but rather that the material was retained at the reactor entrance. Here, it formed a relatively thick layer limited in size by six mm cutouts in the rotor blades. These cutouts were designed to create an entrance zone where particles could be gently accelerated to full speed without hitting the blades. However, as shown in Figure 8, the cutouts combined with the shape of the tangential inlet caused the feed material to be retained at the entrance, and when a sufficient amount of material had collected, a pulse rapidly moved down the reactor. Since the amount of material trapped at the inlet corresponded to the capacity of the reactor surface, if it had been filled with a mono layer of particles, this behavior had wrongly been interpreted as proof for that the flow was as desired. Accordingly, the particle flow pattern could more appropriately be compared to a stirred tank reactor where the main part of the residence time was spent in a relatively thick layer at the cold reactor inlet, while most of the reactor surface was not utilized for heat transfer.

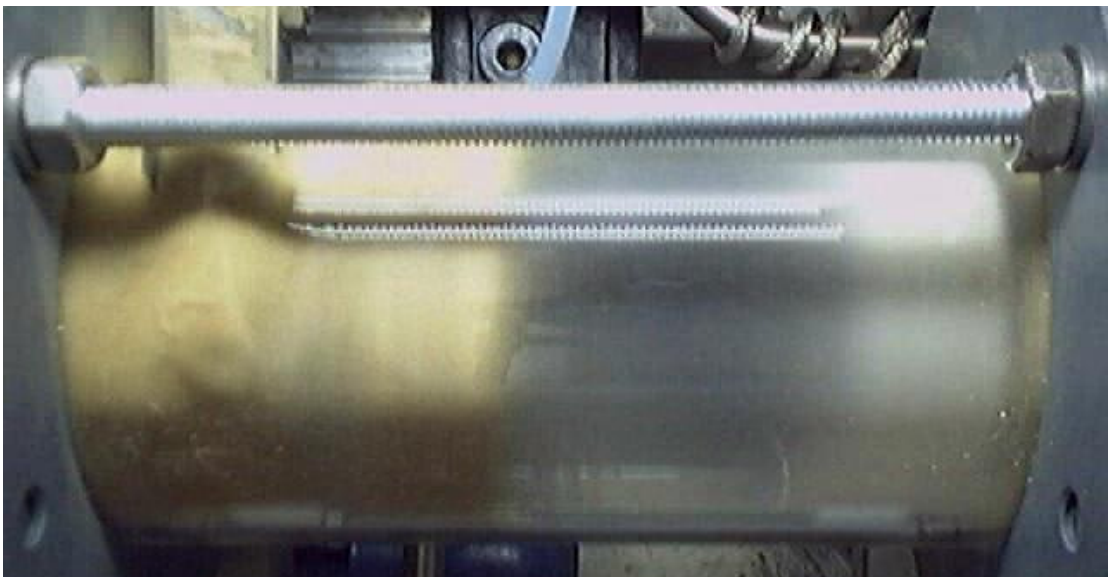

Figure 8: Reactor fitted with glass pipe during a cold run before it was modified. Notice the thick layer of material retained at and to the left of the entrance and the separating ring-shaped pulse that is moving towards the exit situated at the lower right hand corner (not visible).

The observed particle flow behavior supported the findings of the preliminary experimental runs. When the feed material was retained at the entrance, and only shortly utilized the remainder of the reactor surface, the heat transfer at this position was dominating. Since the temperature controller was connected to a thermocouple mounted at the center of the pipe, where heat transfer was insignificant, the temperature distribution was further skewed compared to the profiles shown in Figure 5. Accordingly, the material was pyrolyzed at temperatures which as a minimum were 100 °C lower than the temperature set point whereby slow pyrolysis was promoted. Furthermore, condensation in the piping had earlier been observed if the tracing

temperature was not maintained above 400 °C, and since vapors were released within the cold layer, condensation on solid particles could be expected. Condensation followed by re-pyrolysis lead to a reduction of the liquid organic yield and an increase in the yield of char, gas, and water. Although the char surface does not participate actively, this process is analogous to the mechanism for heterogeneous char induced tar cracking through adsorption proposed in Appendix C.

Further experimentation with the glass reactor revealed that a flow approaching the desired mono layer plug-flow could be established by eliminating the dead volume formed by the rotor cutouts and by attaching several rings to the inside wall. As a further precaution, a twisted strip was attached to the wall at the entrance in order to sweep the feed material away and preventing it from being trapped. The rings were found to slow down particle speed across the surface whereby surface coverage and particle residence time were increased. The effectiveness of these modifications was ascertained in the glass reactor by photographing the flow of altering portions of straw particles undyed and dyed at feed rates and centrifugal accelerations comparable to those used in the experimental runs (~24 g min^{-1}; $4.9 \cdot 10^3$, $1.0 \cdot 10^4$, $1.7 \cdot 10^4$ g) and in the later pilot runs (~40 g min^{-1}; $1.0 \cdot 10^4$ g). In the series of pictures, the dividing line between the differently colored feeds could be identified as it moved through the reactor. By converting the pictures to monochrome and analyzing the pixel count, it was computed that at $1.0 \cdot 10^3$ g centrifugal acceleration 41 % and 53 % of the reactor surface was covered by particles at the feed rates mentioned above, respectively. Accordingly, it was concluded that the desired plug flow was established but the reactor surface was still not fully utilized at the employed feed rates. These modifications were implemented in the steel reactor as shown in Figure 9 (top left and right) and described in Appendix B in detail.

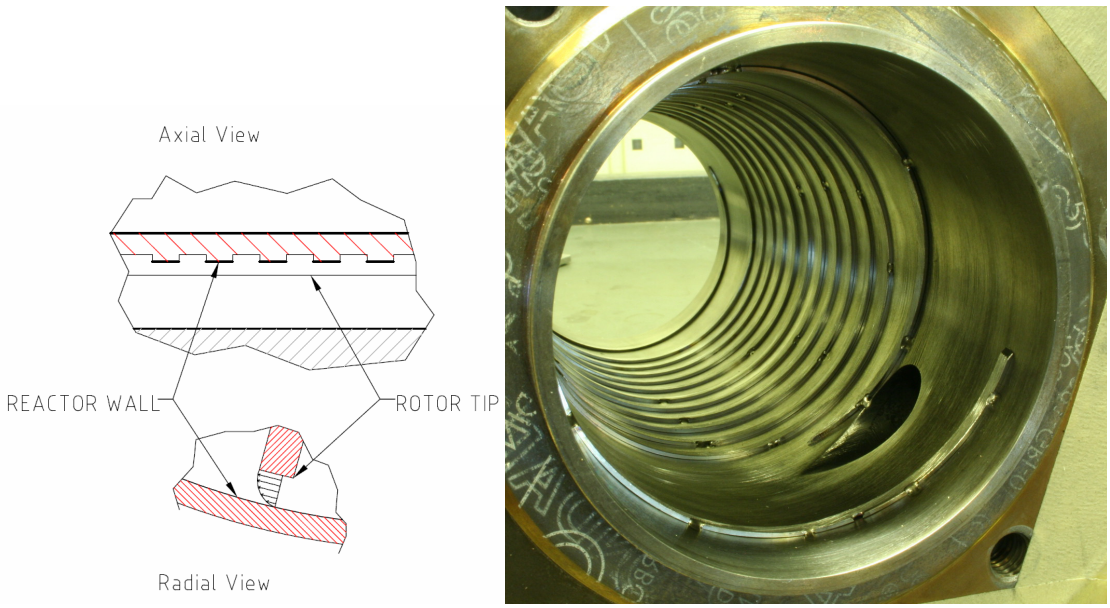

Figure 9: Reactor details: One mm thick by four mm wide flow guide rings on the reactor wall (top left) and assumed gas velocity profile in the gap between rotor tip and reactor wall (bottom left). To the right, a view in to the modified reactor pipe with the entrance port in the foreground, the helix strips at both ends, and the rings welded to the wall.

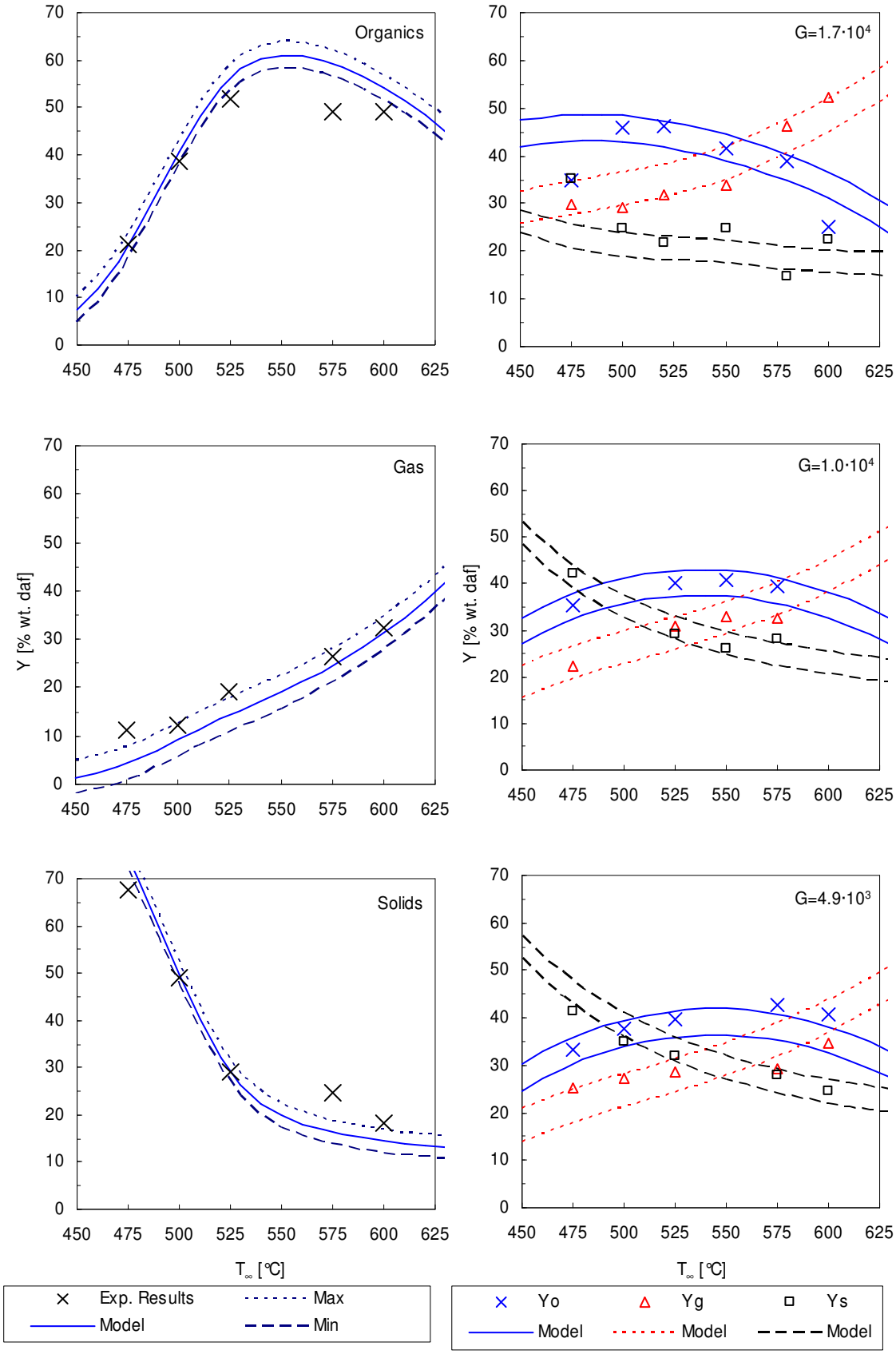

Figure 10: Yield of liquid organics (o), gas (g), and solids (s) and model predictions (lines) with temperature for pine wood at $1.7 \cdot 10^3$ g (left) and wheat straw at three centrifugal accelerations (right).

The heating system was split into four zones with independent temperature control in order to assure that the entire pipe surface was supplied with the heat necessary to maintain the set point. Finally, the char separator and catch pot were separated in order to limit contact between char and vapor whereby char-induced heterogeneous tar cracking could be further suppressed.

3.1.4 Final Experimental Results and Modeling

After the system had been modified, a new series of experimental runs were performed in order to collect data for modeling. In addition to wheat straw, runs with pine wood were again included in order to use the results as a reference in the modeling work. The conditions employed were similar to those used in the preliminary runs, but the vapor residence time was reduced to 0.6±0.3s and 0.7±0.2s for wheat and pine, respectively. A full description and discussion of results can be found in Appendix D.

As seen from Figure 10, the yields of the principal fractions now varied markedly with reactor conditions. The liquid organics yield of pine wood increased steeply with temperature from the lowest investigated temperature of 475 °C but stabilized or declined slightly from 525 °C and up to 600 °C. The opposite behavior was observed for the collected solids (*i.e.* unreacted wood and char). The gas yield increased steadily over the investigated temperature domain. For pine wood, all the experiments were conducted at a nominal centrifugal acceleration of $1.0 \cdot 10^3$ g, and the highest yield of liquid organics was 52 % daf. (51 % db.) obtained at 525 °C.

The influence of temperature on the yields of the principal fraction for wheat straw followed the same pattern as pine wood. However, yields of char and gas were generally higher and the increase in liquid organics yield not as rapid with temperature. The temperature at which the maximum yield of liquid organics was obtained decreased with centrifugal acceleration whereas the yield increased from 43 % daf. (40 % db.) at 575 °C and $4.9 \cdot 10^3$ g to 46 % daf. (43 % db.) at 520 °C and $1.7 \cdot 10^4$ g.

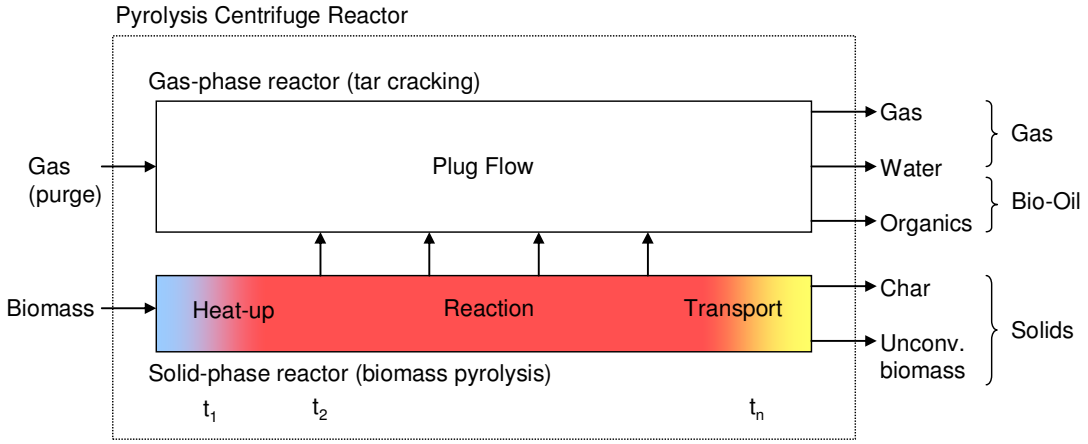

Figure 11: Model outline and convention for reactor streams.

As detailed in Appendix D and references [40-42], a model was developed to describe the yield of the principal fractions with reaction parameters. Figure 11 outlines the overall approach taken to model the reactions in the PCR. Conceptually, solid-phase

primary pyrolysis and secondary tar cracking in gas phase were treated in separate reactors although numerically solved simultaneously. Particles are introduced in the solid reactor where they travel in plug flow undergoing heat up, reaction, and transport of char. For some particles, conversion is not completed before they are discharged from the reactor, whereby the collected solids are a mixture of char and unconverted biomass. Following solid pyrolysis reaction, the formed pyrolysis gas and vapors are injected into the plug flow gas-phase reactor where the vapors undergo cracking to gas. The numerical method resulted in a number of discrete time steps which were automatically sized to avoid numerical inaccuracies.

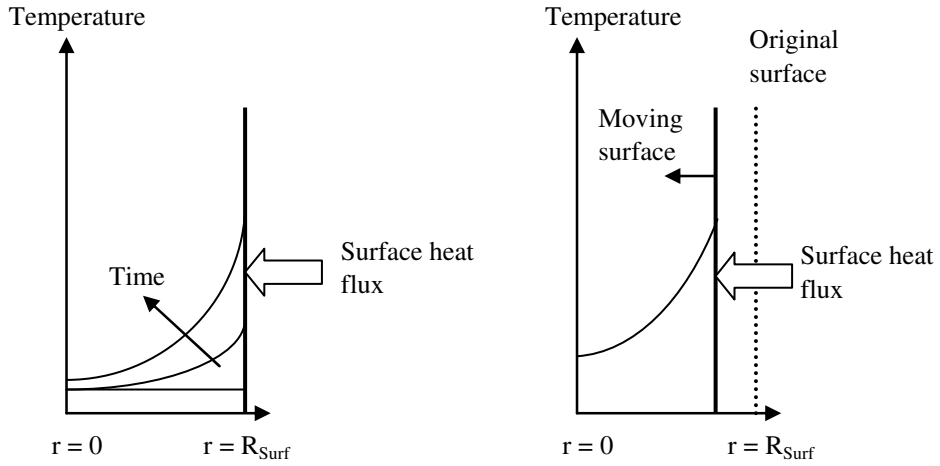

Figure 12: Schematic illustration of solid material undergoing surface decomposition at time t (left) and t +Δt.

Conversion of the biomass particles was treated as a pseudo-surface reaction. As discussed in Appendix D, for ablative pyrolysis, the steep temperature gradient earlier observed experimentally combined with a reaction rate which is strongly dependent on temperature suggested that reaction is concentrated in a relatively thin shell at the surface. The reaction scheme was coined *pseudo* in order to stress that particle density was considered constant, whereby any reaction within the particle also resulted in movement of the surface towards the centre rather than formation of a porous system. Figure 12 illustrates the surface decomposition of a solid material under high heat flux conditions. Drying of the particles was not considered in the model and the enthalpy of reaction assumed to be insignificant compared to the sensible heat.

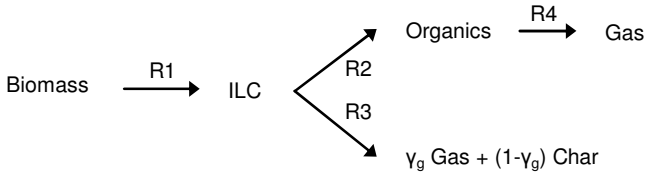

Figure 13: The Broido-Shafizadeh model for biomass pyrolysis.

The modified Broido-Shafizadeh kinetic scheme was applied in the modeling, see Figure 13. The shrinking particle is converted to an Intermediate Liquid Compound (ILC) which in turn is further degraded to the final pyrolysis products tar, gas, and

char. Only the formation of ILC was assumed to determine the degradation rate of the particle, whereas the split between products was determined by the surface temperature of the particle. Heat transfer to the particle was assumed to originate from wall-particle contact only. In addition, slabs and cylinders were assumed to be indefinite and during conversion particles of slab geometry only submitted to wall contact on one side, whereas cylinders and spheres were evenly exposed to the hot surface due to rotation. Further, it was established that the gas flow was turbulent and it was assumed that the velocity profile between rotor tip and wall (Figure 9, left bottom) could be described by a power law. Particle residence times for the investigated combinations of rotor speed and feed rate were measured directly in cold flow experiments with the modified glass reactor.

Discretization by orthogonal collocation was used to approximate the transient temperature profile inside the particle. Integration of the coupled differential equations was performed using the FORTRAN-based semi-implicit Runge-Kuta integration routine SIRUKE. As the feed materials used in the experiments were not homogeneous with regard to particle size, the code was set up to repeat the calculations for each ASTM screen size between 106 and 1180 μm using the arithmetic mean as twice the characteristic particle dimension. Results for the combined feed were obtained by taking the weighted average yields using the sieve mass fraction as weights. Pine particles were modeled as cylinders and wheat as spheres based on their appearance in a light microscope.

Kinetic parameters were directly available for pine wood (see Appendix D), whereby the model for this material had no free parameters. For wheat straw it is known [43] that the higher ash content has a pronounced catalytic effect on the pyrolytic reactions favoring formation of char and gas by reducing the activation energies of the corresponding reactions. Accordingly, the distribution between char and gas (γ_g) and the pre-exponential factors were left equal to those of pine, and the gas phase cracking of tar was assumed to be unaffected by the ash which to a large degree was found to be retained in the solids for the investigated temperature domain. Thus, the activation energies for R1 and R3 were left as free parameters and visually fitted to the experimental data simultaneously for the three investigated rotor speeds. Reductions of 14 % and 4.5 %, for the two reactions, respectively, were found suitable.

As seen from the correspondence between model predictions and experimental results shown in Figure 10 and Figure 14 (left) the model described the PCR acceptably for both raw materials. Figure 14 (right) shows the predicted influence of particle size on the yield of liquid organics. Optimum liquid organics yield under the investigated conditions at $1.7 \cdot 10^4$ g for straw was predicted for particle sizes close to the mean mass diameter (MMD) of the investigated distribution. It is noted that the optimum temperature for this particle size was lower than what was predicted for the entire distribution. The reason for this behavior is that particles below approximately 0.8·MMD require considerably higher temperatures to minimize the fraction of biomass passing through the reactor unconverted. In contrast, particles several times lager than MMD require a relative long residence time for conversion and the optimum temperature is limited upwards by the rapidly increasing organics cracking above 500 to 550 °C, an effect which is less pronounced for the smaller particles where the decreasing centrifugal acceleration and thus heat transfer tend to favor higher temperatures. It was found that loss of potential organic yield due to char

formation was not responsible for the decrease in liquid yield for particle sizes different from the MMD as the result of the increased optimum reactor temperature was to increase gas but lower char yield. The implications would be that in order to maximize the yield of organics the reactor should be designed to suit the relevant particle size and that fines and over-sizes should be avoided (or removed) in the preceding size-reduction process.

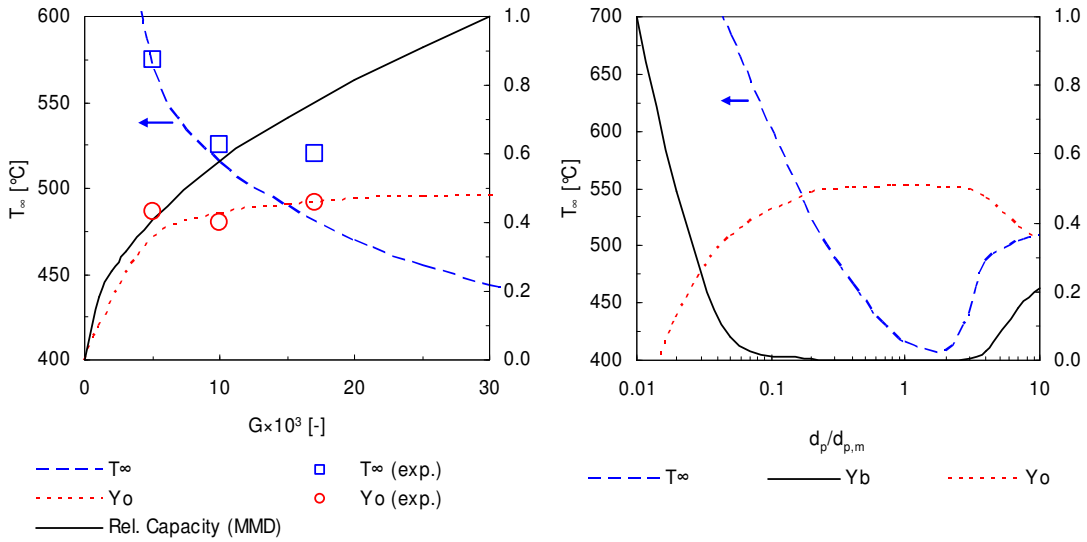

Figure 14: Left: Simulated optimum reactor temperature (broken line) needed to maximize liquid organics yield expressed on daf. basis (dots) as functions of dimensionless centrifugal acceleration compared with experimental results (symbols). Full line shows relative reactor capacity (proportional to inverse conversion time) with dimensionless centrifugal acceleration for straw particles of mean mass diameter (MMD). Right: Simulated reactor temperature for optimum organic yield (broken line) with relative particle size for wheat straw (MMD≡1). Optimum organic yield (dots) and unconverted straw yield for particle size also shown (full line). All conditions equal to those investigated experimentally at $1.7 \cdot 10^4$ g.

The model also revealed a relatively flat spatial temperature profile for a straw particle of MMD throughout conversion under typical conditions (550 °C; $1.7 \cdot 10^3$ g) and that the criterions for ablative pyrolysis, defined by bounds on the Biot number *Bi* and Thermal Thiele modulus *Th*, were not satisfied [44, 45]:

$$Bi \geq 1$$

$$Th >> 1$$

The ablative envelope is characterized by internal control of particle heating and that solid degradation proceeds faster than the inward solid heating rate. Therefore reactor parameters in combination with particle properties determine whether the conditions under which a particle is converted can be defined as ablative. Simulations with particles with diameters five times higher than the MMD employed in the experiments and unchanged reactor parameters showed that the ablative conditions were satisfied here. Under these conditions the surface temperature of the particles is almost constant during conversion, for straw particles 319 °C compared to 405 °C for wood. Although the ablative conditions favor the yield of liquid organics, this is not observed for the investigated reactor parameters since particles sufficiently large to be converted ablatively leave the reactor before they are fully converted (Figure 14 right).

The ability of the model to describe the system despite the invalidated surface reaction assumption was attributed to that cracking of tar within the particle had been found [46] to be negligible under similar conditions and that the violent movement of the particle across the reactor surface would hinder formation of an insulating char layer. Furthermore, despite the computation of the primary distribution between products was based on the surface temperature, this would not have introduced significant error due to the homogenous spatial temperature. Accordingly, it was suggested that the terms *ablative char peeling* (see Figure 15) or *solid convective* should be used in place of *ablative* to more accurately describe the form of flash pyrolysis taking place in the PCR with the employed reactor parameters and particle properties, even though the latter term generally is applied to systems where heat transfer takes place on a metal surface directly.

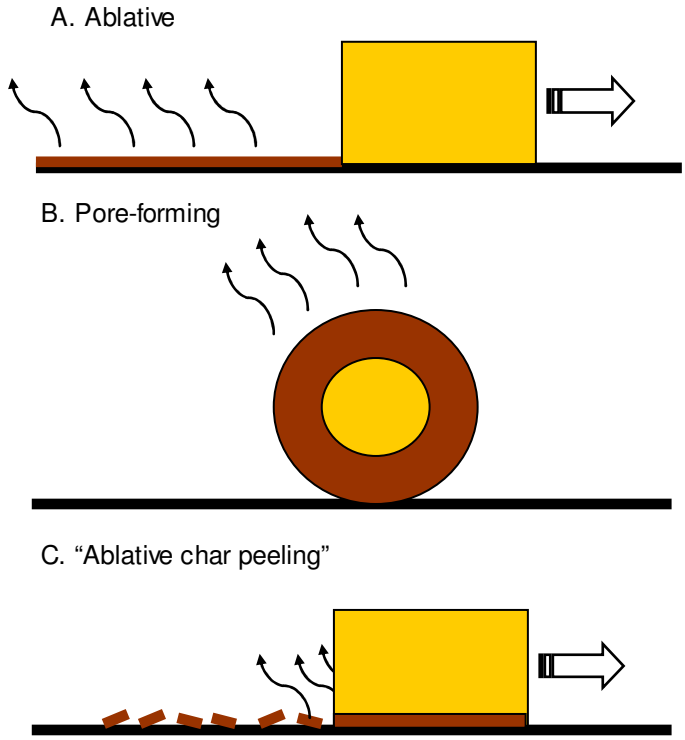

Figure 15: Idealized visual presentation of flash pyrolysis schemes.

3.1.5 Extension of Model Results

The experimental results represent the first reported systematic investigation of straw flash pyrolysis in an ablative (*i.e.* solid convective) reactor defined as a reactor where heat transfer takes place directly between a heated wall and the biomass. Modeling of the yield distribution has shown that the same approach as used for wood feedstock is applicable if the catalytic effect of the ash content is incorporated. It has been demonstrated that this can be accomplished simply by fitting the activation energy of the two solid pyrolysis reactions.

Straw has been shown experimentally to generate lower yields of liquid organics and increased yields of gas and char compared to wood under the same reaction conditions. These differences are the result of the changed kinetics caused by the catalytic ash content. Straw has been shown by modeling to be depolymerized at a temperature on the order of 80 °C lower than that of wood which in combination with

the catalyzed slow pyrolysis reaction increase the char and gas yields. However, the lower temperature of reaction also results in a higher heat transfer to the reacting particle and that less energy is required to bring the particle to the reaction temperature whereby the particle is converted faster. This in turn results in a higher conversion for a given solid residence time and shifts the temperature of maximum liquid organics yield down compared to wood. These effects are not evident from the experimental results due to differences in particle morphology, size distribution, and physical properties between straw and wood feeds but are demonstrated in Figure 16 where the reactor parameters and feed material properties from the straw runs at 10^4 g are simulated with straw and wood kinetics.

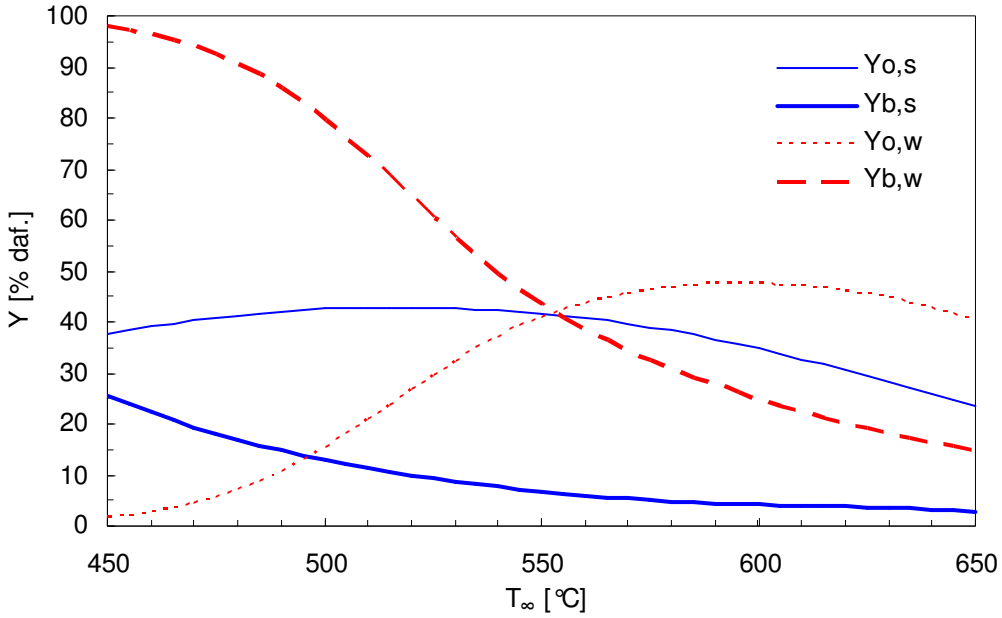

Figure 16: Simulated yield of liquid organics (Yo) and unconverted biomass (Yb) with reactor temperature. All conditions identical to straw experimental runs at 10^4 g except kinetics: Straw kinetics (s) and wood kinetics (w).

The experimental runs have demonstrated that liquid organics yields for wheat straw similar to the results reported in Table 2 are possible with the PCR. For the reactor parameters investigated in the experimental unit, modeling has shown that yields exceeding 50 % daf. are possible if centrifugal acceleration is increased to above $3 \cdot 10^4$ g or the particle size distribution is monodisperse within 0.3·MMD to 3·MMD. However, due to the stable and higher surface (*i.e.* reaction) temperature which is predicted for larger particles where pyrolysis takes place in the ablative regime, the yield is expected to increase somewhat if larger particles are employed in a reactor designed to provide sufficient residence time. The predicted influence of particle size has not been confirmed experimentally but indicates that the PCR is well suited for flash pyrolysis of straw without having to finely mill the feed. The challenge is rather to prepare a flowable material without creating fines.

For the investigated straw particles and reactor parameters, the experimental results and the model have established that the yield of liquid organics does not increase significantly above a centrifugal acceleration of 10^4 g. The highest yield at this level is predicted to be 43 % daf. at a reactor temperature of 515 °C. However, it should be

considered that maximization of liquid organic yield is not a sufficient criterion if the reactor relies on pyrolysis gas for heating. The yield of combustible gas is not directly available from the model, because the water of reaction is included in the predicted gas yield, but based on a run performed at 10^4 g and 525 °C the yield will be on the order of 15 % daf. The higher heating value of the pyrolysis gas was in Appendix D determined to be 11.2 MJ kg^{-1} and the heat capacity of straw is 2.4 kJ kg^{-1} K^{-1} [47]. Accordingly, the ratio between needed and available thermal energy will for these conditions roughly be 0.7 based on that the raw material is heated to the reaction temperature. This estimate does not include the heat load from water evaporation from the raw material and that the burner efficiency will be lower than unity. Accordingly, for a pyrolysis gas fired reactor, it may be necessary to increase the reactor temperature in excess of that determined optimal in terms of liquid organics yield and thereby reduce the yield of liquid organics.

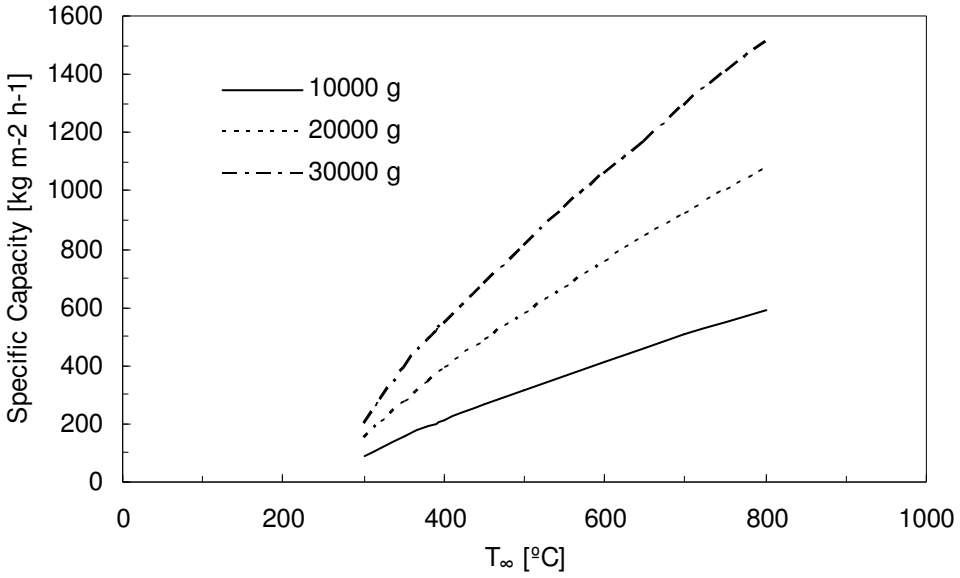

Figure 17: Simulated specific straw capacity of the PCR with reactor wall temperature and centrifugal acceleration for spherical wheat straw particles with a diameter of 630 µm. Particles are assumed arranged in a hexagonal lattice on the surface and converted 99 % wt.

The specific capacity of the reactor is of interest because it determines the size of a reactor for a given production. Since the solid movement in the reactor is still poorly understood, and has not been modeled, the specific capacity can not be accurately computed but an estimate may be given based on calculated particle conversion time. Assuming that the reactor surface is fully occupied by particles arranged in a hexagonal lattice (close-packed) and particle residence time is equal to the time of conversion (*i.e.* particles reach reactor exit when 99 % converted), Figure 17 shows the specific straw capacity of the reactor for particles of the MMD used in the experimental investigations. Since heat transfer to particles increase with reactor wall temperature and centrifugal acceleration, the specific capacity is promoted by increasing both these parameters. At the conditions discussed above, 10^4 g and 515 °C, the specific capacity is predicted to be 330 kg m^{-2} h^{-1}. However, unlike the effect on liquid organic yield, specific reactor capacity is strongly influenced by centrifugal acceleration and increasing it to $2 \cdot 10^4$ g results in a specific capacity of 600 kg m^{-2} h^{-1}. Accordingly, exceeding 10^4 g of nominal centrifugal accelerations may be interesting

not because it increases the yield of liquid organics but because it is predicted to significantly increase the capacity of a given reactor. However, the heat transfer will ultimately be limited by the gas burner acting on the reactor pipe and thereby define an upper centrifugal acceleration above which the specific reactor capacity does not increase further.

3.1.6 Bio-oil Properties and Combustion

Pilot plant runs and combustion trials were conducted in order to test the reactor system over longer runs and at higher feed rates, obtain representative samples of straw bio-oil for characterization, and to test the suitability of straw bio-oil as a liquid fuel replacement. The results of the investigation are reported in detail in Appendix F.

The reactor system had at the time of the optimization been modified whereby longer runs were made possible, and two pilot runs each producing about two liters of bio-oil with the properties shown in Table 4 were conducted. Feedstock properties were as shown in Table 5 and experimental conditions as in Table 6. The wheat straw feedstock, which had been prepared similarly to the feed used for the scientific investigations, had an expected mass mean diameter of ~ 630 μm.

Table 4: Comparison of fuel properties between the October (10/07) and November (11/07) straw bio-oil samples and typical specifications for Dynamotive wood-derived bio-oil (Wood).

Property	**Method** [a]	**10/07**	**11/07**	**Wood** [b]
Density @ 20°C (kg dm^{-3})	Hydrometer	1.18	1.20	1.2
Water content (% wt.)	Refractive index [c]	25.8	28.1	20-25
Ash content (% wt.)	ASTM D1102 (550 °C)	1.2	0.36	<0.02
HHV (MJ kg^{-1})	DIN 51,900	15.4	15.5	16-19
HHV db. (MJ kg^{-1})	DIN 51,900	20.7	21.5	21-25
C (% wt. daf)	Calorimetry [d]	50	52	*n.a.*
H (% wt. daf)	Calorimetry [d]	6.6	6.4	*n.a.*
O+N+S (% wt. daf)	Calorimetry [d]	42	41	*n.a.*
Dynamic viscosity (cP)	Rotation viscometer [e]			
- @ 20 °C		108	53	84
- @ 40 °C		24	18	23
- @ 60 °C		9.2	8.9	10
- @ 80 °C		6.4	6.0	5

[a]For straw-derived samples; [b]From Dynamotive [48]; [c]See Appendix C; [d]See Appendix E; [e]DIN SC4-18/13R spindle

The yield of bio-oil was 53 and 48 % wt. for run 10/07 and 11/07, respectively. Although not statistically significant, this was in average somewhat lower than the 54 % obtained in one of the earlier experiments with similar feedstock and conditions but at a lower specific feed rate of 41 kg m^{-2} h^{-1}. The yield of liquid organics was on average 44 % daf. or somewhat higher than obtained earlier under similar conditions. Accordingly, the increased specific feed rate did not result in a lower yield of liquid organics. As the runs were conducted at the maximum capacity of the feeder and the heating system in zone one and two was not able to maintain the desired temperature, the ultimate reactor capacity could not be determined.

The properties of the samples were in Appendix F compared to proposed specifications for bio-oil used as boiler fuel, and it was concluded that straw-derived

bio-oil produced by the PCR is expected to be able to obtain a proposed *light-medium* specification [49, 50] if char separation is improved, water content reduced by fractional condensation, and nitrogen partitioning controlled. Whereas the former two were expected to be relatively straightforward to achieve, the latter may require further investigation to determine the effect of process conditions and raw material properties because herbaceous feed stocks are known to contain more nitrogen than wood. If the nitrogen portioning can not be controlled declassification to *medium* or *heavy* may result which may affect the value of the product negatively.

Table 5: Properties of straw feed used for the pilot runs.

Property	**Method**	**Value**
Water content (% wt.)	Mettler-Toledo Moisture Analyzer MA40 [a]	9.2
Ash content (% wt. db.)	ASTM D1102 (550 °C)	7.0
HHV (MJ kg^{-1})	DIN 51,900	17.0
HHV db. (MJ kg^{-1})	DIN 51,900	18.2
C (% wt. daf)	Calorimetry [b]	49
H (% wt. daf)	Calorimetry [b]	6.2
O+N+S (% wt. daf)	Calorimetry [b]	45

[a] Drying at 105 °C until change in weight < 0.01% in 120s; [b] See appendix E

Table 6: Experimental conditions during pilot runs.

Property	**Unit**	**Value**
Nominal centrifugal acceleration	g	$1.0 \cdot 10^4$
Reactor temperature, zone 1	°C	420
Reactor temperature, zone 2	°C	480
Reactor temperature, zone 3+4	°C	550
Gas preheater temperature	°C	60 - 70
Tracing temperature	°C	420
Gas residence time	ms	~ 500
Solid feed rate	kg h^{-1}	2.4
Specific feed rate	kg m^{-2} h^{-1}	69

It was attempted to combust the samples in two small (~25 kW) domestic furnaces normally operating on rapeseed oil. These small-scale systems were selected due to the relatively small sample sizes and because the viscosity of the samples was significantly higher than diesel oil but similar to rapeseed oil (18 cP at 60 °C [51]). In neither of the tested furnaces could the bio-oil be ignited by the electric spark ignition system. However, if either ethanol or rapeseed oil was used, combustion could be initiated but stable operation with acceptable flue gas values was not possible. It was concluded that the observed behavior was caused by significantly more specific pre-ignition energy needed by bio-oil compared to rapeseed oil and that combustion of straw bio-oil with these burners was possible if relatively simple measures were taken to increase heat transfer to fuel droplets immediately after atomization. As discussed in Appendix F, these findings were supported by reported experiences with bio-oil combustion were it had been found that the combustion chamber should be redesigned in order to partially enclose the flame and that combustion air swirl should be increased to support the combustion. Further findings included that a cold furnace can

not be started on pure bio-oil but must be preheated and that air-assisted atomization of bio-oil preheated to 60 ºC is a suitable way of introducing bio-oil in to the furnace.

3.2 Commercial Results

The most suitable option for commercializing the intellectual property rights (IPR, *i.e.* patent rights and experience) obtained during the project was identified by using strategic marketing planning techniques combined with analysis of selected scenarios. As shown in Figure 18, internal and external factors were analyzed to provide the basis for a SWOT analysis from which scenarios were developed. Analysis of the scenarios resulted in recommendations regarding participation in alliances, needed management capabilities, and optimum capital structure. The detailed analysis is available in Appendix I.

The analysis concentrated on a three year time frame, corresponding to the time which was considered necessary to develop a mobile prototype pyrolyzer. As seen in Figure 19, a proof of concept reactor system and a pilot plant, both stationary, were contemplated prior to building a mobile prototype. It was selected not to expand the time frame further into the future in order to focus on the commercialization process.

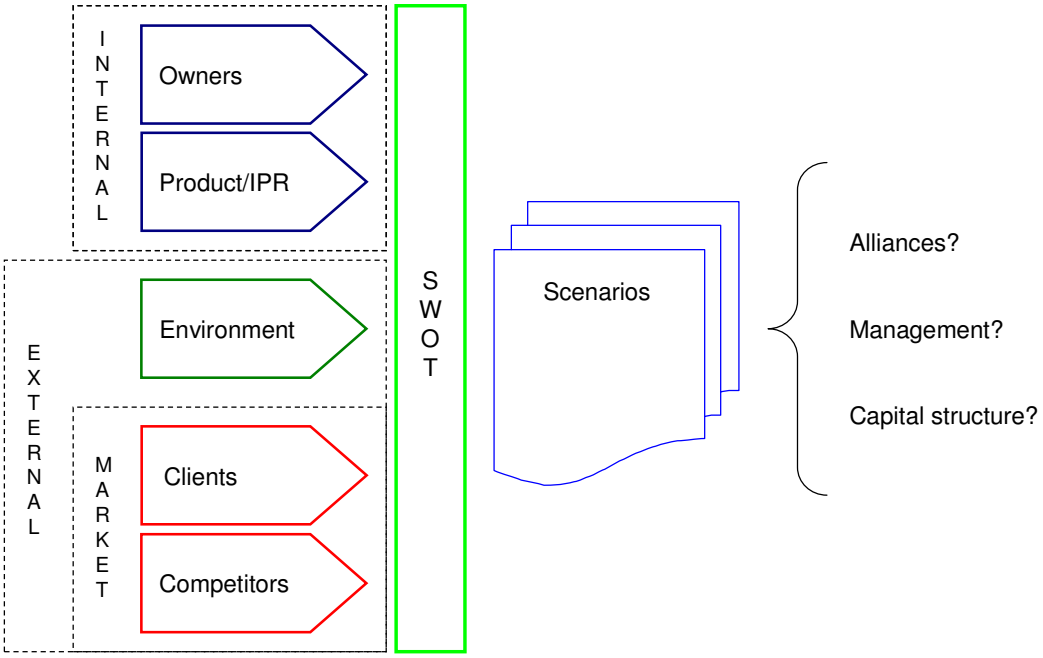

Figure 18: Framework for the developed business plan. SWOT: Strengths, Weaknesses, Opportunities, and Threats.

The IPR is owned by the inventor, co-inventors, the department, and the university. The risk profiles of the owners were found to span from risk averse to risk neutral. Apart from especially the inventor and co-inventors' wish to maximize the outcome of the commercialization, other objectives also affect their attraction to a particular mode of commercialization. The inventor is interested in continuing his work with the project to realize his ideas whereas his co-inventors prefer a more passive role. For DTU and the department, strategy and PR considerations favor the formation of a spin-off company with Danish participation. However, provided a more favorable solution involving foreign participation exits this may also be acceptable especially if it offers the institute the possibility to establish a long term scientific co-operation. In

any case, DTU and the department prefer to be sleeping partners and do not have ambitions of long term ownership. None of the owners demand to have control over the project in the form of a controlling stock share or otherwise.

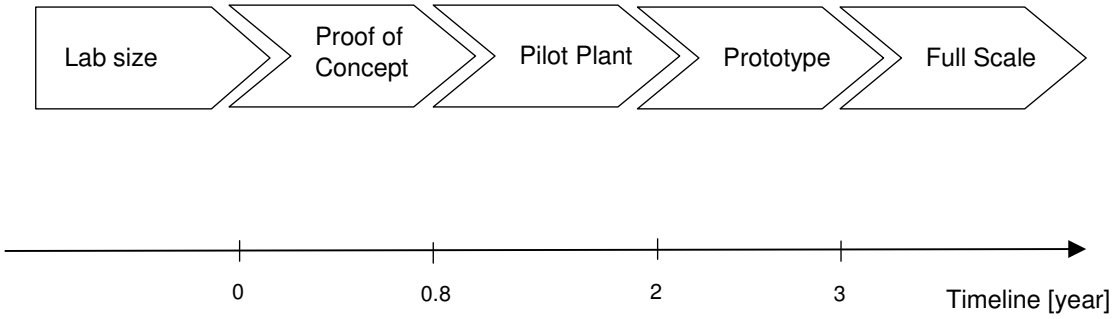

Figure 19: Timeline for bringing the PCR from the lab to the field.

The environment for the commercialization process was analyzed in a PEST (Political, Economic, Social and Technological) analysis, and the factors shown in Table 7 were considered. It was found that for the coming three years superior conditions for commercialization exit in the EU. As the total market for energy is expected to stagnate, this is mainly due to implementation of the first phase of the Kyoto Protocol's initiatives to reduce carbon dioxide emissions in the period 2008 to 2012. Furthermore, the focus in the EU on utilizing alternative energy sources to reduce carbon dioxide emissions, and not primarily gain national independence from oil exporting regions like in the US, also acts in favor of energy technologies focused on the production of electricity and heat. However, on a longer time scale (*i.e.* beyond the one considered), conditions in the US are likely to improve if the expected shift in priorities towards those in the EU takes place. Macroeconomic conditions were expected to be favorable for business investment during the period due to economic growth and low real interest rates. However, further support to alternative energy technologies from increasing prices of traditional fuels or a higher demand for energy was not foreseen. Accordingly, this in turn further strengthened the position of the EU as the driver will be the increased costs of traditional fuels brought about by regulations to reduce carbon dioxide emissions.

Table 7: Selected PEST factors in the environment.

Group	**Topic**	**Influence**
Technology	Global Warming	Curb CO_2 emissions (interest in alternative fuels)
	Use of subsidies	Distribution of subsidies between alternative fuels
Government	UN CO_2 Regulations	Interest in alternative fuels
	EU	Interest in alternative fuels
	Foreign policies	Access to energy resources
Macro Economy	Fossil fuel prices	Relative fuel prices (competitiveness of alternative fuels)
	Economic growth	Demand for all fuels
Culture	Individualism/ Collectivism	Priority for specific alternative fuels

The competitive pressure on the pyrolyzer was found to be extorted by alternative uses of straw primarily in the production of high-value transport fuels. In the period of interest, none of the potential entrants were expected to be important, but they could potentially be in the longer run if they resolve the cost challenges they face. Their set-ups rely on production economies of scale which are off-set by the mounting costs of logistics as their plants increase in size. Furthermore, the giant initial investment in a production facility will form a barrier to entry. All the competing technologies were found to rely on low-cost access to straw which drive them to take opportunistic advantage of the farmers. The pyrolyzer would, on the other hand, be his chance to integrate forward in the value-adding process. This opportunity is not provided by the baler that only allows him to deliver locally to one of the potential entrants. Accordingly, the manufacturers of agricultural machinery are not in a favorable position to expand the market for big balers even though they have raised large barriers to entry through scale economies in production and marketing and through their effective distribution networks.

On this account, it appeared that the pyrolyzer will have freedom to operate in the market for the entire time frame. The potential straw supply and the virtually unlimited market for bio-oil to large installations (see Figure 20) indicate that a significant share of the market for machinery to turn straw into energy could be claimed. In the EU this potential was found to be as high as 26,000 pyrolyzers representing a total value of DKK 70 billion. However, the organization of the well established agricultural machinery industry that presently supply balers clearly indicated that access to effective production, marketing, and distribution will form effective barriers to entry which will have to be circumvented.

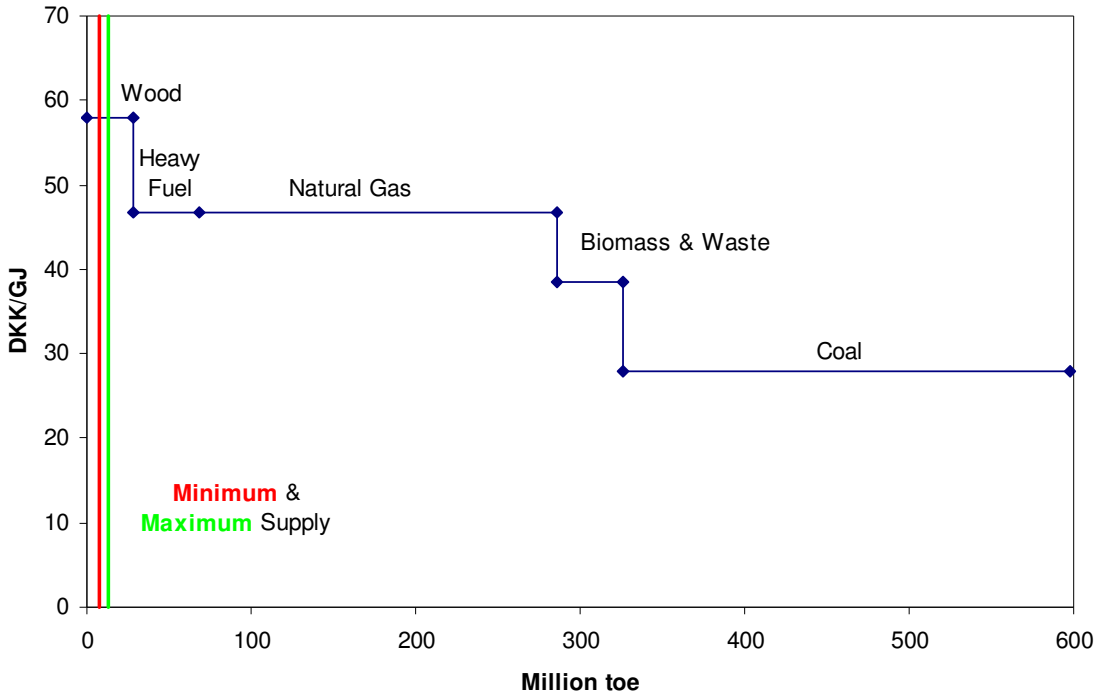

Figure 20: Forecast of the aggregated demand curve for the identified primary segment for bio-oil (industry, power production, and district heating) for the EU in 2008. Supply curves for bio-oil shown for comparison. TOE: tons of oil equivalents.

Based on the SWOT analysis two scenarios for commercialization were identified, establishing an independent research company or transferring the IPR to a multinational producer of agricultural equipment. It was concluded that the objectives of the owners for the commercialization are better achieved by transferring the project to an established company in the agricultural machinery industry. This company will be able to overcome the barriers to entry and thereby profit on the favorable market conditions for the pyrolyzer in the time frame. However, if possibilities to receive government grants arise this could be pursued by the owners in order to increase the value of the project before it is sold. It was not recommended to transfer the project to an independent research company as the financing of this venture would rely on venture capital which is not expected to increase the owners' financial gain. Furthermore, incorporating a research company based on a partnership with an outside company was not found to be a viable route as the gain to the latter is expected to be negative. By nature the recommended mode of commercialization does not require any specialized management capabilities or capital.

Chapter 4: Limitations

The proceeding chapters have revealed that the main goals set for the project were achieved. A suitable reactor for *in situ* flash pyrolysis of straw, a model to predict the distribution of the reaction products with reactor parameters, and a business plan were all developed. However, several issues are still poorly understood or have not been investigated.

The effect of feed particle size on product distribution was not investigated experimentally. In the model the particle size distribution of the feed was handled by dividing the distribution in to a number of discrete fractions and pooling the results to obtain the product distribution for the combined feed. However, since experimental runs were not conducted with monodisperse fractions, it was not ascertained that the model conveys the effect of particle size correctly. The same is true for gas phase residence time since this parameter was not investigated systematically and the model relied on kinetic data previously reported for the homogeneous cracking of wood-derived organics.

Water content of the feed and evaporation of water was ignored in the model. The straw feed materials used experimentally were at 5.8 and 9.2 % wt. for the scientific and pilot runs, respectively, relatively dry. However, straw on the field has a water content of approximately 15 % wt. which may lead to inaccurate predictions.

Establishing satisfactory particle movement in the reactor proved to be more challenging than expected. For the modeling this parameter was measured in cold runs for each combination of centrifugal acceleration and feed rate and specified in the code. However, the basic understanding of this issue and the ability to predict solid residence time still lack.

At the outset of the project it was foreseen that combustion of pyrolysis gas for heat generation would be investigated. However, since the bench-scale reactor could not easily be converted to utilize gas for heating, it was decided to focus on optimizing performance of the reactor. Accordingly, operation on pyrolysis gas still needs to be confirmed.

Two batches of straw bio-oil were produced and it was made probable that by optimizing char separation and employing partial condensation, the PCR could be optimized to produce bio-oil from straw with the same classification as wood-derived bio-oils. However, it still remains to be demonstrated that this is the case and that straw bio-oil can substitute conventional liquid fuels.

The developed model and the experience obtained from the experimental set-up will provide valuable support in the engineering of a future up-scaled reactor. However, it

has not been possible to accurately determine the area specific capacity of the reactor neither experimentally nor by modeling due to the limited capacity of the experimental set-up and the inability to describe solid transport in the reactor, respectively. Since this parameter will ultimately determine the capacity of a given reactor the dimensions for a full-scale plant have not been determined.

Chapter 5: Conclusion

The results obtained during this Ph.D. project have increased the knowledge on and helped advance *in situ* flash pyrolysis of straw. Through a literature study the requirements of the process were established and a suitable reactor identified. Based on the concept of ablative pyrolysis, a bench-scale model of the Pyrolysis Centrifuge Reactor was developed and installed in the laboratory. Data from the optimized reactor was applied to develop a mathematical model whereby yields of the principal products could be predicted. The reactor was operated in pilot plant mode and it was attempted to use the produced bio-oil as replacement for rapeseed oil in domestic furnaces. Even though the combustion trials were not successful, the produced samples showed promise to that the reactor system could be further optimized whereby the product can obtain a classification similar to wood-derived bio-oil.

Several technical aspects of the reactor developed in the project are still poorly understood or require experimental verification. The latter include the effect on yield distribution of feed water content and particle size. Solid particle movement in the reactor needs to be investigated more fundamentally and heating by combustion of pyrolysis gas verified.

The conceptual *in situ* pyrolyzer and the developed reactor represent the intellectual property created during the project, and by submitting two patent applications steps were taken to secure the IPR for the owners. The compiled business plan demonstrated that the technology is commercially interesting especially within the EU but also in the USA and other countries on a longer time scale. It was found that the owners better accomplish their objectives by transferring the IPR to a multinational producer of agricultural machinery rather than establishing a research company.

The project has demonstrated that *in situ* pyrolysis of straw is a promising concept both technically and commercially. A great deal of effort still remains, but significant steps have been taken toward realizing the vision on which the project was initiated.

Chapter 6: Further Work

The following list includes the future work identified during the course of the project:

1) Confirm experimentally the effect of feed particle size. This could be accomplished by performing a series of experiments with monodisperse particle fractions and varying reactor parameters.

2) Investigate the effect of feed moisture content experimentally, and incorporate moisture evaporation in the model. This could be accomplished by performing a series of experiments under varied reactor conditions with feeds prepared by adding controlled amounts of water.

3) Establish the area specific capacity of the reactor. Due to the importance in the engineering of a full scale pyrolyzer and the commercial application, this parameter should be established experimentally.

4) Confirm that the reactor can be heated by combustion of pyrolysis gas.

5) Investigate solid particle movement within the reactor in detail, possibly by CFD modeling.

6) Confirm the suitability of straw bio-oil as a liquid fuel substitute. Based on the findings, this could be accomplished by conducting new combustion trials with a rapeseed oil burner installed in a modified furnace.

7) Investigate nitrogen partitioning between products as influenced by reactor parameters. This investigation could be carried out by analyzing the products from the experimental runs proposed above.

8) Develop partial condensation of bio-oil in order to control water content in the final product. This development could be initiated with the present experimental set-up by observing the effect of varying the temperature in the direct condenser.

References

[1] Sander, B. Properties of Danish Biofuels and the Requirements for Power Production. Biomass Bioenerg, 12, 1997, 177-183.

[2] Nielsen, V. Teknik til Halmbjærgning siden 1950. DJF rapport markbrug, 95, 2003.

[3] Bech, N., Jensen, P.A., Dam-Johansen, K. Cost-Effective Straw Utilization: Harvesting Bio-Oil on the Field. 15th European Biomass Conference, Berlin, 2007.

[4] Bech, N., Jensen, P.A., Dam-Johansen, K. Harvesting Straw Bio-Oil on the Field. 6th European Congress of Chemical Engineering, Copenhagen, 2007.

[5] Hinge, J., Maegaard, E. Prisen på halm til kraftvarme? Landbrugets Rådgivningscenter, Skejby, 1997.

[6] Jensen, P.A., Stenholm, M., Hald, P. Deposition Investigation in Straw Fired Boilers. Energ Fuels, 11, 1997, 1048-1055.

[7] Nielsen, H.P., Larsen, O.H., Frandsen, F.J., Dam-Johansen, K. Deposition and High-Temperature Corrosion in a 10MW_{th} Straw-Fired Grate. Fuel Proces Techn, 54, 1998, 95-108.

[8] Jensen, P.A., Frandsen, F.J., Hansen, J., Dam-Johansen, K., Henriksen, N., Hörlyck, S. SEM Investigation of Superheater Deposits from Biomass-Fired Boilers. Energ Fuels, 18, 2004, 378–384.

[9] Frandsen, F.J. Utilizing Biomass and Waste for Power Production - a decade of Contributing to the Understanding, Interpretation and Analysis of Deposits and Corrosion Products. Fuel, 84, 2005, 1277–1294.

[10] Hjalmarsson, A. NO_x Control Technologies for Coal Combustion. IEA Coal Research IEACR/24, 1990.

[11] Kling, Å., Andersson, C., Myringer, Å., Eskilsson, D., Järås, S.G. Alkali Deactivation of High-Dust SCR Catalysts used for NO_x Reduction Exposed to Flue Gas from 100 MW-Scale Biofuel and Peat Fired Boilers: Influence of Flue Gas Composition. Appl Cat B: Environ, 69, 2007, 240–251.

[12] Sander, B., Nielson, L. Industrial Utilization of Fly Ash from Co-Firing of Coal and Straw. In: Mitchell, C.P., Bridgewater, A.V. (eds). Proc International Energy Agency Bioenergy Agreement Seminar, Snekkersten, Denmark, 1993.

[13] Bech, N. In-Situ Flash Pyrolysis of Straw. In: Dam-Johansen, K., Skjøth-Rasmussen, M.S. (eds). Graduate Schools Yearbook 2004. Department of Chemical Engineering, DTU, Kgs. Lyngby, 2005, 13-14.

[14] Oasmaa, A., Leppämäki, E., Koponen, P., Levander, J., Tapola, E. Physical Characterisation of Biomass-based Pyrolysis Liquids. Application of standard fuel oil analyses. VTT Energy, Espoo, 1997.

[15] Oasmaa, A., Kytö, M., Sipilä, K. Pyrolysis oil combustion tests in an industrial boiler. In: Bridgwater, A.V. (ed.) Progress in Thermochemical Biomass Conversion. Blackwell Science, Oxford, 2001, 1468-1481.

[16] Diebold, J.P., Czernik, S. Additives To Lower and Stabilize the Viscosity of Pyrolysis Oils during Storage. Energ Fuel, 11, 1997, 1081-1091.

[17] Bridgwater, A.V., Peacocke, G.V.C. Fast Pyrolysis Processes for Biomass. Renew Sustain Energ Rev, 4, 2000, 1-73.

[18] Scott, D.S., Majerski, P., Piskorz, J., Radlein, D. A. J. A Second Look at Fast Pyrolysis of Biomass - The RTI Process. Anal Appl Pyrolysis, 51, 1999, 23-37.

[19] Raffelt, K., Henrich, E., Koegel, A., Stahl, R., Steinhardt, J., Weirich, F. The BTL2 Process of Biomass Utilization Entrained-Flow Gasification of Pyrolyzed Biomass Slurries. Appl Biochem Biotech, 129-132, 2006, 153-164.

[20] Leibold, H., Hornung, A., Seifert, H. HTHP Syngas Cleaning Concept of Two Stage Biomass Gasification for FT Synthesis. Powder Tech, 180, 2008, 265 -270.

[21] Mann, C.C. The Real Dirt on Rainforest Fertility. Science, 297, 2002, 920-923.

[22] Marris, E. Black is the New Green. Nature, 442, 2006, 624-626.

[23] Chan, K.Y., Van Zwieten, L., Meszaros, I., Downie, A., Joseph, S. Agronomic Values of Greenwaste Biochar as a Soil Amendment. Australian J Soil Res, 45, 2007, 629-634.

[24] Christensen, B.T. Kulstofindhold i dyrket jord. In: Christensen, B. (red). Biomasseudtag til energiformål – konsekvenser for jordens kulstofbalance i land- og skovbrug. DJF rapport markbrug, 72, 2002.

[25] Luxhøi, J., Bech, N., Bruun, S. Bio-oil Production in the Field. BioSci, 57, 2007, 469.

[26] Lehmann, J., Gaunt, J., Rondon, M. Bio-Char Sequestration in Terrestrial Ecosys-tems – a Review. Mitigation and Adaptation Strategies for Global Change, 11, 2006, 403-427.

[27] Bech, N., Jensen, P.A., Dam-Johansen, K. Ablative Flash Pyrolysis of Straw and Wood: Bench-Scale Results. Proc 15th European Biomass Conference and Exhibition, Berlin, 7-11 May, 2007 (in press).

[28] Bech, N., Larsen, M.B., Jensen, P.A., Dam-Johansen, K. Modelling Ablative Flash Pyrolysis of Straw and Wood in the Pyrolysis Centrifuge Reactor. Submitted for publication, 2008.

[29] Bech, N., Jensen, P.A., Dam-Johansen, K. Predicting Fuel Elementary Composition by Bomb Calorimetri. Submitted for publication, 2008.

[30] Bech, N., Dam-Johansen, K. A Method and a Mobile Unit for Collecting and Pyrolysing Biomass. PCT Application WO 2006/117006. Geneva, World Intellectual Property Organization, 2006.

[31] Bech, N., Jensen, P.A., Dam-Johansen, K. Pyrolysis Method and Apparatus. PCT Application WO 2006/117005. Geneva, World Intellectual Property Organization, 2006.

[32] Chang, P.W., Preston, G.T. The Occidental Flash Pyrolysis Process. In: Sofer, S.S., Zaborsky, O.R. (eds). Biomass Conversion Processes for Energy and Fuel, Plenum Press, New York, 1981, 173-185.

[33] Scott, D.S., Piskorz, J. The Continuous Flash Pyrolysis of Biomass. Can J Chem Eng, 62, 1984, 404-412.

[34] Lidén, A.G., Berruti, F., Scott, D.S. A Kinetic Model for the Production of Liquids from the Flash Pyrolysis of Biomass. Chem Eng Comm, 65, 1988, 207-221.

[35] Reed, T.B. Principles and Operation of a Novel “Pyrolysis Mill”. In: Thermochemical Conversion Program Annual Meeting, Solar Energy Research Institute, Golden, CO, 1988, 248-258.

[36] Samolada, M.C., Vasalos, I.A. A Kinetic Approach to the Flash Pyrolysis of Biomass in a Fluidized Bed Reactor. Fuel, 70, 1991, 883-889.

[37] Peacocke, G.V.C., Bridgwater, A.V. Ablative Plate Pyrolysis of Biomass for Liquids. Biomass Bioenergy, 7, 1994, 147-154.

[38] Wagenaar, B.M., Prins, W., van Swaaij, W.P.M. Pyrolysis of Biomass in the Rotating Cone Reactor. Chem Eng Sci, 49, 1994, 5109-5126.

[39] Czernik, S., Scahill, J., Diebold, J.P. The Production of Liquid Fuel by Fast Pyrolysis of Biomass. In: Proc 28th Intersociety Energ Conv Eng Con, 1993, 2429-2436.

[40] Bech, N. In-Situ Flash Pyrolysis of Straw. In: Dam-Johansen, K., Bøjer, M. (eds). Graduate Schools Yearbook 2005. Department of Chemical Engineering, DTU, Kgs. Lyngby, 2006, 5-8.

[41] Bech, N. In-Situ Flash Pyrolysis of Straw. In: Dam-Johansen, K., Bøjer, M. (eds). Graduate Schools Yearbook 2006. Department of Chemical Engineering, DTU, Kgs. Lyngby, 2007, 15-20.

[42] Bech, N. In-Situ Flash Pyrolysis of Straw. In: Dam-Johansen, K., Bøjer, M. (eds). Graduate Schools Yearbook 2007. Department of Chemical Engineering, DTU, Kgs. Lyngby, 2008, 23-26.

[43] Fahmi, R., Bridgwater, A.V., Darvell, L.I., Jones, J.M., Yates, N., Thain, S. et al. The Effect of Alkali Metals on Combustion and Pyrolysis of Lolium and Festuca Grasses, Switchgrass and Willow. Fuel, 86, 2007, 1560-1569.

[44] Lédé, J. Reaction Temperature of Solid Particles Undergoing an Endothermal Volatilization. Application to the Fast Pyrolysis of Biomass. Biomass Bioenerg, 7, 1994, 49-60.

[45] Di Blasi, C. Heat Transfer Mechanisms and Multi-Step Kinetics in the Ablative Pyrolysis of Cellulose. Chem Eng Sci, 51, 1996, 2211-2220.

[46] Janse, A.M.C., Westerhout, R.W.J., Prins W. Modelling of Flash Pyrolysis of a Single Wood Particle. Chem Eng Proc, 39, 2000, 239-252.

[47] Jensen, P.A., Sander, B., Dam-Johansen, K. Pretreatment of Straw for Power Production by Pyrolysis and Char Wash. Biomass Bioenerg, 20, 2001, 431-446.

[48] Available at: http://dynamotive.com/en/biooil/index.html#demonstration

[49] Diebold, J.P., Milne, T.A., Czernik, S., Oasmaa, A., Bridgwater, A.V., Cuevas, A., Gust, S., Huffman, D., Piskorz, J. Proposed Specifications for Various Grades of Pyrolysis Oils. In: Bridgwater, A.V., Boocock, D.G.B. (eds). Developments in Thermochemical Biomass Conbersion. Blackie Academic, London, 1997, 433-447.

[50] Oasmaa, A., Czernik, S. Fuel Oil Quality of Biomass Pyrolysis Oils – State of the Art for the End Users. Energ Fuels, 13, 1999, 914-921.

[51] Santos, J.C.O., Santos, I.M.G., Souza, A.G.. Effect of Heating and Cooling on Rheological Parameters of Edible Vegetable Oils. J Food Eng, 67, 2005, 401–405.

Appendix A:

Reactor Design for In Situ Flash Pyrolysis

1 Introduction

Constituting the heart of a pyrolyzer, the reactor differentiates the various flash pyrolysis plant designs. This appendix will identify the requirements to a reactor installed in a pyrolyzer that, in addition to being mobile, will operate *in situ* (*i.e.* as it moves across the growth site of the biomass) with the main objective to convert straw to bio-oil. The appendix is divided in to three sections. First, the requirements and constraints pertinent to *in situ* operation are identified. Second, existing reactor designs are discussed in relation to the identified requirements. Finally, recommendations regarding the design of the experimental unit are proposed.

2 Considerations for *In Situ* Operation

In situ flash pyrolysis differs from conventional stationary operation because the unit is not only mobile but also needs to operate in motion whereby some additional constraints regarding size and maneuverability have to be considered. This section is not an attempt to treat the engineering of a flash pyrolyzer in detail but merely to gather information to support the choice of reactor design. For details on the general requirements for flash pyrolysis reactors, an exhaustive review article is available elsewhere [1].

2.1 Yield Maximization

The desired product of flash pyrolysis is bio-oil subsequently used as boiler fuel. As a first approximation, it is assumed that the product quality in terms of heating value (*i.e.* elemental composition), viscosity, and storage stability (*i.e.* reactivity) is not critically affected by reaction parameters whereby maximization of liquid organics yield is a central parameter for evaluating reactor performance. It is generally recognized [2] that the formation of volatiles has a greater activation energy factor than the competing char forming reactions. Therefore, the yield or liquid organics will increase with temperature whereas the char yield decreases, as demonstrated in Figure 1. However, due to temperature-accelerated secondary degradation of tar to gas, an optimum temperature for liquid organics yield is established, in this case for sorghum bagasse somewhere between 500 and 520 °C. Accordingly, a particle at ambient temperature will when subjected to heating pass through the low temperature domain before reaching the temperature for optimum tar yield. Thus, in order to minimize

char formation during, the heating period the heating rate should be as high as possible.

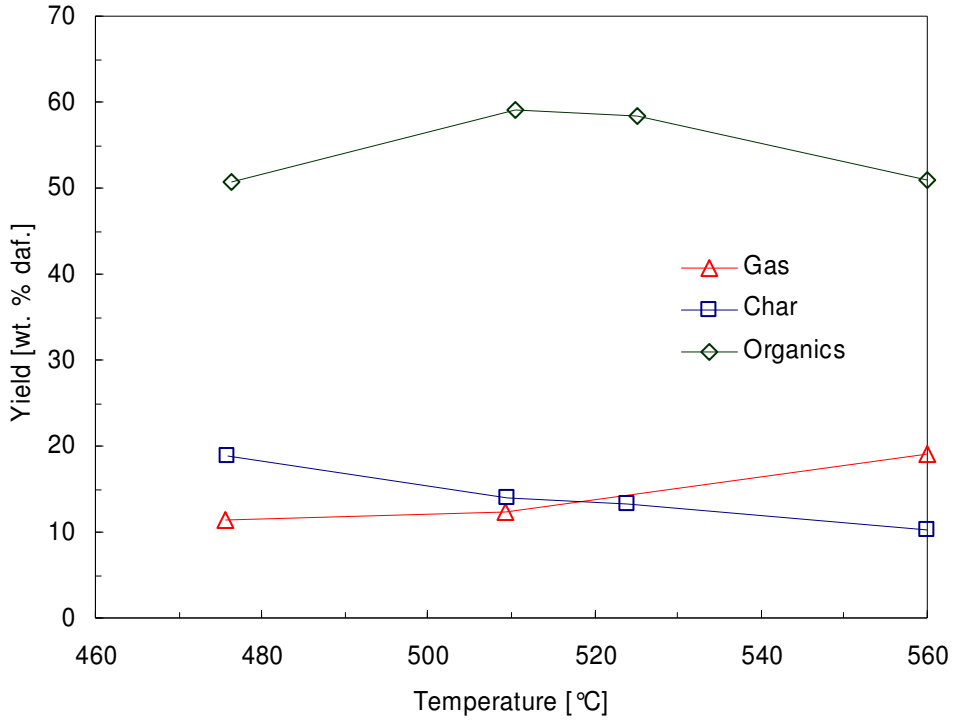

Figure 1: Yields of reaction products with reactor temperature for flash pyrolysis of raw sorghum bagasse at 500 ms vapor residence time. Data from [3].

2.2 Plant Capacity

In order to minimize the variable costs of production, the capacity of the *in situ* pyrolyzer needs to as high as possible but will ultimately be determined by the physical size available on the vehicle. However, for the sake of this discussion a minimum target capacity of 10 t h^{-1} is selected because the objective for the pyrolyzer is to substitute the Hesston baler which has a similar capacity [4].

2.3 Raw Material Characteristics

In fluid bed reactors, high heating rates are promoted by reducing the particle size [5] and the mass-average particle size is generally of the order 0.5 mm. The power input needed to mill straw is dependent on plant species, equipment, water content, and the desired particle size of the product [6]. Mani *et al.* [7] found that for wheat straw containing 12.1 % wt. water, a specific power input of 43.6 kW h t^{-1} was need with hammer mill fitted with a 1.6 mm screen in order to obtain a material with a mass

mean particle size of 0.34 mm and 95 % wt. below 0.85 mm. The results reported by Mani *et al.* appear to be representative for wheat as their results were similar to those found by Cadoche and Lopez [8] who also used a hammer mill. However, for fibrous materials knife mills use significant less power than hammer mills in order to obtain the same average final particle size but also produce a significantly broader size distribution [9]. Thus, the apparent power saving is offset because a smaller screen is required in order to narrow the particle size distribution. Accordingly, for an *in situ* pyrolyzer processing 10 t h^{-1}, a power input of approximately 440 kW is needed in order to maximize liquid organic yield if the reactor is of the fluid bed type. Even though size reduction is the most power intensive process of the machine, even more power will be needed and since only the largest agricultural tractors are rated above 150 kW this is a potential pitfall for the widespread acceptance of the process. One of the market leaders for big balers, Case New Holland, recommend a tractor power output minimum of minimum 112 kW for their largest bailer [10]. Consequently, if the power requirement of the pyrolyzer is significantly larger than this figure investment in a new tractor will be a financially heavy prerequisite in order to operate a pyrolyzer.

2.4 Energy Management

In addition to the mechanical energy required by the *in situ* pyrolyzer, thermal energy is also needed in order to heat the raw material to the reaction temperature and supply the enthalpy of reaction, and this must be provided by combusting the permanent gasses released from the reaction. In contrast to a stationary plant where the primary focus is to reduce the energy consumption in order to maximize the amount available for export, the situation with an *in situ* pyrolyzer is also a matter of balance. Storage of pyrolysis gas, which requires a high pressure to liquefy, is not practicable due to the increased size and weight of tank, condenser, and compressor. The goal is therefore to balance thermal energy supply and demand by adjusting parameters influencing gas yield while aiming at tar maximization. Furthermore, since the gas can not be stored on board it is required that the pyrolyzer utilize this product for heating rather than using char which may be left on the field or collected for export.

2.5 Plant Size

The *in situ* flash pyrolyzer operates in the field and must be able to drive between fields on public roads. Consequently, it needs to be maneuverable in terrain without damaging soil structure and to comply with traffic statutes. The latter imposes constraints on length (12.0 m), height (4.0 m), and width (3.3 m) [11]. As mentioned above, these constraints will ultimately limit the capacity, and thereby the profitability, of the machine thus underlining that it is of great priority to specify a compact design both in term of volume and weight.

2.6 Heat-up Time

The pyrolyzer must be restarted every time it is moved to a new field. Time used for setting up the equipment to resume operation reduces the operational window and net capacity. Therefore it is necessary to minimize the time it takes for the reactor to reach its working temperature when it is restarted.

2.7 Time between Service

The pyrolyzer is a piece of harvest equipment and as such will be used seasonally. Unlike a stationary plant where operation may be scheduled non-stop for 8,000 h y^{-1} or more, the pyrolyzer can only be utilized when straw is available on the field. As discussed in Appendix I, the present operational time of a Hesston baler (250 h y^{-1}) is a reasonable estimate for the yearly time of operation. However, since straw is only available in this time frame prolonged out-of-service can not be accepted during the harvest. Accordingly, service intervals should not be shorter than 250 h.

2.8 Summary

Table 1 summarizes the identified requirements and constraints for an in situ pyrolyzer.

Table 1: Requirements and constraints for an *in situ* pyrolyzer.

Specification	Value
Weight/volume specific capacity	As **high** as possible
Acceptable particle feed size	As **high** as possible
Bio-oil yield	As **high** as possible
Maximum weight	As **low** as possible
Heat-up time	As **low** as possible
Source of thermal energy	Pyrolysis gas
Time between service	> 250 h
Capacity	> 10 t h^{-1}
Mechanical power demand	< 112 kW
Length	< 12 m
Width	< 3.3 m
Height	< 4.0 m

3 Basic Reactor Designs

Although only a few full-scale flash pyrolyzers are in operation several designs have been published and some even evaluated in pilot-plants [12]. In order to evaluate their applicability for *in situ* flash pyrolysis, this section will summarize their common features and address the issues treated in the foregoing chapter. The existing reactor designs can be divided into three basic categories, namely fluid beds, plug-flow transported beds, and ablative reactors. For a comprehensive review of ongoing research activities and operational flash pyrolyzers the reader is referred to Bridgwater and Peacocke [12].

3.1 Fluid Bed Reactors

The common feature of fluid bed pyrolyzers is that biomass particles are fluidized in a chamber by inert gas. A distinction between designs can be made according to whether an inert solid is present and whether that solid is circulated externally. The latter is referred to as transported fluid beds, not to be confused with the plug-flow transported bed design treated in section 3.2, whereas the former group of reactors is referred to as bubbling fluid beds. Fluid beds without inert solids constitute the group of sprouted beds.

A transported fluid bed reactor system was applied in the pioneering full-scale flash pyrolyzer commissioned by Occidental Research Corporation in the late 1960's [13]. The inert bed material consisted of ash and debris from the municipal solid waste feed

and was circulated between the bed and an external char combustor mechanically. Thermal energy was provided exclusively by combusting pyrolysis char in the presence of the circulating ash. Vapors were removed from the top of the reactor assisted by the recycled pyrolysis gas used for fluidization. Present day circulated fluid beds work much the same as this pioneering project except that the bed material is usually sand. Another difference is that ash from char combustion is entrained in the vapor phase and separated by a secondary cyclone before the pyrolysis liquid is condensed [14]. If a separate char combustor is used, ash is entrained in the exhaust gas whereby contact with vapors is avoided. Due to the expected catalytic effect of ash on vapor cracking the former solution may for straw feed be especially problematic as it contains an order of magnitude more ash than wood.

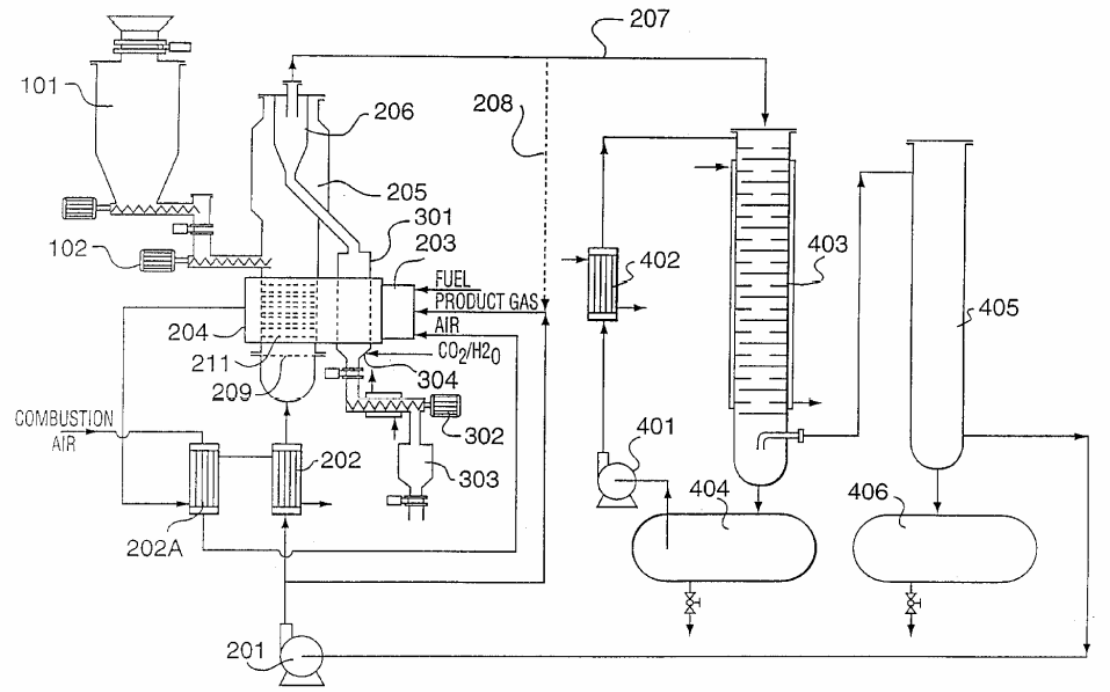

Figure 2: Bubbling fluid bed design used by Dynamotive. Notice the internal cyclone (206) used to separate char from pyrolysis vapors [16].

Dynamotive Energy Systems Corporation is an example of a company working with bubbling fluid bed technology [3, 15]. In their design [16] heat is provided by combusting either the pyrolysis gas, or alternatively gasified char, in fire tubes installed in the bottom section of the reactor. Fluidization is accomplished by re-circulating pyrolysis gas preheated by the fire tube exhaust, see Figure 2.

The spouted bed reactor represents yet another type of fluid bed design but it is operated without inert material. Here, the function of the gas is both to fluidize the biomass particles and to provide most or all the process heat [17]. This increases the gas recirculation rate considerably due to the low volumetric gas heat capacity.

Overall, the major advantage of fluid bed systems seems to be their apparent simplicity, high liquid organics yield, and easy scale up [1]. On the other hand, they generally require the feed to be milled to less than one millimeter in order to obtain efficient heat transfer and thus a competitive tar yield. Other disadvantages include the vertical orientation and thus excessive height when scaled (*i.e.* in relation to traffic statutes), the blower and piping associated with the transport of gas for fluidization (*i.e.* in relation to power demand and plant volume), and increased difficulties in liquefying aerosols due to gas-phase dilution. Furthermore, for transported fluid beds a sieving step needs to be added if it is desired to utilize pyrolysis gas for heating in order to export char.

3.2 Plug-Flow Transported Bed Reactors

The rotating cone [18] and the twin-screw reactors [19] are examples of reactor configurations where biomass and a solid heat carrier are transported in plug flow mode, while evolved volatiles are removed cross-currently. For the rotating cone (Figure 3), biomass and heated sand are introduced and mixed at the center of the cone and transported in spiral motion on the sloping cone by centrifugal force and finally pass over the edge. Evolved vapors escape the solid phase perpendicularly and are withdrawn though a connection located near the cone center. The twin-screw reactor (Figure 4) relies on two augers with intervening flights to transport and mix the solid phase horizontally, while vapors are removed from the space above the solids. For both reactor types, heat is supplied by combusting pyrolysis char externally by blowing air through the hot re-circulating sand/char mixture and may for the rotating cone be supplemented by a gas burner acting directly on the cone. Ash is removed by entrainment in the exhaust. If all heat is transported via sand the weight of sand fed constitutes on the order of 20 times the biomass input in order to heat it to the optimum reaction temperature [19]. Naturally, both sand and systems to handle it adds weight and increase power demand and heat-up time whereby net capacity is reduced.

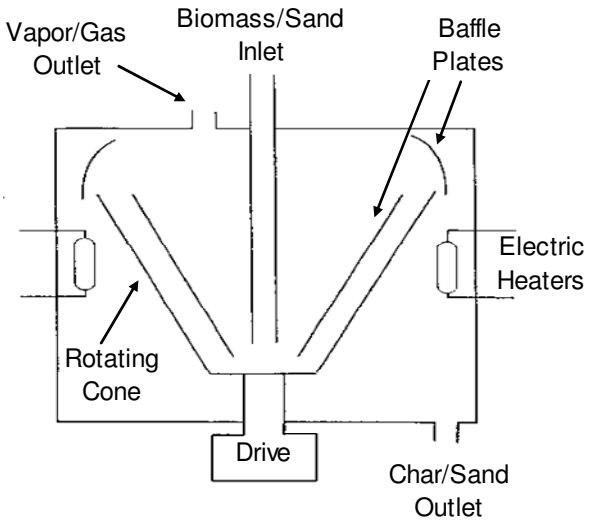

Figure 3: Laboratory version of the Rotating Cone Reactor that unlike the full-scale version employ electric heating. Based on [18].

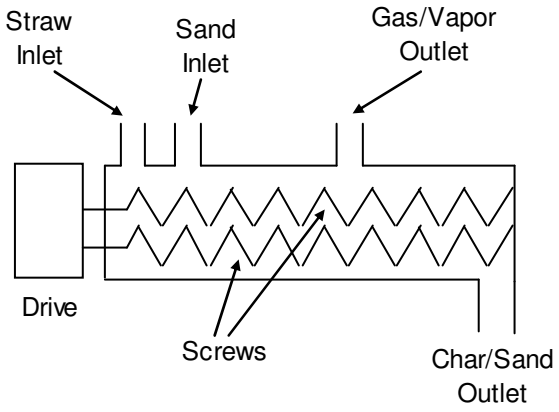

Figure 4: Twin-screw reactor with hot sand as heat carrier for fast pyrolysis of straw chops. Screws are positioned next to each other. Based on [19].

Especially the twin-screw reactor appears to be a simple and compact horizontally arranged reactor for pyrolyzing biomass. However, the large amounts of circulating hot sand and the need to mechanically remove char from the sand in order to use gas as the heating source limit its effectiveness for *in situ* pyrolysis.

3.3 Ablative Reactors

Ablation signifies a process of removal by erosion, melting, evaporation, or vaporization. A familiar example is the entering of meteorites in the upper atmosphere where the surface of the meteorite exposed to the high-speed flow of air melts and is rapidly blown away without affecting the internal structure significantly due to a steep

temperature gradient [20]. The underlying principle as related to biomass pyrolysis can be demonstrated in the simple spinning disk experiment. If a rod of biomass is pressed on to a heated spinning disk it will exhibit a fusion-like behavior [21]. Between the rod and the disk a layer of liquid with a thickness on the order of 10^{-6} to 10^{-5} m will be formed and continuously be removed from below the rod. The liquid will then undergo further de-polymerization before evaporating from the open disk surface. Heat transfer coefficients of the magnitude 10 kW m^{-2} K^{-1} are realized possibly as a result of the liquid establishing good conduction between plate and rod and insulating char being continuously removed [21-24].

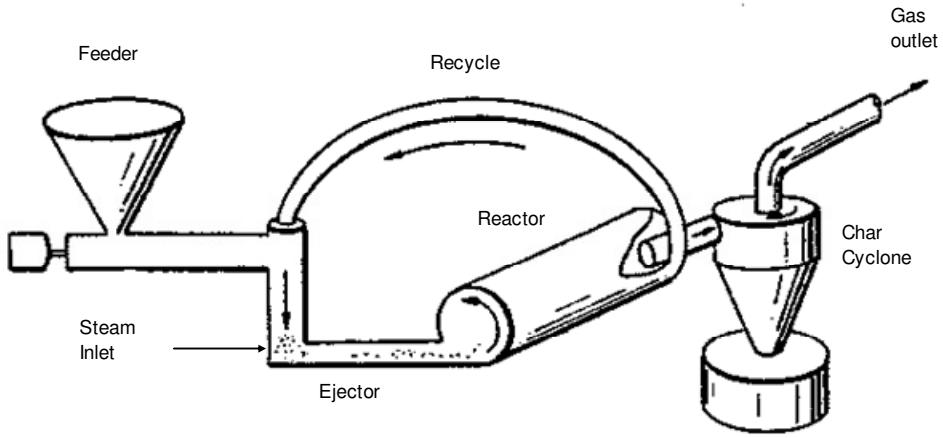

Figure 5: Vortex reactor schematic. Based on [25].

One way to achieve ablative pyrolysis, is to accelerate biomass particles in a stream of steam or other inert gas and introduce them tangentially in to a heated tube [26-28] as illustrated in Figure 5 with the vortex reactor. A consequence of the particles traveling virtually in plug flow is that unpyrolyzed particles will have to be recycled. Vapors and entrained char are removed axially at the reactor end and solids separated in a cyclone. The speed of the particle inside the tube is close to 100 m/s and the centrifugal force ensures, that it is maintained in good contact with the wall [29]. The main drawback of this is reactor seems to be the need to heat and cool the gas needed to transport the particles, the resulting dilute vapor phase, and the coupling between solid and gas residence times.

The Continuous Ablative Regenerator (CAR) flash pyrolysis system developed by Enervision, Inc. relies on a design very similar to the vortex reactor's but in order to

closely define the trajectory of the particle, a coiled steel tube constitutes the heated wall [30]. In the Cyclone Reactor [31], simultaneous pyrolysis and char/vapor separation is accomplished by introducing the entrained particles to the heated walls of a cyclone and collecting char in the catch pot. This integration of reactor and solid separation offers the possibility of a potentially very compact arrangement with minimum piping.

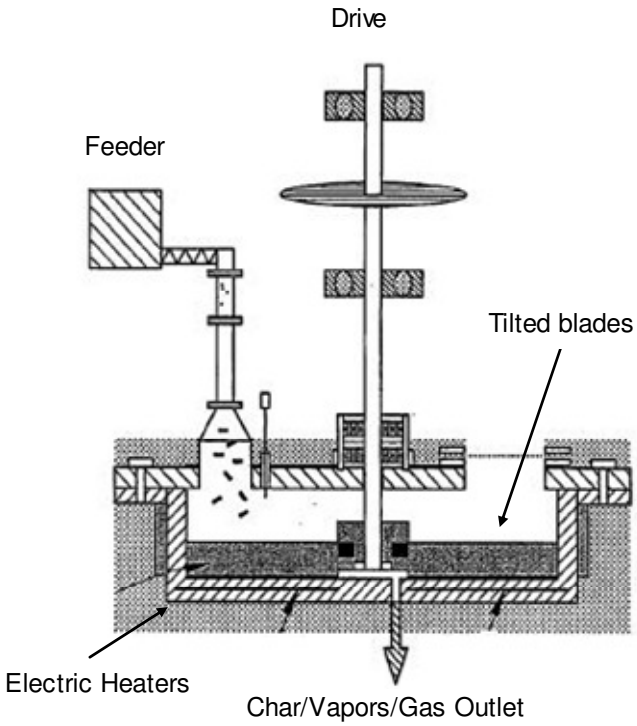

Figure 6: Ablative Thermolysis Reactor. Based on [32].

Yet another ablative reactor is the Ablative Thermolysis Reactor [32, 33] which employs mechanical sweeping to move the particles across the hot surface, see Figure 6. Biomass is introduced onto a circular heated plate and dragged by four tilted propellers, whereby pressing the particles against the plate is simultaneously achieved. The asymmetric form of the propellers allows char to be transported towards the center of the plate where it is removed through an outlet. The Pyrolysis Mill reactor shown in Figure 7 is similar to the Ablative Thermolysis Reactor but instead of blades the material is squeezed and transported between two heated copper discs [34]. Both these reactors have eliminated pneumatic transport of particles but are prone to wear due to close contact between biomass and rotors. Furthermore, scaling

of neither has been demonstrated and may present several problems, also in terms of heating by combustion of gas or char.

As a result of the step temperature gradient inside a particle undergoing ablative pyrolysis there is no bond on the maximum particle size and thus the task of particle reduction is minimized or even eliminated. As noted earlier, this is advantageous in relation to a mobile unit as both power demand and size of the unit are reduced. Combined with the absence of a circulated gas for fluidization in a mechanically driven arrangement (*i.e.* as in the Ablative Thermolysis or the Pyrolysis Mill reactors) and the compact horizontal arrangement, an ablative arrangement could potentially be well suited for an *in situ* pyrolyzer. Finally, since char is not mixed with sand or other inerts there is no need for separation before export of char and the heat transfer through wall contact facilitates gas heating.

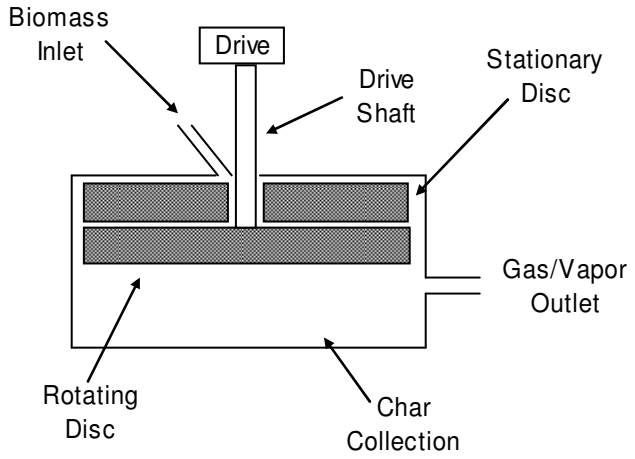

Figure 7: The Pyrolysis Mill: The lower rotating disc is pressed against the upper counterpart by a spring (not shown). On this laboratory model discs are heated electrically and feed is introduced in the center and move out between them. Based on [34].

4 Conclusions

Based on the review of existing reactor designs and the requirements for a flash pyrolysis reactor operating *in situ* it can be concluded that although the fluid bed reactor is the most commonly applied configuration for stationary pyrolysis it is not well suited for *in situ* operation. The same is true for transported beds due to the inherent circulation of hot sand and need to separate char from sand. In contrast ablative reactors seem to be well suited due to especially their flexibility regarding

raw material particle size provided a mechanical system for pressing the straw against the heated wall can be devised in a horizontal arrangement.

5 References

[1] Mohan, D., Pittman, C.U., Steele, P.H. Pyrolysis of Wood/Biomass for Bio-oil: A Critical Review. Energ. Fuel, 20, 2006, 848-889.

[2] Miller, R.S., Bellan, J. A Generalized Biomass Pyrolysis Model Base on Superimposed Cellulose, Hemicellulose and Lignin Kinetics. Combust. Sci. and Tech., 126, 1997, 97-137.

[3] Scott, D.S., Majerski, P., Piskorz, J., Radlein, D. A Second Look at Fast Pyrolysis of Biomass – The RTI Process. J. Anal. Appl. Pyrolysis, 51, 1999, 23-37.

[4] Håndbog til Driftsplanlægning, Dansk Landbrugsrådgivning (Landscentret), Skejby, 2003.

[5] Di Blasi, C. Kinetic and heat Transfer Control in the Slow and Flash Pyrolysis of Solids. Ind. Eng. Chem. Res., 35, 1996, 37-46.

[6] Hoque, M., Sokhansanj, S., Naimi, L., Bi, X., Lim, J., Womac, A.R. Review and analysis of performance and productivity of size reduction equipment for fibrous materials. Proc. ASABE Ann. Int. Meet, Minneapolis (MN), USA, June 17-20, 2007.

[7] Mani, S., Tabil, L.G., Sokhansanj, S. Grinding performance and physical properties of wheat and barley straws, corn stover and switchgrass. Biomass Bioenerg., 27, 2004, 339-352.

[8] Cadoche, L., Lopez, G.D. Assessment of size reduction as a preliminary step in the production of ethanol from lignocellulosix wastes. Biolog. Wastes, 30, 1989, 153-157.

[9] Himmel, M., Tucker, M., Baker, J., Rivard, C., Oh, K., Grohmann, K. Comminution of Biomass: Hammer and Knife Mills. Biotech. Bioeng. Symp., 15, 1985, 39-58.

[10] New Holland B9090. Marketing material for big baler. CNH Global N.V., 2007. Available on the web at: http://www.newholland.com.

[11] Bekendtgørelse om detailforskrifter for køretøjers indretning og udstyr. Færdselsstyrelsen, 2007.

[12] Bridgwater, A.V., Peacocke, G.V.C. Fast Pyrolysis Processes for Biomass. Renewable Sustainable Ener. Rev., 4, 2000, 1-73.

[13] Chang, P.W., Preston, G.T. The Occidental Flash Pyrolysis Process. In: Sofer, S.S., Zaborsky, O.R. (eds.) Biomass Conversion Processes for Energy and Fuel, Plenum Press, New York, 1981, 173-185.

[14] Lappas, A.A., Samolada, M.C., Iatridis, D.K., Voutetakis, S.S., Vasalos, I.A. Biomass Pyrolysis in a Circulating Fluid Bed Reactor for the Production of Fuels and Chemicals, Fuel, 81, 2002, 2087-2095.

[15] Dynamotive Energy Systems Coorporation. Fast Pyrolysis of Bagasse to Produce BioOil Fuel for Power Generation, presentation at the 2001-Sugar Conference, 2001.

[16] Piskorz, J., Majerski, P., Radlein, D. Energy Efficient Liquefaction of Biomaterials by Thermolysis. US Patent 5,853,548, 1998.

[17] Aguado, R., Olazar, M., Barona, A., Bilbao, J. Char-formation Kinetics in the Pyrolysis of Sawdust in a Conical Spouted Bed Reactor, J. Chem. Tech. Biotech., 75, 2000, 583-588.

[18] Wagenaar, B.M., Prins, W., van Swaaij, W.P.M., Janse, A.M.C. Method and Apparatus for Thermal Treatment of non-Gaseous Material. US Patent 6,274,095, 2001.

[19] Henrich, E., Dinjus, E., Weirich, F. A new Concept for Biomass Gasification at High Pressure, 12th European Conference on Biomass, Amsterdam, 2002.

[20] Lédé, J. Comparison of Contact and Radiant Ablative Pyrolysis of Biomass, J. Anal. Appl. Pyrolysis, 70, 2003, 601-618.

[21] Lédé, J., Li, H.Z., Villermaux, J. Pyrolysis of Biomass. Evidence for a Fusionlike Phenomenon. ACS Symposium Series, 376, 1988, 66-78.

[22] Lédé, J., Li, H.Z., Villermaux, J., Martin, H. Fusion-Like Behaviour of Wood Pyrolysis. J. Anal. Appl. Pyrolysis, 10, 1987, 291-308.

[23] Lédé, J., Panagopoulos, J., Li, H.Z., Villermaux, J. Fast Pyrolysis of Wood: Direct Measurement and Study of Ablation Rate. Fuel, 64, 1985, 1514-1520.

[24] Martin, H., Lédé, J., Li, H.Z., Villermaux, J., Moyne, C., Degiovanni, A. Ablative Melting of a Solid Cylinder Perpendicularly Pressed Against a Heated Wall, Int. J. Heat Mass Transfer, 29, 1986, 1407-1415.

[25] Diebold, JP., Scahill, JW. Improved Vortex Reactor System. US Patent 5,413,227, 1995.

[26] Scahill, J., Diebold, J.P. Adaptation of the SERI Vortex Reactor for RDF Pyrolysis, Thermochemical Conversion Program Annual Meeting, 1988.

[27] Diebold, J.P, Scahill, J. Ablative Pyrolysis of Biomass in Solid-Convective Heat Transfer Environments. In: Overend, R.P., Milne, T.A., Mudge, L.K. (Eds.). Fundamentals of Thermochemical Biomass Conversion, Elsevier, London, 539-555.

[28] Miller, R.S., Bellan, J. Numerical Simulation of Vortex Pyrolysis Reactors for Condensable Tar Production from Biomass, Energy Fuels, 12, 1998, 25-40.

[29] Diebold, J., Power, A. Engineering Aspects of the Vortex Pyrolysis Reactor to Produce Primary Pyrolysis Vapors for Use in Resins and Adhesives. In: Bridgwater, A.V. (Ed.). Research in Thermochemical Biomass Conversion, Elsevier, London, 1988, 609-628.

[30] Helleur, R., Popovic, N., Ikura, M., Stanciulescu, M., Liu, D. Characterization and Potential Applications of Pyrolytic Char from Ablative Pyrolysis of used Tires, J. Anal. Appl. Pyrolysis, 58-59, 2001, 813-824.

[31] Lédé, J. The Cyclone: A Multifunctional Reactor for the Fast Pyrolysis of Biomass, Ind. Eng. Chem. Res., 39, 893-903.

[32] Bridgwater, A.V., Peacocke, G.V.C., Robinson, N.M. Ablative Thermolysis Reactor. US Patent Application 2005/0173237, 2005.

[33] Peacocke, G.V.C., Bridgwater, A.V. Design of a Novel Ablative Pyrolysis Reactor. In: Bridgwater, A.V. (Ed.). Advances in Thermochemical Biomass Conversion, Blackie, London, 1994, 1134-1150.

[34] Reed, T.B. Principles and Operation of a Novel ”Pyrolysis Mill”. Proc. Thermochem. Conver. Prog. Ann. Meet., June 21-22, Golden (CO), USA, 1988, 248-258.

Appendix B:

Bench-Scale Reactor Design

1 Introduction

In this appendix the experimental equipment used during the project is treated. This equipment is a simplified bench-scale model of the full-scale Pyrolysis Centrifuge Reactor (PCR) as presented in Appendix H.

The appendix is divided in to three sections. First the specific objectives for constructing the equipment are illustrated. Second, the operational principle of the bench-scale system is presented. Third, the modifications added to the equipment in order to achieve the present version are explained along with the construction drawings. Finally, suggestions for further improvements to the system are presented.

The experimental equipment was designed by the author who provided the construction drawings to the workshop at the department for fabrication. Improvements to the initial design and changes added later as operational experience accumulated were conceived in a close corporation with the workshop where especially Engineer Assistant and Machinist S. V. Madsen has provided invaluable assistance and input.

2 Specific Objectives

The experimental set-up was constructed after the concept for the PCR was conceived with the intension to test its principle of operation. Furthermore, provided the system performed as expected it was also desired to obtain data for an engineering model which could mimic the yield of the flash pyrolysis products with varying operational conditions. Additionally, since the bulk of the flash pyrolysis results research reported in the literature concerns wood, it was desired to construct a system which could increase the general knowledge on straw flash pyrolysis. However, in order to be able to test other raw materials both for comparison with published results but also for more exotic fuels in the future, a flexible system regarding raw materials was desired.

It was decided that the experimental set-up should be sized as a bench-scale system even though the uncertainty regarding the functionality traditionally would have weighed in favor of a lab unit in order to minimize the investment. However, due to the need for very high rotational speeds in order to achieve a significant level of centrifugal acceleration when the PCR is miniaturized, and thereby specialized

knowledge on mechanical construction, this option was disregarded. Furthermore, although a pilot plant was initially planed, a unit which could provide sufficient bio-oil for analysis and small-scale boiler testing was perceived as an attractive option if those plans were not realized. Finally, it was decided to size the unit so it would just fit into an available fume hood where unexpected mishaps would not compromise the safety of the operator and other researchers present at the departmental pilot hall.

3 Operational Principle

In line with the objectives, the bench-scale reactor system was designed as a simplified version of the conceived full-scale PCR described in Appendix H. The simplifications are reflected in the operation and design of the heating system, the char/vapor separation system, and the condensations train. First, in order to provide more accurate control over reactor temperature an electric heating system was selected instead of heating by pyrolysis gas. Second, due to size constraints the condensation system was not integrated into the reactor rotor but was placed more conventionally outside the reactor. Third, in order to accommodate the external condenser system char was not separated from the vapor within the reactor but externally in a catch-pot and a cyclone.

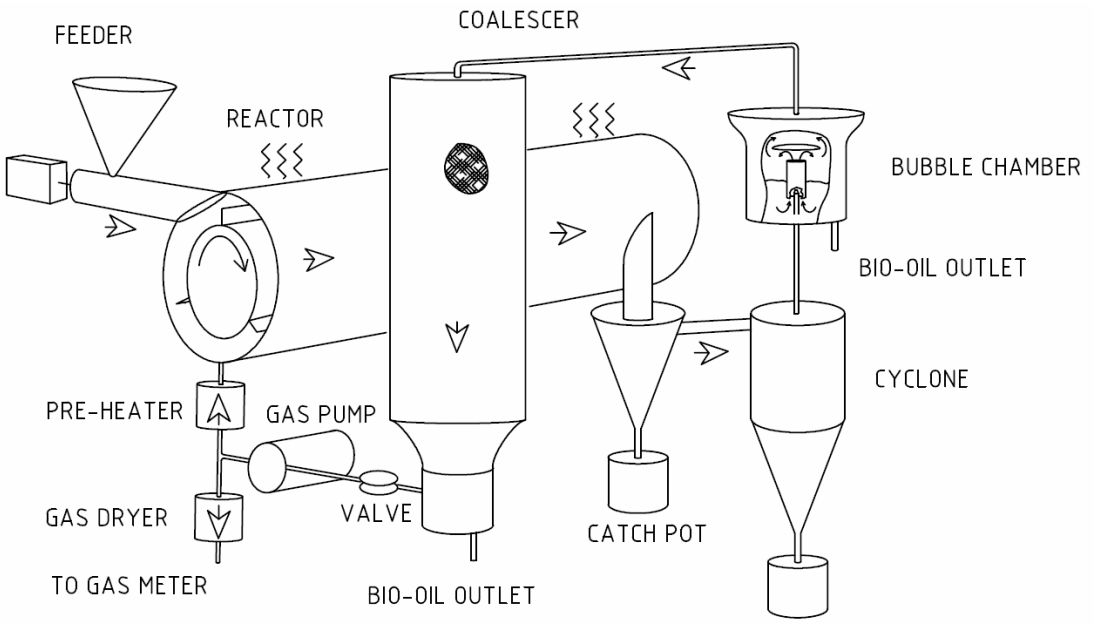

Figure 1: Simplified flow chart for the final version of the bench-scale reactor system.

Figure 1 depicts a simplified flow char for the experimental set-up. Biomass particles are introduced in to the horizontally oriented reactor body by a screw feeder. Within the reactor a three-winged rotor causes the gas to swirl and the suspended particles are forced against the heated reactor wall on which they circulate while they move towards the outlet. At the outlet char particles are suspended in the vapors before they are removed by a change-in-flow separator and a cyclone. The particle-free vapors are then condensed in a direct condenser by bubbling them through a pool of bio-oil maintained at approximately 60 °C by a water cooled coil. In order to remove aerosols from the gas, a coalescer follows before the gas enters a gas pump. Following the pump, a fraction of the gas is preheated before it enters the reactor near the particle inlet whereas produced gas flows to a gas dryer and a gas meter. The system ensures that the reactor and feeder are automatically maintained at atmospheric pressure.

In addition to the elements depicted on Figure 1 utilities and support systems are needed for the system to operate. The reactor rotor is fixed by bearings at either end and these are lubricated and cooled by circulating lubricating oil maintained at 100 °C through them in order to ensure the correct oil viscosity and bearing temperature. Nitrogen is used to displace air from the system before it is operated. Tracing in the form of heating cables are mounted on all piping and components outside the reactor which is in contact with pyrolysis vapors in order to avoid premature condensation. Figure 4 depicts the detailed PI&D diagram for the system.

4 Development Outline

The PCR went through several modifications before the present shape materialized. The development of those subsystems which were changed significantly during the project is summarized below.

4.1 Condensation Train

The condensation train was originally designed as an indirect condenser where the liquid was condensed inside a metal tube cooled on the outside with cooling water. However, during the test runs this arrangement proved to be unsuited as the highest boiling organic fractions would plug the tube near the entrance. Therefore the condenser was modified in order for the vapors to condense on the outside of the tube whereby plugging could be avoided. However, condensation of high boiling

components was favored by this system and the condensed liquid would stick to the surface whereas the lighter components left the condenser in form of aerosols. It was concluded that the optimum system should cool the vapors rapidly in a direct condenser which would not leave the high boiling components any surface to stick to and also provide some scrubbing action in order to combat aerosols and retain the light ends. This lead to the development of the present condenser which was put in place before the experimental program started.

Devising a system to collect the aerosols escaping the condenser also took several tries. First a simple laboratory glass condenser cooled by liquid nitrogen was installed but it proved to be only partially effective. Then a wad of mineral wool was added to the exit of the condenser which was so effective that it worked even without the preceding cryogenic cooling. Accordingly, in order to avoid the hassle of the liquid nitrogen, the present system was constructed in which the gas after leaving the bubble chamber at approximately 60 °C is somewhat cooled in the top section of the un-insulated coalescer and then passes through a bed of ROCKWOOL® mineral insulation material where coalescing takes place. After a few runs this material is soaked in liquid and will begin to discharge the collected aerosols to a conical flask mounted below. This system was also installed before the experimental program was started.

4.2 Char Separating System

The initial char separation consisted merely of a traced catch pot mounted directly below the reactor exit where a change of flow direction was supposed to deposit the char particles. The test runs showed that a significant amount of char was not removed by this simple system and a cyclone was added after the catch pot before the experimental program was started in order to clean the vapors more thoroughly.

Following the first part of the experimental program, the contact between char and vapors in the catch pot was found to be partly responsible for the disappointing yields of liquid organics. Furthermore, as the catch pot was mounted directly on the reactor the system had to cool down before it could be removed for emptying which limited the maximum duration of an uninterrupted run to about 15 minutes due to the holding capacity. However, since the modified system had proved to work satisfactory the principle of operation was retained but the catch pot was substituted with a change-in-

flow separator from which the char was continuously removed by gravity and stored in a glass char collector below. At the same time an optimized cyclone with an extended solid exit pipe and a glass char collector was put in place. Both char collectors were fitted with stop valves whereby emptying could be accomplished during a run by simply interrupting feeding for the short time it takes to replace the collectors. This system was used for the later experimental runs.

4.3 Reactor Heating

Initially the reactor was heated by an electric tubular heating element wrapped around the reactor pipe and controlled by one temperature probe located at the center of the pipe and a PID controller. At the end of the initial experimental runs it was decided as part of the effort to improve liquid organics yield to check the temperature distribution on the reactor pipe. It was found that the temperature was substantially below the set point at either end of the reactor (*i.e.* due to heat loss from the flanges) and that the system had to be optimized in order to obtain reliable data. Therefore, four independent heating zones were added, each controlled by a separate PID controller, and the insulation on the flanges was improved. This system was used for the later experimental runs.

4.4 Reactor Pipe and Rotor

After the char removal system had been modified the glass char collectors revealed that char would exit the reactor in short bursts rather than continuously and it was decided to check the solid flow within the reactor. For this purpose a glass copy of the reactor pipe was made and cold runs were conducted. Both with the naked eye and on the movies made with a high speed camera it could be observed that the particles accumulated at the reactor entrance. When a certain amount of material had accumulated a ring of material would shoot down the reactor pipe (see Figure 2) which could explain the bursts of char observed during operation. This flow pattern where the main part of the reaction took place in a thick relatively cold layer contributed to the disappointing results mentioned above and it was decided to modify the system in order to eliminate the accumulation at the entrance and use the entire surface of the reactor more efficiently. After testing several modifications by gluing strips of plastic to the glass reactor it was found that inserting thin rings into the reactor tube would slow down the speed of the material as it traveled down the tube.

The accumulation at the entrance was eliminated by fitting a ring to the rotor whereby the excess space between the entrance and the end flange was removed and by adding a helix ring on the reactor tube near the entrance which guided the material in the flow direction. The steel reactor tube was modified with these changes as seen in Figure 3 and in order to maintain the same distance between the fitted rings and the rotor wings as had previously been between the wings and the reactor wall, the rotor wings were machined. These modifications were in place during the later experimental runs.

Figure 2: Picture of the material flow in the unmodified glass reactor taken with an exposure time of 1/4000 s, feed rate 23 g s^{-1}, and rotor speed of 14,784 rpm. The feed port is to the left and a "ring" of material (below the timer) has just separated and is rapidly moving towards the outlet in the lower right corner (out of view). In this picture the rotor has been fitted with end rings that limit the accumulation of material to the left of the feed port.

4.5 Final Version

The main specifications for the final version of the bench-scale reactor system which was used for the later part of the experimental program and the pilot plant runs are given in Table 1. Figure 4 to Figure 10 show the detailed construction drawings for the system.

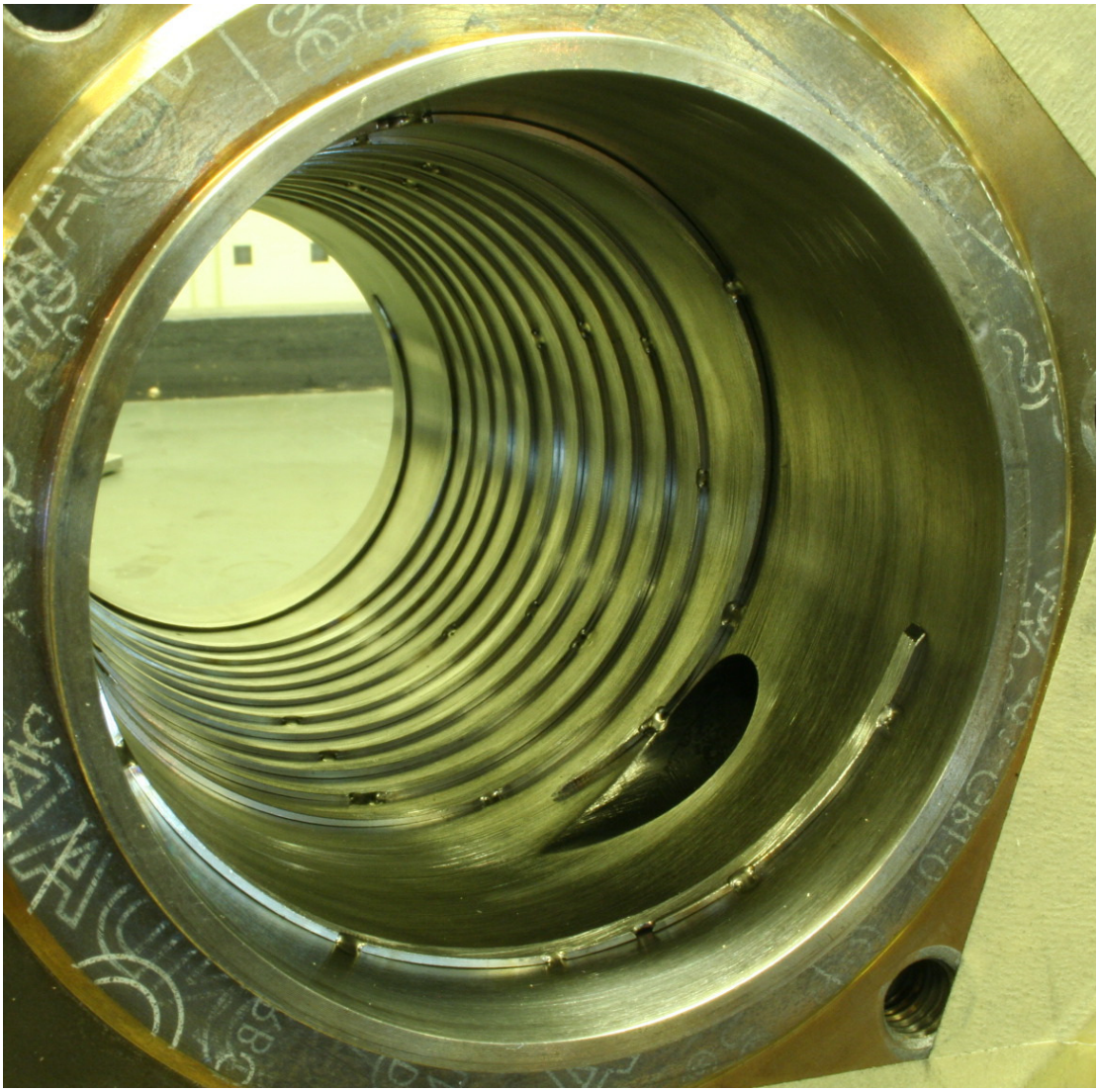

Figure 3: View into the reactor tube after 202 hours of operation. Notice the entrance port in the foreground, the helix strips at both ends welded to the wall to guide the flow towards the exit, and the strip rings welded to the wall to slow axial velocity.

Table 1: Specifications and main dimensions for the experimental set-up.

Reactor Specifications	**Value**	**Unit**
Overall pipe length	200	mm
Pipe length, entrance to exit (c-c)	137	mm
Pipe inner diameter, avg.	81.4	mm
Pipe particle-swept area	$3.50 \cdot 10^{-2}$	m^2
Rotor diameter	60.3	mm
Wall-to-rotor-wing clearance, min	2.2	mm
Motor, rated power max	0.37	kW
Rotor speed, max	$2.0 \cdot 10^4$	rpm
Centrifugal force at wall, max	$1.8 \cdot 10^4$	g
Reactor Heating	Horst heating cable HSQ, 4 zones	
Zone split over full pipe length	3:1:3:4	(length)
Cable temperature, max	900	ºC
Heating power, all zones	1870	W
Tracing Temperature, max	450	ºC
Gas preheater temperature, max	540	ºC
Gas preheater power	750	W
Temperature Sensors	K-type thermocouple	
Accuracy @ 500 ºC	±2.0	ºC
Gas Pump	Rietschle Thomas VTE8 (rotary vane)	
Reactor gas volume	0.44	L
System total hot gas volume	0.50	L
Feeder	AccuRate MOD304M with centerless helix	
Feed rate (straw particles), max	2.4	kg/h
Gas Meter	IGA AC5M, positive displacement, temp. comp.	
Gas flow, max	5	nm^3/h
Accuracy	±0.5	% vol.

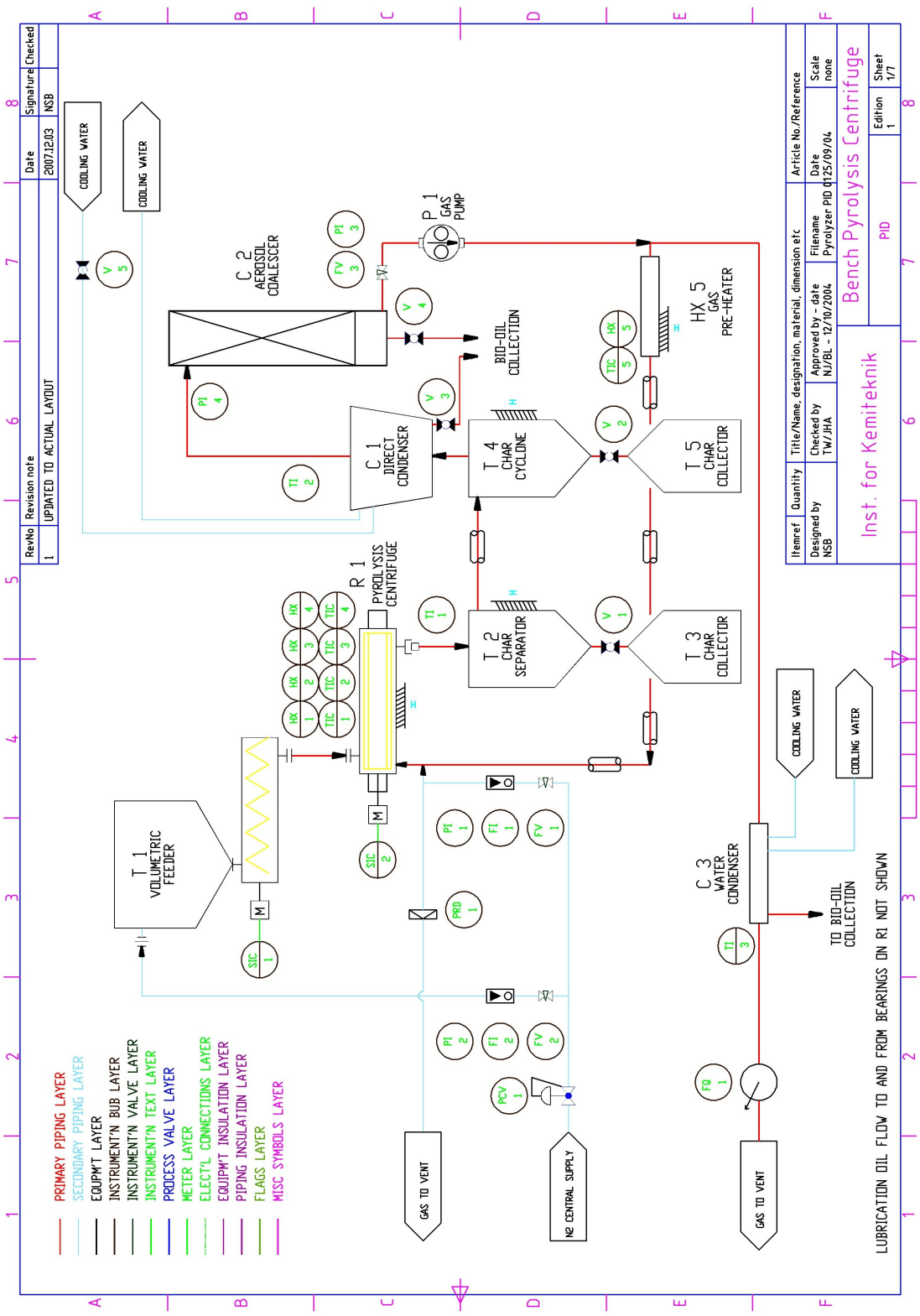

Figure 4: Pyrolyzer construction drawings: P&ID Diagram.

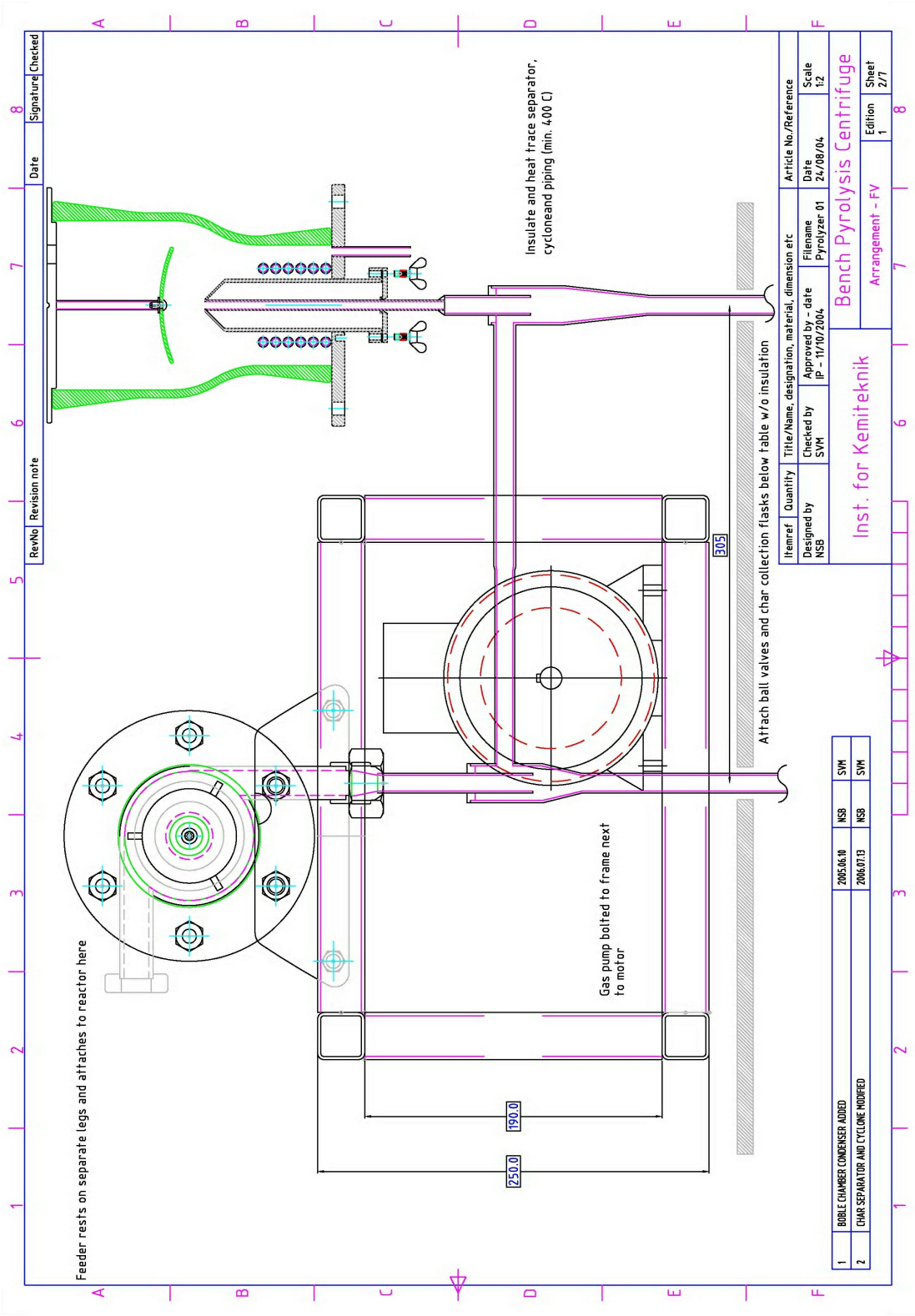

Figure 5: Pyrolyzer construction drawings: Front view.

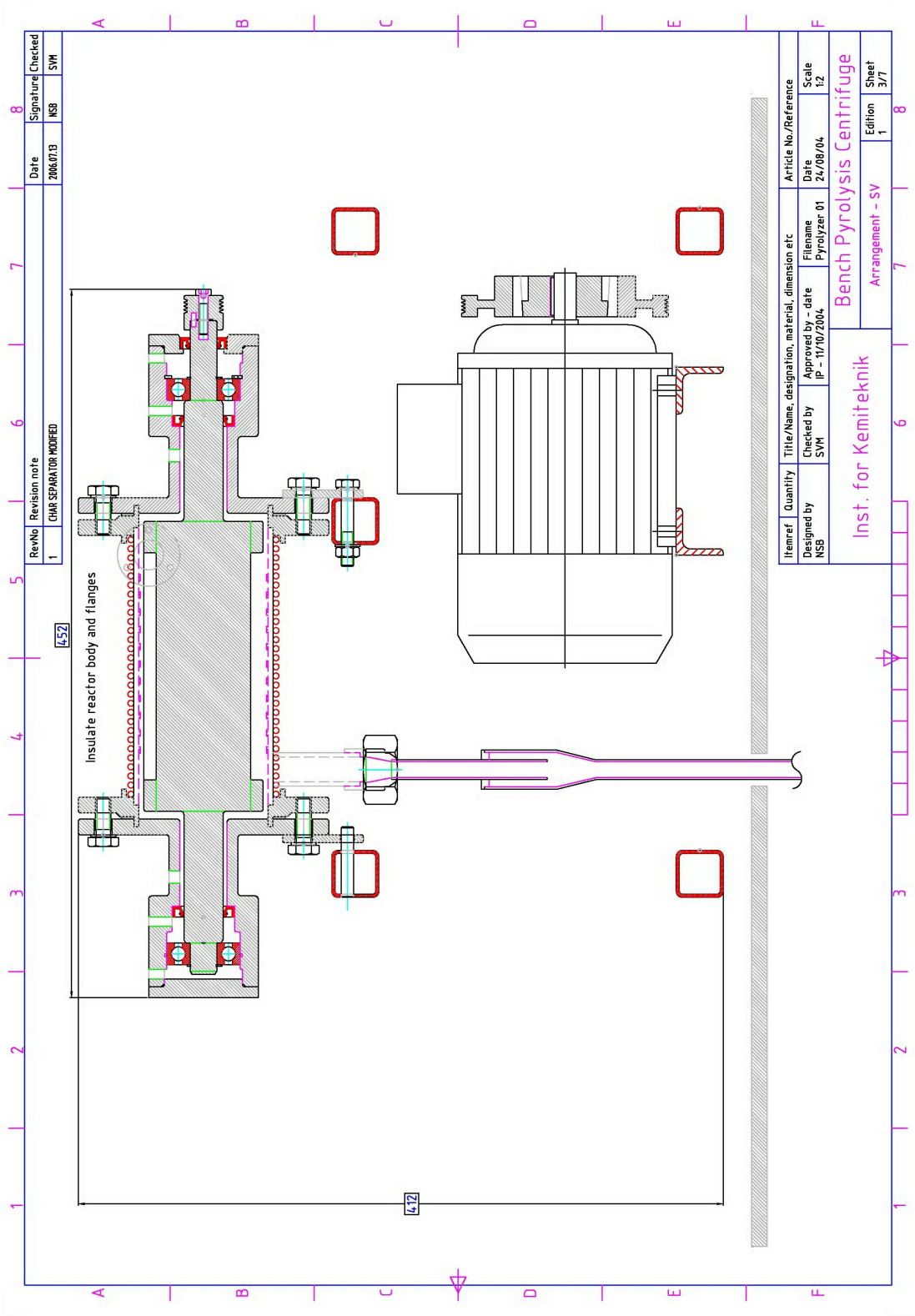

Figure 6: Pyrolyzer construction drawings: Side view.

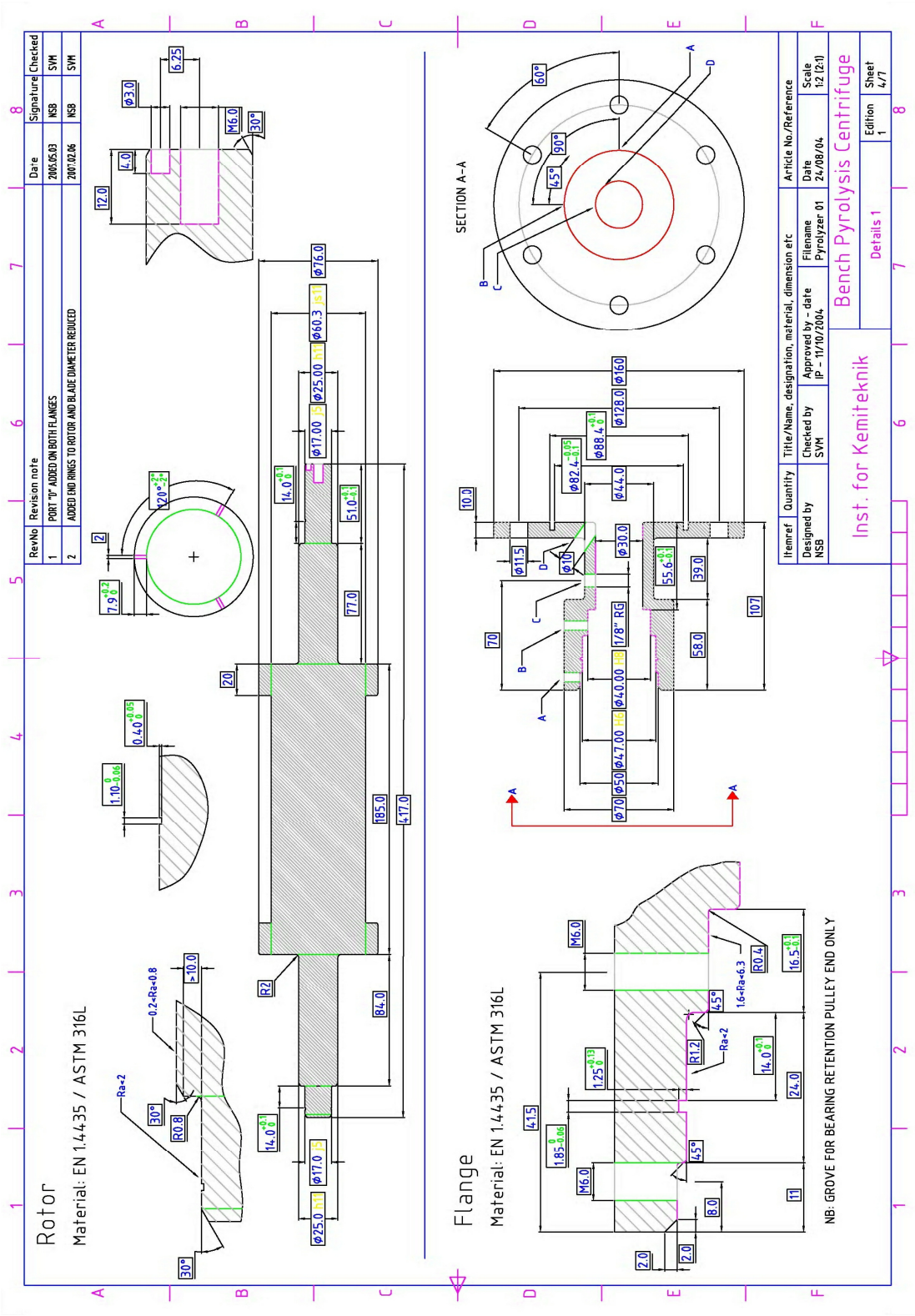

Figure 7: Pyrolyzer construction drawings: Rotor and end flange details.

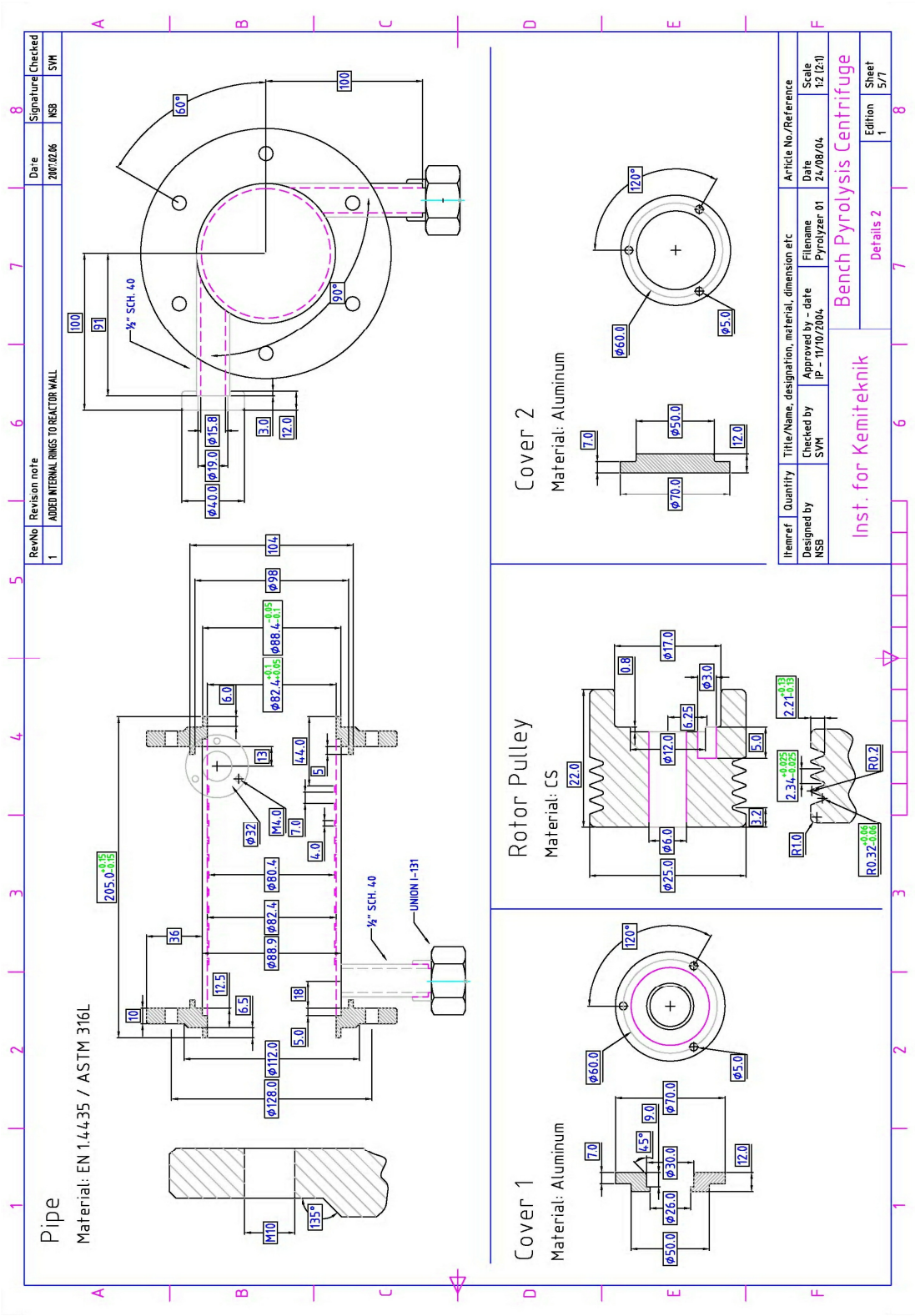

Figure 8: Pyrolyzer construction drawings: Reactor pipe, bearing covers, and pulley details.

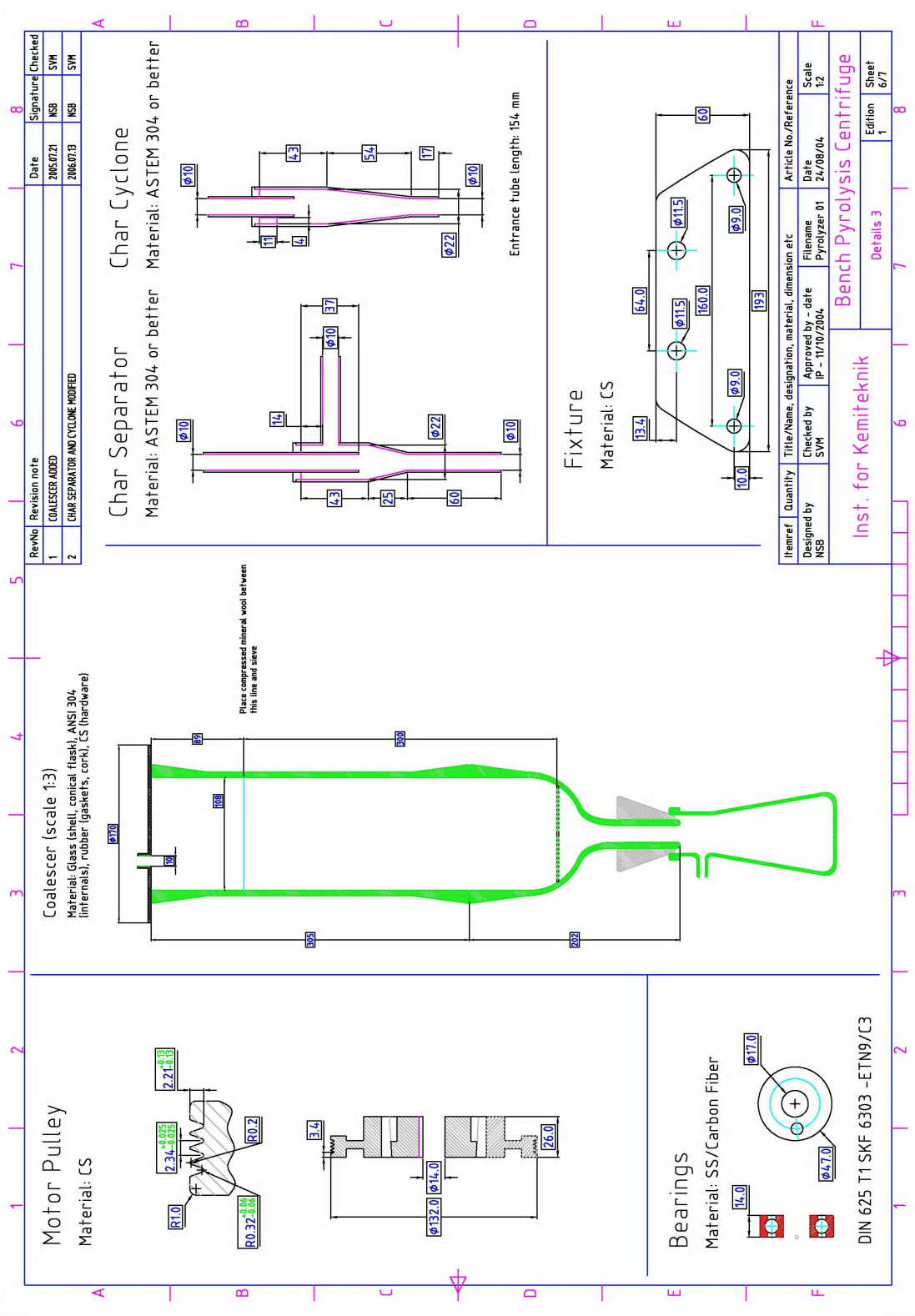

Figure 9: Pyrolyzer construction drawings: Motor pulley, bearings, coalescer, char separator, char cyclone, and reactor support details.

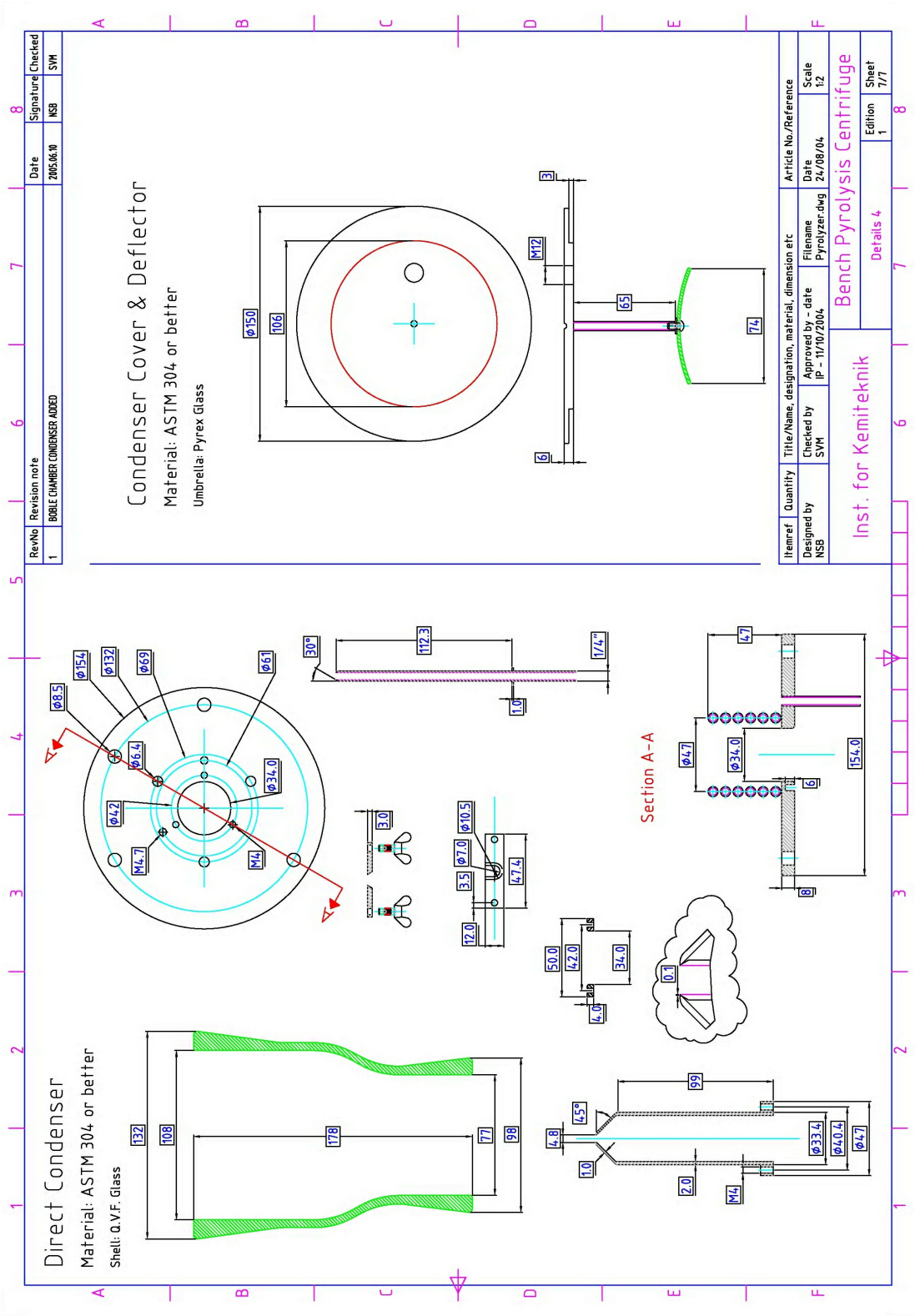

Figure 10: Pyrolyzer construction drawings: Direct condenser (bubble chamber) details.

5 Further Improvements

The optimization of the experimental set-up has resulted in a reactor system which is suitable for collecting data for yield modeling and the production of smaller quantities of products. However, if more than a few hundred grams of bio-oil or char is desired it needs to be produced over several runs as the vapor nozzle in the bubble chamber will plug up after approximately 20 minutes of operation. The char plug develops at the nozzle outlet due to heat conduction whereby the tip of the traced nozzle cools below the condensation temperature of the higher boiling components. A simple suggestion for solving this issue is to install a nozzle with a larger diameter than the present size of 4 mm whereby the formation of char eventually will come to a hold due to its insulating effect without affecting the flow in the nozzle significantly.

6 Conclusions

A simplified version of the PCR was constructed in the form of a bench-scale experimental unit. After several modifications the system performs well and is suitable for the production of smaller quantities of product and for obtaining data for yield modeling. Only a minor modification is needed in order to prepare the system for runs lasting more than 20 minutes whereby larger amounts of product may be obtained in a single run.

Appendix C:

Ablative Flash Pyrolysis of Straw and Wood: Bench-Scale Results

ABLATIVE FLASH PYROLYSIS OF STRAW AND WOOD: BENCH-SCALE RESULTS

Bech, N.; Jensen, P.A.; Dam-Johansen, K.
Department of Chemical Engineering, CHEC Research Centre, Technical University of Denmark
Søltoft Plads, Building 229, DK-2800 Kgs. Lyngby, Denmark

ABSTRACT: A novel ablative reactor, the Pyrolysis Centrifuge Reactor (PCR), is presented and bench-scale results with wheat straw and pine wood feedstock reported. In the tubular reactor, biomass particles are forced against the heated reactor wall by the centrifugal force caused by the circular motion of the particles. Particle residence time is controlled by solid feed rate. In the investigate temperature (480 to 620 °C) and centrifugal force (4,900 to 17,000 G), the yields of liquid, char and gas are relative insensitive to these parameters. The sluggish yield response is attributed to a non-uniform temperature profile on the reactor pipe, whereby the particle undergoing pyrolysis may do so partially through pore formation promoting char and gas formation. In addition, heterogeneous tar cracking also seems to influence the observed behavior. The presented results give promise to a reactor that with due adjustments will deliver good liquid yield from biomass at a high area specific feed rate without carbon build-up on the active surface and excessive mechanical wear. Also, an empirical correlation between water content in the liquid product (bio-oil) as measured by Karl-Fisher titration and the mixtures refractive index is presented.
Keywords: Flash pyrolysis, Straw, Bio-oil

1 INTRODUCTION

With flash pyrolysis organic materials may thermally be decomposed into liquid, gaseous and solid fuels. Due to the attractive features of liquid fuels, the aim is universally to achieve conditions where the energy content of the parent material is concentrated in this fraction, commonly referred to as bio-oil or biocrude. Although the liquid can not substitute motor vehicle fuels without further upgrading, the simplicity and relative good yield of the process makes it attractive as a route for utilizing bulky and otherwise difficult fuels in applications formerly unable to operate on bio-fuels. Converting wheat straw or other high-ash herbaceous waste into a practically ash-free liquid by flash pyrolysis appears especially promising as these fuels contain volatile inorganic fractions known to cause slagging and corrosion in boilers [1-3].

A multitude of reactor designs for carrying out flash pyrolysis of biomass with the aim to achieve a high liquid yield on a large scale has been proposed over the past three decades [4, 5]. Generally, the configurations may be subdivided into shallow transported beds (atmospheric and vacuum) [6, 7], fluid beds [8, 9], and ablative reactors [10-15]. The latter have received a great deal of attention due to the promise of low char yield as initially demonstrated by the hot wire [16] and rotating disk [17] experiments. However, to this date the fluid bed reactors have been the technology of choice for facilities engaged in bio-oil production on commercial scale.

Ablative reactor development has pursued several directions. In the Vortex [10] and Cyclone [11] reactors, biomass particles are suspended in a flow of high-velocity gas which after tangential introduction in the reactor forces the particles against the heated reactor wall by centrifugal action. Despite their inherent mechanical simplicity, both reactors require large volumes of motive gas relative to the biomass feed and the area specific feed rate must be maintained below a critical value in order to avoid build-up of carbon residue on the reactor wall [18]. Other reactors, including the Pyrolysis Mill [12] and the Ablative Plate or Tube reactors [14, 15], have resolved these issues by utilizing mechanical systems in the form of mill stones or scrapers, respectively, to force the biomass against the reactor wall. This obviously introduces mechanical complexity and wear to components.

This article reports the results obtained with the novel ablative Pyrolysis Centrifuge Reactor (PCR) developed in an attempt to exploit the potential benefits of ablative pyrolysis without the above drawbacks. Focus is on the yield of pyrolysis products for wheat straw and pine wood feedstock with changes to the operational parameters and a discussion of the observed results. Further, a simple method for determining the water content in pyrolysis liquids by measurement of the mixtures refractive index is presented.

Table I: Analysis of wheat and pine samples

			Wheat Straw	Pine Wood
Particle Size (MMD)		µm	633	632
Particle Size (PAMD)		µm	316	314
Proximate	Moisture	% wt.	5.8	7.1
	VM	% db.	75	85
	Ash	% db.	6.8	0,50
	HHV	MJ/kg db.	18.4	20.5
Ultimate	C	% daf.	49.2	49.9
	H	% daf.	6.39	6.30
	S	% daf.	0.21	<0.022
	N	% daf.	1.2	<0.1
	O (by difference)	% daf.	43.0	43.7
Ash Composition*	Cl	% wt.	9.3	2.4
	Si	% wt.	21	14
	Al	% wt.	0.44	1.7
	Fe	% wt.	0.43	1.8
	Ca	% wt.	5.7	28
	Mg	% wt.	1.4	5.9
	Ti	% wt.	0.04	0.10
	Na	% wt.	0.32	0.55
	K	% wt.	27	7.3
	P	% wt.	2.2	1.0
	O (by difference)	% wt.	32.2	37.4

db.: dry basis; daf.: dry, ash-free basis; MMD: Mass Mean Diameter; PAMD: Projected area mean diameter.
** Ash composition measured on untreated straw.*

2 MATERIALS

Wheat straw and pine wood pellets were crushed in a Retsch SM 2000 cutter mill fitted with a 4 x 4 mm screen and fractions above 1400 µm were removed by sieving. Table I displays the proximate and ultimate analysis of the wheat and pine samples in addition to the composition of the inorganic constituents. Wheat straw particles tended to be spherical whereas the pine wood particles were more cylindrical (splinters). Average particle sizes were determined by sieve analysis.

3 EXPERIMENTAL APPARATUS

3.1 Bench Reactor System

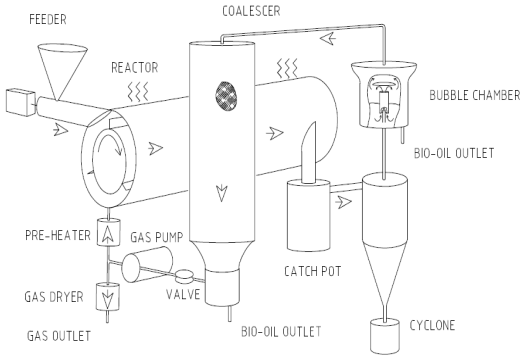

Figure 1: Experimental bench reactor system.

Wheat and pine particles were treated in the experimental set-up depicted schematically in figure 1. A variable rate screw feeder carried the feed material to the tangential inlet on the horizontally oriented ø 82 x 200 mm tubular reactor. Within the reactor a solid rotor with three radial wings having a wing-to-wall clearance of 2 mm turned at a fixed speed between 10,000 and 20,000 rpm creating a centrifugal force at the pipe wall of nominally 4,900 to 17,000 G. At the inlet, the wing-to-wall clearance was increased by 6 mm to form an acceleration zone in order to minimize the damage to the particles by collision with the wings upon entry. Heat was supplied to the reactor wall by a single electric resistance heater coiled around the pipe and controlled by a digital PI controller receiving a signal from a K-type thermocouple placed in a grove machined into the outside of the pipe at a central position. A temperature deviation from the set-point of less than 5 °C was generally achieved for the controlling thermocouple. Figure 2 shows the realized axial temperature profile over the reactor surface. For a more detailed description of the PCR, please refer to Bech *et al.* [19, 20].

Pyrolysis vapors and char evolved upon contact with the hot wall traveled axially to a catch pot, where part of the char was deposited, followed by a cyclone for smaller char particles to be separated from vapors. Catch pot, cyclone and piping were heat traced to maintain a surface temperature of about 420 °C to avoid premature condensation. The particle-free gas was cooled rapidly by bubbling it through a pool of liquid obtained from earlier runs, in which the temperature was restricted to 55 to 65 °C by means of a pipe coil cooled by tap water. Typically 40 pct. of the collected liquid by weight was condensed in this bubble chamber and the aerosol-laden gas was further treated in a coalescing filter consisting of a vertically oriented ø 150 x 400 mm pipe section loosely packed with fibrous commercially available rock wool thermal insulation. In the coalescer, the aerosols accumulated to larger droplets and traveled downward due to gravity and gas flow and were collected.

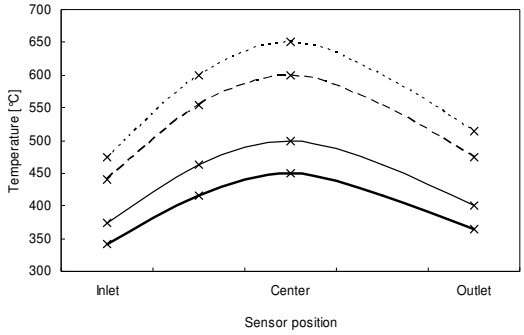

Figure 2: Temperature profile on reactor pipe with position and set point (equal to center value).

Gas recirculation was maintained by a dry-running rotary vane vacuum pump in order to control the gas residence time. Reactor, feeder, catch pot, and cyclone were kept at atmospheric pressure whereas the forced flow of gasses created a vacuum of typically -150 mbar within the bubble chamber and coalescer. The recirculation rate was controlled by adjusting a valve on the pump suction side, and an electric heater was placed on the pressure side in order to preheat the gas to 400 °C before reintroducing it axially into the reactor through the end-flange near the particle inlet. Excess incondensable pyrolysis gas was purged to a condenser cooled by tap water to achieve a temperature of 22 to 24 °C, before measuring the flow in a temperature compensated gas meter and collecting it in a gas bag. The molecular weight of the incondensable gas was determined by weighing a 5 L gas bag on an analytical scale and compensating for air buoyancy by using pure nitrogen as reference. The influence of the initial purge nitrogen was compensated for by assuming the nitrogen would leave the system as in a perfectly stirred reactor. The gravimetrical method for gas molecular weight determination was tested with both pure carbon dioxide and oxygen which indicated a precision of ± 2 pct.

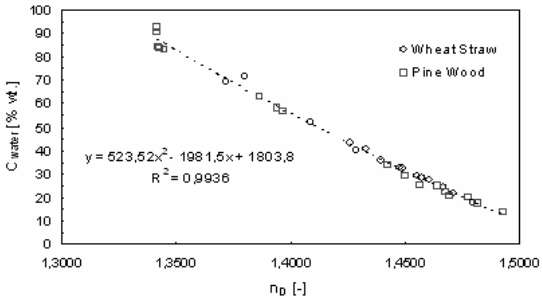

Figure 3: Water content determined by Karl Fischer titration with refractive index at 30.0 °C for wheat straw and pine wood tar/water mixtures.

3.2 Water–in-Liquid Measurement

The relationship between water content in the liquid product and the refractive index was determined by correlating Karl Fisher titration results with

measurements of the refractive index by a Bellingham & Stanley Abbe 60 refractometer (estimation to within ±0.0002). Figure 3 shows the obtained relationship and the empirical correlation given by:

$$C_{water} = 523.52(n_D)^2 - 1981.5(n_D) + 1803.8 \qquad (1)$$
$$R^2 = 0.9936$$

4 EXPERIMENTAL PROCEDURES

4.1 Pyrolysis Experiments

A 500.0 g sample of feed material was placed in the feeder and the system was purged with nitrogen. The heater was turned on and after the reactor had reached the temperature set point and the rotor speed had been adjusted, feeding was started at approximately 24 g min^{-1}. Due to semi batch operation of the catch pot and cyclone, feeding could not be extended beyond 20 minutes and a value of 14 minutes was used for all runs. Steady state operation was achieved after three to four minutes of feeding as witnessed by the stabilization of temperature readings.

After the system had cooled, liquid and char yield in addition to spend raw material were determined gravimetrically. Gas yield was calculated on the basis of the measured gas volume and the molecular weight measurement obtained immediately after the run in order to minimize the potential effect of light gasses diffusing through the gas bag. Liquid samples were filtered through Whatman #4 filter paper on a Buchner funnel and the residue re-suspended in 200 ml ethanol, filtered again, and washed with 100 ml acetone. After drying under an infrared light bulb for 45 minutes, the residual mass (typically 1.5 pct. or less of total liquid) was determined and added to the char yield. Average mass balance closure was 93.9 and 97.3 pct. for wheat and pine experiments, respectively. Water content in the liquid products from the bubble chamber and the conical flask below the coalescing filter was determined by refractive index measurement and eq. 1. The fraction left in the coalescer was assumed to be similar in composition to the fraction condensed in the bubble chamber and was determined by weighing the coalescer before and after the run.

4.2 Cold Flow Runs

In order to measure reactor particle residence time the char catch pot, cyclone, and the condensation train were removed from the reactor and substituted by a cyclone of the improved Stairmand design developed by Zhu and Lee [19]. A flask was coupled to the cyclone particle exit port by a flexible coupling and placed on a scale equipped with continuous logging. After adjusting rotor and gas velocity, feeding of either wheat or pine particles was started and continued until approximately 10 g had been collected in the flask. As the time-weight curve showed a linear response, the hold-up time was determined as the time of intersection between a linear regression curve and the abscissa. For each set of conditions, the experiment was repeated 10 times and an average hold-up time taken to represent the particle residence time. In the cold flow experiments the reactor was unheated and air at ambient temperature was used as purge gas.

5 RESULTS

5.1 Particle Flow in Reactor

The cold flow particle residence time measurements presented in figure 4 did not show any systematic variation with neither rotor speed nor gas velocity (*i.e.* gas residence time) but was related to the inverse feed rate according to the equation:

$$\tau_b = m_b Q_b^{-1} \qquad (2)$$

A good description was observed for Q_b^{-1} greater than ~7,500 and ~25,000 s kg^{-1} for pine and wheat, respectively, with m_b and m_b/a equal to $5.5 \cdot 10^{-3}$ kg and $102 \cdot 10^{-3}$ kg m^{-2} in both cases (full line, figure 4). However, for higher feed rates the residence time deviated positively from eq. (2), apparently due to increasing particle loading m_b/a . It was concluded that the axial particle movement across the reactor surface took place through a succession of particle-particle collisions whereby particles were pushed across the surface in plug flow. Accordingly, particle residence time was controlled by the feed rate directly and by affecting the specific particle loading on the reactor surface.

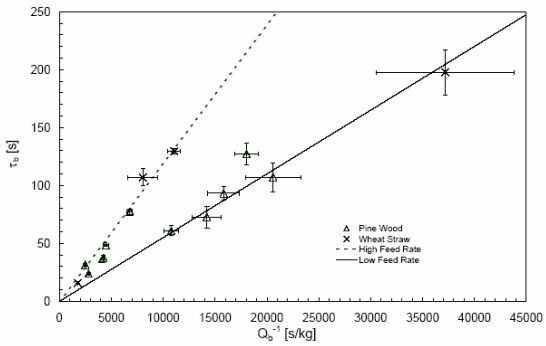

Figure 4: Particle residence time obtained in cold flow experiments with inverse feed rate for pine wood and wheat straw particles.

5.2 Visual Observations

Following six hours of hot operation (including heat-up and shut down) the reactor was dismantled for inspection. The reactor tube had a brown color typical of stainless steel heated to 500 to 600 °C and appeared from the smooth touch and fine scratches to have been polished by the biomass particles and associated grains of sand. No signs of carbon deposits on the hot active surface were observed. On the rotor body, thin (approximately 1 mm) flakes indicated that some tar had condensed and later carbonized but was slung off before a more extensive layer would build up. It was noted that tar condensation on the solid rotor could have been caused by allowing insufficient time for the rotor to reach 400 °C before feeding was started. Except for the particle acceleration zone, the wing tips did not appear to have been in contact with the particles as they were covered by a faint vanish-like material.

5.3 Yields

Yields of liquid, char and gas were expected to be influenced by reactor temperature, rotational speed of the rotor (*i.e.* centrifugal force), and gas residence time.

However, examination of the results reported in figure 5 revealed that for both feedstocks the effect of centrifugal force was undetectable and trend lines were drawn with respect to temperature only. Even though the effect of reactor temperature on yields was not expected to follow a linear empirical relationship, the trend lines were observed to provide a rather good fit to the observed data. For liquid yield from wheat and pine, the reactor temperature had a positive effect as yield increased 0.8 and 0.7 pct. (daf of feedstock), respectively, for 100 °C increase in temperature. However, liquid yield for pine was 60.8 pct. at 550 °C compared to 52.8 pct. for wheat and this difference was reflected in the gas yields which were projected to be 14.0 and 21.3 pct., again with only a slight effect from reactor temperature. The same was true for char but here the feedstock difference was comparable smaller with pine giving 21.9 pct. and wheat 22.5 pct. at 550 °C.

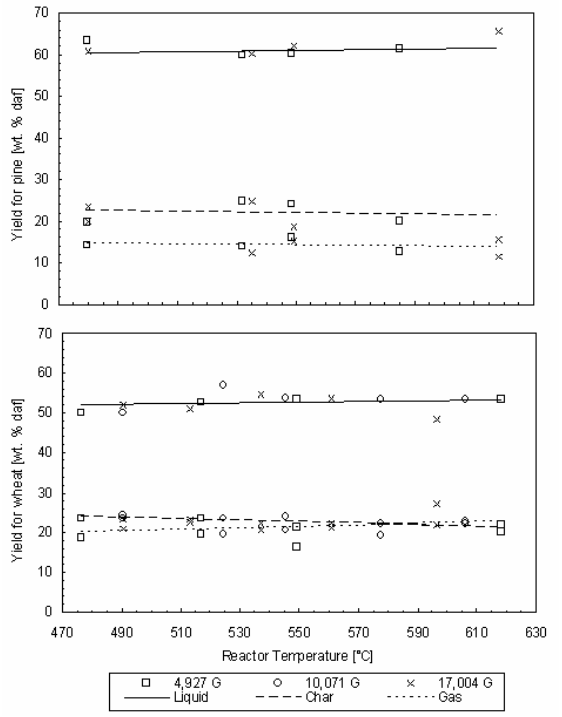

Figure 5: Yield of liquid, char, and gas for pine (top) and wheat with reactor wall temperature and centrifugal force.

5.4 Water Content in Liquid Product

As shown in figure 6 the water content of the liquid product did not wary with reactor temperature. However, a noticeable difference was observed between wheat and pine as liquid obtained from the former contained 40 pct. more water. It was observed that the scatter for data in figure 6 is comparable larger than that observed for yield data in figure 5. This scatter did not seem to originate from errors introduced by the refractive index water measurement technique employed, but was likely caused by the tendency of the liquid to separate into two phases if the water content was above approximately 35 wt. pct. Thus, for high water-content samples, separation was suspected to have caused inaccuracies due to difficulties in obtaining a representative sample even after thorough homogenization [20].

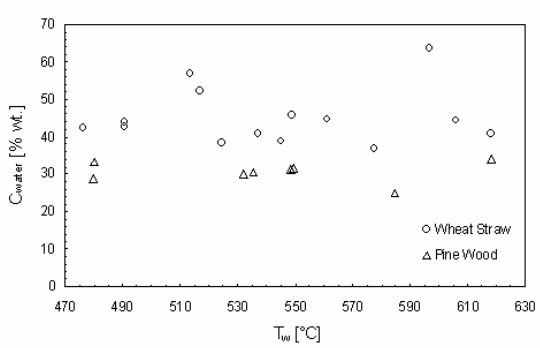

Figure 6: Water content in the liquid product from pyrolysis of wheat straw and pine wood with reactor wall temperature.

5.5 Char Analysis

Wheat char obtained from the catch pot proved to be highly reactive and would self-ignite within minutes when exposed to air, even if allowed to cool to room temperature overnight under a nitrogen blanket. In contrast, wheat char from the cyclone and pine char (irrespectively of origin) did not show any sign of self-ignition. The reactivity of the wheat char was thought to be related to a high specific surface area but as table II displays, the analyzed values were two to three orders of magnitude lower than that generally observed for activated carbon. The tendency to self-ignition was probably caused by the high ash content and concentration of alkali salts of the wheat char as the inorganic constituents in straw are known to increase the pyrolytic reactivity [23].

The content of volatile matter (table II) in wheat and pine chars was relatively insensitive to reactor conditions and indicated that the chars roughly had the same volatile matter content left after pyrolysis irrespectively of feedstock. However, due to the considerably higher ash content of the wheat chars, it appeared that the organic fraction left in this char was noticeably more volatile as reflected by the lower fixed carbon content. To ensure this difference did not reflect different ash composition and thus volatility, the ash retention α was calculated:

$$\alpha = Y_c \frac{Ash_c\left(100 - Ash_b\right)}{Ash_b\left(100 - Ash_c\right)} \qquad (3)$$

Ignoring sample #6, which seemed to be erroneous, the ash retention for pine was approximately 77 pct. and that for straw 91 pct. The cause for the lower retention for pine was not apparent but was suspected to be the result of the increased sensitivity introduced by the low initial ash content or the less than 100% mass balance closure. In any case, Knudsen *et al.* [2] found that for fixed bed pyrolysis of wheat straw up to 600 °C, approximately 47 pct. of the initial chloride would be released from the organic matrix. As chloride constituted 9.3 wt. pct. of the straw ash this seemed to provide an explanation for the fate of the major part of the disappeared ash. Further, Knudsen *et al.* found that for pyrolysis up to 950 °C, another 20 pct. of the chloride in addition to 14 pct. of the potassium, summing in our case to 6 pct. of the ash content, would disappear. As the volatile content was measured at 950 °C, only up to 4 pct. of the measured volatile matter could therefore be attributed to further

Table II: Analysis of wheat and pine chars.

Sample ID	Feed	T_w [°C]	G [-]	BET [m^2 g^{-1}]	VM % db.	Ash % db.	FC % db.
#1	Wheat	476	4,927	1.3	32.8	21.8	45.4
#2	Wheat	537	17,004	1.2	31.2	22.0	46.8
#3	Wheat	606	10,071	1.5	28.4	23.3	48.3
#4	Pine	480	4,927	-	32.9	1.68	65.4
#5	Pine	549	17,004	-	34.1	1.74	64.2
#6	Pine	618	17,004	-	32.0	2.54	65.5

high temperature ash evaporation. For pine char, the low chloride and potassium concentrations combined with low ash content implied that ash evaporation was insignificant. This indicated that the lower fixed carbon content of straw char did in fact reflect higher volatility of the residual organic material. It could therefore be noted that for pine, the total volatilization (*i.e.* that observed during pyrolysis plus that measured as volatile matter in the char) was equal to that measured by volatile matter determination on the virgin material. For straw, the total volatilization on the other hand was approximately 80 pct. compared to 75 pct. when measuring volatile matter content on the untreated straw. These observations were seen as indicative for that straw char yields below that predicted by the fixed carbon content of the raw straw were obtainable.

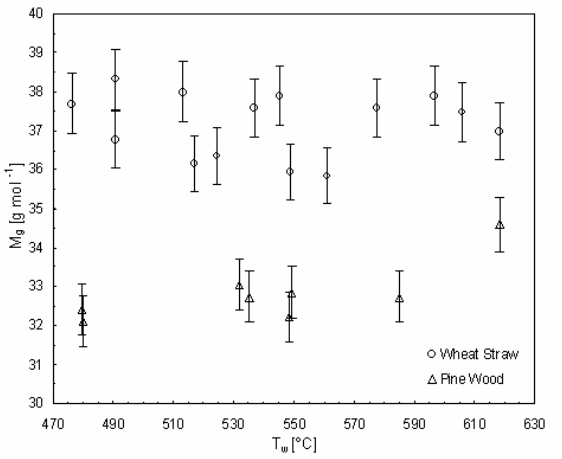

Figure 7: Molecular weight of pyrolysis gas from wheat straw and pine wood pyrolysis with reactor wall temperature.

5.6 Gas Molecular Weight

The molecular weight of the pyrolysis gas (figure 7) proved to be unaffected by reactor temperature but a detectable difference was observed between wheat and pine as the average gas molecular weights were 37.2 and 32.6 g mol^{-1}, respectively. The data scatter was presumed to be related to the analytical method as two standard deviations, or approximately the 95 pct. confidence interval, for both wheat (4 pct.) and pine (5 pct.) were comparable to the indicated precision of the method. The observed difference between the pyrolysis gases produced from the feedstocks was thought to be the result of a change in the gas composition, especially the CO_2/CO ratio, caused by the high potassium content of wheat straw [24].

6 DISCUSSION

6.1 Particle flow

To evaluate whether particles were distributed on the reactor surface in a mono layer, a metal plate was subjected to the same area specific particle loading observed in the low feeding rate regime. Even though it was difficult by hand to evenly distribute the particles due to the large variation in sizes, it did give the visual impression that the reactor surface was less than 50 pct. covered by material. Another way to reach this conclusion is to compare the weight of a mono layer of particles with the amount contained within the reactor during the experiment. Taking the true density for both wheat and pine to be 700 kg m^{-3} [25], a continuous layer of particles with a thickness equal to the particle Projected Area Mean Diameter (PAMD) would have a specific mass of $221 \bullet 10^{-3}$ kg m^{-2} or roughly double that observed for lower feed rates. As can be seen from the dotted line in figure 4, this specific loading, effectively forming a mono layer without particle spacing, gives a good fit at higher feed rates. For the investigated feed rates the particles will therefore form a mono layer on the reactor surface and the surface coverage will attain asymptotic values for both high and low feed rates. The observed difference between wheat and pine particles with regard to the transition between high and low feed rate regimes can be speculated to be related to the exact particle morphology, as the mean diameters for the two feedstocks (table I) are nearly identical.

It should be pointed out that the fixed rotor tip/reactor wall clearance was larger than the maximum particle size, and the particle motion across the reactor wall could therefore not have been caused by impact between particles and rotor, as also indicated by the visual inspection. Accordingly, circular particle motion must be the result of the spinning gas volume in a similar way as in the both the Vortex and Cyclone reactors. Diebold [26] described the motion of wood chips in the former to be visually comparable to cars traveling at the same velocity down a highway, as the particles would swirl through the tubular reactor in widely spaced discrete helical bands. This behavior was apparently caused by the flow pattern of the motive gas which was similar to that observed in Ranque-Hilsch vortex tubes [10]. In the cyclone reactor, it was also indicated from measurements of particle residence times that the solid phase was transported in plug flow [18, 27] which would be a logical consequence of the similar way of accomplishing particle motion in the cyclone and vortex reactors. In the light of these observation it appears plausible that the particle residence time in the PCR is independent of both gas flow and rotor speed, as there is no discrete tangentially introduction of gas capable of forming a vortex. Consequently, the active surface area

available for particle contact is not limited by the gas flow pattern, and particle residence time can be controlled independently of the gas flow rate and the rotor speed.

6.2 Yields

As noted in the introduction, the focus of flash pyrolysis is the production of liquid in high energy yields and, accordingly, minimization of solid and gaseous by-products. Peacocke and Bridgwater [14] operated their Plate reactor with pine wood at a wall temperature near 600 °C and obtained 73.4 pct. (on dry, ash-free feed) total liquid yield with a water content of 26 pct. d.b. and yields of char and gas of 19.7 and 10.7 wt. pct., respectively. With the Vortex reactor operating at a wall temperature of 625 °C, Czernik *et al.* [28] obtained 72.5 pct. (on dry, ash-free feed) liquid yield from Southern Pine and a water content of 19 pct. d.b., whereas char and gas yield were 19.3 and 13.9 wt. pct., respectively. Although definite conclusions are hard to derive due to the somewhat poor mass balance closures, these reactors produce a liquid product with noticeably less water than reported here (32 pct. on dry feedstock for pine) and simultaneously achieve lower yields of char and gas. It is therefore of interest to investigate which factors have resulted in relatively high gas and char yields, and further what led to the high water concentrations.

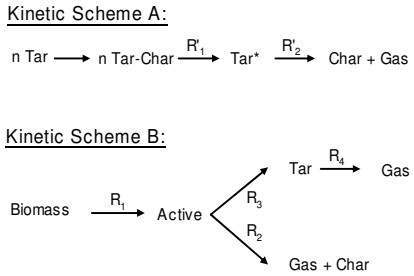

Figure 8: Kinetic model for heterogeneous secondary tar cracking via tar adsorption (A) and the Broido-Shafizadeh model for biomass pyrolysis (B).

6.2.1 Homogeneous Thermal Tar Cracking

It is well established that tar produced by primary pyrolysis may crack in the gas phase before cooled sufficiently or condensed, see R_4 on figure 8. An estimate for the gas residence time can be obtained by comparing the empty volume of the system with the volumetric flow rate of gas. Assuming that the average tar molecular weight (excluding water) was 350 g mol^{-1} [29] and all reactions (including water formation, see below) were completed instantaneously at the reactor entrance, the realized hot gas residence times for wheat and pine runs were 2.0±0.5 and 2.2±0.6 s, respectively (average ± 2 std. deviations). On account of the severe vapor cracking which would result in fluid beds from such long residence times (see *e.g.* [30]), it is therefore of interest if this could also be the case here. However, because the temperature of the gas phase was maintained at 400 °C, supposedly due to the thermally insulating blanket formed by the particles on the reactor wall, homogeneous tar cracking does not seem to be important. One way to ascertain this is to compare the half time of the tar cracking reaction, using data from Liden *et al.* [31], to the gas residence time whereby it is found that 36 s would be needed to reduce the tar yield by half. The lower-than-expected yield of organics and higher gas yields can therefore not to a large extent be the effect of secondary homogeneous gas phase tar degradation.

6.2.2 Heterogeneous Activated Tar Cracking

Another pathway for secondary tar degradation is the poorly understood heterogeneous cracking of tar on (or within) char particles. Boroson *et al.* [32] investigated the effect of passing freshly produced hardwood tar through a bed of char produced from the same material and found that the net tar yield would decreased independently of temperature (400 to 600 °C) and space time (2.5 to 100 ms). They interpreted this behavior as indicative for that a certain tar fraction, supposedly composed mainly of lignin-derived material, was reactive whereas others were unaffected. Increasing char yield with vapor residence time in a fluid bed reactor [33] with sorghum bagasse feedstock could possible be a result of such heterogeneous tar cracking, although operation with maple wood did not confirm this [30]. However, Boroson *et al.* found that the char-induced cracking may be responsible for increases in gas yield of up to 12 wt. pct. and char yield of up to 23 wt. pct. of the virgin tar. Correcting our pine yield data for heterogeneous tar cracking with these estimates and assuming that this mode of tar degradation was insignificant in both the Plate and Vortex reactors, the deviations observed for liquid and gas yield may be well accounted for. It is noteworthy, however, that Boroson *et al.* did not find that the heterogeneous reactions would increase the yield of water to any significant degree, but rather that the main gaseous (at reactor conditions) products were CO_2 and CO.

Due to the lack of detailed knowledge on heterogeneous tar cracking, the exact locations within the reactor system where heterogeneous tar cracking could have taken place is difficult to establish, but the relatively cold zones formed at the entrance and exit of the reactor in addition to the catch pot (located at the reactor outlet) appear to possible candidates. From Boroson *et al.*'s investigation it appears that tar may in reality be adsorbed on the char particles, followed by polymerization and char forming reactions leading to the elimination of light gasses, see kinetic scheme A on figure 8. This would be analogous to the polymerization (Tar* on figure 8) observed for bio-oil samples stored at ambient temperature for months [34], but here greatly accelerated by the higher temperatures. Further, if the mechanism does in fact proceed through adsorption, it would appear reasonable that this would preferably take place at relatively cold locations as tar formed and released to the vapor phase and later adsorbed on particles, would likely be desorbed if the particles were still are in contact with the hot portion of the reactor wall. Future investigation of the chars with TGA may shed further light on this.

6.2.3 Slow pyrolysis conditions

The so-called Broido-Shafizadeh model [35] for cellulose pyrolysis extended to include tar thermal cracking [36] has also been employed to explain the behavior of biomass [18] as detailed in kinetic scheme B, figure 8. Under this framework pyrolysis takes place

Table III: Simplified reactions considered in the mass balance.

Reaction	Reaction scheme
R_1 (Activation)	Biomass → "Active" + CO_2 + CH_4 + H_2O
R_2 (Slow Pyrolysis)	"Active" → Char + H_2O + CO_2
R_3 (Tar evaporation)	"Active" (s) → Prim. Tar (g)
R' (Het. Tar Cracking)	Prim. Tar → Char + Sec. Tar + CO_2 + CO

Table IV: Composition of mass balance components.

	Component	Composition	Source
Wheat	Feed	$CH_{1.6}O_{0.66}$	Table I
	"Active"/Prim. Tar	$CH_{1.2}O_{0.49}$	Diebold [29]
	Char	$CH_{0.43}O_{0.087}$	Jensen *et al.* [25]
	Gas	61% CO_2, 33% CO, 6% CH_4* (w/w)	GC gas analysis[§]
	Secondary Tar	$CH_{1.6}O_{0.23}$	From overall balance
Pine	Feed	$CH_{1.5}O_{0.66}$	Table I
	"Active"/Prim. Tar	$CH_{1.2}O_{0.49}$	Diebold [29]
	Char	$CH_{0.53}O_{0.12}$	Diebold [29]
	Gas	56% CO_2, 38% CO, 6% CH_4* (w/w)	Diebold [26]
	Secondary Tar	$CH_{1.4}O_{0.43}$	From overall balance

** by difference*

[§] *Reactor conditions: T_w=550 °C ; G=10,071; Wheat feed.*

through the initial formation of an active specie ("Active") with a reduced degree of polymerization [37], followed by competitive reactions resulting in either tar or char and gas. Due to differences in activation energies, the later reaction will dominate in the low temperature domain. As the product "gas" from reaction 2 includes both incondensable gasses (CO_2 primarily [38]) and water, the relatively high observed yields of gas, char and water could therefore be the result of pyrolysis taking place at a relatively low temperature. It follows that if "Active" is produced on the particle surface (ablative conditions) and is deposited on the warmer reactor wall the formation of tar will be favored to a higher degree than if it would be formed and further react within the core of the particle. The relatively cold zone at the reactor entrance is therefore expected to promote yields of char and gas compared to conditions where ablative conditions are more favored.

It can be noted, that Lédé *et al.*'s [39] concept of a "fusion" temperature for wood would imply that the thermal conditions of the reactive part of a particle undergoing pyrolysis is only slightly altered by reactor severity (*i.e.* the combined effect of T_w and G). Therefore, if intra particle conversion is significant, one would expect the yield profiles to be only slightly affected by changes in reactor wall temperature. Thus, if the sluggish yield profiles with reactor temperature and centrifugal force were ascribable mainly to this mode of pyrolysis, significant pore formation would be expected. However, the observed level of specific surface area is only a fraction of that observed for charcoal produced by slow pyrolysis. Nunoura *et al.* [40] used the Flash Carbonization process to carbonize corncob, and observed that the specific surface area dropped from 447 to 1 $m^2\ g^{-1}$ from the top to the bottom of the char bed. They suggested that tarry vapors released at the reactor top, and forced downward through the char bed, would deposit on the lower-location char and thereby reduce the specific surface area there. Considering these observations and the char SEM photographs (figure 9), it seems likely that both slow pyrolysis conditions and heterogeneous tar cracking have lead to the yield profiles observed in this study.

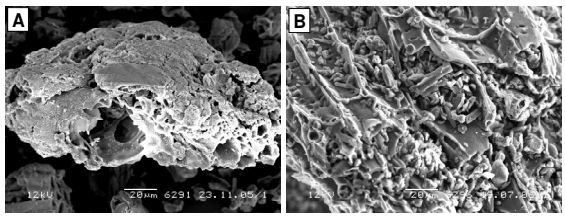

Figure 9: SEM photo of wheat straw char obtained at 606 °C (A) and 596 °C (B), both at a nominal centrifugal force of 10,071 G.

6.3 Component Mass Balance

The main assumptions upon which the mass balance rests are listed in table III and IV. In addition, "Active" for both wheat and pine pyrolysis is assumed to have the same composition as the primary tar obtained from softwood pyrolysis under conditions with minimal tar cracking and char formation, and tar is therefore simply formed by evaporation of "Active". From the results presented in table V, it appears that water is a major product of biomass activation which is consistent with that even with minimal char formation the liquid product will contain some water. However, the extraordinarily high water content reported in this study seems to be directly related to the extensive char formation and to a smaller degree, through dilution, to the tar cracking caused by the heterogeneous reactions. The latter on the other hand seems to be the main source of the higher than expected gas yield, whereas its contribution to char formation is less important. It should be noted that the predicted degree of heterogeneous cracking, and thereby the extent to which gas is formed in the activation step, is strongly influenced by the content of hydrocarbons in the pyrolysis gas. Combined with the lack of more comprehensive gas data, it is somewhat uncertain to which degree char is a product of heterogeneous tar cracking in this system. On the other hand, the assumptions regarding the CO_2/CO ratio in each of the reactions influence the relative importance of each

reaction to a much smaller degree due to the relative low gas yields in the activation and char forming steps.

Table V: Source of products as predicted by mass balance.

		Wt. % of feed daf.		
	Reaction	Char	Water	Gas
Wheat	R_1 (Activation)	*n.a.*	13	2
	R_2 (Slow Pyrolysis)	24	12	1
	R' (Het. Tar Cracking)	0	*n.a.*	17
Pine	R_1 (Activation)	*n.a.*	11	5
	R_2 (Slow Pyrolysis)	20	9	1
	R' (Het. Tar Cracking)	3	*n.a.*	8

6.4 Concluding Remarks

In light of the above discussion, it appears that for the investigated feedstocks the yield of char and water is most effectively reduced by maintaining the entire reactor wall temperature at a temperature above 500 °C. Regarding gas yield, it seems likely that heterogeneous tar cracking is not only limiting liquid yield in the PCR but will be active to a certain extent in any reactor system. Otherwise, the mass balance would predict that gas yield for wheat and pine could be reduced to 3 and 6 wt. pct. daf., respectively, simply by maintaining the temperature of char in contact with pyrolysis vapors. In the light of results discussed above [14, 28] this level of gas yield for pine appears rather low.

7 CONCLUSIONS

The Pyrolysis Centrifuge Reactor, a novel ablative reactor, has been presented and the initial bench-scale results with wheat and pine feedstock reported. In the tubular reactor biomass particles are forced against the heated reactor wall by the centrifugal force caused by the circular motion of the particles. This motion is caused by a rotor located centrally on the axial axis of the reactor and is transmitted to the particles by the spinning gas volume created by the rotor wings. Particle residence time is controlled by solid feed rate directly and through its effect on particle loading which attains asymptotic values at high and low feed rates. In the investigate temperature (480 to 620 °C) and centrifugal force (4,900 to 17,000 G) domain, the yields of liquid, char and gas proved to be relative insensitive to these parameters. The cause seems to be that a significant part of the particle reacts in the kinetic regime, where the balance between tar and char forming reactions, as determined by reaction temperature, is only slightly altered with reactor severity. Further, these conditions appear to have lead to significant char and water formation. The observed larger than expected gas formation is likely the result of heterogeneous tar cracking on the surface of char particles, possibly promoted by an uneven temperature profile of the reactor pipe and the design of the char separation system where conditions appear to favor this reaction. Due to poor heat transfer between reactor wall and gas, the gas temperature within the system was maintained at approximately 400 °C whereby thermal tar cracking did not contribute to the observed increased gas yield. A uniform reactor temperature and optimization of the char separation system to reduce vapor-char contact is expected to reduce the gas yield somewhat, whereas increased reactor severity through a uniform temperature on the active reactor wall will promote conversion in the ablative regime where char and water production will be comparable lower. The presented results give promise to a reactor that will be able to obtain high liquids yield from biomass at a high specific feed rate without carbon build-up on the active surface and excessive mechanical wear.

ACKNOWLEDGEMENTS

CHEC is financially supported by the Technical University of Denmark, DONG Energy A/S, Energinet.dk, the Danish Research Council for Technology and Production Sciences, the Danish Energy Research Program, Nordic Energy Research Program, EU, and many industrial partners. This particular project is financed by the DTU Innovation Program and the Nordic Energy Research Program.

GLOSSARY

Latin letters

a	Reactor inside surface area [m^2]
Ash	Ash content by ASTM D 1102 [% db.]
BET	Specific surface area of particles [m^2 g^{-1}]
C_{water}	Water content in liquid product [% wt.]
FC	Fixed carbon: 100-VM-Ash [% daf.]
g	Force of gravity [m s^{-2}]
G	Centrifugal force subjected to particles divided by g [-]
M	Molecular weight [g mol^{-1}]
m	Mass [kg]
n_D	Liquid refractive index at 30° and sodium D-lines [-]
Q	Mass flow rate [kg s^{-1}]
R	Reaction [-]
T	Temperature [°C]
VM	Volatile matter determined by ASTM E 872 [% db.]
Y	Yield of feedstock [% daf.]

Greek letters

α	Ash retention [% wt.]
ρ	Density [kg m-3]
τ	Residence time [s]

Subscripts

b	Biomass; wheat or pine
c	Char
g	Incondensable pyrolysis gas
t	Tar (organic and water fraction)
w	Reactor wall
v	Vapors; gaseous tar and incondensable gas

REFERENCES

[1] Frandsen, F.J. Fuel 2005, 84, 1277-1294.

[2] Knudsen, J.N.; Jensen, P.A.; Dam-Johansen, K. Energ. Fuel. 2004, 18, 1385-1399.

[3] Hansen, L.A.; Nielsen, H.P.; Frandsen, F.J.; Dam-Johansen, K.; Hørlyck, S.; Karlsson, A. Fuel Proc. Tech. 2000, 64, 189-209.

[4] Bridgwater, A.V.; Peacocke, G.V.C. Renew. Sust. Energ. Rev. 2000, 4, 1-73.

[5] Bridgwater, A.V.; Maier, D.; Radlein, D. Org. Geochem. 1999, 30, 1479-1493.

[6] Wagenaar, B.M.; Prins, W.; van Swaaij, W.P.M. Chem. Eng. Sci. 1994, 49 (24B), 5109-5126.
[7] Roy, C.; Blanchette, D.; de Caumia, B.; Labrecque, B. In: Bridgwater, A.V., editor. Advances in thermochemical biomass conversion; Blackie Academic & Professional: Edinburgh, 1994, pp. 1165-1186.
[8] Graham, R.G.; Bergougnout, M.A.; Freel, B.A. Biomass Bioenerg. 1994, 7, 33-47.
[9] Scott, D.S.; Piskorz, J. Can. J. Chem. Eng. 1982, 60, 666-674.
[10] Diebold, J.P.; Scahill, J. In: Overend, R.P.; Milne, T.A.; Mudge, L.K., editors. Proceedings of Fundamentals of thermochemical biomass conversion, Estes Park, 1982, pp. 539-555.
[11] Lédé, J.; Verzaro, F.; Antoine, B.; Villermaux, J. Chem. Eng. Proc. 1987, 20, 309-317.
[12] Reed, T.B. In: Proceedings of the Thermochemical Conversion Program Annual Meeting, Solar Energy Research Institute: Golden, CO, 1988; pp. 248-258.
[13] Brown, D.B.; Black, J. Patent WO 92/09671, 1992.
[14] Peacocke, G.V.C.; Bridgwater, A.V. Biomass Bioenerg. 1994, 7, 147-54.
[15] Bridgwater, A.V.; Peacocke, G.V.C.; Robison, N.M. Patent WO 03/057800, 2003.
[16] Diebold, J.P. In: Proceeding of the Specialist's Workshop on the Fast Pyrolysis of Biomass: Solar Energy Research Institute: Copper Mountain, CO, 1980; pp. 237-251.
[17] Lédé, J.; Panagopoulos, J.; Li, H.Z.; Villermaux, J. Fuel 1985, 64, 1514-1520.
[18] Lédé, J. Ind. Eng. Chem. Res. 2000, 39, 893-903.
[19] Bech, N.; Dam-Johansen, K. PCT Application, WO 2006/117006, 2006.
[20] Bech, N.; Dam-Johansen, K.; Jensen, P.A. PCT Application WO 2006/117005, 2006.
[21] Zhu, Y.; Lee, K.W. J. Aerosol Sci. 1999, 30, 1303-1315.
[22] Lee, K.H.; Kang, B.S.; Park, Y.K.; Kim, J.S. Energ. Fuel. 2005, 19, 2179-2184.
[23] Stenseng, M.; Jensen, A.; Dam-Johansen, K. J. Anal. Appl. Pyrol. 2001, 58/59, 765-780.
[24] Jensen, A.; Dam-Johansen, K.; Wójtowicz, M.A.; Serio, M.A. Energ. Fuel. 1998, 12, 929-938.
[25] Jensen, P.A.; Sander, B.; Dam-Johansen, K. Biomass Bioenerg. 2001, 20, 431-446.
[26] Diebold, J.P.; Power, A. In: Bridgwater, A.V., editor. Research in thermochemical biomass conversion; Elsevier Applied Science: London, 1988; pp. 609-628.
[27] Lédé, J.; Li, H.Z.; Soulignac, F.; Villermaux, J. Chem. Eng. Proc. 1987, 22, 215-222.
[28] Czernik, S.; Scahill, J.; Diebold, J.P. In: Proceeding of the 28th Intersociety Energy Conversion Engineering Conference, 1993, pp. 2429-2436.
[29] Diebold, J.P. The cracking kinetics of depolymerised biomass vapors in a continuous, tubular reactor, (Master Thesis); Colorado School of Mines: Golden, CO, 1985, p. 67.
[30] Scott, D.S.; Piskorz, J.; Bergougnou, M.A.; Graham, R.; Overend, R.P. Ind. Eng. Chem. Res. 1988, 27, 8-15.
[31] Liden, A.G.; Berruti, F.; Scott, D.S. Chem. Eng. Comm. 1988, 65, 207-221.
[32] Boroson, M.L.; Howard, J.B.; Longwell, J.P.; Peters, W.A. Energ. Fuel. 1989, 3, 735-740.
[33] Scott, D.S.; Majerski, P.; Piskorz; J.; Radlein, D. J. Anal. Appl. Pyrol. 1999, 51, 23-37.
[34] Diebold, J.P.; Czernik, S. Energ. Fuel. 1997, 11, 1081-1091.
[35] Bradbury, A.G.W.; Sakai, Y.; Shafizadeh, F. J. Appl. Polym. Sci. 1979, 23, 3271-3280.
[36] Di Blasi, C. Biomass Bioenerg. 1994, 7, 87-98.
[37] Lédé, J.; Diebold, J.P.; Peacocke, G.V.C.; Piskorz, J. In: Bridgwater, A.V *et al.*, editors. Fast pyrolysis of biomass: A handbook; CPL Scientific Publishing Services ltd: Newbury, UK, 1999, pp. 51-65.
[38] Diebold, J.P. Biomass Bioenerg. 1994, 7, 75-85.
[39] Lédé, J.; Li, H.Z.; Villermaux, J.; Martin, H. J. Anal. Appl. Pyrol. 1987, 10, 291-308.
[40] Nunoura, T.; Wade, S.R.; Bourke, J.P.; Antal, M.J. Ind. Eng. Chem. Res. 2006, 45, 585-599.

Appendix D:

Modelling Ablative Flash Pyrolysis of Straw and Wood
in the Pyrolysis Centrifuge Reactor

Modelling Ablative Flash Pyrolysis of Straw and Wood in the Pyrolysis Centrifuge Reactor

*Niels Bech [a, *], Morten Boberg Larsen [b], Peter Arendt Jensen [a], Kim Dam-Johansen [a]*

[a] Department of Chemical Engineering, CHEC Research Centre, Technical University of Denmark, Building 229, DK-2800 Lyngby, Denmark

[b] FLSmidth A/S, Vigerslev Allé 77, DK-2500 Valby, Denmark

Abstract

Less than a handful of ablative pyrolysis reactors for the production of liquid fuel from biomass have been presented and for only a single reactor has a detailed mathematical model been presented. In this article we present a predictive mathematical model of the pyrolysis process in the Pyrolysis Centrifuge Reactor, a novel ablative flash pyrolysis reactor. The model relies on the original concept for ablative pyrolysis of particles being pyrolysed through the formation of an intermediate liquid compound which is further degraded to form liquid organics, char, and gas. To describe the kinetics of the pyrolysis reactions the Broido-Shafizadeh scheme is employed with cellulose parameters for wood and modified parameters for straw to include the catalytic effect of its alkali-containing ash content. The model describes the presented experimental results adequately for engineering purposes for both wood and straw feedstock even though conditions for ablative pyrolysis from a reaction engineering point of view are not satisfied. Accordingly, even though the concept of an ablatively melting particle may constitute a limiting case, it can still be used to model flash pyrolysis provided that the reacting particle continuously shed the formed char layer.

Keywords: Alative flash pyrolysis; Pyrolysis Centrifuge Reactor; wheat straw; pine wood; modelling; bio-oil; biocrude

[*] Corresponding author: Tel. +45 45252851; Fax +45 45882258; e-mail: nsb@kt.dtu.dk

1. Introduction

The Pyrolysis Centrifuge Reactor (PCR) is a novel flash pyrolysis reactor developed for the production of liquid fuel from biomass. Due to the reactor currently being scaled-up from bench to pilot scale, a model to help understand its behaviour and optimise the yield of bio-oil was needed. As the PCR belongs to the ablative branch of flash pyrolysis reactors this model is believed to be of general value to other researchers studying flash pyrolysis, as the vast effort to create engineering models for flash pyrolysis reactors has concentrated on the more common fluid bed reactor designs [1-4].

To our knowledge less than a handful of ablative reactor designs for the production of liquid fuels from biomass have been published to date. Peacocke and Bridgwater presented a design where biomass is squeezed between a tilted slow moving scraper and a hot plate [5, 6], and later a pipe [7], but did not attempt to model neither of them. The same is true for Reed's Pyrolysis Mill [8] in which biomass is forced to pass between two heated metal "mill stones". The initial and most widely known ablative design is properly Diebold's Vortex Reactor [9] in which biomass is forced centrifugally against a heated pipe due to high-speed circular flow within a heated pipe. This reactor was thoroughly modelled by Miller and Bellan [10] who assumed the biomass particles to react by forming pores and shedding char from the surface when a critical porosity was reached.

In this paper we wish to investigate whether the original concept of ablative pyrolysis in which the particle is thought to react from the surface inwards through the formation of a liquid intermediate [11] can be useful for predicting the behaviour of an ablative reactor. The process is assumed to be controlled by chemical kinetics, external and internal heat transfer, that is, the decomposition kinetics are coupled to the physical properties of the material and the external heat transfer environment. The model constitutes a limiting case within the field of solid fuel pyrolysis, since a porous char layer may also be formed due to the action of competing pyrolysis reactions. However, given the right combination of mechanical influence on the char layer and char properties (*i.e.* brittleness), the layer may be removed continuously causing the virgin particle surface to remain exposed to the hot reactor surface.

The paper is organised as follows: First, the PCR and the experimental procedures are presented. Then follow the derivation of the numerical model and presentation

of the experimental results. Finally, the experimental and model results are compared and conclusions drawn.

2. Experimental

The PCR decomposes organic material by sliding particles across a heated wall in a circular motion, whereby the generated centrifugal acceleration press the particles against the wall and improves heat transfer. Referring to Figure 1, particles are fed tangentially to the horizontally oriented reactor cylinder where the centrally mounted tri-winged rotor creates a swirling gas wherein the particles are suspended and accelerated. While circulating on the wall, the particles simultaneously move axially toward the tangential reactor outlet. External to the reactor, the flow of gas and particles is first directed to a simple change-in-flow-direction separator and then a cyclone to remove coarse and fine solid particles, respectively. The liquid product is condensed in a direct condenser and aerosols are collected by a coalescer. A gas pump and a gas pre-heater allow for inert hot gas recirculation delivered axially to the reactor entrance, and excess gas is further cooled before being metered. Further details on the PCR, the bench reactor system, materials, and analytical methods can be obtained elsewhere [12, 13].

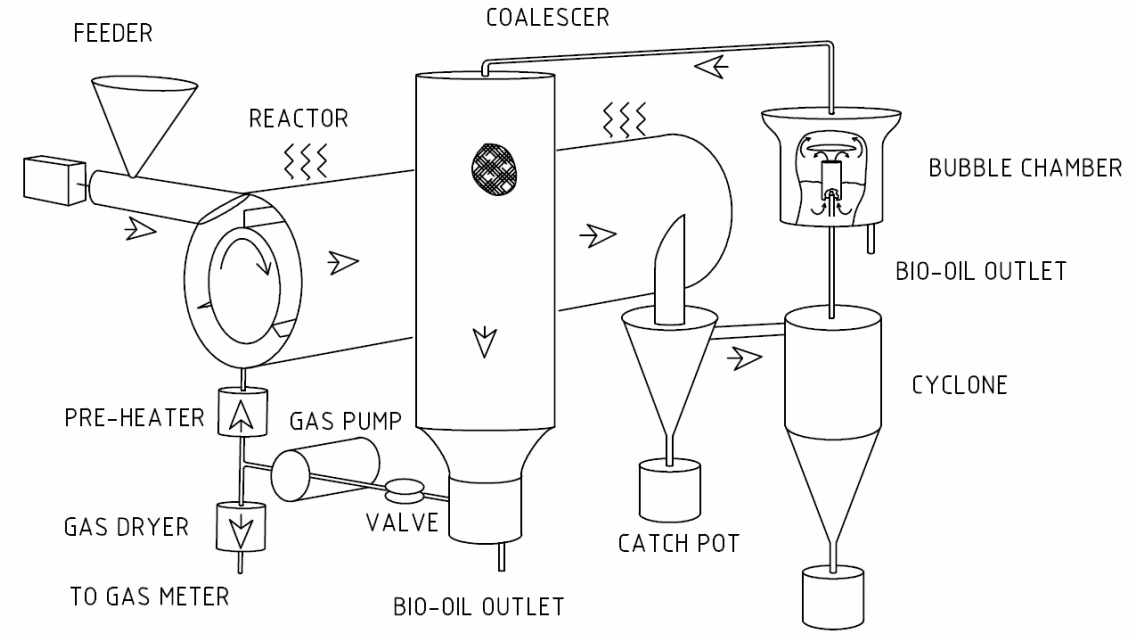

Figure 1: PCR reactor system.

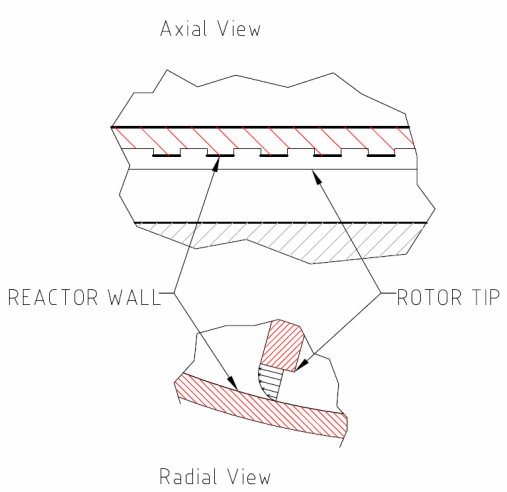

Figure 2: Reactor details: One mm thick by four mm wide flow guide rings on reactor wall (top) and assumed gas velocity profile in the three mm gap between rotor tip and reactor wall.

Prior to the present experimental runs were made the PCR was optimised based on the experience with the initial system [12] and high-speed video clips of a cold flow glass cylinder model. The reactor heating system was divided into four independently controlled zones to ensure a uniform temperature of the reactor pipe. Char storage in connection with the first separator was separated from the gas flow to eliminate the risk of catalytic vapour cracking. Flow guide rings were welded to the inside of the cylindrical reactor wall (Figure 2 (top)) to distribute the particles evenly on the reactor surface. The rotor was machined to maintain a rotor-tip-ring clearance well above the greatest particle diameter. Finally, spirally-twisted flow guides were welded at both the entrance and the exit to guide particles from the former to the latter.

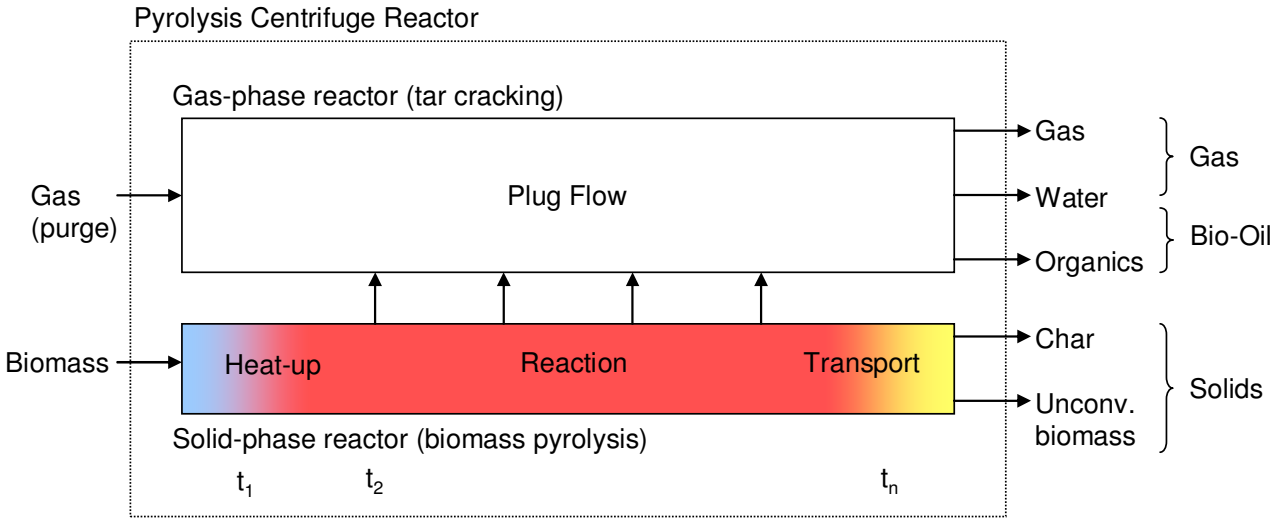

Figure 3: Model outline and convention for reactor streams.

3. Model

3.1 Model Outline

Figure 3 outlines the overall approach taken to model the reactions in the PCR. Conceptually, solid-phase primary pyrolysis and secondary tar cracking in gas phase are treated independently in separate reactors although numerically solved simultaneously. Particles are introduced in the solid reactor where they travel in plug flow undergoing heat up, reaction, and transport of char. For large (and small, see below) particles conversion is not completed before they are discharged from the reactor whereby the collected solids are a mixture of char and unconverted biomass. During reaction the formed pyrolysis gas and vapours are injected into the plug flow gas-phase reactor where the vapours undergo cracking to gas. The numerical method results in a number of discrete time steps which are automatically sized to avoid numerical inaccuracies. It should be noted that the term "gas" denotes all small molecules including water whereby "organics" does not equal the experimentally collected mixture "bio-oil".

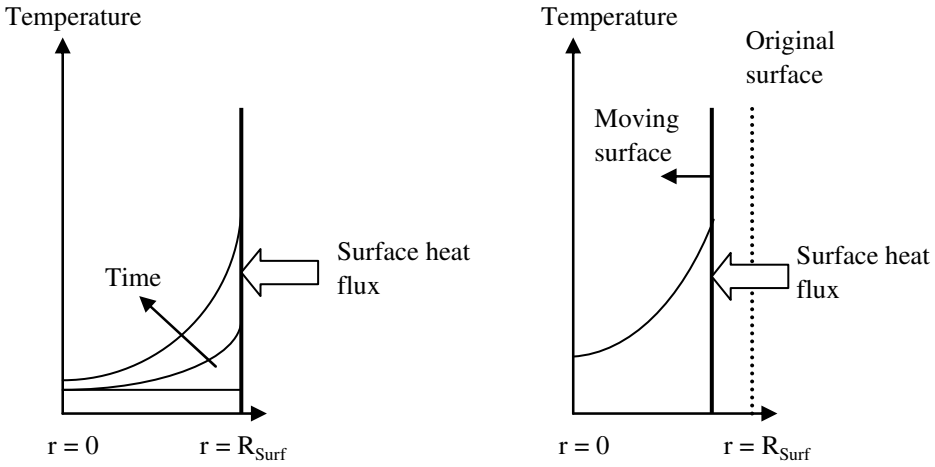

Figure 4: Schematic illustration of solid material undergoing surface decomposition at time t (left) and t +Δt.

Conversion of the biomass particles is treated as a pseudo-surface reaction. For ablative pyrolysis, the steep temperature gradient observed experimentally [14] combined with a reaction rate which is strongly dependent on temperature suggest, that reaction is concentrated in a relatively thin shell at the surface. The reaction scheme is coined *pseudo* in order to stress that particle density is considered constant, whereby any reaction within the particle also results in movement of the surface towards the centre rather than formation of a pore system [15]. The situation is depicted in Figure 4,

where the left pane shows the initial transient temperature profile for the situation where the particle surface has not yet moved. Under continued heating the spatial temperature increases successively with time until the particle surface is heated to a temperature, where decomposition causes the surface to retreat. After a finite movement of the particle surface, the situation is as depicted in the right pane. Again the heating continues followed by movement of the surface. The movement of the front continues until the particle is consumed (*i.e.* $R_{surf} \rightarrow 0$) or the particle is ejected from the reactor.

The shrinking particle is converted to an Intermediate Liquid Compound (ILC) which in turn is further degraded to the final pyrolysis products tar, gas, and char. Only the formation of ILC is assumed to influence the degradation of the particle whereas the split between products is determined by the surface temperature of the particle.

3.2 Spatial Temperature Profile and Particle Shrinkage

An expression for the movement of the surface is obtained by setting up a shell mass balance for a particle to obtain the differential equation:

$$\frac{d}{dr}\left(r^s v\right) + r^s r_{p,1} = 0 \qquad \textbf{(1)}$$

Here v is the velocity of the retracting surface, r is the particle characteristic size, s the particle shape factor, and $r_{p,1}$ the rate of reaction for the initial reaction. Integration within limits and substituting $r_{p,1}$ with the Arrhenius first order expression gives:

$$\frac{dR_{surf}(t)}{dt} = -\frac{1}{R_{surf}^s}\int_0^{R_{surf}} r^s A_1 \exp\left(\frac{-E_1}{R_g T(r)}\right) dr \qquad \textbf{(2)}$$

where R_{surf} is the initial characteristic size of the particle, E_1 the activation energy, A_1 the pre-exponential factor, R_g the gas constant, and $T(r)$ describes the temperature profile within the particle. The transient temperature distribution in the solid is described with the following partial differential equation [16]:

$$\rho \cdot c_p \frac{\partial T}{\partial t} = \frac{1}{r^s}\frac{\partial}{\partial r}\left(k \cdot r^s \frac{\partial T}{\partial r}\right) \qquad \textbf{(3)}$$

where s is the shape factor, ρ is the solid density, c_p is the specific solid heat capacity and k is the thermal conductivity and since these are considered constant, (3) is rewritten as:

$$\frac{\partial T}{\partial t} = \alpha \frac{1}{r^s}\frac{\partial}{\partial r}\left(r^s \frac{\partial T}{\partial r}\right) \qquad \textbf{(4)}$$

where α is the thermal diffusivity ($=k/\rho c_p$). The initial and boundary conditions for the system of differential equations (2) and (4) are:

IC1 : $R_{surf}(t=0) = R_0$ **(5)**

IC2 : $T(t=0, r) = T_0$ **(6)**

BC1: $k \left. \frac{\partial T}{\partial r} \right|_{r=R_{surf}} = h\left(T^{\infty} - T_{R_{surf}}\right)$ **(7)**

BC2: $\left. \frac{\partial T}{\partial r} \right|_{r=0} = 0$ **(8)**

IC1 states the initial size of the particle considered, IC2 states that the initial spatial temperature profile is uniform, BC1 states that heat transferred to the external surface by convection is transported into the material by conduction and finally BC2 states that the particle is symmetric around the particle centre.

The model is made dimensionless by introducing a number of variables. Thus, the dimensionless temperature θ is selected in such a way that the dimensionless temperature ranges between 0 and 1:

$$\theta = \frac{T - T_0}{T_0^{\infty} - T_0} \quad \textbf{(9)}$$

For this moving boundary problem the time is scaled according to a fixed size, namely the initial distance from the surface to centre. The dimensionless time τ is given by:

$$\tau = \frac{\alpha\, t}{R_0^{\,2}} \quad \textbf{(10)}$$

The dimensionless position within the particle x is scaled so the moving surface is always located at 1 and the centre of the particle is located at 0:

$$x = \frac{r}{R_{surf}(t)} \quad \textbf{(11)}$$

To satisfy the symmetry boundary condition at the centre, (8), a variable substitution is used:

$$u = x^2 \quad \textbf{(12)}$$

To track the position of the surface in time, a dimensionless position η is introduced:

$$\eta = \frac{R_{surf}(t)}{R_0} \quad \textbf{(13)}$$

A dimensionless activation energy γ is also introduced based on the initial temperature:

$$\gamma_i = \frac{E_i}{R_g T_0} \quad \textbf{(14)}$$

The dimensionless variables are introduced into the original equations (2) to (8). The conservation of energy in the particle becomes:

$$\frac{\partial\theta}{\partial\tau}\eta^2 = 2\left(s+1+u\eta\frac{\partial\eta}{\partial\tau}\right)\frac{\partial\theta}{\partial u}+4u\frac{\partial^2\theta}{\partial u^2} \qquad \textbf{(15)}$$

with corresponding initial and boundary conditions:

$$\left.\frac{\partial\theta}{\partial u}\right|_{u=1} = \frac{1}{2}\frac{hR_{surf}}{k}\left(\theta^{\infty}-\theta|_{u=1}\right) = \frac{Bi(R_{surf})}{2}\left(\theta^{\infty}-\theta|_{u=1}\right) \qquad \textbf{(16)}$$

or

$$\left.\frac{\partial\theta}{\partial u}\right|_{u=1} = \frac{1}{2}\frac{hR_{surf}}{k}\left(\theta^{\infty}-\theta|_{u=1}\right) = \frac{Bi(R_0)}{2}\eta\left(\theta^{\infty}-\theta|_{u=1}\right)$$

$$\theta(t=0,u)=0 \qquad \textbf{(17)}$$

where it is noted that the dimensionless Biot number is introduced:

$$Bi = \frac{hR_{surf}}{k} \qquad \textbf{(18)}$$

Finally, the movement of the surface is also made dimensionless yielding:

$$\frac{d\eta}{d\tau} = -\frac{R_0^2 A_1}{2\alpha}\eta\int_0^1 u^{\frac{s-1}{2}}\exp\left(-\frac{\gamma_1}{\left(\frac{T_0^{\infty}}{T_0}-1\right)\theta(u)+1}\right)du \qquad \textbf{(19)}$$

with the initial condition:

$$\eta(\tau=0)=1 \qquad \textbf{(20)}$$

Biomass is decomposed on a metal wall having a constant temperature T^{∞} in time. A special feature is that the heat transfer coefficient changes during conversion with the characteristic length of the particle. For a rod of cellulose in contact with a rotating disk, the heat transfer coefficient has been experimentally established to be correlated to the contact pressure between rod and disk, provided the relative velocity is above 1.0 to 1.5 m/s [14]:

$$h = \frac{1}{59}\,p \qquad \textbf{(21)}$$

where h is the overall heat transfer coefficient [W m^{-2} K^{-1}] and p the contact pressure [Pa]. Following the idea of Diebold and Power [17], heat transfer to the particle is assumed to originate from wall-particle contact only. In addition, particles are assumed to be indefinite and during conversion particles of slab geometry are only submitted to

wall contact on one side, whereas cylinders and spheres are evenly exposed to the hot surface due to rotation. Under these conditions, it can be shown that *h* is given by:

$$h = \frac{1}{59(s+1)} r \rho g G \qquad \textbf{(22)}$$

where G is the dimensionless centrifugal acceleration. Table 1 and Table 2 contain information regarding the kinetic and physical properties. Note that the heat of reaction has been ignored due to its insignificance relative to the latent heat [17, 22]. Finally, particles are assumed to be fully converted when the characteristic size is reduced to below 5 μm.

Table 1: Model parameters used to simulate pine wood and wheat straw experiments.

	Parameter	Value	Source
Pine	S	1 (cylinder)	Bech *et al.* [12]
	MMD	$632 \cdot 10^{-6}$ m	Bech *et al.* [12]
	ρ	650 kg m^{-3}	Miller and Bellan [10]
	c_p	2300 J kg^{-1} K^{-1}	Miller and Bellan [10]
	k	0.13 W m^{-1} K^{-1}	Miller and Bellan [10]
	A_1	$2.8 \cdot 10^{19}$ s^{-1}	Diebold [18]
	E_1	240 kJ mol^{-1}	Diebold [18]
	A_2	$6.79 \cdot 10^{9}$ s^{-1}	Diebold [18]
	E_2	140 kJ mol^{-1}	Diebold [18]
	A_3	$1.30 \cdot 10^{10}$ s^{-1}	Diebold [18]
	E_3	150 kJ mol^{-1}	Diebold [18]
	A_4	$4.3 \cdot 10^{6}$ s^{-1}	Liden *et al.* [19]
	E_4	108 kJ mol^{-1}	Liden *et al.* [19]
	γ_g	0.65	Di Blasi [20]
Wheat	s	2 (sphere)	Bech *et al.* [12]
	MMD	$633 \cdot 10^{-6}$ m	Bech *et al.* [12]
	ρ	700 kg m^{-3}	Jensen *et al.* [21]
	c_p	2446 J kg^{-1} K^{-1}	Jensen *et al.* [21]
	k	0.21 W m^{-1} K^{-1}	Jensen *et al.* [21]
	A_1	$2.8 \cdot 10^{19}$ s^{-1}	Like pine
	E_1	206 kJ mol^{-1}	Fitted
	A_2	$6.79 \cdot 10^{9}$ s^{-1}	Like pine
	E_2	140 kJ mol^{-1}	Like pine
	A_3	$1.30 \cdot 10^{10}$ s^{-1}	Like pine
	E_3	143 kJ mol^{-1}	Fitted
	A_4	$4.3 \cdot 10^{6}$ s^{-1}	Like pine
	E_4	108 kJ mol^{-1}	Like pine
	γ_g	0.65	Like pine

Table 2: Reactor parameters.

Parameter	Pine Wood Runs	Wheat Straw Runs
V_r	$5 \cdot 10^{-4}$ m^3	
d_r	$8.2 \cdot 10^{-2}$ m	
l_r	$2.0 \cdot 10^{-1}$ m	
G	$4.9 \cdot 10^3$; $1.0 \cdot 10^4$; $1.7 \cdot 10^4$	
τ_∞	2.8, 3.3, and 6.0 ± 0.3 s	
T_∞	475 to 600 °C	
T_0	20 °C	
M_o *	350 g mol^{-1}	
P	10^5 pa	
F_b	20 ± 7 g min^{-1}	23 ± 2 g min^{-1}
F_g	17 ± 5 g min^{-1}	19 ± 8 g min^{-1}
M_g	31 ± 3 g mol^{-1}	35 ± 1 g mol^{-1}

* Source: Diebold [9]

3.3 Particle Velocity

In order to find the true acceleration acting on a particle for use in (22), the nominal acceleration G at the rotor tips needs to be corrected. Similar to cyclonic separator modelling it is assumed that the slip between gas and particles can be ignored [23]. Furthermore, as the Reynolds number for experimental conditions investigated here range from $3 \cdot 10^4$ to $5 \cdot 10^4$, based on the rotor tip diameter [24], it is assumed that the flow is turbulent and the velocity profile between rotor tip and wall (Figure 2, bottom) can described by a power law of the form:

$$\frac{v}{v_0} = \left(\frac{r}{\delta}\right)^{1/n} \qquad \textbf{(23)}$$

where δ is the rotor-to-wall distance, r the particle radius (*i.e.* the distance from the wall), v_0 the rotor speed, v the speed at r, and n an empirical exponent taken as 6 in accordance with the Reynolds number range [25]. Since the centrifugal acceleration is proportional to the squared particle speed, the acceleration correction factor κ becomes:

$$\kappa = \left(\frac{r}{\delta}\right)^{1/3} \qquad \textbf{(24)}$$

Accordingly, reacting particles will experience progressively lower centrifugal acceleration as they disappear.

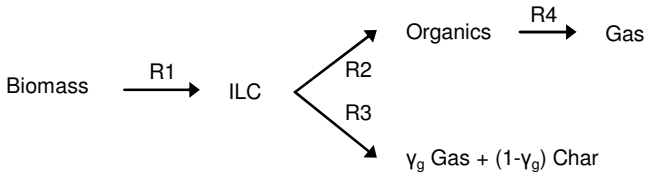

Figure 5: The Broido-Shafizadeh model for biomass pyrolysis.

3.4 Product Yields

To predict the fate of the ILC we employ the extended Broido-Shafizadeh (BS) kinetic scheme [20] depicted in Figure 5 to model the pyrolysis reaction. Although the BS kinetic scheme has been criticised for not providing an adequate fit to thermogravimetric weight loss curves [26], and more accurate schemes have been suggested for both cellulose [26, 18] and biomass [27], it continues to be popular within papers on flash pyrolysis [28, 29] along with the similar three-parallel reaction Shafizadeh scheme [1]. Although extrapolation of both models must be done with caution [30], considering that the operational envelope for flash pyrolysis reactors is relatively narrowly defined with respect to temperature (i.e. 450 to 600 ºC), the popularity of the BS kinetic scheme can properly be attributed to the products being easily identified and that it intuitively reduces a complex system with adequate precision for engineering purposes. All reactions are assumed to be irreversible first order with an Arrhenius type of rate expression.

The respective mass balances for tar, gas, biomass, and char in dimensionless form reduce to:

$$\frac{\partial X_o}{\partial \tau} = -S_o \frac{\partial X_b}{\partial \tau} - B \frac{X_o}{X_o e_o^{-1} + X_g e_g^{-1}} \quad \textbf{(25)}$$

$$\frac{\partial X_g}{\partial \tau} = -(1 - S_o)\gamma_g \frac{\partial X_b}{\partial \tau} + B \frac{X_o}{X_o e_o^{-1} + X_g e_g^{-1}} \quad \textbf{(26)}$$

$$\frac{\partial X_b}{\partial \tau} = X_{b,0}(s+1)\eta^s \frac{\partial \eta}{\partial \tau} \quad \textbf{(27)}$$

$$X_c = 1 - X_b - X_g - X_o \quad \textbf{(28)}$$

where the X_i's are mass fractions of feed and products with dimensionless time τ and γ_g is the gas/char selectivity of R3. The reactor factor B, the dimensionless molar masses e_i's, and the organics selectivity S_o are given by:

$$B = \frac{V \cdot r_{p,4} \cdot p \cdot M_b}{F \cdot R_g \cdot T \cdot \tau_\infty}, \qquad e_i = \frac{M_i}{M_b}, \qquad S_o = \frac{r_{p,2}}{r_{r,2} + r_{p,3}} \tag{29}$$

where the organics cracking rate $r_{p,4}$ (and thereby B) is taken as constant as it is assumed that the gas temperature will approach the reactor wall temperature rapidly due to the highly turbulent gas flow discussed above. In contrast $r_{p,2}$ and $r_{p,3}$ (and S_o) are evaluated at the particle surface temperature because ILC is assumed to be consumed immediately when formed due to the experimentally observed very short life time of the compound [11]. Product yields Y_i's are computed by solving the system of equations to obtain corresponding mass fractions X_i's at the reactor outlet (*i.e.* at $\tau = \tau_\infty$).

3.6 Solution Procedure

Discretization by orthogonal collocation is used to approximate the transient temperature profile described by (15) inside the particle. Integration of the coupled differential equations and (25) to (27) is performed using the FORTRAN-based semi-implicit Runge-Kuta integration routine SIRUKE [31]. Equation (19) is solved by Gauss integration.

As the feeds used in the experiments were not homogeneous with regard to particle size (see Figure 6), the code was set up to repeat the calculations for each ASTM screen size between 106 and 1180 µm using the arithmetic mean as twice the characteristic particle dimension. Results for the combined feed were obtained by taking the weighted average using the sieve mass fraction as the weight.

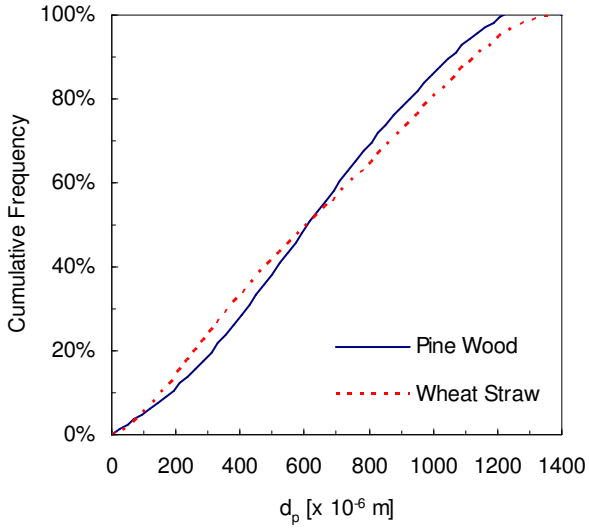

Figure 6: Characteristic particle diameter for feed material.

4. Results

4.1 Mass Balance

Mass balance closures were generally good for both wood and straw experiments with average losses of 7.6 ± 2.2 % wt. and 2.8 ± 2.2 % wt., respectively, and in all cases the loss was positive. However, in order to assign the balance for modelling purposes the ultimate analysis presented in Table 3 was used to compute the composition of the lost material. The analysis revealed that based on the organic constituents the lost fraction had a composition similar to char, although with an increased hydrogen content, and therefore it was assumed that the loss was due to condensation of vapours on the reactor pipe flanges which were somewhat inadequately insulated and prone to promote condensation. Thus, in the following material not collected experimentally has been assigned to char.

Table 3: Ultimate analysis (wt. %) and measured higher heating value (HHV) of feed material and products from flash pyrolysis of straw at 550 °C and $G=17\cdot10^3$. For products, averages and two standard deviations of three experimental runs are reported.

	Straw	Liquid	Solids	Gas [d]
C	44	37 ±2.3	53 ±2.0	40 ±0.6
H	6.3	7.7 ±1.4	3.6 ±0.23	2.8 ±0.2
S	0.19	0.10 ±0.01	0.4 ±0.05	n/a [b]
N	1.1	1.1 ±0.12	1.0 ±0.17	n/a [b]
O	42 [a]	52 ±1.4 [a]	17 ±1.0 [a]	57 ±0.8
Ash	6.4	1.3	25 ±1.2	n/a [b]
HHV (MJ/kg)	17.3	15.2	20.1	11.2 [c]

[a] By difference; [b] Not analysed; [c] Calculated from ultimate analysis [32]; [d] Based on Table 4

Table 4: Gas analysis (% vol.) by GC/TCD and GC/FID for flash pyrolysis of straw at 550 °C and $G=17\cdot10^3$. Averages for three repeated runs shown.

CO_2	CO	H_2	CH_3CHO	CH_4	CH_2CH_2	CH_3CH_3	CH_2CHCH_3	$CH_3CH_2CH_3$	C_4+ [a]
50	37	1.1	1.6	2.2	0.6	0.3	0.3	0.1	6.8

[a] Includes balance (assumed composition C_4H_{10}).

Table 5: Ash composition and mass balance (% wt.) for inorganic components determined by wavelength dispersive (WXRF) x-ray fluorescence spectrometry of feed and products from flash pyrolysis of straw at 550 °C and $G=17\cdot10^3$.

	Na	Mg	Al	Si	P	Cl	K	Ca	Mn	Fe	Zn	O [a]
Straw	0.32	1.4	0.44	21	2.2	9.3	27	5.7	n.d.[b]	0.43	n.d.[b]	32
Liquid	0.31	0.87	0.31	0.26	0.77	13	31	6.1	0.08	17	0.08	30
Solids	0.23	1.1	0.19	14	2.0	8.4	30	6.2	0.07	0.45	0.03	37
In liquid	11	7.2	8.0	0.14	4.0	16	13	12	-	450	-	11
In solids	70	80	43	68	90	90	110	110	-	100	-	110
Total	81	87	51	68	94	110	120	120	-	550	-	120

[a] By difference; [b] Not detected (<0.001%)

Assigning the observed loss to char was apparently contradicted by an ash mass balance which would overestimate the amount of ash. However, detailed analysis of the ash in the parent material and the two products (Table 5) revealed that for all components but silica and iron the distribution between the products was roughly equal. It is therefore believed that the ash observed in the liquid product resulted from leaching of inorganic components from carried-over char (roughly 10 to 15 % wt. of total char yield) before it was removed by filtration and quantified. However, since silica is expected to be present in the form of SiO_2 which is insoluble in the mildly acidic bio-oil this component was retained in the solid phase. The highly increased amount of iron in the products could likely originate from either wear on the reactor pipe from particle movement or corrosion of the equipment by bio-oil. This is, however, not supported by the presence of neither nickel nor chromium which constitutes 12 and 17 % wt., respectively, of the reactor construction material.

4.2 Yield Modelling for Wood

Results for pine wood are shown in Figure 7 which includes the limits of a credible interval established by repeating an experiment five times with fixed reactor parameters at 550 °C and for each product estimating the interval as twice the standard deviation. Rather than calculating error bars for each experimental observation based on the analytical uncertainty, this procedure was thought to give a more correct picture as the observed experimental scatter seemed to arise from experimental variations and not from the analytical methods [12]. Thus, the credible interval can be perceived as: given the model correctly represents the true mean for a number of repeated experiments, the interval should encompass any single experimental observation with 95 % probability.

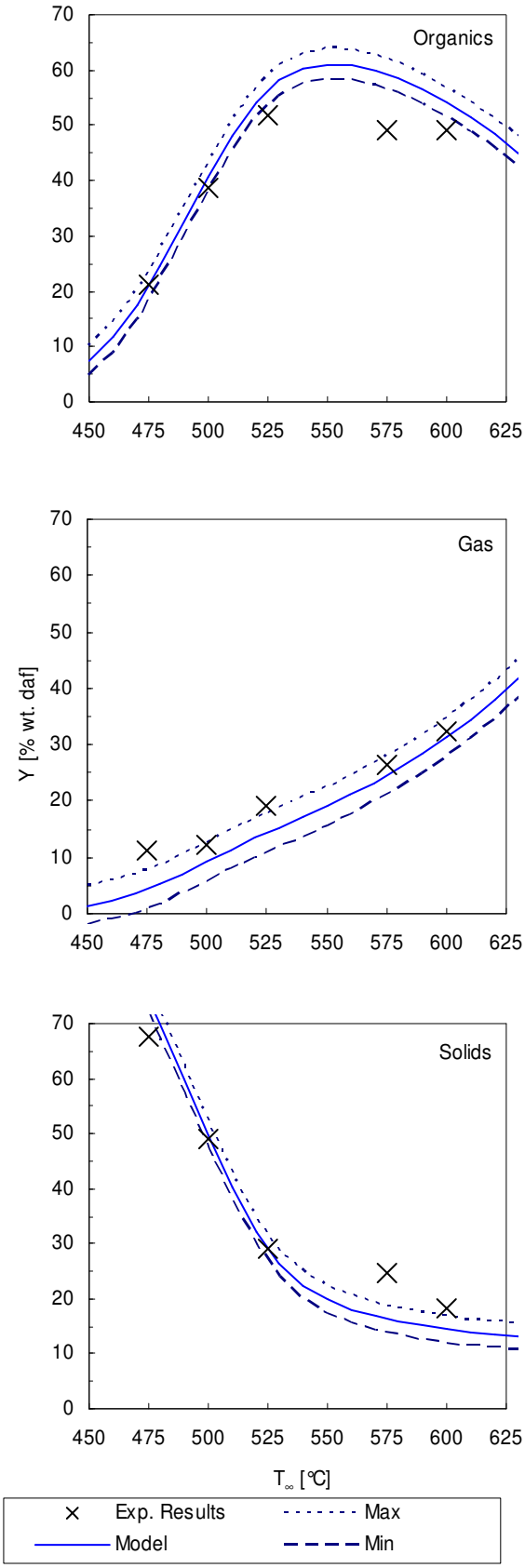

Figure 7: Experimental yields (symbols) and model predictions with reactor temperature for pine wood at $G=1.7\cdot10^3$. Full line shows predictions and broken lines encompass the credible interval.

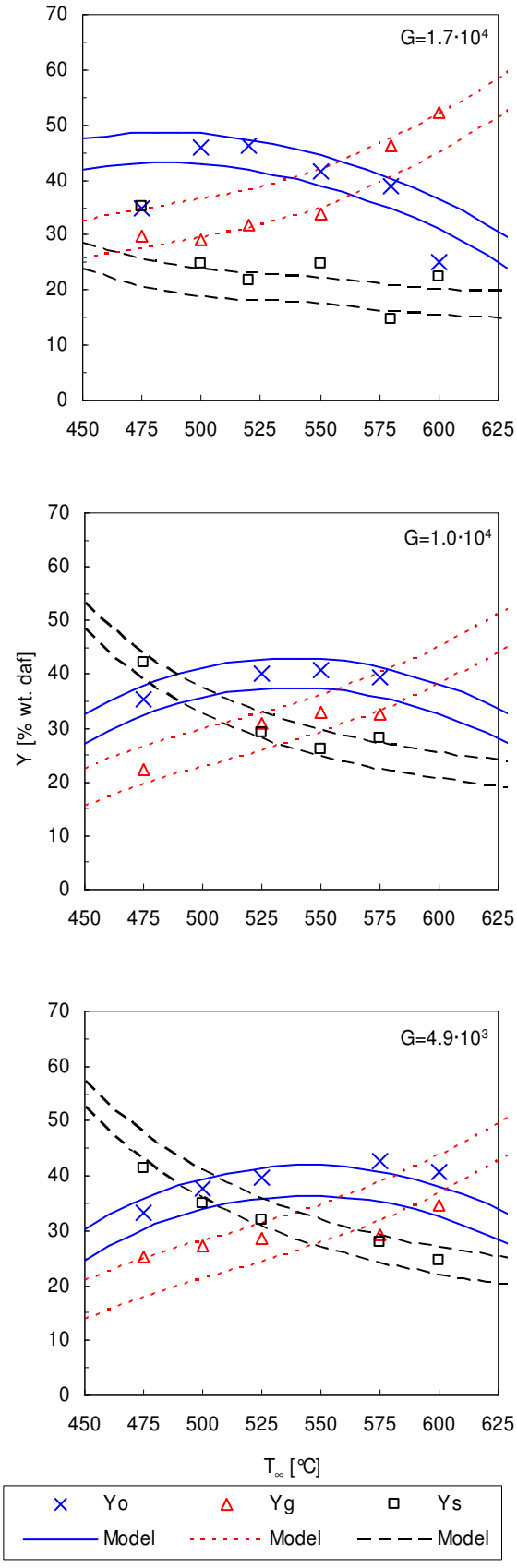

Figure 8: Experimental results (symbols) and model predictions for yield of main fraction with reactor temperature for wheat straw pyrolysis at three centrifugal accelerations. Only the credible interval shown for model predictions.

From the plots it can be seen that the model accurately predicts the yield of gas in the entire investigated domain and to a lesser extent also of organics and char. For the latter two the predictions appear to be biased such that above approximately 550 °C organic yields are overestimated whereas char yields are too conservative. A possible explanation could be the before-mentioned condensation of organics on the reactor internals. However, given that the main discrepancy between model and experimental results is observed for the single experiment at 575 °C and that the mass balance was closed with char, it is uncertain whether this is the result of poor collection of organics for this data point. In any case the model appears to be satisfactory for engineering purposes.

As the modelling results were obtained with kinetic data for cellulose they support earlier findings [28] that a satisfactory description can be obtained by simplifying the pyrolytic degradation of wood to include only its main constituent. However, since the kinetic data were not for pine wood it is not clear whether the observed inaccuracies could be eliminated by improved kinetic data or are artefacts introduced by the model.

4.3 Yield Modelling for Straw

Due to the lack of published kinetic data for wheat straw, it was attempted to employ the superposition kinetic scheme of Miller and Bellan [33]. By dividing each size fraction into its three main organic components cellulose, hemicellulose, and lignin and modelling each separately using kinetic data for the pure components the result was obtained by averaging over composition and then particle size. However, not unexpectedly this approach proved unsuccessful properly because the influence of ash components [34] is of more importance than the organic composition for the yield of products. Interestingly, for pine the simple cellulose kinetics more accurately described the experimental results than the detailed superposition model. Accordingly, it was decided to use the cellulose kinetic data which had been given good results with wood but modify them to obtain an acceptable fit.

It was assumed that the higher ash content in the wheat straw has a pronounced catalytic effect on the pyrolytic reactions favouring the formation of char and gas [34] by reducing the activation energies of the affected reactions. Accordingly, the distribution between char and gas (γ_g) and the pre-exponential factors were left equal to those of cellulose, whereas the gas phase cracking of tar was assumed to be unaffected by the ash content which largely stays in the solid state for the investigated temperature domain. Furthermore, as the distribution between gas/char and organics can be described by one parameter, the activation energy for R2 was kept unchanged for simplicity. Fit-

ting the remaining two activation energies for R1 and R3 simultaneously to the three investigated rotor speeds visually, the result shown in Figure 8 were obtained. Although the predictive power of the model was somewhat reduced compared to the pine modelling, reducing the activation energies by 14 % and 4.5 %, respectively, produced an acceptable fit but could likely be improved by investigating the kinetics for straw in more detail.

5. Discussion

5.1 Ablative Conditions

The conditions necessary to obtain ablative pyrolysis have suggestively been defined by means of the Biot number and the thermal Thiele modulus [35, 36]:

$$\begin{aligned} Bi &\geq 1 \\ Th &>> 1 \end{aligned} \qquad \textbf{(30)}$$

where the latter is given by:

$$Th = -\frac{d\eta}{d\tau}\eta \qquad \textbf{(31)}$$

The physical interpretation of *Th* is that it gives the ratio between a characteristic time of solid heating and a characteristic time of solid degradation. The ablative envelope is thus characterized by internal control of particle heating and that solid degradation proceeds faster than the inward solid heating rate. With this definition in mind, it can be questioned whether ablative conditions ever materialized during the conversion discussed here, judging from the simulation presented in Figure 9 (left). It is noted that the temperature profiles remained relatively flat throughout the conversion. Further, early investigators in the field of ablative pyrolysis compared the observed behaviour of cellulose (and biomass) undergoing decomposition on a moving hot moving surface to a process of fusion due to the almost constant surface temperature observed in the ablative regime [37-39]. It was therefore expected that the surface temperature would stabilize on a constant level after the process was initiated but this is not observed, most likely due to the lack of ablative conditions. In contrast, Figure 9 (right) presents the results for a spherical particle with a five times larger diameter. Here it can be observed that the transient heating period is considerably shorter due to the five times higher initial heat transfer coefficient whereby the particle is within the ablative regime almost immediately. Following the definition (30), it stays here until conversion has reached

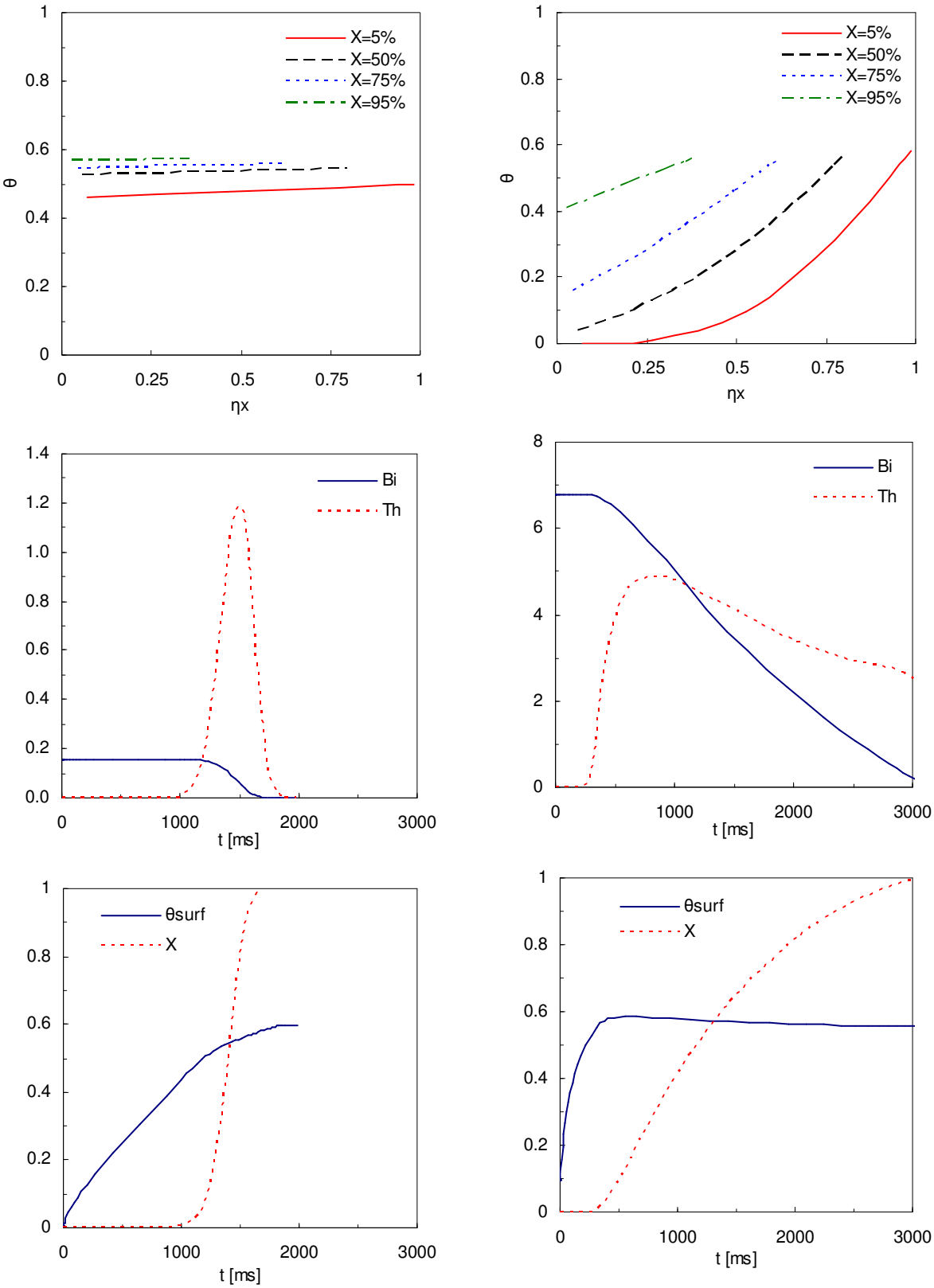

Figure 9: Simulated values for spherical straw particle (d_p=633 µm (left) and d_p=3265 µm (right)) at T_∞=550 °C and G=1.7·10^4: Dimensionless temperature profiles at selected conversions (top), Biot number and Thiele modulus with reaction time (centre), and dimensionless surface temperature and conversion with reaction time (bottom).

more than 99% as can also be confirmed by the steep parallel temperature profiles. It is noted that the almost constant surface temperature is at 319 ºC for straw whereas a similar wood (cellulose) particle under unchanged conditions is converted at 405 ºC or somewhat lower than earlier estimates of 467 ºC [38] or 437 ºC [40].

Following from the above discussion, the reaction mechanism for the investigated conditions can from a fundamental reaction engineering point of view not be classified as ablative even though the term is generally applied to flash pyrolysis processes in the sense of *solid convective*. Accordingly, the reaction proceeds for the investigated conditions predominantly in the kinetic or thermally thick regime [36] where the particle is partly consumed from within. This situation is graphically presented in Figure 10 along with the pure ablative and pore-forming (kinetically controlled regime) and is for the PCR characterised by the continuous char peeling or ablation of char formed on the particle surface (cf. Miller and Bellan's concept of a critical porosity [10]) due to high centrifugal acceleration and particle velocity across the metal surface. It can be hypothesised that there are two primary explanations for the model being able to mimic the obtained results well even though the surface reaction assumption does not hold.

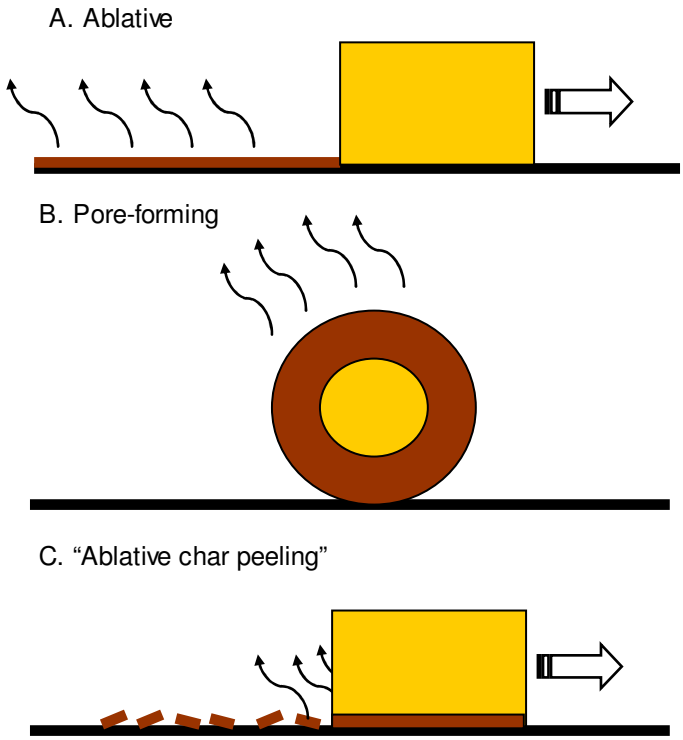

Figure 10: Idealised visual presentation of flash pyrolysis schemes.

First, it has been observed for fluid beds that cracking of product vapours can be neglected inside a pyrolysing particle of 100 to 1000 µm at reactor temperatures between 500 and 600 ºC [41]. Secondly, due to the high speed and centrifugal acceleration a char layer developing on the surface and thus changing the heat flow in to the particle is continuously removed.

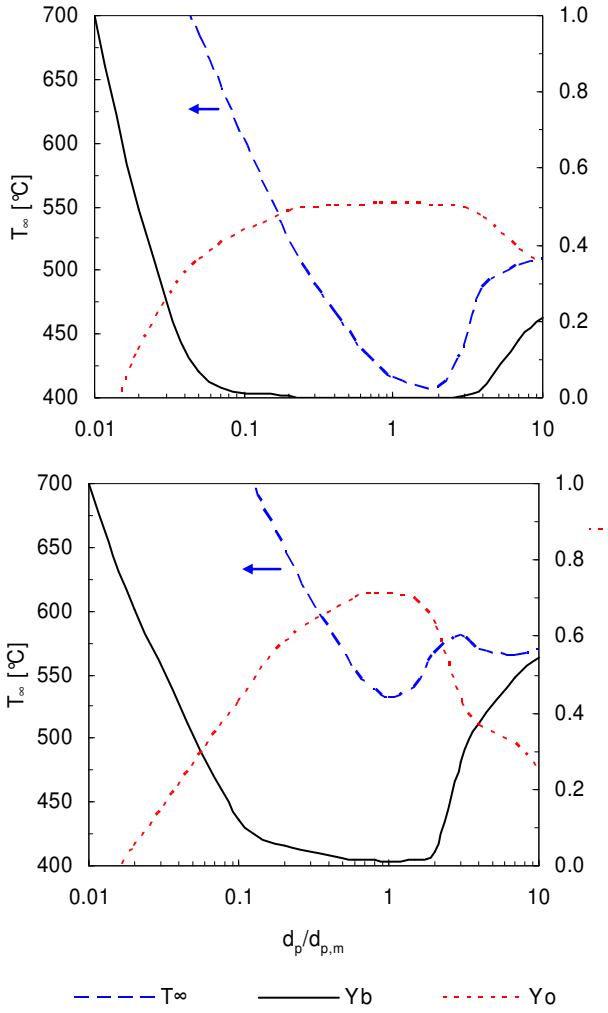

Figure 11: Simulated reactor temperature for optimum organic yield (broken line) with relative particle size for straw (top) and wood. Optimum organic yield (dots) and unconverted straw yield for particle size also shown (full line). All conditions equal to those investigated experimentally at $G=1.7 \cdot 10^4$.

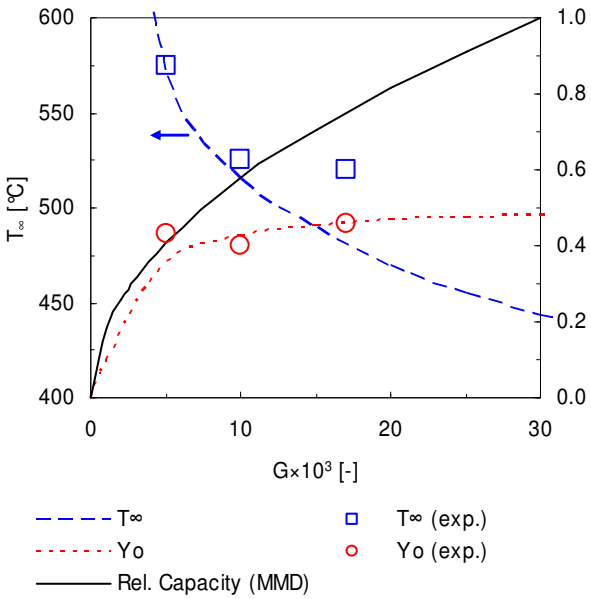

Figure 12: Simulated optimum reactor temperature (broken line) needed to maximise organic yield (dots) with centrifugal acceleration compared with experimental results (symbols) for conditions equal to those for straw experimental runs. Full line shows relative reactor capacity with centrifugal acceleration for straw particles of MMD.

5.2 Reactor Optimisation

Having established that the pyrolytic degradation is not ablative from a reaction engineering point of view, it seems appropriate to investigate which effect particle size has on the yield of organics. Referring to Figure 11, it is interesting to note that for both straw and wood optimum organics yield are predicted for particle sizes close to the mean mass diameter (MMD) of the investigated distributions. It is noted that the optimum temperature for this particle size is lower than what is predicted for the entire distribution and that the reason for this behaviour is that particles below approximately 0.8 MMD require considerably higher temperatures to minimise the fraction of biomass passing through the reactor unconverted. In contrast, particles several times lager than MMD require a relative long residence time for conversion and for them the optimum temperature is limited upwards by the rapidly increasing organics cracking above 500 to 550 °C, an effect which is less pronounced for the smaller particles where the decreasing centrifugal acceleration and thus heat transfer tend to favour higher temperatures. Loss of potential organic yield due to char formation is for both biomasses not responsible for the observed decrease in liquid yield for particle sizes different from the MMD as the result of the increased optimum reactor temperature is to lower the char yield somewhat (not shown). The implications would be that in order to maximise the yield of

organics the reactor should be designed to suit the relevant particle size and that fines and oversizes should be avoided or removed in the preceding size-reduction process.

From the experimental results with straw it was noted that the maximum yield of organics did not change significantly with increasing centrifugal acceleration which merely lowered the optimum temperature. In order to investigate this issue further, it is necessary to make some assumptions regarding the particle residence time within the reactor as a function of rotor speed. Assuming that the particles follow the same narrowly pitched helical path the residence time will be given by:

$$t_{p,\infty} = \frac{l_{p,\infty}}{\sqrt{Ggr_r}} \qquad \textbf{(32)}$$

where $l_{p,\infty}$ is the length of the assumed path. Employing the measured residence times for the three investigated rotor speeds an estimate for $l_{p,\infty} = 237 \pm 61$ m is obtained and used to compute the curves shown in Figure 12. From this figure it can be noted that increasing G above approximately $5 \cdot 10^3$ has only a moderate effect on organics yield and that 90 % of the yield at $G=30 \cdot 10^3$ is obtained at $G=10 \cdot 10^3$. However, assuming that the surface loading (or average particle-particle distance) is independent of rotor speed, the decreasing conversion time with rotor speed will result in a progressively higher area-specific throughput as demonstrated in Figure 12 (full line) for particles of MMD. Consequently, increasing the centrifugal acceleration to above the domain investigated here is not expected to contribute significantly to the yield of organics but is predicted to increase throughput.

6. Conclusions

For engineering purposes, the presented pseudo surface reaction model has been shown to describe the yields from flash pyrolysis of wood and straw in the PCR satisfactorily. It was shown that with the Broido-Shafizadeh kinetic scheme, parameters for cellulose represented wood very well whereas fitting cellulose parameters in accordance with the influence of the higher ash content led to an acceptable fit for the straw data. As this simplified kinetic scheme achieved a better fit than a superimposed based on the organic composition of the material, it again stresses that ash constituents are of more importance than organic composition for the yield distribution in flash pyrolysis of herbaceous biomass. However, the predictive power of the model for straw could possibly

be improved by determining the kinetic parameters for this material in a dedicated study.

Simulations showed that for the conditions investigated, the assumption of ablative degradation involving a steep temperature gradient and consumption of the reacting particle from the surface inwards did not hold. However, due to the minor importance of the pore system on the yields for the investigated particle size and temperature domain and the ability to keep the particle free of an insulating char layer by mechanical action in the reactor, the model could still describe the experimental data well. Accordingly, it appears that even though the concept of an ablatively melting particle may constitute a limiting case, it can still be used to model flash pyrolysis provided the reacting particle continuously shed a build up char layer.

Acknowledgements

CHEC is financially supported by the Technical University of Denmark, DONG Energy A/S, Vattenfall A/S, FLSmidth A/S, Hempel A/S, Energinet.dk, the Danish Research Council for Technology and Production Sciences, the Danish Energy Research Program, Nordic Energy Research Program, EU and many industrial partners. This particular project is financed by the DTU Innovation Program and the Nordic Energy Research Program.

Glossary

A	Pre-exponential factor	1/s
B	Reactor factor	-
Bi	Biot number	-
c_p	Specific heat capacity	J/kg/K
d	Diameter	m
e	Dimensionless molar mass	-
E	Activation energy	J/mol
F	Flow rate	kg/s
g	Gravitational acceleration	9.81 m/s^2
G	Acceleration/g	-
h	Heat transfer coefficient	W/m^2/K
k	Thermal conductivity	W/m/K
l	Length	m

M	Molar mass	kg/mol
MMD	Particle mass mean diameter	m
n	Particle velocity power law constant	-
p	Pressure	Pa
R	Distance from centre to surface or wall	m
R	Reaction	-
R_g	Universal gas constant	8.31 J/mol/K
r	Spatial coordinate for particle or in reactor	m
r_p	Rate of reaction	1/s
S	Product selectivity	-
s	Shape factor (0,1 & 2 for slab, cylinder & sphere)	-
T	Temperature	°C or K
t	Time	s
Th	Thermal Thiele modulus	-
u	Dimensionless position ($\equiv x^2$)	-
V	Gas volume of reactor	m^3
v	Velocity of retracting surface	m/s
X	Mass fraction or conversion	- or %
x	Dimensionless position	-
Y	Product yield (daf)	- or %
α	Thermal diffusivity	m^2/s
δ	Rotor-to-wall clearance	m
γ	Dimensionless activation energy	-
γ_g	Gas/char selectivity	-
η	Dimensionless position of surface	-
κ	Acceleration correction factor	-
θ	Dimensionless temperature	-
ρ	Density	kg/m^3
τ	Dimensionless time	-

Sub- and superscripts

b	Biomass (wood or straw)
c	Char

g	Gas (permanent gasses and water)
m	Mean (on mass basis)
o	Liquid organics
p	Particle
r	Reactor
s	Solids (char and biomass)
surf	Surface
0	Initial or nominal
∞	Surroundings or final

References

[1] Kersten SRA, Wang X, Prins W, van Swaaij WPM. Biomass Pyrolysis in a Fluidized Bed Reactor. Part 1: Literature Review and Model Simulations. Ind Eng Chem Res 2005;44:8773-85.

[2] Boukis IPh, Grammelis P, Bezergianni S, Bridgwater AV. CFB Air-Blown Flash Pyrolysis. Part I: Engineering Design and Cold Model Performance. Fuel 2007;86:1372-86.

[3] Luo Z, Wang S, Cen K. A Model of Wood Flash Pyrolysis in Fluidized Bed Reactor. Renew Energ 2005;30:377-92.

[4] Wang X, Kersten SRA, Prins W, van Swaaij WPM. Biomass Pyrolysis in a Fluidized Bed Reactor. Part 2: Experimental Validation of Model Results. Ind Eng Chem Res 2005;44:8786-95.

[5] Peacocke GVC, Bridgwater AV. Design of a Novel Ablative Pyrolysis Reactor. In: Bridgwater AV, editor. Advances in Thermochemical Biomass Conversion, vol. 2, London, UK: Blackie Academic and Professional; 1994, pp. 1134-50.

[6] Peacocke GVC, Bridgwater AV. Ablative Pyrolysis of Biomass for Liquids. Biomass Bioenerg 1994;7:147-54.

[7] Bridgwater AV, Peacocke GVC, Robison NM. Ablative Thermolysis Reactor. PCT Application WO 03/057800, 2003.

[8] Reed TB. Principles and Operation of a Novel “Pyrolysis Mill”. In: Proceedings of the Thermochemical Conversion Program Annual Meeting, Golden, USA: Solar Energy Research Institute; 1988, pp. 248-58.

[9] Diebold JP. The Cracking Kinetics of Depolymerised Biomass Vapors in a Continuous, Tubular Reactor. Master Thesis. Golden, USA: Colorado School of Mines, 1985.

[10] Miller RS, Bellan J. Numerical Simulation of Vortex Pyrolysis Reactors for Condensable Tar Production from Biomass. Energy Fuels 1998;12:25-40.

[11] Lédé J, Diebold JP, Peacocke GVC, Piskorz J. The Nature and Properties of Intermediate and Unvaporized Biomass Pyrolysis Materials. In: Bridgwater AV, Czernik S, Diebold JP, Meier D, Oasmaa A, Peacocke GVC et al., editors. Fast pyrolysis of biomass: A handbook, Newbury, UK: CPL Scientific Publishing Services ltd; 1999, pp. 51-65.

[12] Bech N, Jensen PA, Dam-Johansen K. Ablative Flash Pyrolysis of Straw and Wood: Bench-Scale Results. Proc 15th European Biomass Conference and Exhibition, Berlin, 7-11 May, 2007 (in press).

[13] Bech N, Dam-Johansen K, Jensen PA. Pyrolysis Method and Apparatus. PCT Application WO 2006/117005, 2006.

[14] Lédé J, Panagopoulos J, Li HZ, Villermaux J. Fast pyrolysis of wood: direct measurement and study of ablation rate. Fuel 1985;64:1514-20.

[15] Galgano A, Di Blasi C. Modelling Wood Degradation by the Unreacted-Core-Shrinking Approximation. Ind Eng Chem Res 2003;42:2101-11.

[16] Bird RB, Stewart WE, Lightfoot EN. Transport Phenomena, 2nd edition, New York, USA: Wiley; 2002.

[17] Diebold J, Power A. Engineering aspects of the vortex pyrolysis reactor to produce primary pyrolysis oil vapors for use in resins and adhesives. In: Bridgwater AV, editor. Research in thermochemical biomass conversion, London, UK: Elsevier; 1988, pp. 609-28.

[18] Diebold JP. A Unified, Global Model for the Pyrolysis of Cellulose. Biomass Bioenerg 1994;7:75-85.

[19] Liden AG, Berruti F, Scott DS. A Kinetic Model for the Production of Liquids from the Flash Pyrolysis of Biomass. Chem Eng Comm1988;65:207-21.

[20] Di Blasi C. Numerical Simulation of Cellulose Pyrolysis. Biomass Bioenerg 1994;7:87-98.

[21] Jensen PA, Sander B, Dam-Johansen K. Pretreatment of Straw for Power Production by Pyrolysis and Char Wash. Biomass Bioenerg 2001;20:431-46.

[22] Stenseng M. Pyrolysis and Combustion of Biomass. PhD Thesis. Kgs. Lyngby, DK: Department of Chemical Engineering, DTU; 2001.

[23] Boysan F, Ayers WH, Swithenbank J. A Fundamental Mathematical Modelling Approach to Cyclone Design. Trans IChemE 1982;60:222-30.

[24] Meyer KA. Three-Dimensional Study of Flow between Concentric Rotating Cylinders. Phys Fluids, II 1969;165-70.
[25] Schlichting H. Boundary Layer Theory. 4th ed. New York: McGraw-Hill; 1962.
[26] Várhegyi G, Jakab E, Antal MJ Jr. Is the Broido-Shafizadeh model for Cellulose Pyrolysis True? Energ Fuels 1994;8:1345-52.
[27] Lanzetta M, Di Blasi C. Pyrolysis Kinetics of Wheat and Corn Straw. J Anal Appl Pyrolysis 1998;44:181-92.
[28] Lédé J. The Cyclone: A Multifunctional Reactor for the Fast Pyrolysis of Biomass. Ind Eng Res 2000;39:898-903.
[29] Boutin O, Ferrer M, Lédé J. Flash Pyrolysis of Cellulose Pellets Submitted to a Concentrated Radiation: Experiments and Modelling. Chem Eng Sci 2002;57:15-25.
[30] Stenseng M, Jensen A, Dam-Johansen K. Thermal Analysis and Kinetic Modelling of Wheat Straw Pyrolysis. In: Bridgwater AV, editor. Progress in Thermochemical Biomass Conversion, Oxford, UK: Blackwell Science; 2001, pp. 1061-75.
[31] Villadsen J, Michelsen ML. Solution of Differential Equation Models by Polynomial Approximation. New Jersey, USA: Prentice-Hall; 1978.
[32] Channiwala SA, Parikh PP. A Unified Correlation for Estimating HHV of Solid, Liquid, and Gaseous Fuels. Fuel 2002;81:1051-63.
[33] Miller RS, Bellan J. A Generalized Biomass Pyrolysis Model based on Superimposed Cellulose, Hemicellulose, and Lignin Kinetics. Combust Sci Tech 1997;126:97-137.
[34] Fahmi R, Bridgwater AV, Darvell LI, Jones JM, Yates N, Thain S et al. The Effect of Alkali Metals on Combustion and Pyrolysis of Lolium and Festuca Grasses, Switchgrass and Willow. Fuel 2007;86:1560-69.
[35] Lédé J. Reaction Temperature of solid particles undergoing an endothermal volatilization. Application to the fast pyrolysis of biomass. Biomass Bioenerg 1994;7:49-60.
[36] Di Blasi C. Heat Transfer Mechanisms and Multi-Step Kinetics in the Ablative Pyrolysis of Cellulose. Chem Eng Sci 1996;51:2211-20.
[37] Martin H, Lédé J, Li HZ, Villermaux J, Moyne C, Degiovanni A. Ablative Melting of a Solid Cylinder Perpendicularly Pressed against a Heated Wall. Int J Heat Mass Trans 1986;29:1407-15.
[38] Lédé J, Li HZ, Villermaux J, Martin, H. Fusion-Like Behaviour of Wood Pyrolysis. J Anal Appl Pyrolysis 1987;10:291-308.

[39] Lédé J, Li HZ, Villermaux J. Pyrolysis of Biomass. Evidence for a Fusion-Like Phenomenon. ACS Symposium Series 1988;376:66-78.
[40] Peacocke GVC. Ablative Pyrolysis of Biomass. PhD Thesis. Birmingham, UK: University of Aston; 1994.
[41] Janse AMC, Westerhout RWJ, Prins W. Modelling of Flash Pyrolysis of a Single Wood Particle. Chem Eng Proc 2000;39:239-252.

Appendix E:

Predicting Fuel Elementary Composition by Bomb Calorimetry

Short Communication:

Predicting Fuel Elementary Composition by Bomb Calorimetry

Niels Bech [*], *Peter Arendt Jensen, Kim Dam-Johansen*

Department of Chemical Engineering, CHEC Research Centre, Technical University of Denmark, Building 229, DK-2800 Lyngby, Denmark

Abstract

Analysis of the elementary composition a fuel's organic fraction is important in many fields but unfortunately elementary analysers require a considerable monetary investment and skill to operate. This article presents a method to obtain a simplified elementary analysis of an organic sample in which the oxygen, nitrogen, and sulphur are lumped. The method uses a simple bomb calorimeter combined with a numerical procedure based on a generalised equation for predicting higher heating value. By analysing pure organic substances, literature data, and fuels it is demonstrated that the method can provide a hydrogen estimate within ±0.7% daf. and carbon and sum of oxygen, nitrogen, and sulphur estimates within ±2% daf. for fuels containing less than 90 % ash db., 2 % nitrogen daf., and 1% daf. sulphur.

Keywords: Elementary analysis; bomb calorimeter; biomass; coal

[*] Corresponding author: Tel. +45 45252851; Fax +45 45882258; e-mail: nsb@kt.dtu.dk

1. Introduction

Within fuel and combustion research the composition of the organic fraction of a fuel found by elementary analysis is often important. However, due to the special knowledge and high investment in equipment these analyses are often performed at specialised laboratories where a constant flow of samples allows operating the equipment. Correlations to predict the higher heating value (HHV) of a fuel from the ultimate analysis [1, 2, 3], or even the proximate analysis [3, 4], continue to be published whereas the reverse relationship to our knowledge has not received attention. Due to the before-mentioned cost and skill required to operate an elementary analyser we expect that a general procedure to deduce the elementary analysis by means of a bomb calorimeter will be of general interest. In this article we present a procedure developed in our lab by which a simplified elementary analysis may be obtained for fuel samples by means of a simple bomb calorimeter and investigate the applicability on common fuels.

2. Experimental Method

Samples from our material library which had been analysed to determine elementary composition (Flash Dymamic Combustion, Gas Chromatography (FDC-GC)) and ash content (CEN 14775 or ISO 1171) by an external laboratory and samples of simple pure (analytical grade) components with known composition were used. Moisture was for all solid samples determined at the time of the investigation to exclude changes in water content by a Sartorius electronic moisture analyser (model MA40) by drying at 105 °C until the change in weight remained below 0.01% in 120s.

Higher heating value was determined by an IKA C200 bomb calorimeter in isoperibolic mode according to DIN 51900 [5] and recalculated to dry basis. After the measurement the bomb was depressurised and all liquid and solid material in the bomb and crucible was collected by a pre-weighted paper towel and the mass determined on a four decimal laboratory scale. It was assumed that all organic material was combusted and that the collected material represented the sum of free water, water of reaction, and ash. For all samples the procedure was repeated five times and average values reported.

3. Numerical Procedure

Channiwala and Parikh [1] found in a comparative study employing 225 data points of various fuels that the best universal equation to predict the dry basis higher heating value (HHV) based on elementary composition had the form:

$$HHV = A_H H + A_C C + A_O O + A_N N + A_S S + A_A A \quad \textbf{(1)}$$

where *H*, *C*, *O*, *N*, *S*, and *A* is the content of hydrogen, carbon, oxygen, nitrogen, sulphur, and ash, respectively, expressed in percentage on dry basis and A_i's are the numerical coefficients displayed in table 1. For organics containing only H, C, and O the carbon content may predicted by combining (1) and the total mass balance:

$$C = \frac{HHV - (A_H - A_O) H - (A_A - A_O) A - 100 A_O}{A_C - A_O} \quad \textbf{(2)}$$

where *H* can be calculated from the material collected in the calorimeter bomb after correcting for sample ash and moisture content (free water). Finally, oxygen content is predicted by the mass balance:

$$O = 100 - H - C - A \quad \textbf{(3)}$$

This procedure is applicable for simple hydrocarbon fuels such as petroleum fractions. However, many solid fuels such as various biomasses and coal contain more than just traces of sulphur and nitrogen. If no information is available regarding the concentration of nitrogen and sulphur these components can be lumped with oxygen to obtain the equation:

$$C = \frac{HHV - (A_H - A_R) H - (A_A - A_R) A - 100 A_R}{A_C - A_R} \quad \textbf{(4)}$$

where R denotes the combined amount of oxygen, nitrogen, and sulphur. Since oxygen in most cases will be dominating the simplest procedure is taking A_R equal to A_O but if the level of the trace elements is known a priori a better value may be found from:

$$A_R = \sum_{i=O}^{S} \frac{i}{O + N + S} A_i \quad \textbf{(5)}$$

Table 1: Coefficient for equation (1) with HHV expressed in J/g and composition in percentage on dry basis.

A_H	A_C	A_O	A_N	A_S	A_A
1178.3	349.1	-103.4	-15.1	100.5	-21.1

Finally, a mass balance yields:

$$O + N + S = 100 - H - C - A \quad \textbf{(6)}$$

In (4) to (6) it is assumed that neither nitrogen nor sulphur will influence the determined hydrogen content and thereby also the other elements but this may not necessarily be true. During combustion these elements will form the corresponding gaseous oxides which through further oxidation and reaction with water can form nitric and sulphuric acid. For sulphur this can be represented by the reaction scheme [6]:

$$S + O_2 \rightarrow SO_2(g) \quad \textbf{(7)}$$

$$SO_2(g) \rightleftarrows SO_2(aq)$$

$$SO_2(aq) + H_2O \rightleftarrows HSO_3^-$$

$$HSO_3^- \rightleftarrows SO_3^{2-} + H^+$$

$$SO_3^{2-} + H_2O \rightleftarrows SO_4^{2-} + 2H^+$$

The relative proportions of the various sulphite and sulphate ions are dependent on the detailed equilibrium chemistry in both the gaseous and the aqueous phases. Thus, it is expected that a certain, although low, amount of these elements can be tolerated without effecting the hydrogen determination significantly.

Ash in the fuel is also capable of influencing the determined hydrogen content by reaction. During combustion in the pure oxygen atmosphere substantial temperatures may be reached whereby reactions not important in the customary analysis of ash at 580 to 600 ºC [7] can play a role. An example is calcination of carbonates:

$$MCO_3(s) \rightarrow MO(s) + CO_2(g) \quad \textbf{(8)}$$

where M denotes a suitable anion. During biomass combustion, substantial chloride release has been observed [8] and can result in gaseous hydrochloric acid formation:

$$Biomass - HCl(s) \rightarrow HCl(g) + Biomass(s) \quad \textbf{(9)}$$

$$HCl(g) \rightleftarrows H^+(aq) + Cl^-(aq)$$

However, the equilibrium between gaseous HCl and ions in aqueous solution is expected to mediate the effect on hydrogen determination.

4. Results and Discussion

Initially the outlined method was tested with pure organic chemicals containing only hydrogen, carbon, and oxygen. The results depicted in Table 2 show that for these compounds a nearly unbiased result with low variability could be obtained for hydrogen

whereas both carbon and oxygen estimates were biased and with considerably higher absolute variability.

Table 2: Predicted elementary composition (% wt. daf.) and absolute error of prediction for pure organic substances containing only C, H, and O.

Substance	H	C	O	E_H	E_C	E_O
Ethylene glycol	9.7	37.7	52.5	0.0	-1.0	1.0
Ascorbic acid	4.6	39.3	56.1	0.0	-1.6	1.6
Cellulose	6.0	44.1	49.1	-0.2	-0.3	0.6
n-Decane	15.6	83.5	0.9	0.0	-0.9	0.9
Benzene	7.6	92.3	0.1	-0.1	0.0	0.1
n-Dodecanol	14.0	77.1	8.9	0.0	-0.3	0.3
Ethyl acetate	9.1	52.4	38.4	0.0	-2.1	2.1
Polyethylene oxide	9.0	55.5	35.4	-0.1	1.0	-0.9
Methyl cyclohexane	14.3	83.3	2.3	0.0	-2.3	2.3
Benzoic acid	5.0	67.1	27.9	0.1	-1.7	1.7
Average				-0.1	-0.9	1.0
2 x Std. deviation				0.2	2.1	2.0

Table 3: Influence of ash, nitrogen, and sulphur on predicted elementary composition (% wt. daf.).

Substance	E_H	E_C	E_R
Adipic Acid	0.1	-4	4
Adipic Acid, 5% K_2CO_3	-0.2	-3	3
Adipic Adic, 5% KCl	-0.1	-3	3
Adipic Acid, 6.4% S	1.3	-3	2
92% Adipic Acid, 5% Methionine, 3% Urea	0.0	-2	2

Before applying the method on solid fuels the possible influence of reactive ash components, sulphur and nitrogen on hydrogen determination was tested. This was done by observing the effect of adding these components to adipic acid, a crystalline dicarboxylic acid with an elemental composition similar to that of most biomasses (7.0% H, 46% C, 47% O), and is reported in Table 3. As expected both addition of carbonate (as potassium carbonate) and chloride (as potassium chloride) resulted in under prediction of hydrogen through the weigh loss mechanisms proposed above. However, in both cases the effect was small compared with the error standard deviation even for the large additions relative to real fuels. Addition of sulphur on the other hand resulted in a large over prediction of hydrogen. Finally, predicting hydrogen content of a synthetic bio-

mass produced by mixing adipic acid, methionine, and urea (composition: 6.9% H, 48% C, 42% O, 1.1% S, 2.0% N, all daf.) was achieved without error. Therefore, the following will only treat fuels containing less than 2.0% N and 1.0% S as these levels apparently do not affect hydrogen determination significantly.

In order to study the suitability of the method for fuel analysis on a larger set of data, 111 data points of liquid and solid fuels selected only by their nitrogen and sulphur content were taken from the literature [1, 9] and analysed. This was done by assuming that hydrogen could be determined quantitatively and then applying (3) and (4) without adjusting A_R for nitrogen and sulphur (*i.e.* $A_R=A_O$). The data points covered fuels with ash contents from 0 to 90% db. Figure 1 shows the correlation obtained between the analysed and predicted elementary composition. For 95% of the data points carbon and the sum of oxygen, nitrogen, and sulphur were predicted within ±2.8% wt. daf., as found from twice the error standard deviation, or somewhat higher than experimentally found with the simple hydrocarbons (Table 2).

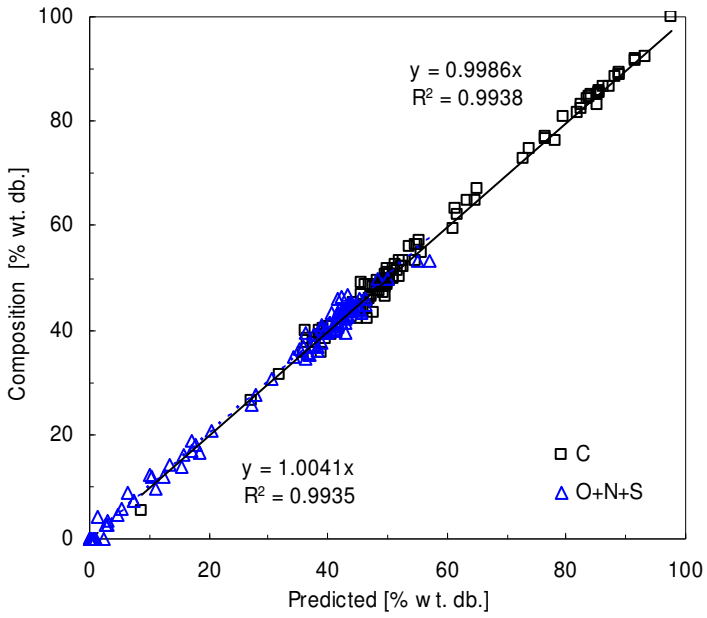

Figure 1: Correlation between composition and prediction of carbon and oxygen, nitrogen, and sulphur content (% wt. db.) for 111 fuels investigated by Channiwalla et al. [1] and reported by Gauer et al. [9].

Since the literature data were originally used to derive (1) and the coefficients of Table 1 and since it was unclear whether the lower accuracy results from the fuels containing ash, nitrogen, and sulphur or is the result of the method used to analyse the fuels elementary, we analysed ten fuels from our own library. Table 4 presents the results ob-

tained and the error standard deviations are seen to be in agreement with those found from the analysis of the literature data. Accordingly, we were confident that these values were representative and could be used to derive the accuracy which can be expected from the present method.

Table 4: Predicted elementary composition and absolute error of prediction for fuels (% wt. daf.).

Fuel	H	C	R	E_H	E_C	E_R
Wheat Straw Pellets	6.2	49	45	-0.2	0	1
Pine Wood Pellets	5.9	51	43	-0.4	1	-1
Spruce Bark	5.9	51	43	-0.3	-3	3
Waste Wood	6.0	50	44	-0.3	-1	1
75% Caragenan Residue, 25% Shea Nut Shell	6.0	50	44	-0.2	0	1
75% Pektin Residue, 25% Potato Starch Residue	6.3	48	46	0.0	-3	3
Olive Residue	6.1	55	39	-0.4	1	0
Coal A (Columbia)	6.2	80	14	0.7	-1	0
Coal B (Poland)	5.8	84	10	0.5	0	0
Coal C (Poland)	5.0	81	14	0.0	-1	1
Average				0.0	-0.8	0.8
2 x Std. deviation				0.7	2.5	2.5

Because the experimentally observed error is the result of both error from the present method and the method used to analyse the fuels elementary, the method error can be found by correcting the former for the latter by standard deviation arithmetics. Table 5 presents the measurement error reported by our external laboratory taken as twice the standard deviation for measurements performed on the same reference material over several days and with different operators. These are conditions under which our material library has been gathered over the years. In addition, the calculated method error which can be expected for the present method is presented. It is observed that for both carbon and the sum of oxygen, nitrogen, and sulphur this estimate is in excellent agreement with the estimate for method error obtained with the pure hydrocarbon samples where the elementary composition was derived without the use of an elementary analyser. Accordingly, for 95% of solid and liquid fuel samples containing less than 90% db. ash, 2% daf. nitrogen, and 1% sulphur it can be expected that elemental analysis by bomb calorimetry can predict the hydrogen content within ±0.7% daf., carbon content within ±2% daf., and the sum of oxygen, nitrogen, and sulphur content within ±2% daf.

Table 5: Measurement error (two std. deviations) for elementary analysis by FDC-GC and bomb calorimetry, % wt. daf.

	E_H	E_C	E_R
FDC-GC	0.2	1.5	1.5
Bomb Calorimetry	0.7	2.0	1.9

5. Conclusions

A simplified elementary analysis can be obtained for fuels with a bomb calorimeter provided ash and moisture contents are known and the fuel contains less than 2% daf. nitrogen and 1% daf. sulphur. Since the method is not capable of distinguishing between oxygen, nitrogen, and sulphur these elements are reported as a lump sum. Study of literature and experimentally obtained data has shown that for 95% of liquid and solid fuel samples with the above restrictions an accuracy of 0.7% daf. can be expected for hydrogen and 2% daf. for both carbon and the sum of oxygen, nitrogen, and sulphur.

Acknowledgements

CHEC is financially supported by the Technical University of Denmark, DONG Energy A/S, Vattenfall A/S, FLSmidth A/S, Hempel A/S, Energinet.dk, the Danish Research Council for Technology and Production Sciences, the Danish Energy Research Program, Nordic Energy Research Program, EU and many industrial partners. The authors wish to acknowledge Edith Thomsen and Kathrine Hansen from DONG Energy A/S for their assistance with and information on elementary analysis.

Glossary

A	Ash content	% wt. db. or daf.
A_i	Elemental coefficient for (1)	J (% wt. db.)$^{-1}$
C	Carbon content	% wt. db. or daf.
E	Absolute measurement error (measured – true value)	% wt. daf.
H	Hydrogen content	% wt. db. or daf.
HHV	Higher heating value on dry basis	J g^{-1}
N	Nitrogen content	% wt. db. or daf.
O	Oxygen content	% wt. db. or daf.

R	Rest (oxygen, nitrogen, and sulphur) content	% wt. db. or daf.
S	Sulphur content	% wt. db. or daf.

Subscripts

C	Carbon
H	Hydrogen
N	Nitrogen
O	Oxygen
R	Oxygen, nitrogen, and sulphur
S	Sulphur

References

[1] Channiwala SA, Parikh PP. A unified correlation for estimating HHV of solid, liquid and gaseous fuels. Fuel 2002;81:1051-63.

[2] Meraza L, Domínguez A, Kornhauserb I, Rojas F. A thermochemical concept-based equation to estimate waste combustion. Fuel 2003;82:1499-1507.

[3] Thipkhunthod P, Meeyoo V, Rangsunvigit P, Kitiyanan B, Siemanond K, Rirksomboon T. Predicting the heating value of sewage sludges in Thailand from proximate and ultimate analyses. Fuel 2005;84:849-57.

[4] Parikh J, Channiwala SA, Ghosal GK. A correlation for calculating HHV from proximate analysis of solid fuels. Fuel 2005;84:487-94.

[5] DIN 5900-2. Determining the gross calorific value of solid and liquid fuels using the isoperibol or static jacket calorimeter and calculation of net calorific value, 2003.

[6] Singh, HB (ed). Composition, Chemistry, and Climate of the Atmosphere. New York: Van Nostrand Reinhold; 1995.

[7] ASTM D 1102. Standard test method for ash in wood, 2001.

[8] Knudsen JN, Jensen PA, Dam-Johansen K. Transformation and release to the gas phase of Cl, K, and S during combustion of annual biomass. Energ. Fuel 2004;18:1385-99.

[9] Gaur S, Reed TB. Thermal Data for Natural and Synthetic Fuels. New York: Marcel Dekker; 1998.

Appendix F:

Pilot Production and Combustion of Straw Bio-Oil

1 Introduction

This appendix reports on the pilot plant operation of the bench-scale Pyrolysis Centrifuge Reactor, on the properties of the produced straw bio-oils, and on attempts to combust the produced samples in domestic rapeseed oil furnaces. The investigation was initiated with the intention to test the reactor system over longer runs and at higher feed rates, obtain representative samples of straw bio-oil for characterization, and to test the suitability of straw bio-oil as a liquid fuel replacement. First, the experimental equipment, procedures, and results are presented. Second, the properties of the produced samples are compared to specifications for a future standard for bio-oil and recommendations for improvements to the pyrolysis pilot plant proposed. Third, the combustion behavior of bio-oil and rapeseed oil is reviewed in order to explain the observed behavior of the fuels during the trials and propose suitable modifications to the equipment. Finally, the findings are compared with the practical experience of bio-oil combustion reported in the literature.

The combustion trials would not have been possible without the consent of M. Jørgensen from the company Firegreen and M.P. Roesen from KSM-Roesen. The author wishes to thank both for their invaluable assistance during these trials.

2 Pilot Plant Runs

2.1 Experimental

Two pyrolysis pilot plant runs were completed during October and November of 2007 under identical conditions and approximately two liters of bio-oil were produced in each. The feed material was obtained by crushing wheat straw pellets and removing sizes above 1.4 mm by sieving. Properties for the feed material are displayed in Table 1.

For the pilot runs the procedure for operating the equipment was slightly changed compared to the previous experimental runs of shorter duration (see appendix C and E). The solid feed rate was set to the feeder's maximum in order to test reactor operation at higher feed rates and since the electric heating elements for zone 1 and 2 (*i.e.* near the reactor entrance) were not able to supply adequate power to maintain the set point of 550 °C the realized temperature in these zones were considerably lower.

Furthermore, since the preheater was out of service at the time the re-circulated gas was returned to the reactor unheated. Also, the produced bio-oil was continuously removed from the direct condenser in order to remove carry-over char by filtration on a vacuum filter. Finally, since heavy compounds condensed at the vapor nozzle tip of the direct condenser feeding was interrupted approximately five minutes every 20 minutes and the direct condenser was emptied in order to clean char buildup in the nozzle. Table 2 displays the realized experimental conditions for both runs.

Table 1: Properties of straw feed used for the pilot runs.

Property	**Method**	**Value**
Water content (% wt.)	Mettler-Toledo Moisture Analyzer MA40 [a]	9.2
Ash content (% wt. db.)	ASTM D1102 (550 °C)	7.0
HHV (MJ kg^{-1})	DIN 51,900	17.0
HHV db. (MJ kg^{-1})	DIN 51,900	18.2
C (% wt. daf)	Calorimetry [b]	49
H (% wt. daf)	Calorimetry [b]	6.2
O+N+S (% wt. daf)	Calorimetry [b]	45

[a] Drying at 105 °C until change in weight < 0.01% in 120s; [b] See appendix E

Table 2: Experimental conditions during pilot runs.

Property	**Unit**	**Value**
Nominal centrifugal acceleration	g	$1.0 \cdot 10^4$
Reactor temperature, zone 1	°C	420
Reactor temperature, zone 2	°C	480
Reactor temperature, zone 3+4	°C	550
Preheater temperature	°C	60 - 70
Tracing temperature	°C	420
Gas residence time	ms	~ 500
Solid feed rate	kg h^{-1}	2.4
Specific feed rate	kg m^{-2} h^{-1}	69

The yield of bio-oil for the pilot runs operating at a specific straw feed rate of 69 kg m^{-2} h^{-1} was 53 and 48 % wt. of wet feedstock, respectively. Although not statistically significant, this is in average somewhat lower than the 54 % obtained in an earlier experiment with similar feedstock and conditions but at a lower specific feed rate of 41 kg m^{-2} h^{-1}. However, this does not need to be caused by the higher feed rate *per se* but rather by the relatively low temperatures realized in zone 1 and 2, the cold re-circulated gas, and less careful collection of product.

2.2 Bio-Oil Properties

The fuel properties of the bio-oil samples obtained from the pilot runs were analyzed and compared with typical properties of a wood-derived bio-oil, see Table 3. Both samples were homogeneous liquids with an intense burgundy/maroon color that appeared black in larger containers and had a characteristic smell of smoke with a note of acid. In Figure 1 the dynamic viscosity with temperature for the samples and for the wood-derived bio-oil is compared with that of rapeseed oil (RSO) and rapeseed bio-diesel, two alternative liquid fuels suitable for combustion in small furnaces. The bio-oil properties are further discussed in section 3.4.

Table 3: Comparison of fuel properties between the October (10/07) and November (11/07) straw bio-oil samples and typical specifications for Dynamotive wood-derived bio-oil (Wood).

Property	**Method** [a]	**10/07**	**11/07**	**Wood** [b]
Density @ 20°C (kg dm^{-3})	Hydrometer	1.18	1.20	1.2
Water content (% wt.)	Refractive index [c]	25.8	28.1	20-25
Ash content (% wt.)	ASTM D1102 (550 °C)	1.2	0.36	<0.02
HHV (MJ kg^{-1})	DIN 51,900	15.4	15.5	16-19
HHV db. (MJ kg^{-1})	DIN 51,900	20.7	21.5	21-25
C (% wt. daf)	Calorimetry [d]	50	52	*n.a.*
H (% wt. daf)	Calorimetry [d]	6.6	6.4	*n.a.*
O+N+S (% wt. daf)	Calorimetry [d]	42	41	*n.a.*
Dynamic viscosity (cP)	Rotation viscometer [e]			
- @ 20 °C		108	53	84
- @ 40 °C		24	18	23
- @ 60 °C		9.2	8.9	10
- @ 80 °C		6.4	6.0	5

[a]For straw-derived samples; [b]From Dynamotive [1]; [c]See Appendix C; [d]See Appendix E; [e]DIN SC4-18/13R spindle

3 Combustion Trials

3.1 Burners

Combustion trials were carried out with burners developed for combustion of RSO in domestic furnaces. These small-scale burners were chosen due to the relatively small samples of produced bio-oil and the availability of test facilities locally.

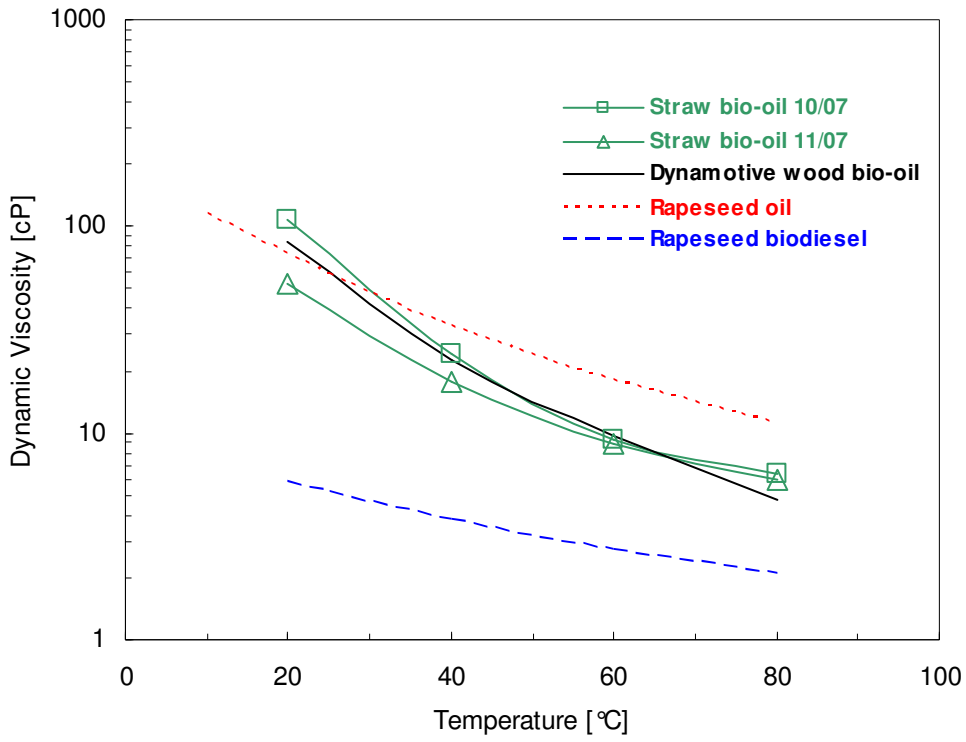

Figure 1: Dynamic viscosity with temperature for RSO [2], rapeseed bio-diesel [3], and straw and wood derived bio-oil samples. Data for bio-oils from Table 3.

3.1.1 Firegreen

The Firegreen burner [4] is intended for replacing a conventional heating oil burner of a domestic furnace and has a rated capacity of 15 to 70 kW. The liquid fuel is pumped to a level-controlled open tank where an electric thermostat-controlled heater maintains it at the desired set-point. From the tank the fuel is drawn to an air-assist spray nozzle by the vacuum created by the compressed air supplied to the nozzle. The liquid nozzle is a Delavan #30609-5 producing a solid cone spray. Secondary combustion air is delivered by a blower to the pipe enclosing the nozzle within the combustion chamber and swirl is created by a disk distributor, see Figure 2. The system can be regulated by changing the liquid pre-heat temperature, the nozzle air pressure, and the amount of secondary air but fuel flow can not be controlled independently but increases with nozzle air pressure. Ignition of the fuel is accomplished by an electric spark between two ignition electrodes positioned just above the nozzle tip.

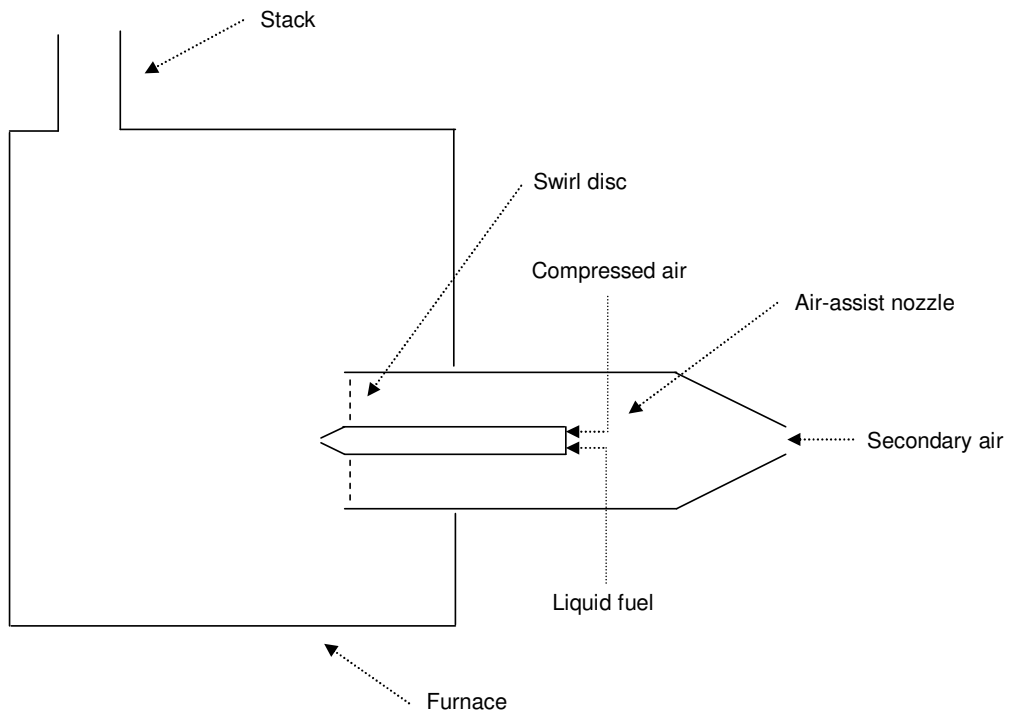

Figure 2: Firegreen burner installed in furnace.

3.1.2 KSM-Roesen

The KSM-Roesen burner [5] is an experimental unit developed by M. P. Roesen and intended for the same market as the Firegreen but not yet in production. In this design fuel is metered by a step motor coupled to a gear pump and feed to an inline preheater before entering the air-assist nozzle which similar to the Firegreen's but rated at a higher flow (Delavan #30610-8). In the combustion chamber the nozzle and the surrounding secondary air supply pipe is located within a horizontally oriented ø 250 mm radiation reflector pipe extending approximately 500 mm beyond the tip of the nozzle, see Figure 3. The secondary air supply system is similar to the Firegreen's but is without a distributor for inducing swirl. The system is controlled by regulating liquid pre-heat temperature, liquid flow rate, nozzle air pressure, and amount of secondary air.

3.2 Flue Gas Analysis

For both burners, flue gas was continuously drawn from the stack, filtered, dried in a refrigeration dryer, and analyzed by Rosemount UV gas analyzers. Results for CO, CO_2, O_2, NO, and SO_2 were logged on a laptop computer.

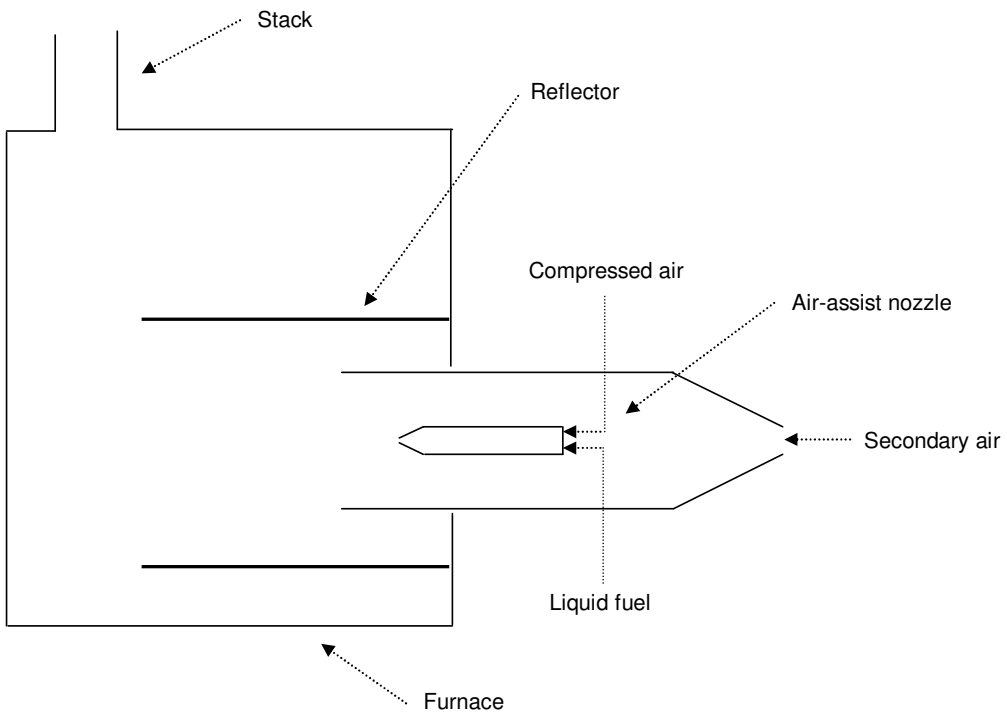

Figure 3: KSM-Roesen burner installed in furnace.

3.3 Results

In the first run sample 10/07 was tested in the Firegreen burner. The bio-oil was initially preheated to 60 °C which had been established to be suitable for RSO in order to reduce the viscosity sufficiently for good atomization. As expected, atomization was excellent at this temperature due to the lower viscosity of the bio-oil. However, since ignition proved difficult the preheating temperature was adjusted to 90 °C in order to increase the gaseous concentration of flammable components in the igniter vicinity. Nevertheless, even at this temperature approximately 50 ml of ethanol had to be added to the top of the preheating tank in order to establish a flame. After ignition with ethanol the pure bio-oil burned with an unstable flickering flame about 100 mm in front of the nozzle. This was unlike the performance with RSO where a stable flame was observed approximately 40 mm from the nozzle tip.

The CO emission reflected the poor bio-oil performance as concentrations varied between 3500 and 7300 ppm (150 ppm for RSO). In contrast, nitric oxide and sulfur dioxide emissions were comparable to RSO at 50 to 80 ppm (45 for RSO) and 35 to 50 ppm (12 for RSO), respectively. Oxygen concentrations at 16 to 18 % vol. (4.5 % for RSO) and CO_2 concentrations at 2 to 5 % vol. (13 % for RSO) indicated that

secondary air should be reduced. However, any attempt to do so resulted in loss of flame.

The KSM-Roesen burner was selected for a new attempt with sample 11/07 due to its ability to control liquid flow rate independently of primary air supply. It was speculated that the poor flame stability observed with the Firegreen burner and thus small operational window with regard to secondary air was caused by an excessive primary air to fuel ratio. Due to the fixed ratio between compressed air and liquid flow and the difference in elemental composition the Firegreen burner supplied 5% of the stoichiometric air demand when operating on RSO but 10% for bio-oil. This indicated that conditions were too lean near the nozzle tip and that doubling the liquid flow rate would create similar conditions to those for RSO operation whereby ignition and flame stability could be improved.

The KSM-Roesen burner had the same difficulties igniting the fuel as had been experienced with the Firegreen. The liquid temperature was initially maintained at 60 °C. Due to the plug flow design of liquid feeding system it was possible to ignite the bio-oil by operating the burner on RSO for several minutes and then switch to bio-oil. Visually the clear feed hose revealed when the bio-oil reached the preheater and at that time the flow rate was doubled in order to maintain the same primary air to fuel ratio. Immediately after changing fuel the operation of the burner was unaffected but after approximately 30 seconds the flame went out. Attempts to rectify this behavior by changing nozzle air pressure, fuel flow rate, secondary air admission, and preheater temperature was unsuccessful. Due to the short duration of each successful start on bio-oil no meaningful data for emissions of this fuel were collected. However, when firing RSO the burner achieved excellent emission values with CO concentration at 15 to 20 ppm, NO at 70 ppm, SO_2 at 2 ppm. Carbon dioxide and oxygen values were comparable to those achieved with the Firegreen firing RSO at 11 and 5.5 % vol., respectively.

3.4 Discussion

3.4.1 Bio-Oil Properties

For commercial hydrocarbon and some biomass-based liquid fuels national and international standards specify the accepted chemical and physical properties relevant

for combustion, handling, and safety. Due to the at present low production volume this is not the case for bio-oil even though suggestions for a future standard have been published, see Table 4. This framework operates with four grades defined in term of viscosity at a reference temperature and ash content analogous to how hydrocarbon fuel oils are classified [7]. According to the suggested classification the produced samples, as well as the reference wood-derived bio-oil, can be classified as *light-medium* products if the ash content of the samples was below 0.05 % wt. (see Table 3). However, it has earlier been established that the relatively high ash content of the samples is caused by leaching of soluble inorganic components from carry-over char particles before they are removed by filtration (see Appendix D). Accordingly, by optimizing the char separation system it is expected that the product can be brought within the ash content specifications.

Table 4: Proposed specifications for various grades of bio-oils [6, 7].

Property	**Light**	**Light-medium**	**Medium**	**Heavy**
Kin. viscosity @ 40ºC (cSt)	1.9-3.4	5.5-24	17-100 [a]	100-638 [a]
Ash (% wt.)	<0.05	<0.05	<0.10	<0.10
Solids (% wt.)	<0.01	<0.05	<0.10	<0.25
Water (% wt.)	<32	<32	<32	<32
LHV (MJ l^{-1})	>18	>18	>18	>18
S (% wt.)	<0.1	<0.1	<0.2	<0.4
N (% wt.)	<0.2	<0.2	<0.3	<0.4
Phase stability, 8 h @ 90 ºC	single	Single	single	Single
Flash point (ºC)	>52	>55	>60	>60

[a] *@ 50 ºC*

Energy content of bio-oils produced by flash pyrolysis (expressed by HHV or LHV) depends on water content, raw material, and to some degree on pyrolysis process and conditions. Table 5 displays properties of five bio-oil samples produced by larger pilot or commercial production units. On dry basis the HHV of the bagasse-derived samples is seen be significant lower than those produced from hard and softwoods. Oasmaa *et al.* [8] found that the dry basis LHV was 19 to 22 MJ kg^{-1} for wood-derived oils, 18 to 21 MJ kg^{-1} for wheat straw oils, and 22 to 23 MJ kg^{-1} for oils rich in lignin-derived water insolubles. Accordingly, materials with relatively low contents of lignin, such as herbaceous feedstocks (*e.g.* wheat straw and bagasse), are expected to have a lower dry basis specific energy contents than the wood-derived bio-oils. On volumetric basis the samples had a LHV of 16.2 MJ L^{-1} (19.5 MJ kg^{-1} db.) and 16.5

MJ L^{-1} (20.3 MJ kg^{-1} db.) for sample 10/07 and sample 11/07, respectively, or approximately 10 % below the minimum LHV specification. Ignoring the effect of increased density with water removal, the water contents must be reduced to 19.4 and 23.5 % wt. for samples 10/07 and 11/07, respectively, in order to bring this figure up to the required 18 MJ L^{-1}.

Table 5: Selected properties of five bio-oils produced in larger production units [9]. Samples A, B, and C produced by Dynamotive, sample D by Forestera and sample E by Ensyn.

Property	**A**	**B**	**C**	**D**	**E**
Feed material	Pine/ spruce	Pine/ spruce	bagasse	spruce	Oak/ maple
Feed moisture content (% wt.)	2.4	3.5	2.1	6-9	
Feed ash content (% wt.)	0.42	2.6	2.9		
Water (% wt.)	23.3	23.4	20.8	23.8	22
Solids (% wt.)	<0.1	<0.1	<0.1	0.05	0.045
Ash (% wt.)	<0.02	<0.02	<0.02	<0.02	0.01
N (% wt.)	<0.1	0.3-0.4	0.7	0.04	0.2
S (% wt.)	<0.01	<0.05	<0.1	<0.01	<0.01
Kin. viscosity @ 20 ºC (cSt)	73	78	57		
Kin. viscosity @ 40 ºC (cSt)				15	50 [a]
Kin. viscosity @ 80 ºC (cSt)	4.3	4.4	4		12
Density (kg dm^{-3})	1.20	1.19	1.20	1.19	1.18
HHV (MJ kg^{-1})	16.6	16.4	15.4	17.6	17
HHV db. (MJ kg^{-1})	21.6	21.4	19.4	23.1	21.8
LHV (MJ kg^{-1})				16.0	15.7

[a] @ 50 ºC

Control of water in the bio-oil product is traditionally achieved by pre-drying the feedstock in order to reduce the moisture content below that used here as can be seen from the raw material characteristics reported in Table 5. An alternative is to employ fractional condensation of vapors whereby the concentration of low boiling oxygenates with poor heating value is simultaneously reduced which has been shown to improved storage stability and increase the flash point [10]. Since bio-oils regardless of feedstock origin have been found to have flash point in the 50 to 66 ºC range [8] fractional condensation appears promising for bringing the product within specifications for heating value, stability, and flash point. However, employing this method for water control also results in a reduced yield of liquid organics in the bio-oil fraction because low boiling components evaporate at lower temperatures or form azeotropes with water and are lost to the condensate. Preliminary experiments with

pine-derived bio-oil where water was evaporated at ~ 65 °C under reduced pressure in a rotavap and the water content reduced from 33.9 % wt. to 14.1 % wt. suggest that the distillate will contain 10-12 % wt. organics. This estimate is in agreement with the findings of Oasmaa *et al.* [10] who evaporated water from pine-derived bio-oil at 40 °C and found the organics/water ratio of the distillate to be relatively constant throughout the process. Accordingly, reducing the water content in the bio-oil by the required 5.5 % wt. (*i.e.* the average value for the two samples) by fractional condensation is expected to result in a loss of less than 1 % wt. of the liquid organics. However, since the heating value of the lost components is below the average for the organics the energy yield calculate on HHV will be decreased by less and may if calculated on LHV basis even increase [10].

Solids, sulfur, and nitrogen contents in addition to phase stability was not determined for the produced samples. Solid char particles are known to reduce the stability of bio-oils [11, 12] and since the high ash content was also caused by carry-over char particles and may accelerate the degradation [13] it is essential to increase the efficiency of the char separation system. The sulfur content of straw-derived bio-oils (400 to 500 ppm) is generally higher than that for the wood-derived oils (60 to 500 ppm) [8] but well below the proposed specifications and is thus not expected to be problematic. This is in contrast to the nitrogen content which has been found to be generally higher for bio-oils derived from herbaceous feedstock as seen in Table 5. Oasmaa *et al.* found that the nitrogen content for wheat straw derived bio-oil was 0.3 to 0.4 % wt. whereas it was below 0.1 % wt. for wood-derived oils [8]. Accordingly, since nitrogen contents at that level will result in declassification to the *medium* or *heavy* category, which could potentially reduce the value of the product, the nitrogen content should be determined and an investigation carried out in order to determine the effect of process conditions and straw properties on nitrogen partitioning between products.

In summary, it is expected that straw-derived bio-oil produced with the PCR can obtain the proposed *light-medium* specification if char separation is improved, water content reduced by fractional condensation, and nitrogen partitioning controlled. Whereas the former two conditions are expected to be relatively straightforward to achieve, the latter may require further investigation to determine the effect of process

conditions and raw material properties. If the nitrogen portioning can not be controlled a declassification to *medium* or *heavy* may result which may affect the value of the product negatively.

3.4.2 Bio-Oil Combustion Behavior

The behavior of bio-oil subjected to heating and combustion has been investigated by thermogravimetric techniques [14-17] and single droplet heating and/or combustion [18-22]. However, for the purpose of this discussion the results obtained with the latter technique are more relevant due to the lower heating rates employed in the former, typically 5 to 20 °C/min. Calabria *et al.* [18] reported five distinct phases during heating of a single wood/bark-derived bio-oil droplet suspended on a thermocouple above a heating coil, see Figure 4. The ø 847 µm droplet initially heated from room temperature to 100 °C where gas bubbles began to cause repeated expansions and collapses followed by a temperature plateau at approximately 130 °C due to the evaporation of water and light organics. In the next phase the droplet heated to 180 °C under continued gas production and fluctuations in diameter although progressively smaller. At 180 °C the gas ignited and burned homogeneously causing droplet heating to accelerate. When the droplet reached approximately 500 °C the blue gas flame extinguished and heterogeneous combustion (yellow flame) of the formed char cenosphere caused the interior temperature to peak. D'Alessio *et al.* [20] observed similar initial behavior when exposing ø 600 µm single droplets of pine or poplar derived bio-oil suspended on a thermocouple to a flow of air heated to 1200 °C (local Re≈20). Under these conditions, water and light organic evaporation initiated at 100 °C after which the droplet heated to 500 °C where a second plateau was observed. The gas ignited at 600 °C followed by a rapid temperature rise during the following sooty cenosphere burnout. In agreement with Calabria *et al.* they observed maximum droplet expansions up to between 1.5 and twice the initial diameter. Droplet pulsation was observed well in to the combustion period.

Wornat *et al.* dropped single ø 320 µm droplets of oak or pine derived bio-oils in to a vertical laminar flow reactor furnace heated to 1327 °C by an internal H_2/CH_4 fueled combustor adjusted to yield a O_2 concentration of 24 % vol. They observed four distinct phases during combustion of the oils. After introduction in to the furnace and ignition the undisturbed droplet was surrounded by a blue flame, a behavior which

they also observed for pure droplets of methanol and acetone under the same conditions. However, suddenly gases were released from within the droplet causing it to distort in shape and release small fragments from the surface. During this microexplosion the droplet was surrounded by a yellow flame indicative of soot formation which they ascribe to gas-phase pyrolysis. Following the eruption, the flame turned blue and the droplet coalesced in to its original spherical shape although vapor release continued but at a markedly reduced rate. Finally, a yellow flame was observed during cenosphere burn-out. In a later study employing the same equipment and conditions Shaddix *et al.* [21] confirmed these findings and found that samples with an increased content of char would distort in microexplosions earlier compared to hot gas filtered samples with a residual char content approximately hundred times lower. The authors offer the explanation that the char particles facilitated the nucleation of gas bubbles leading to microexplosions at lower values of superheat.

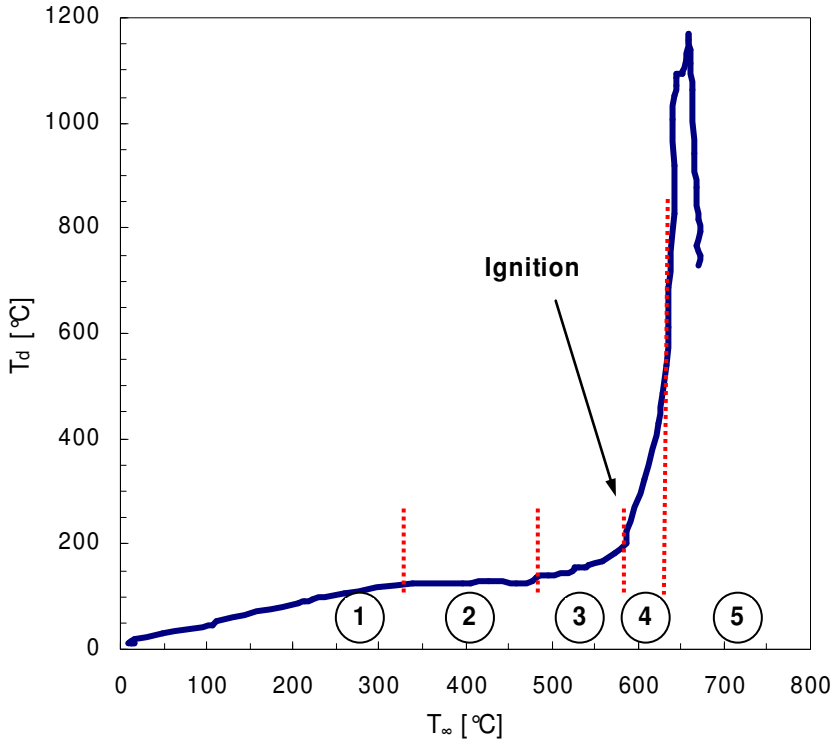

Figure 4: Droplet center temperature with temperature of environment during heat-up (1), evaporation (2), devolitalization (3), homogeneous combustion (4), and heterogeneous cenosphere combustion (5). Initial bio-oil droplet diameter was 847 µm. Data from [23].

From the discussion above it appears that the hanging droplet and the drop tube experiments differ in whether the droplet is superheated before evaporation in the

interior starts. In this connection Wornat *et al.* discuss two limiting cases, that of batch distillation on one hand and that of superheating on the other, and it appears that a continuum of superheat is attainable before bubble formation starts. Furthermore, in addition to the nucleation effect of solid particles, time, and thereby indirectly heating rate, may also play a role. This has been shown to be the case for liquids containing readily activated nucleation centers [24-26] because time during rapid heating may be insufficient for an assumed equilibrium phase change even though nucleation dominates the phase transition process [27]. Comparing the time scales for bubble initiation after the onset of heating for the hanging droplet and drop tube experiments the former operated with values on the order of 500 ms whereas micro explosions were observed for the latter after droplet residence times in the furnace of ~ 40 ms. In addition, given sufficient time the bio-oil may polymerize and form solids whereby new cites for nucleation may be formed or a shell of polymerized material may develop around the bubble whereby bubble formation is not observed before the internal pressure is sufficient to rupture the shell [22].

3.4.3 RSO Combustion Behavior

Despite the ready availability of RSO its behavior during heating under combustion conditions has not been as intensely studied as that of bio-oil. RSO is a mixture of triglycerides with fatty acid lengths ranging from 16 to 22 carbon atoms [28] and trace quantities of phospholipids (<2.5 % wt.), free fatty acids (<1.2 % wt.), unsaponifiables (<1.2 % wt.), and water (<0.3 % wt.) [29]. Due to its homogeneity and the high molecular mass of the main components evaporation is not an important mechanism for droplet gas production during heating but when heated to sufficiently high temperatures the material will pyrolyze. Jóźwiak and Szlęk [30] found that the flash point of RSO determined by the open cup method exceeded 300 °C and accordingly they limited their investigation of the ignition properties of RSO/diesel mixtures to those containing maximum 85 % wt. RSO. Employing an apparatus where ø 1.4 mm droplets suspended on a thermocouple were lowered into a heated cylinder they found that ignition was problematic for this mixture if the cylinder temperature was below 550 ºC. Dweck and Sampaio [31] studied the thermal decomposition of 10 mg canola oil (*i.e.* RSO) samples in air by thermogravimetric techniques using a heating rate of 5 °C/min. They found that the volatilization was initiated around 200 ºC but significant decomposition was delayed to 291 ºC and preceded over three steps

were the last corresponded to char burnout. Their findings are in agreement with those of McDonnell *et al.* [32] who used TGA under the same conditions and found that for crude RSO volatilization commenced at 200 °C whereas decomposition set in at 280 ºC. Idem *et al.* [33] studied the decomposition of refined (*i.e.* free fatty acids, water, and phospholipids removed) RSO in an un-catalyzed fixed bed reactor at atmospheric pressure and found that 58 % wt. of the feed would be converted to light organics and gas without char formation at 300 ºC (*i.e.* the lowest temperature employed) and gas hourly space velocities of 3.3 to 15.4 h^{-1}. Accordingly, for RSO gas release may proceed at a significant rate at 300 ºC, even in an inert atmosphere if sufficient residence time is available, and this temperature appears to be at the lower limit for sufficient gas release to ignite the fuel during dynamic heating of a small quantity as would be the case for a droplet during combustion.

3.4.4 Pre-Ignition Energy

Based on the combustion behavior of bio-oil and RSO it is possible to estimate and compare the specific energy input needed to ignite fuel droplets and establish a self-sustaining flame. For bio-oil it is assumed that the droplet is heated from 60 ºC to 100 ºC where all water evaporates before heating continues to 180 ºC where the droplet ignites. Volatile components with a normal boiling point below 180 ºC are also assumed to have evaporated before ignition. For RSO it is assumed that the droplet is heated from 60 ºC to 300 ºC where it is ignited and evaporation of lighter components prior to ignition is ignored. Table 6 displays the numerical values assumed for physical and chemical properties of the fuels. Under these assumptions the pre-ignition specific input for RSO is estimated to be 456 kJ kg^{-1} whereas bio-oil requires 831 kJ kg^{-1} or 1.8 times that of RSO. Compared on energy (HHV) specific basis bio-oil droplets require 3.6 times the pre-ignition energy of RSO due to its lower heat of combustion. The pre-ignition energy input estimate for RSO depends strongly on the assumed ignition temperature but even if heating to 500 °C is required under combustion conditions bio-oil would still require twice the input of RSO on energy basis. Furthermore, it can be noted that 73 % of the specific energy input for bio-oil is due to water evaporation and bio-oils with relatively high water contents, as was the case for the produced samples, therefore have an increased specific pre-ignition energy demand.

Table 6: Properties of bio-oil and RSO.

Property	Unit	Value	Source
Bio-oil, water content	% wt.	27.0	- [a]
Bio-oil (water), heat of vaporization	kJ kg^{-1}	2257	[34]
Bio-oil (org. fraction), heat of vaporization [b]	kJ kg^{-1}	394.7	[35]
Bio-oil, org. fraction BP<180 °C	% wt.	28.3	[14]
Bio-oil, specific heat capacity 60-100°C	kJ kg^{-1} K^{-1}	1.7	[36, 37]
Bio-oil, specific heat capacity 100-180°C	kJ kg^{-1} K^{-1}	0.84	[36, 37]
RSO, specific heat capacity	kJ kg^{-1} K^{-1}	1.9	[29]

[a] *Average of produced samples;* [b] *Assumed equal to acetic acid*

The higher pre-ignition energy demand for bio-oil droplets seems to explain the behavior observed when attempting to combust this fuel with burners that are suitable for RSO. For the investigated burners pre-ignition energy for fuel droplets preheated to a fixed temperature may be supplied by radiation from the flame, convection from hot flue gas, radiation from the furnace interior, or an electric spark when the burner is started. Convection takes place in a recirculation zone induced by a swirling flow whereby heat can only be supplied by preheating the fuel and by the electric spark at start-up which was not sufficient for bio-oil. For the Firegreen burner droplet heating during operation can only be accomplished through radiation from the flame and convection with flue gas because the nozzle is surrounded by the furnace's heat transfer surfaces which are cooled by relatively cold water (~ 60 °C). However, if adequate swirl is induced to the secondary air these mechanisms may be sufficient, as it was observed, but since swirl and secondary air admission can not be regulated independently with a fixed swirl disc geometry the droplets will not be heated sufficiently when secondary air is reduced. Accordingly, after a flame was established and it was attempted to reduce the secondary air supply swirl was inadequate and the flame extinguished. For the KSM-Roesen burner, where swirl was not induced to the secondary air, the dominating mechanisms for heating droplets were radiation from the flame and the heat shield surrounding the flame. During start-up on RSO the metal heat shield had been heated to glowing red but after switching to bio-oil pre-ignition energy demand was increased and the shield cooled whereby the flame moved forward until it was expelled from the shield and extinguished.

The above discussion indicates that combustion of bio-oil with burners suitable for RSO is possible if measures are taken to increase heat transfer to fuel droplets

immediately after atomization. In the simplest form this may be accomplished by adding a swirl disc at the secondary air supply, changing the geometry of an existing disc, or adding a radiation shield to the furnace.

3.4.5 Macro-Scale Bio-Oil Combustion

Only a single attempt to combust herbaceous-derived bio-oil in a furnace has been found in the literature [38]. It was reported that combustion in a 50 kW furnace of bio-oil samples produced from switchgrass burned with a stable flame provided the water content was below 35 % wt. Atomization was accomplished with an air-assist nozzle. The procedure used for starting the furnace and igniting the bio-oil was not disclosed but since the burner was developed for both single fuel and co-firing with natural gas the latter option might have been employed. The combustion chamber design was also not discussed.

Details on ignition and combustion chamber designs suitable for wood-derived bio-oil are also scarce in the literature. Oasmaa *et al.* [39] studied the combustion of bio-oil derived from hard and softwoods at a firing rate of 4 MW in an industrial hot water boiler. Heavy fuel was used to start the boiler and the bio-oil was atomized with an air-assist nozzle. They found the best results were obtained if the fuel was preheated to 50 to 60 ºC in order to reduce viscosity but also prevent nozzle clocking due to polymerization. The furnace front head had been modified based on the experience of Birka Energi [40] by adding a cylindrical stub in order to prevent heat loss from the flame. The result was a denser flame, higher flame temperature, and thus faster volatilization but it was noted that the design should not allow the flame to touch the wall because it will result in rapid coke deposition. A converging burner head and a modified swirl plate operating with more secondary air was also chosen in order to obtain a stable flame. Bandi and Baumgart [41] combusted pine-derived bio-oil up to 40 kW in a so-called FLOX burner modified to accept an air-assisted spray nozzle. This burner featured an enclosed combustion chamber with internal air preheating and mixing of air and combustion gasses. The burner was started by heating the combustion chamber to 900 ºC with a natural gas flame after which the bio-oil ignited unassisted. They did observed problems with nozzle plugging over time, even though the nozzle feed tube was water jacketed, possibly due to the intense radiation submitted to the tip.

The reported experiences support the finding that combustion of bio-oil without support fuel in smaller conventional furnaces does require equipment modifications. In contrast to the hypothesis of Bridgwater and Peacocke [42] the combustion chamber should be re-designed in order to partially enclose the flame and assist heat transfer to the evaporating fuel spray. Further improvements are obtained by increasing swirl to the combustion air. It follows that a cold furnace can not be started on pure bio-oil but must be preheated. Finally, air-assisted atomization of the bio-oil preheated to somewhat below 60 ºC appears to be a suitable way of introducing the fuel in to the furnace.

4 Conclusions and Further Work

The bench-scale Pyrolysis Centrifuge Reactor was used as a small pilot plant to produce two 2 l samples of bio-oil. At a specific straw feed rate of 69 kg m^{-2} h^{-1} the yield of bio-oil on wet feed basis was somewhat lower than that obtained in an earlier experiment operating at 41 kg m^{-2} h^{-1} mainly due to inadequate capacity of the heating elements. Based on the viscosity of the samples they could be classified as *light-medium* bio-oils but other parameters were not within the specified limits. It is proposed that char separation should be improved in order to reduce ash and fractional condensation implemented to reduce the water and thus increase the specific energy content. The nitrogen content of the samples was not determined but due to the generally higher content in herbaceous feedstocks the effect of reactor operating conditions on nitrogen partitioning should be investigated in order to ensure that the produced bio-oil is not declassified to *medium* or *heavy*.

Combustion of the produced samples was attempted with two burners developed for combustion of rapeseed oil in small domestic furnaces. Atomization with an air-assisted nozzle after preheating the fuel to 60 °C worked well but ignition and stable operation failed. Based on a comparison of the fuels' combustion behavior and properties it is concluded that bio-oil droplets require substantially more energy addition prior to ignition and therefore need the combustion chamber to be partially enclosed and stronger swirl in the secondary air. These findings are in line with earlier studies on practical aspects of bio-oil combustion and indicate that the employed combustion systems could be modified to utilize bio-oil if wanted. However, since

bio-oil requires the furnace to be preheated a support fuel will be needed to start a cold furnace.

5 References

[1] Available at: http://dynamotive.com/en/biooil/index.html#demonstration

[2] Santos, J.C.O., Santos, I.M.G., Souza, A.G.. Effect of heating and cooling on rheological parameters of edible vegetable oils. J Food Eng, 67, 2005, 401–405.

[3] Tate, R.E., Watts, K.C., Allen, C.A.W., Wilkie, K.I.. The viscosities of three biodiesel fuels at temperatures up to 300 C. Fuel, 85, 2006, 1010–1015.

[4] Firegreen website: http://www.firegreen.dk

[5] KSM-Roesen website: http://www.roesen.dk/

[6] Diebold, J.P., Milne, T.A., Czernik, S., Oasmaa, A., Bridgwater, A.V., Cuevas, A., Gust, S., Huffman, D., Piskorz, J. Proposed Specifications for Various Grades of Pyrolysis Oils. In: Bridgwater, A.V., Boocock, D.G.B. (eds.) Developments in Thermochemical Biomass Conbersion. Blackie Academic, London, 1997, 433-447.

[7] Oasmaa, A., Czernik, S. Fuel Oil Quality of Biomass Pyrolysis Oils – State of the Art for the End Users. Energ Fuels, 13, 1999, 914-921.

[8] Oasmaa, A., Leppämäki, E., Koponen, P., Levander, J., Tapola, E. Physical characterisation of biomass-based pyrolysis liquids. Application of standard fuel oil analyses. VTT Energy, Espoo, 1997.

[9] Oasmaa, A., Peacocke, C., Gust, S., Meier, D. McLellan, R. Norms and Standards for Pyrolysis Liquids. End-User Requirements and Specifications. Energ Fuels, 19, 2005, 2155-2163.

[10] Oasmaa, A., Sipilä, K., Solantausta, Y., Kuoppala, E. Quality Improvement of Pyrolysis Liquid: Effect of Light Volatiles on the Stability of Pyrolysis Liquids. Energ Fuels, 19, 2005, 2556-2561.

[11] Scahill, J.W., Diebold, J.P., Feik, C.J. Removal of Residual Char Fines from Pyrolysis Vapors by Hot Gas Filtration. In: Bridgwater, A.V., Boocock, D.G.B. (Eds.)

Proceedings of Developments in Thermochemical Conversion of Biomass. Blackie Academic, London, 1996, 253-266.

[12] Diebold, J.P., Czernik, S. Additives To Lower and Stabilize the Viscosity of Pyrolysis Oils during Storage. Energ Fuels, 11, 1997, 1081-1091.

[13] Agblevor, F.A., Besler, S., Montané, D., Evans, R.J. Influence of Inorganic Compounds on Char Formation and Quality of Fast Pyrolysis Oils. ACS 209th National Meeting, Anaheim, April 2-5, 1995.

[14] Branca, C., Di Blasi, C. Multistep Mechanism for the Devolatilization of Biomass Fast Pyrolysis Oils. Ind Eng Chem Res, 45, 2006, 5891-5899.

[15] Branca, D., Di Blasi, C., Elefante, R. Devolatilization of Conventional Pyrolysis Oils Generated from Biomass and Cellulose. Energ Fuels, 20, 2006, 2253-2261.

[16] Branca, D., Di Blasi, C., Elefante, R. Devolatilization and Heterogeneous Combustion of Wood Fast Pyrolysis Oils. Ind Eng Chem Res, 44, 2005, 799-810.

[17] Branca, C., Di Blasi, C., Russo, C. Devolatilization in the temperature range 300-600 K of liquids derived from wood pyrolysis and gasification. Fuel, 84, 2005, 37-45.

[18] Calabria, R., Chiariello, F., Massoli, P. Combustion fundamentals of pyrolysis oil based fuels. Exp Therm Fluid Sci, 31, 2007, 413-420.

[19] Hallett, W.L.H., Clark, N.A. A model for the evaporation of biomass pyrolysis oil droplets. Fuel, 85, 2006, 532-544.

[20] D'Alessio, J., Lazzaro, M., Massoli, P., Moccia, V. Thermo-optical investigation of burning biomass pyrolysis oil droplets. Proc 27th Int Sym Combustion, The Combustion Institute, Boulder, USA, 1998, 1915-1922.

[21] Shaddix, C.R., Tennison, P.J. Effects of char content and simple additives on biomass pyrolysis oil droplet combustion, Proc 27th Int Sym Combustion, The Combustion Institute, Boulder, USA, 1998, 1907-1914.

[22] Wornat, M.J., Porter, B.G., Yang, N.Y.C. Single droplet combustion of biomass pyrolysis oils. Energ Fuels, 8, 1994, 1131-1142.

[23] Calabria, R., Chiariello, F., Massoli, P. Combustion fundamentals of pyrolysis oil based fuels. Exp Ther Fluid Sci, 31, 2007, 413-420.

[24] Skripov, V.P. Metastable liquids. Wiley, New York, 1974.

[25] Avedisian, C.T. The homogeneous nucleation limits of liquids. J Phys Chem, 3, 1985, 695–729.

[26] Elias, E., Chambré, P.L. Flashing inception in water during rapid decompression. J Heat Transf, 115, 1993, 231–237.

[27] Elias, E., Chambré, P.L. Limit of superheat in uniformly heated fluid. Heat Mass Transf, 43, 2007, 957-963.

[28] Matthäus, B., Brühl, L. Quality of cold-pressed edible rapeseed oil in Germany. Nahrung/Food, 47, 2003, 413-419.

[29] Przybylski, R., Mag, T., Eskin, N.A.M., McDonald, B.E. Canola Oil. In: Shahidi, F (ed.). Bailey's Industrial Oil & Fat Products (vol. 2). Sixth ed., Wiley, New Jersey, 2005.

[30] Jóźwiak, D., Szlęk, A. Ignition characteristics of vegetable fuel oils in fuel sprays. J Energ Inst, 80, 2007, 35-39.

[31] Dweck, J., Sampaio, C.M.S. Analysis of the thermal decomposition of commercial vegetable oils in air by simultaneous TG/DTA. J Therm Anal Calorimetry, 75, 2004, 385-391.

[32] McDonnell, K., Ward, S., Leahy, J.J., McNulty, P. Properties of Rapeseed Oil for Use as a Diesel Fuel Extender. JAOCS, 76, 1999, 539-543.

[33] Idem, R.O., Katikaneni, S.P.R., Bakhshi, N.N. Thermal Cracking of Canola Oil: Reaction Products in the Presence and Absence of Steam. Eneg Fuels, 10, 1996, 1150-1162.

[34] McCab, W.L., Smith, J.C., Harriott, P. Unit Operations of Chemical Engineering. 5th ed., McGraw-Hill, New York, 1993.

[35] Lide, D.R., Frederikse, H.P.R. (eds). Handbook of Chemistry and Physics. 77th ed., CRC Press, Boca Raton, USA, 1996.

[36] Hristov, J., Stamatov V. Physical and mathematical models of bio-oil combustion. Atomization Sprays, 17, 2007, 731-755.

[37] Stroshine, R., Hamann, D. Physical Properties of Agricultural Materials and Food Products. Dept. of Agricultural Engineering, Purdue University, W. Lafayette, IN, 1994.

[38] Brown, M.J., Judd, R.W. Emissions reduction through biomass and gas co-firing – the BAGIT project. Proc 23rd World Gas Conf, Amsterdam, 2006.

[39] Oasmaa, A., Kytö, M., Sipilä, K. Pyrolysis oil combustion tests in an industrial boiler. In: Bridgwater, A.V. (ed.) Progress in Thermochemical Biomass Conversion. Blackwell Science, Oxford, 2001, 1468-1481.

[40] Hallgren, B. Test report of Metlab Miljö AB. Metlab Miljö AB, Skelleftehamn, 1996.

[41] Bandi, A., Baumgart, F. Sterling Engine with Flox® Burner Fuelled With Fast Pyrolysis Liquid. In: Bridgwater, A.V. (ed.) Progress in Thermochemical Biomass Conversion. Blackwell Science, Oxford, 2001, 1459-1467.

[42] Bridgwater, A.V., Peacocke, G.V.C. Fast pyrolysis processes for biomass. Renewable Sustainable Energ Rev, 4, 2000, 1-73.

Appendix G:

A Method and a Mobile Unit for Collecting and Pyrolysing Biomass

(12) INTERNATIONAL APPLICATION PUBLISHED UNDER THE PATENT COOPERATION TREATY (PCT)

(19) World Intellectual Property Organization
International Bureau

(43) International Publication Date
9 November 2006 (09.11.2006)

PCT

(10) International Publication Number
WO 2006/117006 A1

(51) International Patent Classification:
C10B 53/02 (2006.01) *A01D 43/00* (2006.01)
C10B 47/22 (2006.01)

(21) International Application Number:
PCT/DK2006/000242

(22) International Filing Date: 3 May 2006 (03.05.2006)

(25) Filing Language: English

(26) Publication Language: English

(30) Priority Data:
05076034.7 3 May 2005 (03.05.2005) EP
60/676,959 3 May 2005 (03.05.2005) US

(71) Applicant *(for all designated States except US)*: **DANMARKS TEKNISKE UNIVERSITET** [DK/DK]; Anker Engelundsvej 1, Bygning 101A, DK-2800 Lyngby (DK).

(72) Inventors; and
(75) Inventors/Applicants *(for US only)*: **BECH, Niels** [DK/DK]; Frederiksdalsvej 8A, 2.tv., DK-2830 Virum (DK). **DAM-JOHANSEN, Kim** [DK/DK]; Frydsvej 19A, DK-3300 Frederiksværk (DK).

(74) Agent: **INSPICOS A/S**; Bøge Allé 5, P.O. Box 45, DK-2970 Hørsholm (DK).

(81) Designated States *(unless otherwise indicated, for every kind of national protection available)*: AE, AG, AL, AM, AT, AU, AZ, BA, BB, BG, BR, BW, BY, BZ, CA, CH, CN, CO, CR, CU, CZ, DE, DK, DM, DZ, EC, EE, EG, ES, FI, GB, GD, GE, GH, GM, HR, HU, ID, IL, IN, IS, JP, KE, KG, KM, KN, KP, KR, KZ, LC, LK, LR, LS, LT, LU, LV, LY, MA, MD, MG, MK, MN, MW, MX, MZ, NA, NG, NI, NO, NZ, OM, PG, PH, PL, PT, RO, RU, SC, SD, SE, SG, SK, SL, SM, SY, TJ, TM, TN, TR, TT, TZ, UA, UG, US, UZ, VC, VN, YU, ZA, ZM, ZW.

(84) Designated States *(unless otherwise indicated, for every kind of regional protection available)*: ARIPO (BW, GH, GM, KE, LS, MW, MZ, NA, SD, SL, SZ, TZ, UG, ZM, ZW), Eurasian (AM, AZ, BY, KG, KZ, MD, RU, TJ, TM), European (AT, BE, BG, CH, CY, CZ, DE, DK, EE, ES, FI, FR, GB, GR, HU, IE, IS, IT, LT, LU, LV, MC, NL, PL, PT, RO, SE, SI, SK, TR), OAPI (BF, BJ, CF, CG, CI, CM, GA, GN, GQ, GW, ML, MR, NE, SN, TD, TG).

Published:
— *with international search report*

For two-letter codes and other abbreviations, refer to the "Guidance Notes on Codes and Abbreviations" appearing at the beginning of each regular issue of the PCT Gazette.

WO 2006/117006 A1

(54) Title: A METHOD AND A MOBILE UNIT FOR COLLECTING AND PYROLYSING BIOMASS

(57) Abstract: A method for collecting biomass, such as straw, and for producing a pyrolysis liquid, such as oil or tar, from the biomass, comprises the step of collecting the biomass from a growth site, e.g. a field, by means of a mobile unit. The biomass is continuously fed into a pyrolysis apparatus (200) accommodated by the mobile unit, as the mobile unit is moved across the growth site. While the biomass is processed in the pyrolysis apparatus, further biomass is simultaneously being collected. The pyrolysis apparatus may be a flash pyrolysis or fast pyrolysis apparatus relying on centrifugal forces for forcing biomass towards a reactive surface in a pyrolysis reactor. The mobile unit may be self-propelled.

A METHOD AND A MOBILE UNIT FOR COLLECTING AND PYROLYSING BIOMASS

Technical field

The present invention relates to a method and to a mobile device for collecting biomass and for producing a pyrolysis liquid and/or char from the biomass. The biomass liquid may e.g. comprise pyrolysis oil or tar. A novel fast pyrolysis method and apparatus is also disclosed.

Background of the invention

Conventional pyrolysis is a heated process in the range of 200-700°C that converts biomass into pyrolysis liquid, char, and gas, usually in the absence of oxygen and focused on obtaining char in high yield. Fast pyrolysis, also referred to as flash pyrolysis, on the other hand is a process, in which biomass is quickly heated to a controlled pyrolysis temperature, and in which the gas phase is cooled quickly, whereby it partly condenses to pyrolysis liquid. This method generally obtains a higher yield of liquid and thus seeks to minimize the yield of the other two products. When the biomass decomposes at the elevated pyrolysis temperature, e.g. 450-600°C, three primary products are formed: gas, pyrolysis liquid and char.

Various methods and apparatus for producing gas or liquid from organic material have been proposed in the prior art. US 5,413,227 discloses an ablative pyrolysis process in a vortex reactor system, and WO 03/057800 discloses an ablative thermolysis reactor including rotating surfaces. WO 92/09671 discloses a method and apparatus employing a vessel, which forms a torus or helix, through which feedstock can be conveyed at a velocity which sustains the feedstock against the outer periphery of the internal surface of the vessel as it transits the vessel. WO 01/34725 discloses an example of flash-pyrolysis in a cyclone. Further examples of pyrolysis apparatus are provided in WO 88/09364 and CA 2 365 785.

Despite the achievements in pyrolysis and fast pyrolysis, it has been found that one barrier to efficient exploitation of biomass in fuel production is the cost conferred by collection and transportation of the biomass. Biomass is usually collected from growth sites, where it is loaded onto a truck or trailer for transportation thereof to a pyrolysis facility. Due to the relatively low concentration of energy per volume of biomass, production of even small amounts of usable pyrolysis liquid requires collection, transportation and storage of large volumes of biomass. Additionally, though the prior art pyrolysis systems are useful for many purposes, they have been found to have certain limitations, as some of them are bulky, some have a low efficiency, and some require adjustment of e.g. rotor blades, which reduces overall cost efficiency.

Summary of the invention

It is an object of preferred embodiments of the present invention to provide a method and a mobile unit for collecting biomass which improves efficiency in biomass collection and exploitation. It is a further object of preferred embodiments of the present invention to provide a pyrolysis method and apparatus, which allow for a compact and efficient pyrolysis assembly.

In a first aspect, the invention provides a method for collecting biomass and for producing a pyrolysis liquid from the biomass, comprising the steps of:
- collecting the biomass from a growth site, such as a field or forest, by means of a mobile unit;
- continuously feeding the biomass into a pyrolysis apparatus accommodated by the mobile unit, as the mobile unit traverses the growth site;
- decomposing the biomass into pyrolysis liquid, char and pyrolysis gas, the step of decomposing being carried out in the pyrolysis apparatus;
- separating the pyrolysis liquid from the char and pyrolysis gas and collecting the pyrolysis liquid, the method being characterised in that the step of decomposing the biomass is carried out, while further biomass is simultaneously being collected from the growth site by means of the mobile unit.

In a second aspect, the invention provides a mobile unit for collecting biomass and for producing pyrolysis liquid from the biomass, the unit comprising:
- a pyrolysis apparatus for decomposing the biomass into pyrolysis liquid, char and pyrolysis gas;
- a biomass collector for collecting the biomass from a growth site;
- a biomass conveyor for continuously feeding the biomass into the pyrolysis apparatus;
- a separation system for separating the pyrolysis liquid from the char and pyrolysis gas, the mobile unit being characterised in that the biomass collector, the biomass conveyor and the pyrolysis apparatus are operable such that the pyrolysis apparatus can decompose the biomass, while further biomass is simultaneously collected from the growth site by means of the biomass collector.

The pyrolysis takes place while further biomass is simultaneously being collected and continuously fed to the pyrolysis apparatus. Hence, pyrolysis takes place while the mobile unit traverses the growth site, and while biomass is being collected simultaneously. Transportation of relatively large volumes of biomass from the growth site to a remote pyrolysis facility may thus be avoided. As pyrolysis liquid has a significantly higher energy concentration per volume than biomass, a certain amount of energy requires less space when

present in the form of pyrolysis liquid than when present in the form of biomass, and the energy may thus be more conveniently conveyed to the intended consumer in the form of pyrolysis liquid. Pyrolysis liquid may be transported from the growth site to the intended consumer or to a storage facility by means of tank trucks or vessels (e.g. ISO tank containers), or conveyed through pipe lines under adequate pumping action.

The pyrolysis apparatus may include any apparatus known per se, such as e.g. any one of the apparatus disclosed in US 5,413,227, WO 03/057800, WO 92/09671, WO 01/34725, WO 88/09364 or CA 2 365 785. The present inventors have devised an alternative and novel pyrolysis apparatus, which is particularly well suited for the purpose of a mobile pyrolysis unit, and which will be described below.

The mobile unit may comprise a wheeled support structure. A coupling system may be provided for coupling the unit to a power-driven vehicle. Alternatively, the mobile unit may incorporate an engine or motor, so that the mobile unit is self-propelled. The engine or motor of the mobile unit may utilize the pyrolysis gas, pyrolysis liquid and/or char as fuel, whereby the need for a separate fuel source of the mobile unit may be reduced or even eliminated. Likewise, in embodiments of the invention, in which the mobile unit is not self-propelled, the propelling drive means, e.g. tractor or truck, may utilize the pyrolysis gas, pyrolysis liquid and/or char as a fuel source.

In the present context, biomass is to be understood as any organic matter, such as plants and animals or residues thereof, such as wood, agricultural and forestry process waste materials, or industrial, human and animal waste, including petrochemical-based waste feedstock. The chemical energy stored in plants and animals derives from solar energy photosynthesis and can be converted to usable liquid, such as oil or tar, in a heated process, i.e. pyrolysis.

The term pyrolysis liquid is to be understood as any organic liquid derived from biomass in a pyrolysis process, such as bio-oil or tar, the components having a boiling point in the range 0-500°C. Pyrolysis vapour is to be understood as any vapour or gas derived from biomass in a pyrolysis process, such as vaporized pyrolysis liquid.

To efficiently cool char from the pyrolysis process before possible ejection thereof from the mobile unit, the process may include the step of collecting dirt from the growth site and mixing the dirt with the char to thereby cool the char. In other words, dirt may be utilized as a cooling source for waste matter deriving from pyrolysis, and the need for e.g. water cooling may be eliminated. It will hence be appreciated that the mobile unit may comprise a dirt collector for collecting dirt from the growth site and a mixer for mixing the dirt with the char

to thereby cool the char, as well as a dirt and char ejector for ejecting the mix or slurry of char and dirt from the mobile unit.

A press for pilletizing and collecting the char as a bi-product may be provided.

The mix of char and dirt may be fed into a furrow formed by appropriate means of the mobile unit, such as by a tine. The tine may be arranged such with respect to the dirt and char ejector that the mix of char and dirt can be fed into the furrow during use of the mobile unit. Subsequently, the char mix may be covered with dirt to enhance decomposition of the char.

At least a portion of the pyrolysis gas produced by the pyrolysis process may be combusted in a furnace forming part of the pyrolysis apparatus, the furnace producing heat for the pyrolysis process. Exhaust fume of the furnace may be expelled via a fume outlet of the furnace. In addition to pyrolysis gas, at least a portion of the char may be combusted in the furnace.

Prior to feeding of the biomass into the pyrolysis apparatus, the biomass may be fed to a pre-heating device, in which it is preheated and possibly dried before it enters the pyrolysis apparatus. The exhaust fume produced in the furnace may be utilized as a heat source in the pre-heating device. Exhaust fume from the furnace may also be guided to a first heat exchanger, in which it heats intake air for the furnace. Alternatively or additionally, a conduit, which is connectable to an exhaust outlet of the power-driven vehicle or an exhaust outlet of the engine of the mobile unit, may be provided to allow exhaust gas of the vehicle or of the engine as a heat source in the first heat exchanger or in the process of pre-heating and/or drying the biomass.

The mobile unit may advantageously include a shredder for shredding the collected biomass upstream of the pyrolysis apparatus, e.g. upstream of the pre-heating device. A biomass buffer may be included to allow more biomass to be collected than what is being processed in the pyrolysis apparatus. For example, operation of the collector may be interrupted e.g. for manoeuvring the vehicle or for inspection without interruption of the pyrolysis apparatus. In one embodiment, the pre-heating device serves as the biomass buffer.

At the step of separating the pyrolysis liquid from the char and pyrolysis gas, the pyrolysis liquid and at least a portion of the pyrolysis gas may be conveyed to a separator for separating the pyrolysis liquid from the pyrolysis gas, and at least a portion of the separated pyrolysis gas may be conveyed back to the furnace as a fuel source therein. Further, at least a portion of the separated liquid may be conveyed back to the pyrolysis apparatus as a cooling source in a pyrolysis condenser. The condenser may be integrated in the pyrolysis

apparatus, or it may be constitute a separate unit, which does not form part of the pyrolysis apparatus. Before the liquid enters the condenser, it is preferably cooled in a second heat exchanger, which may utilize air as a cooling source. The air, which exits the second heat exchanger, may be mixed with the intake air for the furnace upstream or downstream of the first heat exchanger, e.g. to improve combustion efficiency in the furnace.

In one embodiment, the pyrolysis apparatus comprises a centrifuge defining a centrifuge chamber, and at the step of decomposing the biomass, the method of the invention may comprise the step imparting rotation on biomass distributed in gas volume in the centrifuge, whereby the biomass is forced towards an outer wall of the centrifuge chamber. The outer wall of the centrifuge chamber is maintained at a temperature of 350 – 700°C to effect a pyrolysis process at or near the outer wall of the centrifuge chamber, whereby the biomass decomposes into the pyrolysis liquid, pyrolysis gas and char, the gas and liquid being on gaseous form.

In a particularly compact embodiment of the pyrolysis apparatus, the condenser is integrated in the pyrolysis apparatus. In this embodiment, the centrifuge chamber of the pyrolysis apparatus is delimited by an inner wall and an outer wall, and an outlet is provided for feeding biomass into the centrifuge chamber. A rotor is arranged to impart rotation on the biomass in the centrifuge chamber to force the biomass towards the outer wall of the centrifuge chamber under the action of centrifugal forces. A heating system is included for maintaining the outer wall of the centrifuge chamber at a temperature of 350 – 700°C to effect the pyrolysis process at or near the outer wall of the centrifuge chamber and to thereby decompose the biomass into char, pyrolysis gas and pyrolysis vapours, which can be condensed into pyrolysis liquid in the condenser. The heating system may include the furnace as describe above, the centrifuge being preferably arranged coaxially within the furnace, whereby heat for the pyrolysis process is transported across the outer wall of the centrifuge by conduction. The inner wall of the centrifuge chamber may be permeable to the pyrolysis vapours and gas, so that the condenser may be arranged centrally within the centrifuge chamber.

The present pyrolysis method and apparatus confer several benefits. No inert gas for fluidization and heat transport is required, thereby reducing overall dimensions of the apparatus at a given capacity. Further, residence time of solids and vapours are decoupled from heat transfer. Additionally, no sand is needed as heat transport or heat transmission medium, thereby reducing wear and tear and eliminating the need for subsequent separation of sand and char. Thanks to the rotational motion imparted on the biomass in the centrifuge chamber, the area of the outer wall of the centrifuge chamber is in contact with the biomass, while centrifugal forces ensure an even pressure of biomass towards the outer wall, thereby

ensuring improved utilization of the reactive surface in the pyrolysis apparatus and consequently higher specific capacity. As char is forced towards the outer wall of the centrifuge chamber, gas separation may occur within the centrifuge chamber, i.e. within the pyrolysis chamber itself. As the char particles are forced towards the wall by centrifugal forces and gas may be filtered by passage from the outer wall of the centrifuge chamber through a layer of biomass to an inner wall of the centrifuge chamber, the need for a separate cyclone may be eliminated. Additionally, as biomass is forced towards the reactive surface, i.e. the outer wall of the centrifuge chamber, by centrifugal forces, the need for additional means for imparting the biomass is reduced, thereby reducing wear and tear and consequently maintenance costs. Thanks to the rotational layout of the centrifuge chamber and rotor, there is no need to adjust e.g. angles of blades or distance between blades and a tube wall, as in certain prior art devices. Further, contact between metal parts may be eliminated, and contact between metal parts and biomass strongly reduced, as the rotating motion is imparted on the biomass particles mainly as a result of a similar movement in the gas phase originating from the motion of the rotor. Operation is accordingly less vulnerable to changes in biomass material properties, such as particle size distribution and humidity as well as to fluctuations of biomass feeding speed to the reactor. As char is conveyed away from the reactor, preferably continuously, a high heat conduction between the reactor wall, i.e. the outer wall of the centrifuge chamber, and the biomass material is ensured, resulting in improved efficiency and improved pyrolysis liquid yield. The improved pyrolysis yield is conferred by a steep temperature gradient in the biomass material.

In embodiments of the present invention, biomass in the rotor is subjected to centrifugal forces greater than 2000 times the force of gravity.

The gas phase retention time in the rotor is preferably at most 5 seconds. The ratio of the diameter of the rotor and the diameter of the centrifuge chamber is preferably at least 0.5, such as at least 0.6, 0.7, 1 or at least 1.2.

It has been found that yield of pyrolysis liquid and, subsequently, gas and char is influenced by choice of feed stock, reactor wall temperature, centrifugal force and a combination of reactor gas phase temperature and residence/retention time. Whereas the former parameters determine the initial split between fractions, the latter two work through degradation of the initially formed pyrolysis liquids in the gas phase. The gas phase reactions will result in rearrangements of the molecules, formation of water (dehydration) and cracking of larger molecules constituting the liquid fraction to smaller ones which subsequently cannot be condensed under the moderate conditions employed. Gas phase reactions will therefore act to modify the liquid product in terms of viscosity and water solubility but will also change the yield both on mass and energy basis.

In order to model the effect of gas phase degradation, the reactions can be approximated by first order irreversible chemical reactions following the well-known Ahrrenius expression and furthermore treating the pyrolysis centrifuge as a plug-flow reactor. As a consequence, the degradation will be promoted by both higher temperature and longer residence/retention time, and theoretically it is possible to obtain a certain degree of degradation by an indefinite number of combinations of the two. For most embodiments of the present invention it may be desired that gas phase residence/retention time does not exceed 1 to 2 seconds in order to obtain a liquid product suitable for fuel in acceptable yield (i.e. Bridgwater, A.V., Peacocke, G.V.C. Fast pyrolysis processes for biomass. Renewable & Sustainable Energy Reviews, 4, 2000).

Gas phase residence/retention time is predominantly determined by the active volume of the reactor in combination with the amount of gas purging this volume. For systems where there is no external inert gas purge, the consequence is that the gasses only originate from the pyrolysis reactions of the feedstock. Therefore the residence/retention time and subsequently the liquid product gas phase degradation is predominantly determined by the capacity or feed rate of raw material to the reactor.

In one design of the pyrolysis centrifuge operating with a wall temperature of approximately 500°C and a centrifugal force of 10000 time the force of gravity on wheat straw, the primary mass yield of fractions will be approximately 34% organics, 22% water (56 % liquids in total), 23 % char and 21 % gas, all on substantially dry ash-free basis. At these conditions the gas phase temperature was found to be approximately 400°C in a reactor with a feed rate of approximately 20 g/min and an active volume of approximately 0.53 L. Utilizing the kinetic expression for gas phase cracking of cellulose found by Linden et al. (Linden, A.G., Berruti, F., Scott, D.S. A kinetic model for the production of liquids from the flash pyrolysis of cellulose. Chem. Eng. Commun., 65, 1988) the yield of organics after gas phase degradation can be computed to approximately 33 % with a corresponding gas residence/retention time of approximately 1.5 s or a relatively minor change from the primary yield. If, on the other hand, gas phase temperature is raised to approximately 600°C the organics yield would be reduced to approximately 5 % whereas a tenfold increase in reactor volume would reduce organics yield to approximately 25 %. From these examples it will be clear that a reactor allowing for minimization of the combined effect of temperature and residence time on the gas phase is beneficial in order to obtain pyrolysis liquids from biomass in acceptable yield.

In embodiments of the present invention, the outer wall of the centrifuge chamber may heat the biomass, so that ablative pyrolysis takes place at or near the outer wall. Preferably, this is achieved without the use of a separate transport medium, such as sand.

At the step of conveying the pyrolysis vapors and char away from the centrifuge chamber, the pyrolysis vapors preferably diffuse into a condenser chamber, in which the step of condensation takes place. In a particularly compact embodiment, the centrifuge chamber has an annular cross-section, and the condenser chamber is arranged centrally i.e. coaxially within the rotor, whereby the pyrolysis vapors diffuse through an inner wall of the centrifuge chamber, which is permeable to the vapors. It will thus be appreciated that the centrifuge chamber and the condenser chamber are separated by the inner wall of the centrifuge chamber, the inner wall comprising perforations, so as to allow the pyrolysis vapors to diffuse from the centrifuge chamber to the condenser chamber, in which the pyrolysis vapors may at least partly condense into said pyrolysis liquid.

The integration of the reactor (centrifuge chamber) and condenser allow for improved utilization of reactor volume. This contributes to the compactness of the apparatus, in which there is no need for an external condenser remote from the reactor with associated pipes. Additionally, thanks to the integrated condenser and reactor, the gas phase retention time may be reduced, which has shown to improve pyrolysis liquid yield, reduced liquid viscosity and reduced water content.

The perforations of the inner wall may define inlet openings of pipe stubs extending radially into the condenser chamber to provide an inlet to the condenser, which is inwardly displaced in relation to an outer periphery of the condenser chamber. The pipe stubs preferably have a length sufficient to extend beyond condensed pyrolysis liquid, such as viscous tar, which may accumulate at the outer periphery of the condenser chamber.

In order to enhance condensation in the condenser chamber, a central portion of the condenser chamber may accommodate a packing material, on which the at least a portion of the pyrolysis vapors condense to pyrolysis liquid.

Condensation may further be enhanced by leading a cold fluid into the condenser chamber, e.g. via a pipe arranged centrally within the condenser chamber. The fluid, which is at a temperature below the dew point of the pyrolysis vapors, may be pyrolysis liquid or a hydrocarbon immiscible with pyrolysis liquid. In case pyrolysis liquid is utilized, such pyrolysis liquid may conveniently be derived from the pyrolysis process, so that no external supply of pyrolysis liquid is needed. Any other fluid is separated from the produced pyrolysis liquid by phase separation and recycled in the process.

The condensation temperature may be controlled by the temperature of the utilized fluid whereby especially the amount of water included in the liquid product may be controlled by partial condensation. At a later stage, the gas may be dried by further cooling in order to

increase energy content of the gas and/or mix condensed water with combustible hot char to form a slurry and thus control reactivity.

At least a portion of the char deriving from pyrolysis of the biomass may be in the form of fine particles, which are conveyed away from the centrifuge chamber through openings provided in the outer wall of the centrifuge chamber and into a channel for conveying the particles further. To enhance the flow of particles into the char separation, a small flow of vapour may be drawn out with the char particles, preferably by arranging the openings tangentially to the main reactor pipe whereby the motion of the rotor blades will force vapour through the pipes. The vapour may be reentered into the reactor through an opening near the raw material intake port. In one embodiment of the apparatus of the present invention, a char conveyor is arranged at or near a bottom portion of the centrifuge. The conveyor may e.g. comprise a worm drive for forwarding char in the channel. Alternatively, char may be conveyed under the action of gravity. Means may be provided for mixing the char with the pyrolysis liquid to form a slurry, or char may be pilletized and collected as a separate high density energy product.

As explained above, centrifugal forces provide an outward pressure on the biomass in the centrifuge chamber toward its outer wall. An even peripheral distribution of material in the centrifuge chamber may be achieved by at least one rotor blade arranged in or extending into the centrifuge chamber, whereby the biomass, char, pyrolysis vapors in the centrifuge chamber are forced in a peripheral direction. The rotation thereby imparted on the material generates the centrifugal forces for forcing the material toward the reactive surface at the outer wall of the centrifuge chamber.

The biomass may be led axially or tangentially into the centrifuge chamber. Preferably, the biomass is led tangentially into the centrifuge chamber at one or more positions along the chamber. The biomass may be led into the centrifuge chamber via a plurality of distinct inlets or via one single inlet, e.g. an extended slit forming a widened mouth of a biomass inlet.

Heat for the pyrolysis process may be derived from a furnace arranged coaxially around the centrifuge, whereby heat for the pyrolysis process is transported across the outer wall of the centrifuge chamber by conduction. This coaxial arrangement of the furnace further contributes to overall compactness. In the furnace, at least a portion of said pyrolysis gas, char, liquid or hydrocarbon may be combusted, preferably without any need for external fuel supply. A porous flame stabilizing material in the form of a ceramic material may be incorporated within the furnace to enhace operation. Heating by electric resistance elements, magnetic induction, a condensing vapour, or a hot fluid e.g. liquid salt constitute alternative ways of heating the process.

The rotor may have an inner diameter of 0.01 – 5 m, and it is preferably rotated at at least 200 rpm. In one embodiment, the diameter of the rotor is approximately 1 meter, the rotor being rotated at approximately 2000 rpm and the biomass particles being subjected to centrifugal forces greater than 2000 times the force of gravity.

In order to efficiently collect and process the biomass, the centrifuge may be comprised in a mobile unit, which may collect the biomass from a growth site, such as a field or forest. The biomass may be continuously fed into the centrifuge, as the mobile unit is moved across the growth site. Further biomass may be collected from the growth site by means of the mobile unit concurrently with the step of decomposing the biomass in the pyrolysis apparatus.

Brief description of the drawings

An embodiment of the invention will now be further described with reference to the drawings, in which:

Fig. 1 is a chart illustrating an embodiment of the method and mobile unit of the present invention;

Fig. 2 is a perspective illustration of a pyrolysis apparatus;

Fig. 3 is a partial cross-sectional view through the pyrolysis apparatus of Fig. 2.

Detailed description of the drawings

Fig. 1 illustrates the flow of air, gas and liquid in a system incorporating a pyrolysis apparatus as disclosed herein. The system may be accommodated on a mobile unit for simultaneously collecting biomass and processing biomass in a pyrolysis process. The system includes a pyrolysis apparatus 200, which will be described in more detail below with reference to Figs. 2 and 3. A motor 102 is provided for driving a rotor of the pyrolysis apparatus. In tar/gas separator, pyrolysis liquid in the form of tar is separated from gas. Part of the separated tar is led to a heat exchanger as described further below, and the remaining tar is collected in tar collector 106. Gas is led from the tar/gas separator into a furnace of the pyrolysis apparatus, in which it is utilized as fuel for producing heat required in the pyrolysis process.

As shown in the right-hand end of Fig. 1, biomass such as straw is picked up from a field or from another growth site and fed into a shredder, such as a roller mill 108, from which it is fed to a buffer and pre-heating device 110. Heat is transported to the pre-heating device with

exhaust gas from the furnace of the pyrolysis apparatus 200 and/or with exhaust gas from an engine of the mobile unit or from a truck or tractor driving the mobile unit. Exhaust gas from the furnace of the pyrolysis apparatus is conveyed through a first heat exchanger 112, in which it heats combustion air for the furnace. As shown in the upper left corner of Fig. 1, a second heat exchanger 114 is provided for cooling that part of the tar separated in the tar/gas separator 104, which is led back into the pyrolysis apparatus. The cooling source for the second heat exchanger 114 is air, which may be led through the first heat exchanger 112 after it has passed the second heat exchanger 114, but before it enters the furnace of the pyrolysis apparatus.

In this configuration, char, which is conveyed away from the pyrolysis apparatus, is mixed with dirt picked up from the growth site in a char/dirt mixer 116 to form a char/dirt mixture. The mixture may advantageously be distributed on the growth site, e.g. a field, for instance into a furrow formed by a tine of the mobile unit.

The pyrolysis apparatus 200 is shown in more detail in Fig. 2. It comprises a biomass inlet pipe 202, through which biomass is conveyed into a centrifuge chamber or reactor 204 surrounded by a furnace 206. The centrifuge chamber 204 has an outer wall 208, through which heat is conducted from the furnace for effecting pyrolysis in the centrifuge chamber at or near the outer wall 208. A rotor 210 forms a perforated inner wall 212 of the centrifuge chamber, the rotor being provided with rotor blades 214 for rotating the gas phase and the biomass suspended herein within the centrifuge chamber. During operation of the apparatus, biomass and other material in the centrifuge chamber, such as char and pyrolysis vapors are forced by centrifugal forces towards the reactive surface at the outer wall 208 of the centrifuge chamber 204, at which pyrolysis is effected. Heat deflectors 216 are secured to the rotor blades for limiting heat radiation from the furnace 206 onto the inner wall 212 of the centrifuge chamber, which surrounds a condenser to be kept at a limited temperature well below the pyrolysis temperature of about 350-700°C.

Condenser 218 is arranged coaxially within the centrifuge chamber 204 and comprises a packing material 220 for enhancing condensation. Equidistant baffle plates 222 provide a support for the packing material and for the shell of the condenser 218, and perforations 224 in the baffle plates 222 guide pyrolysis gas through the condenser to optimize gas/liquid contact. Cold liquid is fed into the condenser via a perforated cooling feed pipe 226.

A bottom portion of the wall 208 may be provided with holes or perforations allowing char to fall into a channel 228, in which the char is conveyed away from the pyrolysis apparatus by means of e.g. a worm drive conveyor 230.

It will be appreciated that the furnace, centrifuge chamber, rotor, condenser, and char conveyor extend the entire length of the pyrolysis apparatus, the various parts being cut-off in Fig. 2 for illustrative purposes only.

Fig. 3 shows a partial cross-section through the pyrolysis apparatus 200. The furnace 206 shown in Fig. 2 is not included in Fig. 3 for the sake of clarity. Biomass in the centrifuge chamber 204 is illustrated as hatched area 232. As illustrated by arrows 234, pyrolysis vapors diffuse into the condenser 218 via perforations in the inner wall 212 of the centrifuge chamber 204 (see Fig. 2), there being provided an inwardly projecting pipe stub 236 at each perforation. Each pipe stub 236 has a plurality of openings 238 located above the surface of the condensed pyrolysis liquid 240, through which gas may escape into the condenser 218. The pipe stubs 236 have a length sufficient to extend through a layer of condensed pyrolysis liquid, e.g. tar, which has accumulated at the outer periphery of the condenser.

CLAIMS

1. A method for collecting biomass and for producing a pyrolysis liquid and/or char from the biomass, comprising the steps of:
- collecting the biomass from a growth site by means of a mobile unit;
- continuously feeding the biomass into a pyrolysis apparatus accommodated by the mobile unit, as the mobile unit traverses the growth site;
- decomposing the biomass into pyrolysis liquid, char and pyrolysis gas, the step of decomposing being carried out in said pyrolysis apparatus;
- separating the pyrolysis liquid from the char and pyrolysis gas and collecting the pyrolysis liquid and/or char,
characterised in that
said step of decomposing the biomass is carried out, while further biomass is simultaneously being collected from the growth site by means of the mobile unit.

2. The method of claim 1, further comprising the steps of:
- collecting dirt from the growth site and mixing said dirt with the char to thereby cool the char;
- ejecting the mix of char and dirt from the mobile unit.

3. The method of claim 2, further comprising the step of forming a furrow in the growth field by means of a tine of the mobile unit, and wherein, at said step of ejecting, the mix of char and dirt is fed into the furrow.

4. The method of any of the preceding claims, wherein the pyrolysis apparatus combusts at least a portion of said pyrolysis gas in a furnace, whereby heat and exhaust fume is produced.

5. The method of claim 4, wherein the pyrolysis apparatus further combusts at least a portion of said char.

6. The method of claim 4 or 5, further comprising, prior to the step of continuously feeding the biomass into the pyrolysis apparatus:
- continuously feeding the biomass to a pre-heating device, in which the biomass is pre-heated before it enters the pyrolysis apparatus;
- conveying said exhaust fume through the pre-heating device, whereby the exhaust fume serves as a heat source for the biomass.

7. The method of any of claims 4-6, comprising conveying the exhaust fume from the furnace to a first heat exchanger, in which the exhaust fume heats intake air for the furnace.

8. The method of any of claims 4-7, wherein, at the step of separating, pyrolysis liquid and at least a portion of said pyrolysis gas is conveyed to a separator for separating the pyrolysis liquid from the pyrolysis gas, the method further comprising:
- conveying at least a portion of the separated pyrolysis gas back to the furnace.

9. The method of claim 8, wherein the pyrolysis apparatus produces vaporized pyrolysis liquid, the mobile unit further comprising a condenser for condensing vapours into liquefied pyrolysis liquid, the condenser being arranged as a separate unit outside the pyrolysis apparatus or as an integrated unit of the pyrolysis apparatus, the method further comprising the step of conveying at least a portion of the separated liquid back to the pyrolysis apparatus as a cooling source in the condenser.

10. The method of claim 9, wherein the condenser is integrated in the pyrolysis apparatus, the method further comprising:
- cooling said portion of the separated liquid in a second heat exchanger before said liquid enters the pyrolysis apparatus, wherein the second heat exchanger uses air as a cooling source:
- mixing air, which exits the second heat exchanger, with said intake air for the furnace upstream or downstream of the first heat exchanger.

11. The method of any of the preceding claims, wherein the pyrolysis apparatus comprises a centrifuge defining a centrifuge chamber, the method further comprising, at said step of decomposing:
- imparting rotation on biomass distributed in gas volume in the centrifuge chamber, whereby the biomass is forced towards an outer wall of the centrifuge chamber;
- maintaining said outer wall at a temperature of 350 – 700 degrees Celsius to effect a pyrolysis process at or near the outer wall of the centrifuge chamber, whereby the biomass decomposes into said pyrolysis liquid, pyrolysis gas and char, the pyrolysis gas and char being on gaseous form.

12. The method of any of the preceding claims, wherein the pyrolysis vapours are partially condensed in a primary condenser, the method further comprising:
- drying the gas originating from the partial condensation and utilizing at least a portion thereof as fuel for a furnace and/or for an engine for propelling the mobile unit;
- mixing the resulting liquid phase consisting largely of water with the char to obtain a slurry;
- distributing the slurry over the growth site and/or collecting it for further processing or

combustion;
- leading the vapours formed in the process of contacting hot char with liquid to a tertiary condenser in order to condense components having a lower boiling point than water;
- admixing the condensed vapour from the tertiary condenser with liquid product produced by the primary condenser.

13. A mobile unit for collecting biomass and for producing pyrolysis liquid from the biomass, the unit comprising:
- a pyrolysis apparatus for decomposing the biomass into pyrolysis liquid, char and pyrolysis gas;
- a biomass collector for collecting the biomass from a growth site;
- a biomass conveyor for continuously feeding the biomass into the pyrolysis apparatus;
- a separation system for separating the pyrolysis liquid from the char and pyrolysis gas, characterised in that
the biomass collector, the biomass conveyor and the pyrolysis apparatus are operable such that the pyrolysis apparatus can decompose the biomass, while further biomass is simultaneously collected from the growth site by means of the biomass collector.

14. The mobile unit of claim 13, further comprising a wheeled support structure and a coupling system for coupling the unit to a power-driven vehicle.

15. The mobile unit of claim 13, further comprising a wheeled support structure and an engine in order for the mobile unit to be self-propelled.

16. The mobile unit of claim 14 or 15, further comprising an engine utilizing said pyrolysis gas, pyrolysis liquid or char as fuel.

17. The mobile unit of any of claims 13-16, further comprising an apparatus for mixing pyrolysis liquid with char to form a slurry.

18. The mobile unit of any of claims 13-17, further comprising:
- a dirt collector for collecting dirt from the growth site and mixing said dirt with the char to thereby cool the char;
- a dirt and char ejector for ejecting the mix of char and dirt from the mobile unit.

19. The mobile unit of any of claims 13-18, further comprising a tine for forming a furrow in the growth field, the tine being arranged such with respect to said dirt and char ejector that the mix of char and dirt or char and water slurry can be fed into the furrow during use of the mobile unit.

20. The mobile unit of any of claims 13-19, wherein the pyrolysis apparatus comprises a furnace for combusting at least a portion of said pyrolysis gas and/or at least a portion of said char, the furnace comprising an exhaust fume outlet for expelling exhaust fume from the furnace.

21. The mobile unit of claim 20, wherein the centrifuge is arranged coaxially within a furnace whereby heat for the pyrolysis process may be transported across the outer wall of the centrifuge by conduction.

22. The mobile unit of claim 20 or 21, further comprising:
- a pre-heating device for preheating the biomass, the pre-heating device being arranged upstream of the pyrolysis apparatus;
- an exhaust fume conduit for guiding said exhaust fume from said exhaust fume outlet of the furnace to the pre-heating device.

23. The mobile unit of claim 22, wherein said exhaust fume conduit is further arranged to guide the exhaust fume to a first heat exchanger, which is arranged to heat intake air for the furnace.

24. The mobile unit of any of claims 13-23, further comprising a separator for separating the pyrolysis liquid from the pyrolysis gas as the pyrolysis liquid and gas exit the pyrolysis apparatus, the mobile unit further comprising:
- a first gas conduit for guiding the separated gas back to the furnace.

25. The mobile unit of any of claims 13-24, wherein the pyrolysis apparatus produces vaporized pyrolysis liquid, the mobile unit further comprising a condenser for condensing vapours into liquefied pyrolysis liquid, the condenser being arranged as a separate unit outside the pyrolysis apparatus or as an integrated unit of the pyrolysis apparatus.

26. The mobile unit of claim 24 and 25, further comprising a fluid conduit for guiding at least a portion of the separated liquid back to the pyrolysis apparatus as a cooling source for the condenser.

27. The mobile unit of claims 23 and 26, further comprising:
- a second heat exchanger arranged in said fluid conduit upstream of the pyrolysis apparatus to cool down said portion of the separated liquid;
- a first air conduit for guiding air to the second heat exchanger as a cooling source;
- a second air conduit for guiding the air, which exits the second heat exchanger, to an inlet

conduit for said intake air for the furnace, so as to mix the air in the second air conduit into said intake air.

28. The mobile unit of claim 23 in combination with any of claims 14-16, further comprising a conduit which is connectable to an exhaust outlet of the power-driven vehicle or an exhaust outlet of said engine to allow exhaust gas of the vehicle or of the engine as a heat source in the first heat exchanger.

29. The mobile unit of any of claims 13-28 further comprising a shredder for shredding the collected biomass upstream of the pyrolysis apparatus.

30. The mobile unit of any of claims 13-29, wherein the condenser is integrated in the pyrolysis apparatus, and wherein the pyrolysis apparatus comprises:
- a centrifuge chamber delimited by an inner wall and an outer wall;
- an inlet through which the biomass can be fed into the centrifuge chamber;
- a rotor arranged to impart rotation on biomass distributed in gas volume in the centrifuge chamber to force the biomass towards the outer wall under the action of centrifugal forces;
- a heating system for maintaining said outer wall at a temperature of 350 – 700 degrees Celsius to effect the pyrolysis process at or near the outer wall of the centrifuge chamber and to thereby decompose the biomass into char, pyrolysis gas and pyrolysis vapors, which can be condensed into pyrolysis liquid in said condenser;
- a char conveyor for conveying the char away from the centrifuge chamber;
wherein:
- the inner wall of the centrifuge chamber is permeable to said pyrolysis vapors and gas.

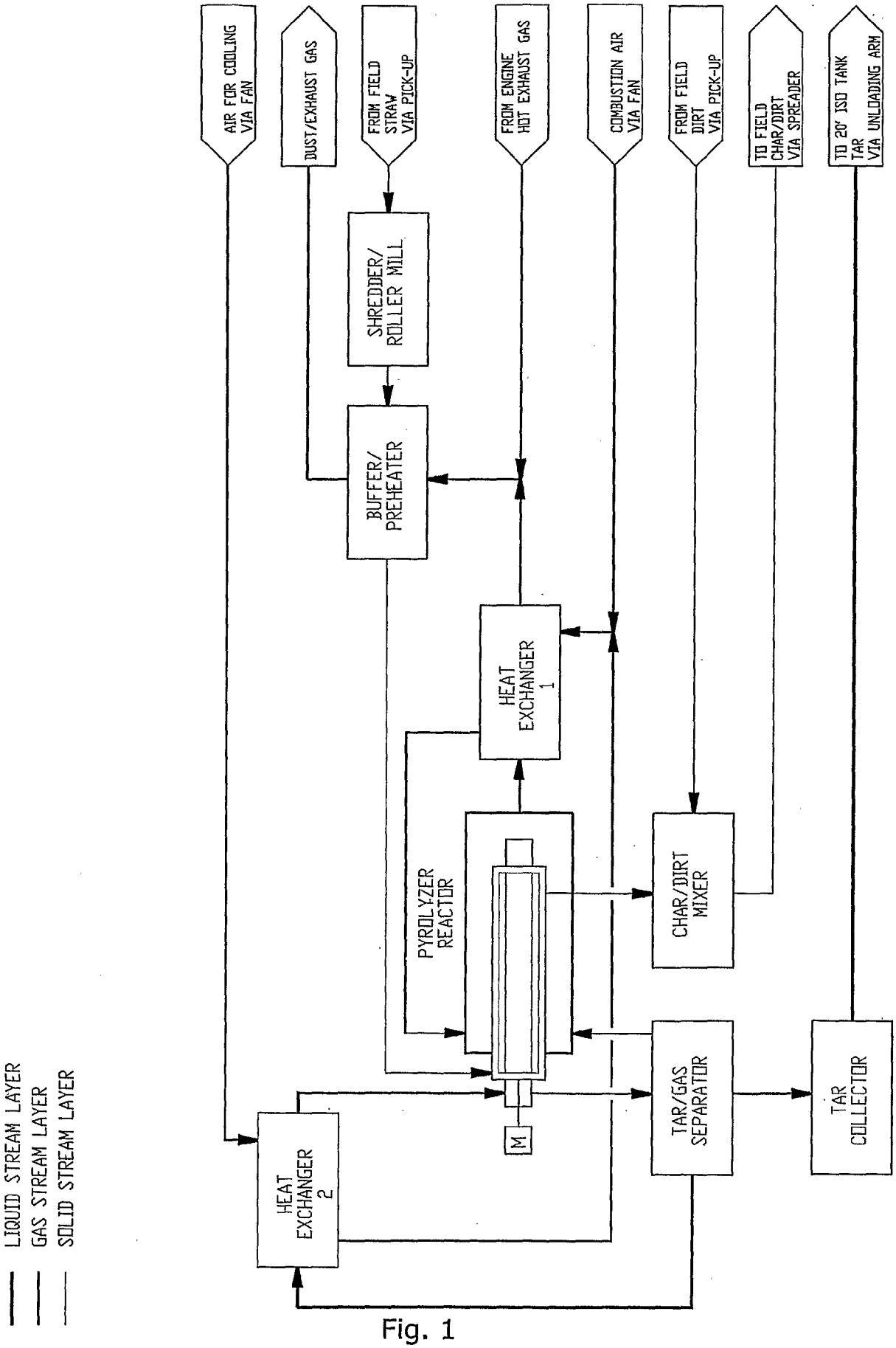
AIR FOR COOLING VIA FAN
DUST/EXHAUST GAS
FROM FIELD STRAW VIA PICK-UP
FROM ENGINE HOT EXHAUST GAS
COMBUSTION AIR VIA FAN
FROM FIELD DIRT VIA PICK-UP
TO FIELD CHAR/DIRT VIA SPREADER
TO 20' ISO TANK TAR VIA UNLOADING ARM
SHREDDER/ ROLLER MILL
BUFFER/ PREHEATER
HEAT EXCHANGER 1
PYROLYZER REACTOR
CHAR/DIRT MIXER
M
HEAT EXCHANGER 2
TAR/GAS SEPARATOR
TAR COLLECTOR
LIQUID STREAM LAYER
GAS STREAM LAYER
SOLID STREAM LAYER

Fig. 1

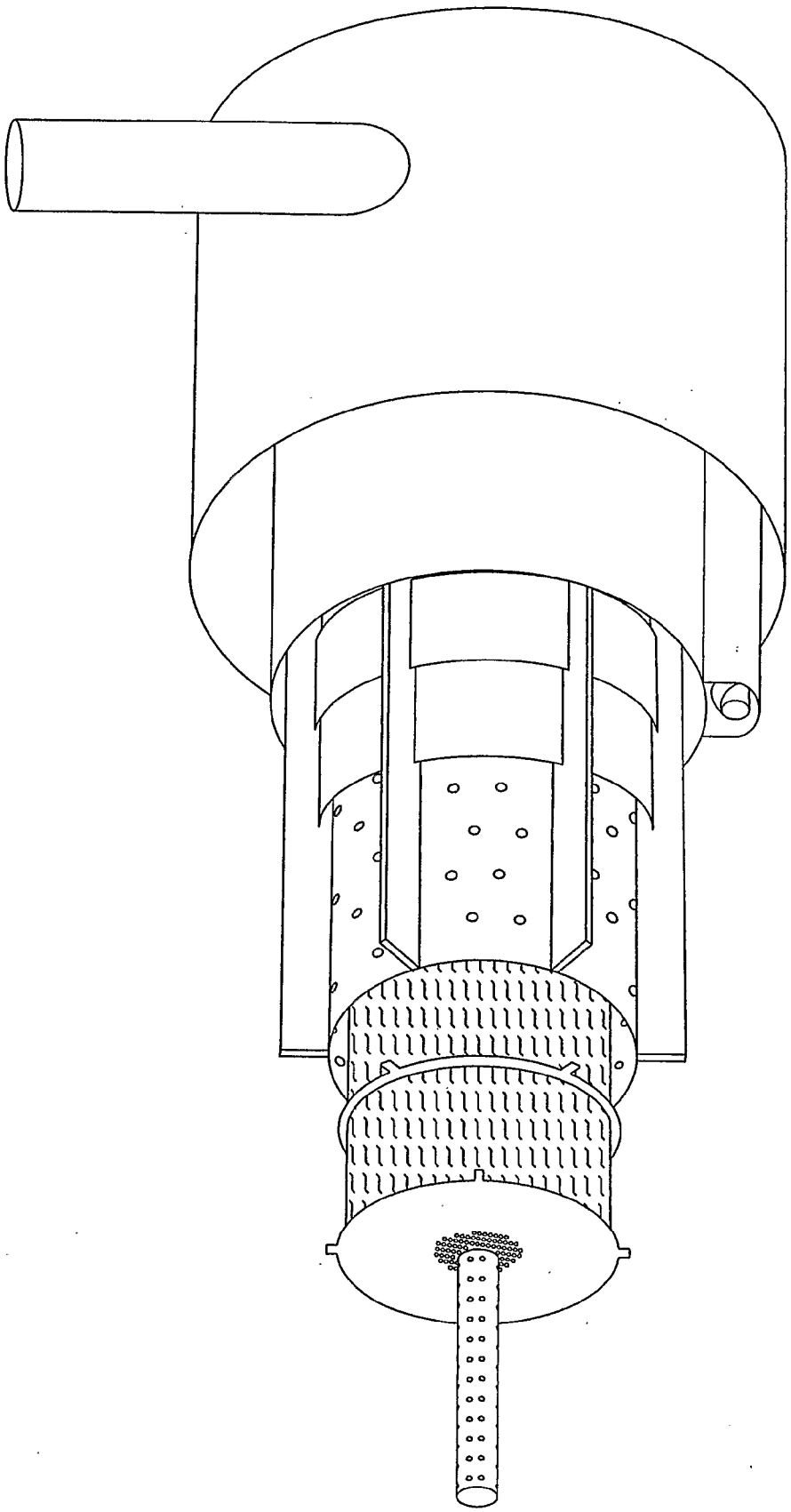

Fig. 2

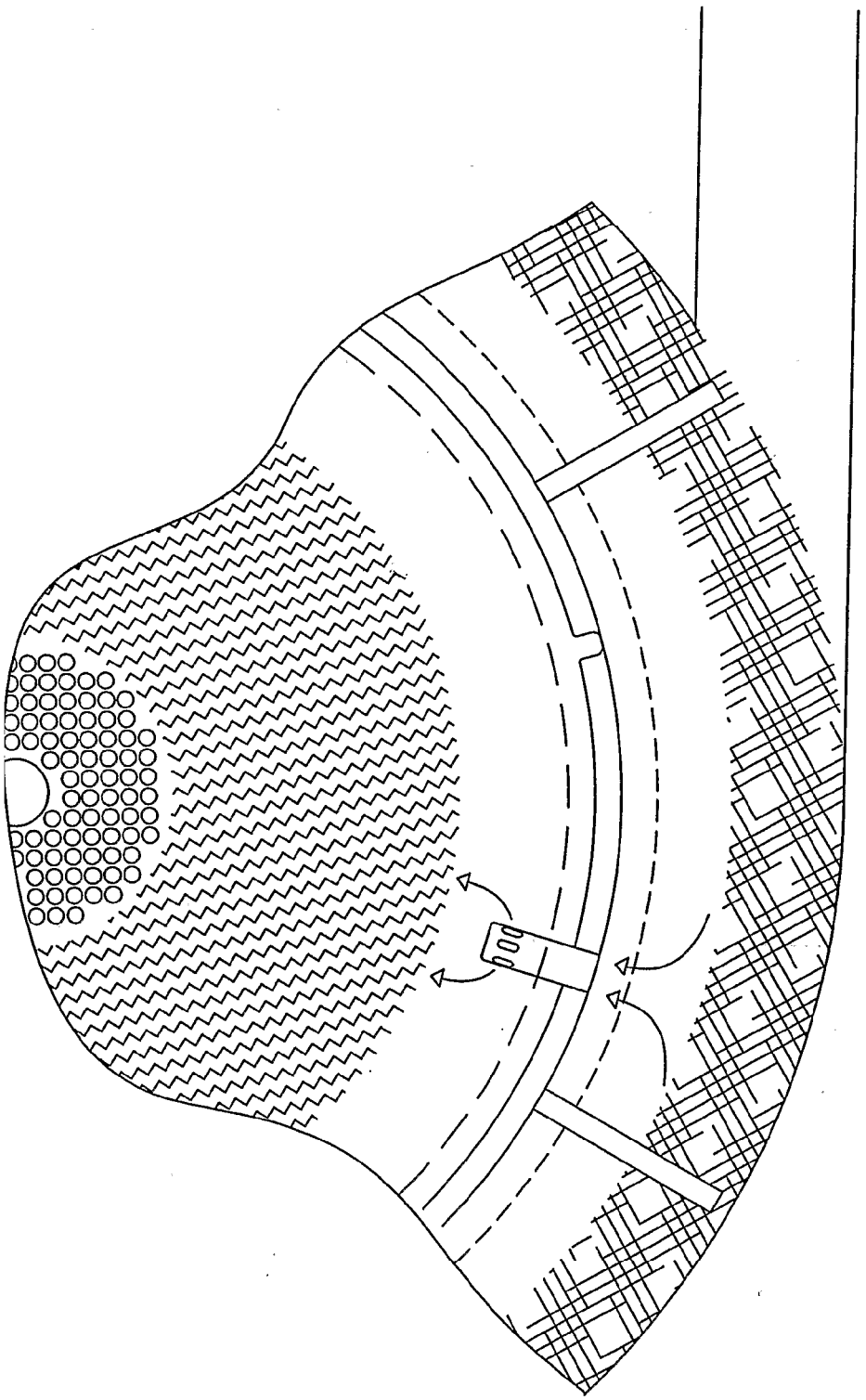

Fig. 3

INTERNATIONAL SEARCH REPORT

International application No
PCT/DK2006/000242

A. CLASSIFICATION OF SUBJECT MATTER
INV. C10B53/02 C10B47/22 A01D43/00

According to International Patent Classification (IPC) or to both national classification and IPC

B. FIELDS SEARCHED

Minimum documentation searched (classification system followed by classification symbols)
C10B A01D C10C

Documentation searched other than minimum documentation to the extent that such documents are included in the fields searched

Electronic data base consulted during the international search (name of data base and, where practical, search terms used)
EPO-Internal, COMPENDEX, WPI Data

C. DOCUMENTS CONSIDERED TO BE RELEVANT

Category*	Citation of document, with indication, where appropriate, of the relevant passages	Relevant to claim No.
A	WIENS JERRY: "MOBILE PYROLYSIS SYSTEM FOR ON-SITE BIOMASS CONVERSION TO LIQUID AND SOLID FUELS" INST OF GAS TECHNOL, 1980, pages 713-720, XP008052810 CHICAGO, ILL, USA page 715 figure 1 ----- -/--	1-30

[X] Further documents are listed in the continuation of Box C.

[X] See patent family annex.

* Special categories of cited documents :

"A" document defining the general state of the art which is not considered to be of particular relevance

"E" earlier document but published on or after the international filing date

"L" document which may throw doubts on priority claim(s) or which is cited to establish the publication date of another citation or other special reason (as specified)

"O" document referring to an oral disclosure, use, exhibition or other means

"P" document published prior to the international filing date but later than the priority date claimed

"T" later document published after the international filing date or priority date and not in conflict with the application but cited to understand the principle or theory underlying the invention

"X" document of particular relevance; the claimed invention cannot be considered novel or cannot be considered to involve an inventive step when the document is taken alone

"Y" document of particular relevance; the claimed invention cannot be considered to involve an inventive step when the document is combined with one or more other such documents, such combination being obvious to a person skilled in the art.

"&" document member of the same patent family

Date of the actual completion of the international search	Date of mailing of the international search report
11 August 2006	18/08/2006

Name and mailing address of the ISA/	Authorized officer
European Patent Office, P.B. 5818 Patentlaan 2 NL – 2280 HV Rijswijk Tel. (+31-70) 340-2040, Tx. 31 651 epo nl, Fax: (+31-70) 340-3016	Zuurdeeg, B

Form PCT/ISA/210 (second sheet) (April 2005)

INTERNATIONAL SEARCH REPORT

International application No
PCT/DK2006/000242

C(Continuation). DOCUMENTS CONSIDERED TO BE RELEVANT

Category*	Citation of document, with indication, where appropriate, of the relevant passages	Relevant to claim No.
A	LINNEBORN JOHANNES ET AL: "MOBILE PYROLYSIS PLANT FOR THE PRODUCTION OF CHARCOAL AND CONDENSABLE HYDROCARBONS FROM BIOMASS" SOLAR ENERGY R&D IN THE EUROPEAN COMMUNITY, SERIES E, ENERGY FROM BIOMASS D. REIDEL PUBL CO, vol. 1, 1981, pages 176-180, XP008052802 DORDRECHT, NETH page 180	1-30
A	WO 99/66008 A (GRAVESON ENERGY MANAGEMENT LTD; MATON, MAURICE, EDWARD, GEORGE) 23 December 1999 (1999-12-23)	
A	BRIDGWATER A V ET AL: "Fast pyrolysis processes for biomass" RENEWABLE AND SUSTAINABLE ENERGY REVIEWS, ELSEVIERS SCIENCE, NEW YORK, NY, US, vol. 4, no. 1, March 2000 (2000-03), pages 1-73, XP004268416 ISSN: 1364-0321	

INTERNATIONAL SEARCH REPORT

Information on patent family members

International application No
PCT/DK2006/000242

Patent document cited in search report	Publication date	Patent family member(s)	Publication date
WO 9966008 A	23-12-1999	AP 1241 A	02-02-2004
		AU 754518 B2	21-11-2002
		AU 4381099 A	05-01-2000
		BG 104230 A	31-08-2000
		BR 9906537 A	15-08-2000
		CA 2299370 A1	23-12-1999
		CN 1130444 C	10-12-2003
		EA 1294 B1	25-12-2000
		EE 200000091 A	15-12-2000
		EP 1012215 A1	28-06-2000
		GB 2342984 A	26-04-2000
		HK 1025594 A1	25-04-2003
		HR 20000087 A2	31-08-2001
		HU 0003735 A2	28-03-2001
		ID 24630 A	27-07-2000
		IL 134423 A	12-09-2002
		IS 5372 A	10-02-2000
		JP 2002518546 T	25-06-2002
		NO 20000747 A	14-04-2000
		NZ 502598 A	30-03-2001
		OA 11319 A	27-10-2003
		PL 338674 A1	20-11-2000
		SK 1962000 A3	11-07-2000
		TR 200000412 T1	23-10-2000
		US 6648932 B1	18-11-2003
		ZA 200000487 A	07-08-2000

Appendix H:

Pyrolysing Method and Apparatus

(12) INTERNATIONAL APPLICATION PUBLISHED UNDER THE PATENT COOPERATION TREATY (PCT)

(19) World Intellectual Property Organization
International Bureau

(43) International Publication Date
9 November 2006 (09.11.2006)

PCT

(10) International Publication Number
WO 2006/117005 A1

(51) International Patent Classification:
C10B 53/02 (2006.01) *C10C 5/00* (2006.01)
C10B 47/22 (2006.01)

(21) International Application Number:
PCT/DK2006/000241

(22) International Filing Date: 3 May 2006 (03.05.2006)

(25) Filing Language: English

(26) Publication Language: English

(30) Priority Data:
05076034.7 3 May 2005 (03.05.2005) EP
60/676,959 3 May 2005 (03.05.2005) US

(71) Applicant *(for all designated States except US)*: **DANMARKS TEKNISKE UNIVERSITET** [DK/DK]; Anker Engelundsvej 1, Bygning 101A, DK-2800 Lyngby (DK).

(72) Inventors; and

(75) Inventors/Applicants *(for US only)*: **BECH, Niels** [DK/DK]; Frederiksdalsvej 8A, 2.tv., DK-2830 Virum (DK). **DAM-JOHANSEN, Kim** [DK/DK]; Frydsvej 19A, DK-3300 Frederiksværk (DK). **JENSEN, Peter, A.** [DK/DK]; Milosvej 3, st., DK-2300 Copenhagen S (DK).

(74) Agent: **INSPICOS A/S**; Bøge Allé 5, P.O. Box 45, DK-2970 Hørsholm (DK).

(81) Designated States *(unless otherwise indicated, for every kind of national protection available)*: AE, AG, AL, AM, AT, AU, AZ, BA, BB, BG, BR, BW, BY, BZ, CA, CH, CN, CO, CR, CU, CZ, DE, DK, DM, DZ, EC, EE, EG, ES, FI, GB, GD, GE, GH, GM, HR, HU, ID, IL, IN, IS, JP, KE, KG, KM, KN, KP, KR, KZ, LC, LK, LR, LS, LT, LU, LV, LY, MA, MD, MG, MK, MN, MW, MX, MZ, NA, NG, NI, NO, NZ, OM, PG, PH, PL, PT, RO, RU, SC, SD, SE, SG, SK, SL, SM, SY, TJ, TM, TN, TR, TT, TZ, UA, UG, US, UZ, VC, VN, YU, ZA, ZM, ZW.

(84) Designated States *(unless otherwise indicated, for every kind of regional protection available)*: ARIPO (BW, GH, GM, KE, LS, MW, MZ, NA, SD, SL, SZ, TZ, UG, ZM, ZW), Eurasian (AM, AZ, BY, KG, KZ, MD, RU, TJ, TM), European (AT, BE, BG, CH, CY, CZ, DE, DK, EE, ES, FI, FR, GB, GR, HU, IE, IS, IT, LT, LU, LV, MC, NL, PL, PT,

[Continued on next page]

(54) Title: PYROLYSIS METHOD AND APPARATUS

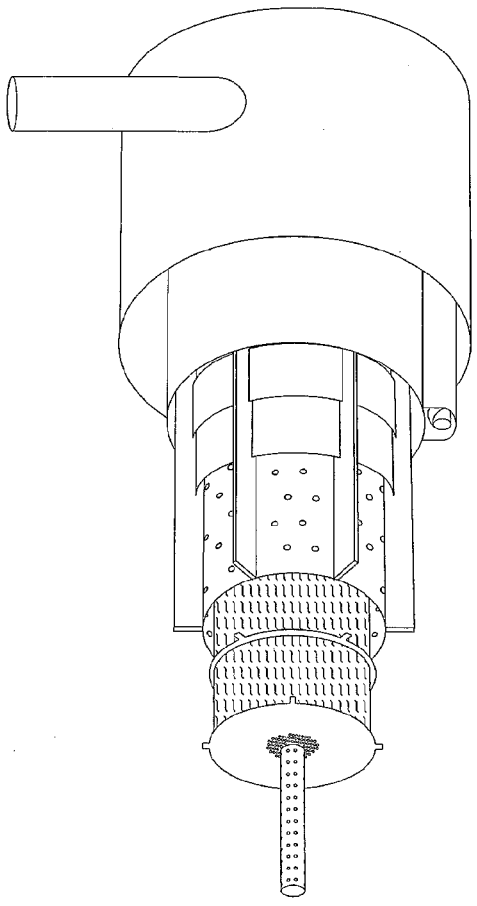

(57) Abstract: A fast pyrolysis apparatus (200) for producing pyrolysis liquid, such as oil or tar, char and pyrolysis gas from biomass, such as straw, comprises a centrifuge chamber (204) and a rotor (210) arranged to impart rotation on the biomass in the centrifuge chamber to force the biomass outwardly under the action of centrifugal forces. A furnace (206) arranged coaxially around the centrifuge chamber (204) maintains the temperature at an outer reactive wall of the centrifuge chamber at an elevated temperature to effect the pyrolysis process at or near the reactive wall. The apparatus comprises a condenser (218) arranged coaxially with and surrounded by the centrifuge chamber (204). The apparatus may be accommodated by a mobile unit for simultaneously collecting biomass from a field and processing the biomass in the apparatus.

WO 2006/117005 A1

RO, SE, SI, SK, TR), OAPI (BF, BJ, CF, CG, CI, CM, GA, GN, GQ, GW, ML, MR, NE, SN, TD, TG).

Published:

— *with international search report*

For two-letter codes and other abbreviations, refer to the "Guidance Notes on Codes and Abbreviations" appearing at the beginning of each regular issue of the PCT Gazette.

PYROLYSIS METHOD AND APPARATUS

Technical field

The present invention relates to a pyrolysis method and a fast pyrolysis apparatus for producing pyrolysis liquid from biomass. The biomass liquid may e.g. comprise pyrolysis oil or tar. A mobile device for collecting biomass and for producing a pyrolysis liquid from the biomass is also disclosed.

Background of the invention

Conventional pyrolysis is a heated process in the range of 200-500°C that converts biomass into pyrolysis liquid, char, and gas, usually in the absence of oxygen and focused on obtaining char in high yield. Fast pyrolysis, also referred to as flash pyrolysis, on the other hand is a process, in which biomass is quickly heated to a controlled pyrolysis temperature, and in which the gas phase is cooled quickly, whereby it partly condenses to pyrolysis liquid. This method generally obtains a higher yield of liquid and normally seeks to minimize the yield of the other two products. When the biomass decomposes at the elevated pyrolysis temperature, e.g. 450-600°C, three primary products are formed: gas, pyrolysis liquid and char.

Various methods and apparatus for producing gas or liquid from organic material have been proposed in the prior art. US 5,413,227 discloses an ablative pyrolysis process in a vortex reactor system, and WO 03/057800 discloses an ablative thermolysis reactor including rotating surfaces. WO 92/09671 discloses a method and apparatus employing a vessel, which forms a torus or helix, through which feedstock can be conveyed at a velocity which sustains the feedstock against the outer periphery of the internal surface of the vessel as it transits the vessel. WO 01/34725 discloses an example of flash-pyrolysis in a cyclone. Further examples of pyrolysis apparatus are provided in WO 88/09364 and CA 2 365 785.

Though the prior art pyrolysis systems are useful for many purposes, they have been found to have certain limitations, as some of them are bulky, some have a low efficiency, and some require adjustment of e.g. rotor blades, which reduces overall cost efficiency. It has also been found that one barrier to efficient exploitation of biomass in fuel production is the cost conferred by collection and transportation of the biomass. Biomass is usually collected from growth sites, where it is loaded onto a truck or trailer for transportation thereof to a pyrolysis facility. Due to the relatively low concentration of energy per volume of biomass, production of even small amounts of usable pyrolysis liquid requires collection, transportation and storage of large volumes of biomass.

Summary of the invention

It is an object of preferred embodiments of the present invention to provide a pyrolysis method and apparatus, which allow for a compact and efficient pyrolysis assembly. It is a further object of preferred embodiments of the present invention to provide a method and a mobile unit for collecting biomass which improves efficiency in biomass collection and exploitation.

In a first aspect, the invention provides a method for producing pyrolysis liquid from biomass, comprising the step of decomposing the biomass into pyrolysis liquid, char and pyrolysis gas in a fast pyrolysis process, the method comprising the steps of:

- feeding the biomass into a centrifuge chamber;
- rotating a rotor to impart rotation on biomass distributed in gas volume in the centrifuge, whereby the biomass is forced towards an outer wall of the centrifuge chamber by centrifugal forces;
- decomposing the biomass into pyrolysis vapors and char by maintaining said outer wall at a temperature of 350 – 700 degrees Celsius to effect the pyrolysis process at or near the outer wall of the centrifuge chamber;
- separating the pyrolysis vapours and char;
- conveying the pyrolysis vapors and char away from the centrifuge chamber;
- condensing the at least a portion of said pyrolysis vapors to obtain said pyrolysis liquid and pyrolysis gas.

In a second aspect, the invention provides a fast pyrolysis apparatus for producing pyrolysis liquid, char and pyrolysis gas from biomass, comprising:

- a centrifuge chamber delimited by an inner wall and an outer wall;
- an inlet through which biomass can be fed into the centrifuge chamber;
- a rotor arranged to impart rotation on biomass distributed in gas volume in the centrifuge to force the biomass towards the outer wall under the action of centrifugal forces;
- a heating system for maintaining said outer wall at a temperature of 350 – 700 degrees Celsius to effect the pyrolysis process at or near the outer wall of the centrifuge chamber and to thereby decompose the biomass into char and pyrolysis vapors, which can be condensed to form pyrolysis liquid and pyrolysis gas;
- a char conveyor for conveying the char away from the centrifuge chamber;

and wherein:

- the inner wall of the centrifuge chamber is permeable to said pyrolysis vapors.

The present pyrolysis method and apparatus confer several benefits. No inert gas for fluidization and heat transport is required, thereby reducing overall dimensions of the

apparatus at a given capacity. Additionally, no sand is needed as heat transport or heat transmission medium, thereby reducing wear and tear and eliminating the need for subsequent separation of sand and char. Thanks to the rotational motion imparted on the biomass in the centrifuge chamber, the area of the outer wall of the centrifuge chamber is in contact with the biomass, while centrifugal forces ensure an even pressure of biomass towards the outer wall, thereby ensuring improved utilization of the reactive surface in the pyrolysis apparatus and consequently higher specific capacity. As char is forced towards the outer wall of the centrifuge chamber, gas separation may occur within the centrifuge chamber, i.e. within the pyrolysis chamber itself. As the char particles are forced towards the wall by centrifugal forces and gas may be filtered by passage from the outer wall of the centrifuge chamber through a layer of biomass to an inner wall of the centrifuge chamber, the need for a separate cyclone may be eliminated. Additionally, as biomass is forced towards the reactive surface, i.e. the outer wall of the centrifuge chamber, by centrifugal forces, the need for additional means for imparting the biomass is reduced, thereby reducing wear and tear and consequently maintenance costs. Thanks to the rotational layout of the centrifuge chamber and rotor, there is no need to adjust e.g. angles of blades or distance between blades and a tube wall, as in certain prior art devices. Further, contact between metal parts is eliminated and contact between metal parts and biomass strongly reduced as the rotating motion is imparted on the biomass particles mainly as a result of a similar movement in the gas phase originating from the motion of the rotor. Operation is accordingly less vulnerable to changes in biomass material properties, such as particle size distribution and humidity as well as to fluctuations of biomass feeding speed to the reactor. As char is conveyed away from the reactor, preferably continuously, a high heat conduction between the reactor wall, i.e. the outer wall of the centrifuge chamber, and the biomass material is ensured, resulting in improved efficiency and improved pyrolysis liquid yield. The improved pyrolysis yield is conferred by a steep temperature gradient in the biomass material.

In the present context, biomass is to be understood as any organic matter, such as plants and animals or residues thereof, such as wood, agricultural and forestry process waste materials, or industrial, human and animal waste, including petrochemical-based waste feedstock. The chemical energy stored in plants and animals derives from solar energy photosynthesis and can be converted to usable liquid, such as oil or tar, in a heated process, i.e. pyrolysis.

The term pyrolysis liquid is to be understood as any organic liquid derived from biomass in a pyrolysis process, such as bio-oil or tar, the components having a boiling point in the range 0-500°C. Pyrolysis vapour is to be understood as any vapour or gas derived from biomass in a pyrolysis process, such as vaporized pyrolysis liquid.

In preferred embodiments of the present invention, biomass in the rotor is subjected to centrifugal forces greater than 2000 times the force of gravity.

The gas phase retention time in the rotor is preferably at most 5 seconds. The ratio of the diameter of the rotor and the diameter of the centrifuge chamber is preferably at least 0.5, such as at least 0.6, 0.7, 1 or at least 1.2.

It has been found that yield of pyrolysis liquid and, subsequently, gas and char is influenced by choice of feed stock, reactor wall temperature, centrifugal force and a combination of reactor gas phase temperature and residence/retention time. Whereas the former parameters determine the initial split between fractions, the latter two work through degradation of the initially formed pyrolysis liquids in the gas phase. The gas phase reactions will result in rearrangements of the molecules, formation of water (dehydration) and cracking of larger molecules constituting the liquid fraction to smaller ones which subsequently cannot be condensed under the moderate conditions employed. Gas phase reactions will therefore act to modify the liquid product in terms of viscosity and water solubility but will also change the yield both on mass and energy basis.

In order to model the effect of gas phase degradation, the reactions can be approximated by first order irreversible chemical reactions following the well-known Ahrrenius expression and furthermore treating the pyrolysis centrifuge as a plug-flow reactor. As a consequence, the degradation will be promoted by both higher temperature and longer residence/retention time, and theoretically it is possible to obtain a certain degree of degradation by an indefinite number of combinations of the two. For most embodiments of the present invention it may be desired that gas phase residence/retention time does not exceed 1 to 2 seconds in order to obtain a liquid product suitable for fuel in acceptable yield (i.e. Bridgwater, A.V., Peacocke, G.V.C. Fast pyrolysis processes for biomass. Renewable & Sustainable Energy Reviews, 4, 2000).

Gas phase residence/retention time is predominantly determined by the active volume of the reactor in combination with the amount of gas purging this volume. For systems where there is no external inert gas purge, the consequence is that the gasses only originate from the pyrolysis reactions of the feedstock. Therefore the residence/retention time and subsequently the liquid product gas phase degradation is predominantly determined by the capacity or feed rate of raw material to the reactor.

In one design of the pyrolysis centrifuge operating with a wall temperature of approximately 500°C and a centrifugal force of 10000 time the force of gravity on wheat straw, the primary mass yield of fractions will be approximately 34% organics, 22% water (56 % liquids in

total), 23 % char and 21 % gas, all on substantially dry ash-free basis. At these conditions the gas phase temperature was found to be approximately 400°C in a reactor with a feed rate of approximately 20 g/min and an active volume of approximately 0.53 L. Utilizing the kinetic expression for gas phase cracking of cellulose found by Linden et al. (Linden, A.G., Berruti, F., Scott, D.S. A kinetic model for the production of liquids from the flash pyrolysis of cellulose. Chem. Eng. Commun., 65, 1988) the yield of organics after gas phase degradation can be computed to approximately 33 % with a corresponding gas residence/retention time of approximately 1.5 s or a relatively minor change from the primary yield. If, on the other hand, gas phase temperature is raised to approximately 600°C the organics yield would be reduced to approximately 5 % whereas a tenfold increase in reactor volume would reduce organics yield to approximately 25 %. From these examples it will be clear that a reactor allowing for minimization of the combined effect of temperature and residence time on the gas phase is beneficial in order to obtain pyrolysis liquids from biomass in acceptable yield.

In embodiments of the present invention, the outer wall of the centrifuge chamber may heat the biomass, so that ablative pyrolysis takes place at or near the outer wall. Preferably, this is achieved without the use of a separate transport medium, such as sand.

At the step of conveying the pyrolysis vapors away from the centrifuge chamber, the pyrolysis vapors preferably diffuse into a condenser chamber, in which the step of condensation takes place. In a particularly compact embodiment, the centrifuge chamber has an annular cross-section, and the condenser chamber is arranged centrally i.e. coaxially within the rotor, whereby the pyrolysis vapors diffuse through an inner wall of the centrifuge chamber, which is permeable to the vapors. It will thus be appreciated that in the apparatus of the invention, the centrifuge chamber and the condenser chamber are separated by the inner wall of the centrifuge chamber, the inner wall comprising perforations, so as to allow the pyrolysis vapors to diffuse from the centrifuge chamber to the condenser chamber, in which the pyrolysis vapors may at least partly condense into said pyrolysis liquid.

The integration of the reactor (centrifuge chamber) and condenser allows for improved utilization of reactor volume. This contributes to the compactness of the apparatus, in which there is no need for an external condenser remote from the reactor with associated pipes. Additionally, thanks to the integrated condenser and reactor, the gas phase retention time may be reduced, which has shown to improve pyrolysis liquid yield, reduced liquid viscosity and reduced water content.

The perforations of the inner wall may define inlet openings of pipe stubs extending radially into the condenser chamber to provide an inlet to the condenser, which is inwardly displaced in relation to an outer periphery of the condenser chamber. The pipe stubs preferably have a

length sufficient to extend beyond condensed pyrolysis liquid, such as viscous tar, which may accumulate at the outer periphery of the condenser chamber.

In order to enhance condensation in the condenser chamber, a central portion of the condenser chamber may accommodate a packing material, on which the at least a portion of the pyrolysis vapors condenses to pyrolysis liquid.

Condensation may further be enhanced by leading a cold fluid into the condenser chamber, e.g. via a pipe arranged centrally within the condenser chamber. The fluid, which is at a temperature below the dew point of the pyrolysis vapors, may be pyrolysis liquid or a hydrocarbon immiscible with pyrolysis liquid. In case pyrolysis liquid is utilized, such pyrolysis liquid may conveniently be derived from the pyrolysis process, so that no external supply of pyrolysis liquid is needed. Any other fluid may be separated from the produced pyrolysis liquid by phase separation and recycled in the process.

The condensation temperature may be controlled by the temperature of the utilized fluid whereby especially the amount of water included in the liquid product may be controlled by partial condensation. At a later stage, the gas may be dried by further cooling in order to increase energy content of the gas and/or mix condensed water with combustible hot char to form a slurry and thus control reactivity.

At least a portion of the char deriving from pyrolysis of the biomass may be in the form of fine particles, which are conveyed away from the centrifuge chamber through openings provided in the outer wall of the centrifuge chamber and into a channel for conveying the particles further. To enhance the flow of particles into the char separation, a flow of vapour may be drawn out with the char particles, preferably by arranging the openings tangentially to the main reactor pipe whereby the motion of the rotor blades will force vapour through the pipes in a fashion similar to a centrifugal compressor. The vapour may be reentered into the reactor through an opening near the raw material intake port(s). In one embodiment of the apparatus of the present invention, a char conveyor is arranged at or near a bottom portion of the centrifuge. The conveyor may e.g. comprise a worm drive for forwarding char in the channel. Alternatively, char may be conveyed under the action of gravity or gas flow. Means may be provided for mixing the char with the pyrolysis liquid to form a slurry or char may be pilletized and collected as a separate high density energy product.

As explained above, centrifugal forces provide an outward pressure on the biomass in the centrifuge chamber toward its outer wall. An even peripheral distribution of material in the centrifuge chamber may be achieved by at least one rotor blade arranged in or extending into the centrifuge chamber, whereby the gas phase and thus suspended biomass, char,

pyrolysis vapors in the centrifuge chamber are forced in a peripheral direction. The rotation thereby imparted on the material generates the centrifugal forces for forcing the material toward the hot surface at the outer wall of the centrifuge chamber, at which surface pyrolysis takes place.

The biomass may be led axially or tangentially into the centrifuge chamber. Preferably, the biomass is led tangentially into the centrifuge chamber at one or more positions along the chamber. The biomass may be led into the centrifuge chamber via a plurality of distinct inlets or via one single inlet, e.g. an extended slit forming a widened mouth of a biomass inlet.

Heat for the pyrolysis process may be derived from a furnace arranged coaxially around the centrifuge, whereby heat for the pyrolysis process is transported across the outer wall of the centrifuge chamber by conduction. This coaxial arrangement of the furnace further contributes to overall compactness. In the furnace, at least a portion of said pyrolysis gas, char, liquid or hydrocarbon may be combusted, preferably without any need for external fuel supply. A porous flame stabilizing material in the form of a ceramic material may be incorporated within the furnace to enhance operation. Heating by electric resistance elements, magnetic induction, a condensing vapour, or a hot fluid e.g. liquid salt constitute alternative ways of heating the process.

In the present invention, the rotor may e.g. have an inner diameter of 0.01 – 5 m, and it is preferably rotated at at least 200 rpm. In one embodiment, the diameter of the rotor is approximately 1 meter, the rotor being rotated at approximately 2000 rpm and the biomass particles being subjected to centrifugal forces greater than 2000 times the force of gravity.

In order to efficiently collect and process the biomass, the centrifuge may be comprised in a mobile unit, which may collect the biomass from a growth site, such as a field or forest. The biomass may be continuously fed into the centrifuge, as the mobile unit traverses the growth site. Further biomass may be collected from the growth site by means of the mobile unit concurrently with the step of decomposing the biomass in the pyrolysis apparatus.

It will be appreciated that the provision of the pyrolysis apparatus in the mobile unit allows the pyrolysis process to take place at or near the growth site. Thus, the need for transportation and possibly intermediate storage of the raw material can be significantly reduced in comparison to those prior art methods, which require the pyrolysis to take place at a stationary installation remote from the growth site. Preferably, the pyrolysis takes place while further biomass is simultaneously being collected and continuously fed to the pyrolysis apparatus. Hence, pyrolysis takes place while the mobile unit traverses the growth site, and while biomass is being collected simultaneously. Transportation of relatively large volumes of

biomass from the growth site to a remote pyrolysis facility may thus be avoided. As pyrolysis liquid has a significantly higher energy concentration per volume than biomass, a certain amount of energy requires less space when present in the form of pyrolysis liquid than when present in the form of biomass, and the energy may thus be more conveniently conveyed to the intended consumer in the form of pyrolysis liquid. Pyrolysis liquid may be transported from the growth site to the intended consumer or to a storage facility by means of tank trucks or vessels (e.g. ISO tank containers), or conveyed through pipe lines under adequate pumping action.

The mobile unit may comprise a wheeled support structure. A coupling system may be provided for coupling the unit to a power-driven vehicle. Alternatively, the mobile unit may incorporate an engine or motor, so that the mobile unit is self-propelled. The engine or motor of the mobile unit may utilize the pyrolysis gas, pyrolysis liquid and/or char as fuel, whereby the need for a separate fuel source of the mobile unit may be reduced or even eliminated. Likewise, in embodiments of the invention, in which the mobile unit is not self-propelled, the propelling drive means, e.g. tractor or truck, may utilize the pyrolysis gas, pyrolysis liquid and/or char as a fuel source.

To efficiently cool waste char from the pyrolysis process before possible ejection thereof from the mobile unit, the process may include the step of collecting dirt from the growth site and mixing the dirt with the char to thereby cool the char. In other words, dirt may be utilized as a cooling source for waste matter deriving from pyrolysis, and the need for e.g. water cooling may be eliminated. It will hence be appreciated that the mobile unit may comprise a dirt collector for collecting dirt from the growth site and a mixer for mixing the dirt with the char to thereby cool the char, as well as a dirt and char ejector for ejecting the mix or slurry of char and dirt from the mobile unit. Alternatively, water derived from drying pyrolysis gas obtained by partially condensing the pyrolysis vapour may be utilized to cool the reactive char by mixing the two ingredients to a slurry.

The mix of char and dirt or the char/water slurry may be fed into a furrow formed by appropriate means of the mobile unit, such as by a tine. The tine may be arranged such with respect to the dirt and char ejector that the mix of char and dirt can be fed into the furrow during use of the mobile unit. Subsequently, the char mix may be covered with dirt to enhance decomposition of the char.

At least a portion of the pyrolysis gas produced by the pyrolysis process may be combusted in a furnace forming part of the pyrolysis apparatus, the furnace producing heat for the pyrolysis process. Exhaust fume of the furnace may be expelled via a fume outlet of the

furnace. In addition to pyrolysis gas, at least a portion of the char may be combusted in the furnace.

Prior to feeding of the biomass into the pyrolysis apparatus, the biomass may be fed to a pre-heating device, in which it is preheated and possibly dried before it enters the pyrolysis apparatus. The exhaust fume produced in the furnace may be utilized as a heat source in the pre-heating device. Exhaust fume from the furnace may also be guided to a first heat exchanger, in which it heats intake air for the furnace. Alternatively or additionally, a conduit, which is connectable to an exhaust outlet of the power-driven vehicle or an exhaust outlet of the engine of the mobile unit, may be provided to allow exhaust gas of the vehicle or of the engine as a heat source in the first heat exchanger or in the process of pre-heating and/or drying the biomass.

The mobile unit may advantageously include a shredder for shredding the collected biomass upstream of the pyrolysis apparatus, e.g. upstream of the pre-heating device. A biomass buffer may be included to allow more biomass to be collected than what is being processed in the pyrolysis apparatus. For example, operation of the collector may be interrupted e.g. for manoeuvring the vehicle or for inspection without interruption of the pyrolysis apparatus. In one embodiment, the pre-heating device serves as the biomass buffer.

At the step of separating the pyrolysis liquid from the char and pyrolysis gas, the pyrolysis liquid and at least a portion of the pyrolysis gas may be conveyed to a separator for separating the pyrolysis liquid from the pyrolysis gas, and at least a portion of the separated pyrolysis gas may be conveyed back to the furnace as a fuel source therein. Further, at least a portion of the separated liquid may be conveyed back to the pyrolysis apparatus as a cooling source in a pyrolysis condenser. The condenser may be integrated in the pyrolysis apparatus, or it may be constitute a separate unit, which does not form part of the pyrolysis apparatus. Before the liquid enters the condenser, it is preferably cooled in a second heat exchanger, which may utilize air as a cooling source. The air, which exits the second heat exchanger, may be mixed with the intake air for the furnace upstream or downstream of the first heat exchanger, e.g. to improve combustion efficiency in the furnace.

In one embodiment, the pyrolysis apparatus comprises a centrifuge defining a centrifuge chamber, and at the step of decomposing the biomass, the method of the invention may comprise the step imparting rotation on the biomass in the centrifuge, whereby the biomass is forced towards an outer wall of the centrifuge chamber. The outer wall of the centrifuge chamber is maintained at a temperature of 350 – 700°C to effect a pyrolysis process at or near the outer wall of the centrifuge chamber, whereby the biomass decomposes into the pyrolysis liquid, pyrolysis gas and char, the gas and liquid being on gaseous form.

In a particularly compact embodiment of the pyrolysis apparatus, the condenser is integrated in the pyrolysis apparatus. In this embodiment, the centrifuge chamber of the pyrolysis apparatus is delimited by an inner wall and an outer wall, and an outlet is provided for feeding biomass into the centrifuge chamber. A rotor is arranged to impart rotation on the gas phase and the biomass suspended herein within the centrifuge chamber to force the biomass towards the outer wall of the centrifuge chamber under the action of centrifugal forces. A heating system is included for maintaining the outer wall of the centrifuge chamber at a temperature of 350 – 700°C to effect the pyrolysis process at or near the outer wall of the centrifuge chamber and to thereby decompose the biomass into char, pyrolysis gas and pyrolysis vapours, which can be condensed into pyrolysis liquid in the condenser. The heating system may include the furnace as describe above, the centrifuge being preferably arranged coaxially within the furnace, whereby heat for the pyrolysis process is transported across the outer wall of the centrifuge by conduction. The inner wall of the centrifuge chamber may be permeable to the pyrolysis vapours and gas, so that the condenser may be arranged centrally within the centrifuge chamber.

Brief description of the drawings

An embodiment of the invention will now be further described with reference to the drawings, in which:

Fig. 1 is a chart illustrating implementation of an embodiment of the method and apparatus of the present invention;

Fig. 2 is a perspective illustration of a pyrolysis apparatus;

Fig. 3 is a partial cross-sectional view through the pyrolysis apparatus of Fig. 2.

Detailed description of the drawings

Fig. 1 illustrates the flow of air, gas and liquid in a system incorporating a pyrolysis apparatus as disclosed herein. The system may be accommodated on a mobile unit for simultaneously collecting biomass and processing biomass in a pyrolysis process. The system includes a pyrolysis apparatus 200, which will be described in more detail below with reference to Figs. 2 and 3. A motor 102 is provided for driving a rotor of the pyrolysis apparatus. In tar/gas separator, pyrolysis liquid in the form of tar is separated from gas. Part of the separated tar is led to a heat exchanger as described further below, and the remaining tar is collected in tar collector 106. Gas is led from the tar/gas separator into a furnace of the pyrolysis apparatus, in which it is utilized as fuel for producing heat required in the pyrolysis process.

As shown in the right-hand end of Fig. 1, biomass such as straw is picked up from a field or from another growth site and fed into a shredder, such as a roller mill 108, from which it is fed to a buffer and pre-heating device 110. Heat is transported to the pre-heating device with exhaust gas from the furnace of the pyrolysis apparatus 200 and/or with exhaust gas from an engine of the mobile unit or from a truck or tractor driving the mobile unit. Exhaust gas from the furnace of the pyrolysis apparatus is conveyed through a first heat exchanger 112, in which it heats combustion air for the furnace. As shown in the upper left corner of Fig. 1, a second heat exchanger 114 is provided for cooling that part of the tar separated in the tar/gas separator 104, which is led back into the pyrolysis apparatus. The cooling source for the second heat exchanger 114 is air, which may be led through the first heat exchanger 112 after it has passed the second heat exchanger 114, but before it enters the furnace of the pyrolysis apparatus.

In this configuration, char, which is conveyed away from the pyrolysis apparatus, is mixed with dirt picked up from the growth site in a char/dirt mixer 116 to form a char/dirt mixture. The mixture may advantageously be distributed on the growth site, e.g. a field, for instance into a furrow formed by a tine of the mobile unit.

The pyrolysis apparatus 200 is shown in more detail in Fig. 2. It comprises a biomass inlet pipe 202, through which biomass is conveyed into a centrifuge chamber or reactor 204 surrounded by a furnace 206. The centrifuge chamber 204 has an outer wall 208, through which heat is conducted from the furnace for effecting pyrolysis in the centrifuge chamber at or near the outer wall 208. A rotor 210 forms a perforated inner wall 212 of the centrifuge chamber, the rotor being provided with rotor blades 214 for rotating the gas phase and the biomass suspended herein within the centrifuge chamber. During operation of the apparatus, biomass and other material in the centrifuge chamber, such as char and pyrolysis vapors are forced by centrifugal forces towards the reactive surface at the outer wall 208 of the centrifuge chamber 204, at which pyrolysis is effected. Heat deflectors 216 are secured to the rotor blades for limiting heat radiation from the furnace 206 onto the inner wall 212 of the centrifuge chamber, which surrounds a condenser to be kept at a limited temperature well below the pyrolysis temperature of about 350-700°C.

Condenser 218 is arranged coaxially within the centrifuge chamber 204 and comprises a packing material 220 for enhancing condensation. Equidistant baffle plates 222 provide a support for the packing material and for the shell of the condenser 218, and perforations 224 in the baffle plates 222 guide pyrolysis gas through the condenser to optimize gas/liquid contact. Cold liquid is fed into the condenser via a perforated cooling feed pipe 226.

A bottom portion of the wall 208 may be provided with holes or perforations allowing char to fall into a channel 228, in which the char is conveyed away from the pyrolysis apparatus by means of e.g. a worm drive conveyor 230.

It will be appreciated that the furnace, centrifuge chamber, rotor, condenser, and char conveyor extend the entire length of the pyrolysis apparatus, the various parts being cut-off in Fig. 2 for illustrative purposes only.

Fig. 3 shows a partial cross-section through the pyrolysis apparatus 200. The furnace 206 shown in Fig. 2 is not included in Fig. 3 for the sake of clarity. Biomass in the centrifuge chamber 204 is illustrated as hatched area 232. As illustrated by arrows 234, pyrolysis vapors diffuse into the condenser 218 via perforations in the inner wall 212 of the centrifuge chamber 204 (see Fig. 2), there being provided an inwardly projecting pipe stub 236 at each perforation. Each pipe stub 236 has a plurality of openings 238 located above the surface of the condensed pyrolysis liquid 240, through which gas may escape into the condenser 218. The pipe stubs 236 have a length sufficient to extend through a layer of condensed pyrolysis liquid, e.g. tar, which has accumulated at the outer periphery of the condenser.

CLAIMS

1. A method for producing pyrolysis liquid from biomass, comprising the step of decomposing the biomass into pyrolysis liquid, char and pyrolysis gas in a fast pyrolysis process, the method comprising the steps of:

- feeding the biomass into a centrifuge chamber;
- rotating a rotor to impart rotation on biomass distributed in gas volume in the centrifuge chamber, whereby the biomass is forced towards an outer wall of the centrifuge chamber by centrifugal forces;
- decomposing the biomass into pyrolysis vapors and char by maintaining said outer wall at a temperature of 350 – 700 degrees Celsius to effect the pyrolysis process at or near the outer wall of the centrifuge chamber;
- separating the pyrolysis vapours and char;
- conveying the pyrolysis vapors and char away from the centrifuge chamber;
- condensing the at least a portion of said pyrolysis vapors to obtain said pyrolysis liquid and pyrolysis gas.

2. The method of claim 1, wherein biomass in the rotor is subjected to centrifugal forces greater than 2000 times the force of gravity.

3. The method of claim 1 or 2, wherein the gas phase retention time in the rotor is at most 5 seconds.

4. The method of any of claims 1-3, wherein the ratio between the diameter of the rotor and the diameter of the centrifuge chamber is at least 0.5.

5. The method of any of claims 1-4, wherein the outer wall of the centrifuge chamber heats the biomass, so that ablative pyrolysis takes place at or near the outer wall.

6. The method of any of the preceding claims, wherein, at the step of conveying, the pyrolysis vapors diffuse into a condenser chamber, in which said step of condensation takes place.

7. The method of claim 6, wherein the centrifuge chamber has an annular cross-section, and wherein the condenser chamber is arranged centrally within the rotor, whereby, at the step of conveying, the pyrolysis vapors diffuse through an inner wall of the centrifuge chamber, which is permeable to the vapors.

8. The method of claim 6 or 7, wherein the condenser chamber accommodates a packing material, on which the at least a portion of the pyrolysis vapors condense to pyrolysis liquid.

9. The method of any of claims 6-8, wherein a cold fluid is led into the condenser chamber, the fluid being at a temperature below the dew point of the pyrolysis vapors.

10. The method of any of claims 6-8, wherein the cold fluid is pyrolysis liquid or a hydrocarbon immiscible with pyrolysis liquid.

11. The method of claim 9 or 10, wherein the cold fluid is led into the condenser chamber via a pipe arranged coaxially within the condenser chamber.

12. The method of any of the preceding claims, wherein at least a portion of said char is in the form of fine particles, which, at the step of conveying, are conveyed away from the centrifuge chamber through openings provided in the outer wall of the centrifuge chamber and into a channel for conveying the particles further.

13. The method of claim 12, wherein the flow of particles through the openings in the outer wall of the centrifuge chamber is promoted by drawing a flow of vapours out of the centrifuge chamber, said openings extending essentially tangentially to a longitudinal axis of the centrifuge chamber, and said channel being dimensioned to provide a stagnant zone, in which said particles essentially separate from the vapour, the method further comprising:
- forcing the vapours through said channel under the influence of a pressure gradient provided by the rotation of the rotor;
- recycling the essentially particle-free vapours to the centrifuge chamber through at least one opening near one or more intake ports of the centrifuge chamber.

14. The method of any of the preceding claims, wherein the char is conveyed in said channel by means of a conveyor and/or under the action of gravity.

15. The method of any of the preceding claims, wherein the gas phase and thus the suspended biomass, char, pyrolysis vapors in the centrifuge chamber are forced in a peripheral direction by means of at least one rotor blade arranged in the centrifuge chamber.

16. The method of any of the preceding claims, wherein, at the step of feeding, the biomass is led tangentially into the centrifuge chamber.

17. The method of any of the preceding claims, wherein the centrifuge is arranged coaxially within a furnace whereby heat for the pyrolysis process is transported across the outer wall of the centrifuge chamber by conduction, the method further comprising the step of combusting at least a portion of said pyrolysis gas, char, liquid or hydrocarbon in the furnace.

18. The method of any of the preceding claims, wherein the centrifuge is comprised in a mobile unit, the method further comprising the steps of:
- collecting the biomass from a growth site by means of a mobile unit;
- at said step of feeding: continuously feeding the biomass into the centrifuge, as the mobile unit is moved across the growth site;
- collecting further biomass from the growth site by means of the mobile unit, the step of collecting further biomass being carried out concurrently with said step of decomposing.

19. The method of any of the preceding claims, wherein the pyrolysis vapours are partially condensed in a primary condenser, the method further comprising:
- drying the gas originating from the partial condensation and utilizing at least a portion thereof as fuel for a furnace and/or for an engine for propelling the mobile unit;
- mixing the resulting liquid phase consisting largely of water with the char to obtain a slurry;
- distributing the slurry over the growth site and/or collecting it for further processing or combustion;
- leading the vapours formed in the process of contacting hot char with liquid to a tertiary condenser in order to utilize components having a lower boiling point than water;
- admixing the vapour from the tertiary condenser with liquid product produced by the primary condenser.

20. The method of any of the preceding claims, wherein rotor has an inner diameter of 0.01 – 5 m and is rotated at at least 200 rpm.

21. A fast pyrolysis apparatus for producing pyrolysis liquid, char and pyrolysis gas from biomass, comprising:
- a centrifuge chamber delimited by an inner wall and an outer wall;
- an inlet through which biomass can be fed into the centrifuge chamber;
- a rotor arranged to impart rotation biomass distributed in gas volume in the centrifuge chamber to force the biomass towards the outer wall under the action of centrifugal forces;
- a heating system for maintaining said outer wall at a temperature of 350 – 700 degrees Celsius to effect the pyrolysis process at or near the outer wall of the centrifuge chamber and to thereby decompose the biomass into char and pyrolysis vapors, which can be condensed to form pyrolysis liquid and pyrolysis gas;
- a char conveyor for conveying the char away from the centrifuge chamber;

and wherein:
- the inner wall of the centrifuge chamber is permeable to said pyrolysis vapors.

22. The apparatus of claim 21, wherein the rotor and its rotation is configured to subject biomass therein to centrifugal forces greater than 2000 times the force of gravity.

23. The apparatus of claim 21 or 22, wherein the rotor is dimensioned and operable to limit the gas phase retention time in the rotor to at most 5 seconds.

24. The apparatus of any of claims 21-23, wherein the ratio between the diameter of the rotor and the diameter of the centrifuge chamber is at least 0.5.

25. The apparatus of any of claims 21-24, wherein the centrifuge chamber constitutes an ablative reactor, in which heat for the pyrolysis process can be transmitted from the outer wall of the centrifuge chamber to the biomass.

26. The apparatus according to any of claims 21-25, wherein the rotor is essentially cylindrical.

27. The apparatus of claim 26, wherein the centrifuge chamber has an annular cross section, and wherein a condenser chamber is arranged centrally within the centrifuge chamber, the centrifuge chamber and the condenser chamber being separated by said inner wall of the centrifuge chamber, the inner wall comprising perforations, so as to allow the pyrolysis vapors to diffuse from the centrifuge chamber to the condenser chamber, in which the pyrolysis vapors may at least partly condense into said pyrolysis liquid.

28. The apparatus of any of claims 21-27, wherein the perforations of the inner wall defines inlet openings of pipe stubs extending radially into the condenser chamber.

29. The apparatus of any of claims 21-28, wherein a central portion of the condenser chamber accommodates a packing material.

30. The apparatus of any of claims 21-29, further comprising a pipe arranged centrally within the condenser chamber for leading a cold fluid into the condenser chamber to promote condensation.

31. The apparatus of any of claims 21-30, wherein the rotor comprises at least one rotor blade extending into the centrifuge chamber.

32. The apparatus of any of claims 21-31, wherein the char conveyor is arranged at or near a bottom portion of the centrifuge.

33. The apparatus of claim 32, further comprising means for mixing the char with the pyrolysis liquid to form a slurry.

34. A mobile unit comprising an apparatus according to any of claims 18-33.

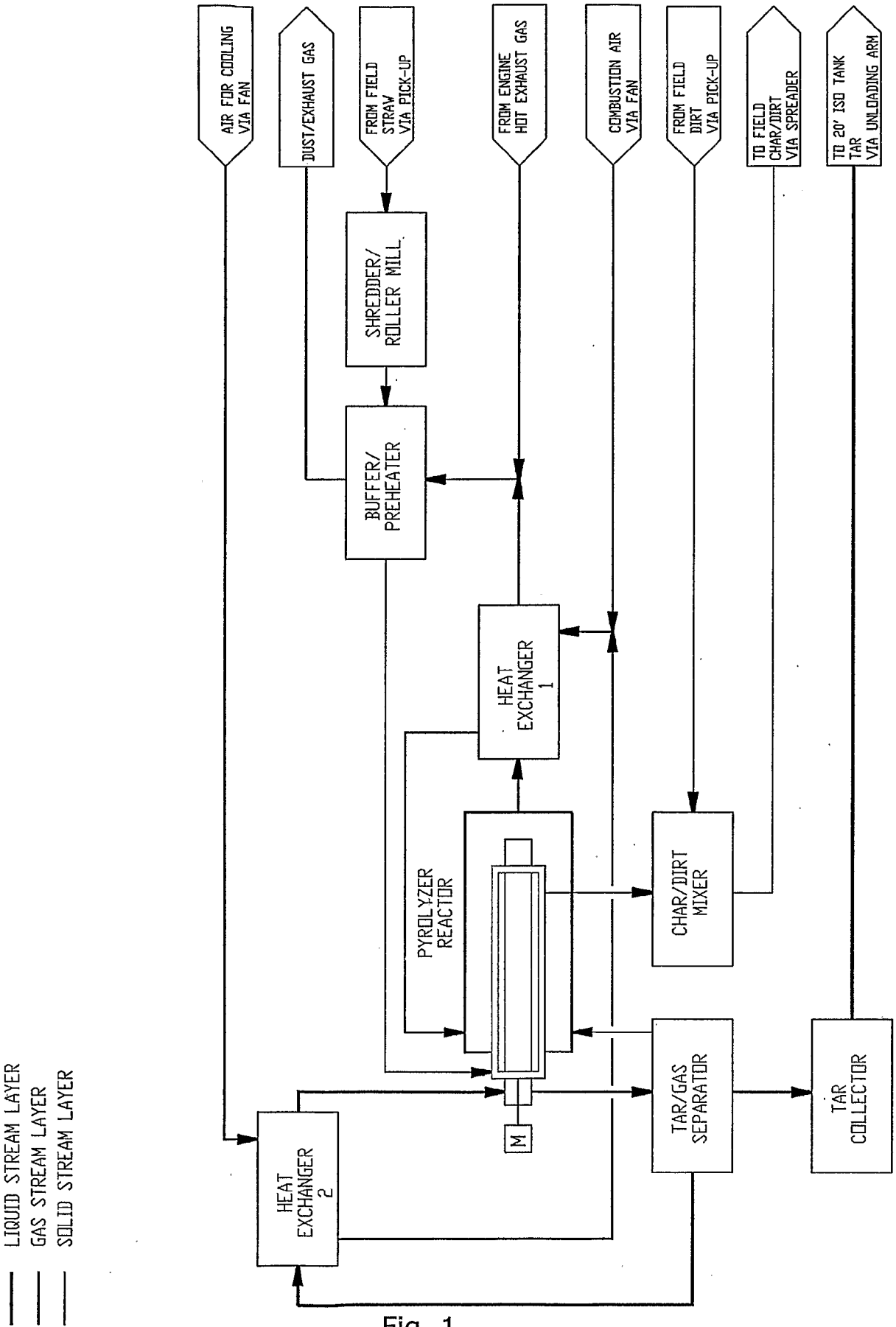
AIR FOR COOLING VIA FAN
DUST/EXHAUST GAS
FROM FIELD STRAW VIA PICK-UP
FROM ENGINE HOT EXHAUST GAS
COMBUSTION AIR VIA FAN
FROM FIELD DIRT VIA PICK-UP
TO FIELD CHAR/DIRT VIA SPREADER
TO 20' ISO TANK TAR VIA UNLOADING ARM
SHREDDER/ ROLLER MILL
BUFFER/ PREHEATER
HEAT EXCHANGER 1
PYROLYZER REACTOR
M
CHAR/DIRT MIXER
TAR/GAS SEPARATOR
TAR COLLECTOR
HEAT EXCHANGER 2
LIQUID STREAM LAYER
GAS STREAM LAYER
SOLID STREAM LAYER

Fig. 1

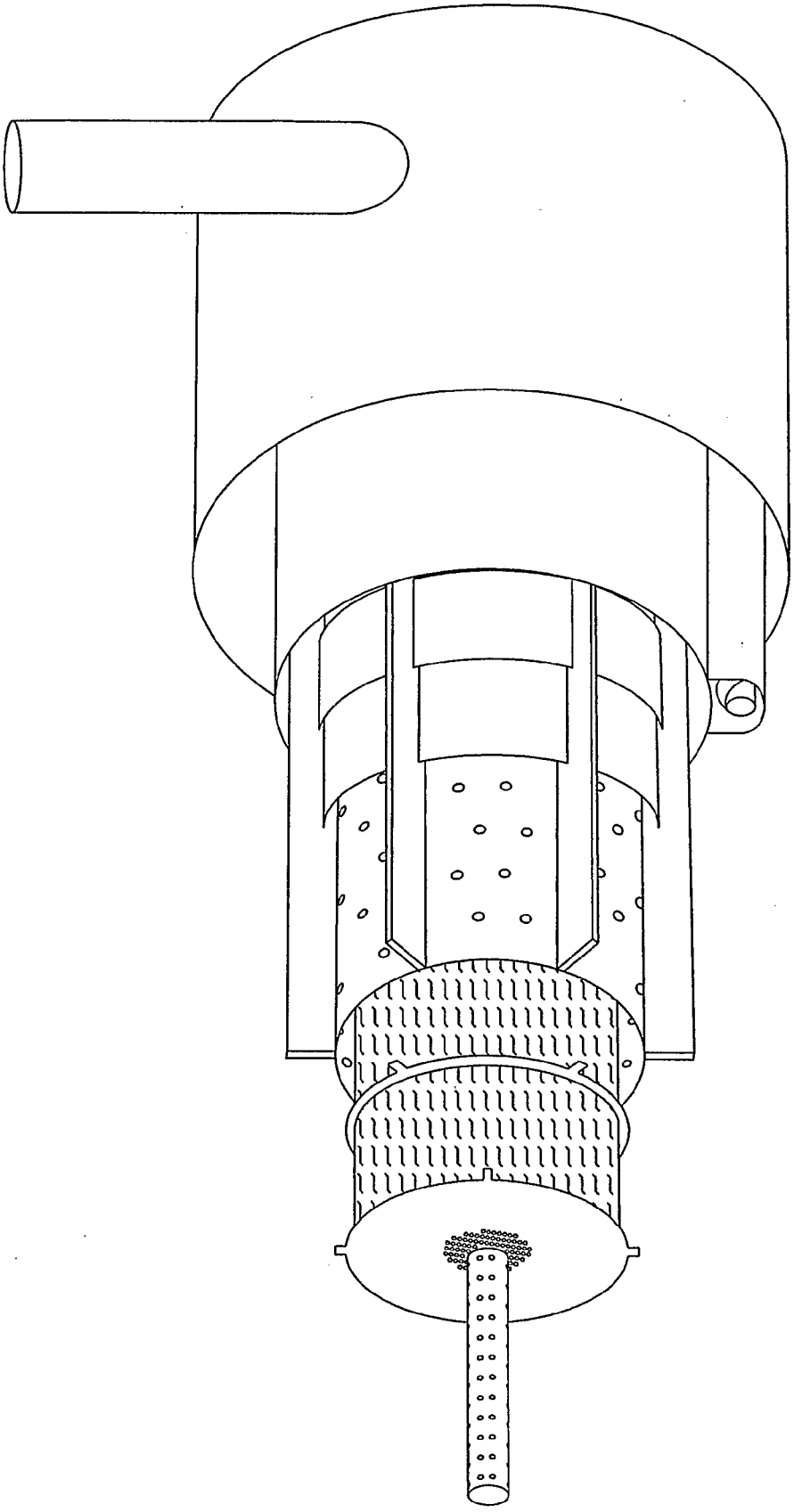

Fig. 2

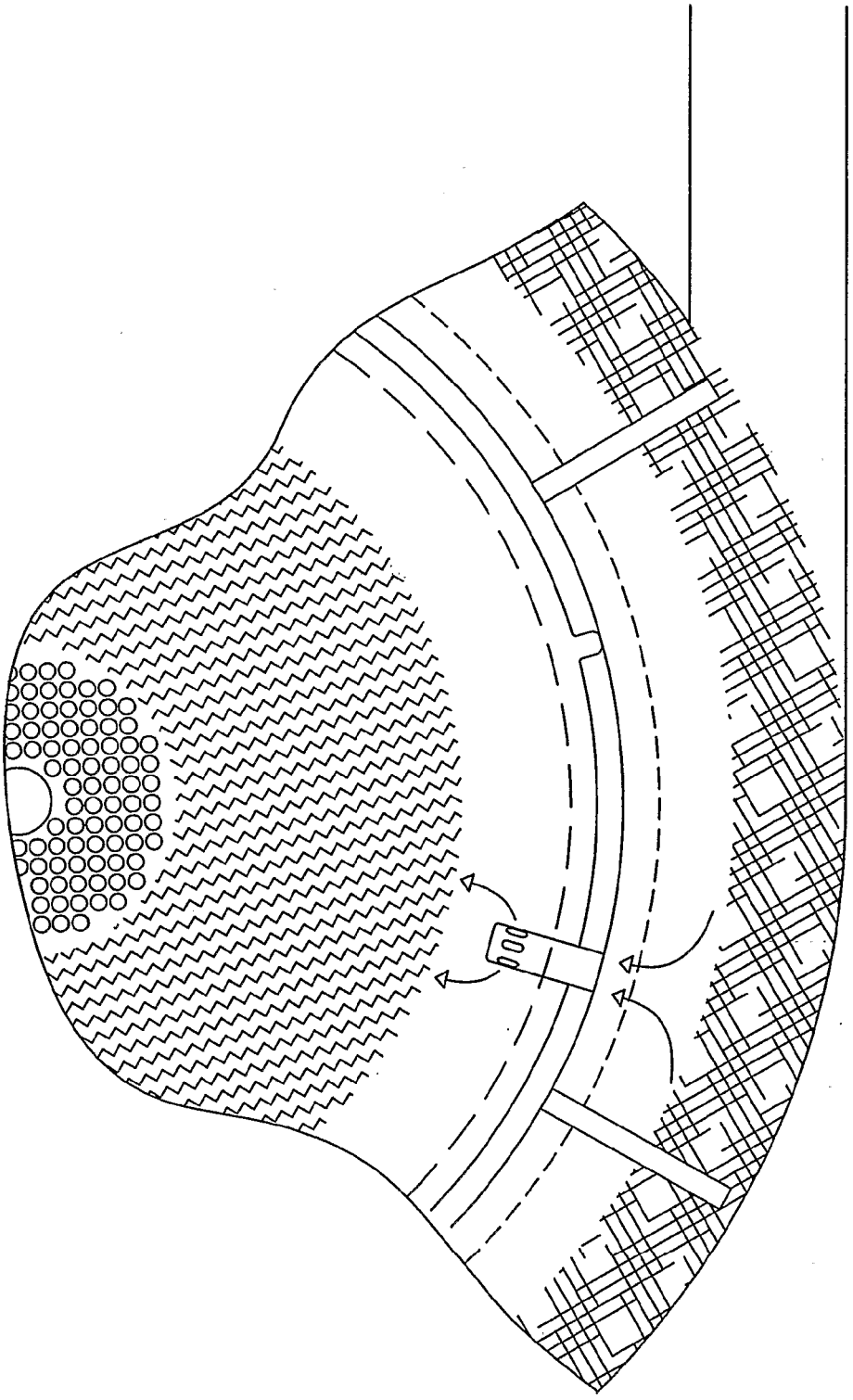

Fig. 3

INTERNATIONAL SEARCH REPORT

International application No
PCT/DK2006/000241

A. CLASSIFICATION OF SUBJECT MATTER
INV. C10B53/02 C10B47/22 C10C5/00

According to International Patent Classification (IPC) or to both national classification and IPC

B. FIELDS SEARCHED

Minimum documentation searched (classification system followed by classification symbols)
C10B C10C

Documentation searched other than minimum documentation to the extent that such documents are included in the fields searched

Electronic data base consulted during the international search (name of data base and, where practical, search terms used)
EPO-Internal, WPI Data, COMPENDEX

C. DOCUMENTS CONSIDERED TO BE RELEVANT

Category*	Citation of document, with indication, where appropriate, of the relevant passages	Relevant to claim No.
X	BRIDGWATER A V ET AL: "Fast pyrolysis processes for biomass" RENEWABLE AND SUSTAINABLE ENERGY REVIEWS, ELSEVIERS SCIENCE, NEW YORK, NY, US, vol. 4, no. 1, March 2000 (2000-03), pages 1-73, XP004268416 ISSN: 1364-0321 page 35 - page 41 page 53 - page 56	1-34
X	WO 99/66008 A (GRAVESON ENERGY MANAGEMENT LTD; MATON, MAURICE, EDWARD, GEORGE) 23 December 1999 (1999-12-23) the whole document	1-34

☐ Further documents are listed in the continuation of Box C.

☒ See patent family annex.

* Special categories of cited documents :

"A" document defining the general state of the art which is not considered to be of particular relevance

"E" earlier document but published on or after the international filing date

"L" document which may throw doubts on priority claim(s) or which is cited to establish the publication date of another citation or other special reason (as specified)

"O" document referring to an oral disclosure, use, exhibition or other means

"P" document published prior to the international filing date but later than the priority date claimed

"T" later document published after the international filing date or priority date and not in conflict with the application but cited to understand the principle or theory underlying the invention

"X" document of particular relevance; the claimed invention cannot be considered novel or cannot be considered to involve an inventive step when the document is taken alone

"Y" document of particular relevance; the claimed invention cannot be considered to involve an inventive step when the document is combined with one or more other such documents, such combination being obvious to a person skilled in the art.

"&" document member of the same patent family

Date of the actual completion of the international search	Date of mailing of the international search report
11 August 2006	18/08/2006

Name and mailing address of the ISA/	Authorized officer
European Patent Office, P.B. 5818 Patentlaan 2 NL - 2280 HV Rijswijk Tel. (+31-70) 340-2040, Tx. 31 651 epo nl, Fax: (+31-70) 340-3016	Zuurdeeg, B

INTERNATIONAL SEARCH REPORT

Information on patent family members

International application No
PCT/DK2006/000241

Patent document cited in search report	Publication date	Patent family member(s)	Publication date
WO 9966008 A	23-12-1999	AP 1241 A	02-02-2004
		AU 754518 B2	21-11-2002
		AU 4381099 A	05-01-2000
		BG 104230 A	31-08-2000
		BR 9906537 A	15-08-2000
		CA 2299370 A1	23-12-1999
		CN 1130444 C	10-12-2003
		EA 1294 B1	25-12-2000
		EE 200000091 A	15-12-2000
		EP 1012215 A1	28-06-2000
		GB 2342984 A	26-04-2000
		HK 1025594 A1	25-04-2003
		HR 20000087 A2	31-08-2001
		HU 0003735 A2	28-03-2001
		ID 24630 A	27-07-2000
		IL 134423 A	12-09-2002
		IS 5372 A	10-02-2000
		JP 2002518546 T	25-06-2002
		NO 20000747 A	14-04-2000
		NZ 502598 A	30-03-2001
		OA 11319 A	27-10-2003
		PL 338674 A1	20-11-2000
		SK 1962000 A3	11-07-2000
		TR 200000412 T1	23-10-2000
		US 6648932 B1	18-11-2003
		ZA 200000487 A	07-08-2000